The *stevor* multigene family of *Plasmodium falciparum*

Submitted by

Jane Elizabeth Blythe

March 2007

To

University College London

For the degree of

Doctor of Philosophy

ProQuest LLC
789 East Eisenhower Parkway
P.O. Box 1346
Ann Arbor, MI 48106-1346

I, Jane Elizabeth Blythe, confirm that the work presented in this thesis is my own. Where information has been derived from other sources, I confirm that this has been indicated in the thesis.

Jane E. Blythe

Abstract

The *stevor* family is the third largest multigene family in the *P. falciparum* 3D7 genome (Gardner *et al.*, 2002). With 30 copies estimated per genome, each encoding a predicted transmembrane spanning protein: a conserved N-terminal domain is followed by hydrophobic regions, a 100 amino acid 'hyper-variable' region (HVR), conserved transmembrane domain and short highly conserved cytoplasmic C-terminus.

In 3D7, *stevor* is transcribed in trophozoites and STEVOR protein was found in cytoplasmic membranous structures known as Maurer's clefts (Kaviratne et al., 2002). The Maurer's clefts are implicated in trafficking of proteins to the infected red blood cell (iRBC) surface, and pre-assembly of proteins destined for knob structures on the surface (Craig and Scherf., 2001). *Stevors* have also been detected in gametocyte stages and a STEVOR peptide found in sporozoite extracts (Sutherland, 2002 and Florens *et al*, 2002).

The HVR of STEVOR may play a role in immune evasion. To investigate this further, we have started to characterise the genomic repertoire and expression profile of *stevor* genes in laboratory lines and field parasite isolates from Kenya, East Africa. Using *stevor* specific primers, we have identified 152 *stevor*s in *P. falciparum* laboratory lines and Kenyan isolates. In addition, 27 *stevors* were identified in the genome of a Ghanaian field isolate (www.plasmodb.org) and 17 in a second laboratory isolate IT.

Western blots identified a protein of approximately 30 kDa; expected STEVOR mean molecular mass is 36.75kDa. Immunofluorescence assays showed that in mature, segmented schizonts, STEVOR is redistributed from the Maurer's clefts to throughout the iRBC cytosol. Interestingly, STEVOR was also observed in the apex of merozoites.

An extremely important observation for the application of *in vitro* cultured *P. falciparum* clones is the huge difference in STEVOR expression to that in the field parasite isolates. STEVOR protein is expressed in only 5% of *P. falciparum* 3D7 schizonts, whereas it is found in 50% of Kilifi field isolate schizonts.

We investigated field isolates further to see whether STEVOR is on the iRBC surface together with other multigene families, such as the *var* encoded PfEMP1 and RIFINS, where STEVOR could play a role in antigenic variation which enables the *P. falciparum* parasite to evade the host immune response. Alternatively, STEVOR may have ligand binding functions/ RBC adherence properties during final schizont stage, rupture and merozoite reinvasion.

Acknowledgements

My thanks go to Peter Preiser for taking me on as an MRC, Ph.D student, for his enthusiasm, ideas and encouragement through tricky times, also for his good company on various tropical islands. I would like to thank Jean Langhorne for her support and help over the many years now, for taking on yet another student and giving me such good advice and guidance (especially in the removal of jargon!). Thank you to Tony Holder for his technical advice, guidance and putting together such a great division of people.

Thank you also to Mike Blackman for time out of your busy schedule for musical interludes and Western blot samples. On a further technical note my thanks to Muni Grainger, and the lovely ladies of the Blackman lab for helping me with parasites (also sharing the Birthday cake responsibilites!), Louise Hinds for trying your best with immunoprecipitations, Ellen Kneupfer, Judith Green and Irene Ling for technical expertise, antibodies, slides, ideas and interesting discussions, Sam Kinyanjui for showing me how to do agglutination assays and live IFAs. Demetrios Vassilakos for help and encouragement with bioinformatics. Bill Jarra for doing the things I can't do myself with all things animal. Salvatore Adinolfi for taking me to protein school and for just being you! Trinny and Chris in the large-scale media laboratory, Steve Howell for Mass spectrometry and Andres Ramos for help with CD analysis, Catherine Braun-Breton for PfSBP1 antibodies, and 'Photographics' for teaching me the art of figure making and generally taking the mickey.

My special thanks go to the wonderful community at KEMRI, Kilifi, and Kevin Marsh for giving me the opportunity to be a part of it. Thank you also to the former members of Nanyang Technological University temporary Biology department and especially Jay Iyer for being so brilliant and such a wonderful friend to work with. Good luck to present members of STEVOR project team in Singapore and thank you for anti-sera and recombinant protein constructs.

There are many people who have taken the trouble to proof-read various parts of my thesis I need to thank Francis Ndungu, Tom Mansell, Deirdre Cunningham, Hannah *aka* 'Bimb' Polson, Vicki Millins, Doug Brown, Ching Li and Sandra Koernig all of whom did a wonderful job in encouraging me along with pointing out the errors. Most of all a big thank you to my supervisors for reading and correcting my whole thesis.

Additional thanks also needs to go to my two personal counsellors Drs. Doug Brown & 'Me' Ndungu without whose support and worldly advice I would not have made it this far (Doug for assuming your position so early in your employment, although to be fair you

nearly killed me on tough guy, and Francis for being an absolutely brilliant friend wherever in the world we were). I must mention the wonderful Langhorne ladies (and gents) thank you for all being such enthusiastic, warm, fun people to work with.

Two very special people without whose support and friendship I cannot imagine having got through the last few years: Sandra Koernig and Robin Stephens thank you both. My gratitude also cannot be expressed enough to my best friends who have kept me sane or perhaps just insane enough over the last year, especially Clive Lunny, the number of times you have rescued me and my mac is just not funny! Also thank you for bringing me almond croissants when all else failed, and Bimb Polson, for bringing the laughter back from Paris with you.

Finally, my love and thanks to Andrew Mellor, Mum, Philippa, and Lauren for all your love, support and believing in me. My fabulous second family the 'Carabines' for providing me with so much more than just a room over my head. Last but by no means least, Dad, thank you for coming back into my life.

Publications

Cunningham DA, Jarra W, Koernig S, Fonager J, Fernandez-Reyes D, Blythe JE, Waller C, Preiser PR, Langhorne J.
Host immunity modulates transcriptional changes in a multigene family (yir) of rodent malaria. Mol Microbiol. 2005 Nov; **58**(3): 636-47

Blythe JE. Surentheran T, Preiser PR.

STEVOR – a multifunctional protein. Mol Biochem Parasitol. 2004 Mar; **134**(1): 11-5

Review

Table of Contents

List of Tables

List of Figures

Chapter 1

Chapter 2

Chapter 3

Chapter 4

Abbreviations

°C	degrees Celsius
A20/B	control (irrelevant) peptide
AB	Blood group antigen type-AB
AE1	Anion-Exchange protein 1 (band 3)
APC	Antigen Presenting Cell
ATS	Acidic Terminal Sequence
BCA	Bicinchoninic acid (assay)
bir	*P. berghei* interspersed repeats (genes)
BLAST	Basic Local Alignment Search Tool
bp	Base pairs (nucleotide)
BSA	Bovine Serum Albumin
C-terminal	Carboxy (COOH-) terminal end
CD	Cluster Designation
cd	Compact Disc
cDNA	Complementary DNA
CIDR	Cysteine rich Inter-Domain Region
cir	*P. chabaudi* interspersed repeats (genes)
CR1	Complement Receptor 1
Da	Dalton
DAPI	4, 6-diamino-2-phenylindole
dATP	Deoxyadenosine triphosphate
DBL	Duffy Binding Ligand
DBP	Duffy Binding Proteins
DC	Dendritic Cell
dCTP	Deoxycytidine triphosphate
dH_2O	Distilled water
dGTP	Deoxyguanosine triphosphate
DNA	Deoxyribonucleic acid (genomic)
dNTP	Deoxyribonucleoside triphosphate
DTT	Dithiothreitol
dTTP	Deoxythymidine triphosphate
EBL	Erythrocyte Binding Ligands
EDTA	Ethylenediaminetetraacetic acid

EGTA	Ethyleneglycotetraacetic acid
ELISA	Enzyme-Linked ImmunoSorbent Assay
EMBL	European Molecular Biology Laboratory
ES	Early Schizont
EST	Expressed Sequence Tags
ET	Early Trophozoite
F	Forward (primer)
FACS	Fluorescence Activated Cell Sorting
FCS	Foetal Calf Serum
FITC	Fluorescein isothiocyanate
FPLC	Fast Protein Liquid Chromatography
g	Gram
xg	Relative centrifugal force (gravities)
GLURP	GLUtamate-Rich Protein
H+L	Heavy + Light (chain)
HCT	Host Cell Targeting (signal)
His	Histidine
HRP	Horse Radish-Peroxidase
HVR	Hyper-Variable Region
IFA(s)	Indirect ImmunoFluorescence Assay(s)
IgG/M	Immunoglobulin G/M
Indels	INsertion-DELetion polymorphisms
iRBC(s)	parasitised/Infected Red Blood Cell(s)
k	Kilo
KAHRP	Knob-Associated Histidine-Rich Protein
kDa	KiloDalton
KEMRI	KEnya Medical Research Institute
KIR	Killer cell Immunoglobulin-like Receptors
kir	*P. knowlesi* interspersed repeats
KLH	Keyhole Limpet Haemocyanin
L	Liter
LB	Luria-Bertani
LIC	Ligation Independent Cloning
LS	Late Schizont
LSR	benchtop flow cytometer

ls	Large-Scale
LT	Late Trophozoite
M	Molar
MACS	Magnetic- Associated Cell Sorting
MAHRP1	Membrane-Associated Histidine-Rich Protein-1
MC	Maurer's Clefts
MEGA	Molecular Evolutionary Genetics Analysis
μ	Micro
μl	Micro Litre
m	Milli
ME	Minimum Evolution (Phylogenetic analysis)
MES	2-(N-morpholino)ethanesulfonic acid (buffer)
MSP1	Merozoite Surface Protein 1
$MSP1_{19}$	Merozoite Surface Protein 1-19kDa fragment
MSP2	Merozoite Surface Protein 2
MWCO	Molecular Weight Cut-Off
n	Nano
Ni-NTA	nickel–nitrilotriacetic acid
NJ	Neighbour Joining (Phylogenetic analysis)
NK	Natural Killer (cell)
N-terminal	Amino (NH_2)-group terminal end
OD	Optimal Density
PAMPs	Pathogen Antigen Molecule Patterns
PBS	Phosphate-buffered saline
PCR	Polymerase Chain Reaction
PECAM1	Platelet/Endothelial Cell Adhesion Molecule-1 (CD31)
PEXEL	*Plasmodium* Export Element
Pf*60*	*Plasmodium falciparum* 60kDa merozoite proteins
PfEMP1	*Plasmodium falciparum* Erythrocyte Membrane Protein -1
PfEMP3	*Plasmodium falciparum* Erythrocyte Membrane Protein-3
PfMC2TM	*Plasmodium falciparum* Maurer's Cleft 2-transmembrane protein
PfSBP1	*Plasmodium falciparum* Skeletal-Binding Protein -1
PfSir2	*Plasmodium falciparum* Sir2 (histone deacetylase)
PHD	Profile fed network systems
p	Pico

pir	*Plasmodium* interspersed repeats
PNPP	p-Nitrophenylphosphate
PVM	Parasitophorous Vacuolar Membrane
*Py*235	*Plasmodium yoelii yoelii* 235kDa rhoptry protein
R	Reverse (primer)
R1/2	Region 1/2
RBC(s)	Red Blood Cell(s)
RBP	Reticulocyte Binding Proteins
RESA 1/2	Ring –associated Erythrocyte Surface Antigen 1/2
rif	Repetitive interspersed family (gene)
RIFIN	Repetitive interspersed family (protein)
RPMI-1640	Roswell Park Memorial Institute -1640 (Medium)
RNA	Ribonucleic acid
Rpm	Revolutions per minute
RT	Room Temperature
RT-PCR	Reverse Transcriptase-PCR
qRT-PCR	Quantitative Real-Time-PCR
ss	Small-Scale (≥1L)
SDS	Sodium dodecyl sulphate
SDS-PAGE	SDS-Polyacrylamide Gel Electrophoresis
SICA*var*	Schizont-Infected Cell Agglutination (assay)
SNPs	Single Nucleotide Polymorphisms
stevor	Sub-telomeric variable open reading frame (gene)
STEVOR	Sub-TElomeric Variable Open Reading frame (protein)
SURFIN	SURFace-associated family INterspersed genes
Taq	*Thermus aquaticus*
TAREs	Telomere-Associated Repetitive Elements
TBE	Tris-borate Electrophoresis
TLR	Toll-Like Receptor
TM	TransMembrane
TRITC	Tetramethylrhodamine isothiocyanate
TSP	ThromboSPondin
var	*P. falciparum* variant PfEMP1 encoding gene family
vir	*P. vivax* interspersed repeats (genes)

Abbreviations

V	Volt
VTS	Vacuolar Transport Signal
w/v	Weight over volume
X	Times

Chapter 1) Introduction

1.1. Malaria: perspective

The discoveries that malaria is caused by the blood-borne protozoan parasite, *Plasmodium falciparum*, and transmitted by mosquitoes were made more than a century ago by Laveran and Ross, respectively. Despite these early discoveries and the subsequent decades of research into many aspects of malaria, we still do not have an effective control strategy, and there is evidence that the burden of malaria continues to rise. Recently, Snow *et al* estimated that there are 300 million to 660 million cases of clinical *P. falciparum* malaria every year (see figure 1.1) (Snow *et al.*, 2005). This burden is spread across a predicted 40% of the world's population and over 90 countries.

Malaria is a devastating disease of unprecedented impact upon the lives and communities of the people it affects. Those at greatest risk are children below the age of 5, and pregnant women and their unborn babies. Almost all of these deaths are caused by *P. falciparum*, one of the four species of malaria parasites that infects humans (reviewed in (Snow *et al.*, 2005). Three other species naturally infect humans including *Plasmodium vivax*, *Plasmodium malariae*, and *Plasmodium ovale*. However, *P. falciparum* produces the most severe manifestations of the malarial disease, usually due to destruction of normal and infected red blood cells (iRBCs), the disruption of blood circulation during the asexual-stage development of the parasite, and an exaggerated immune response to the parasite and its products. Cerebral malaria, severe-anaemia, and respiratory acidosis are the main clinical syndromes of severe life-threatening malaria. Severe malaria is most common in children below 5 years, who suffer a spectrum of symptoms ranging from low birth-weight to death, arising from malaria infections during pregnancy and in the early years of life.

Sadly, the prospect of a malaria-free world continues to fade as the currently available control methods are ineffective and are complicated by a number of factors. Firstly, there

is the spread of insecticide-resistant mosquito populations, evolved through long-term usage of inadequate levels of insecticides, combined with the creation of new breeding sites for mosquitoes through road building, deforestation, mining, irrigation projects, and new agricultural practices. The increased numbers and habitat range of mosquito populations has lead to an increase in malaria transmission. Secondly, the rapid spread of parasites resistant to the first-line anti-malarial drugs is thought to be the primary reason for the dramatic increase in deaths from malaria in the last three decades (reviewed in (Greenwood & Mutabingwa, 2002; Phillips, 2001). The few effective drugs available are too expensive for many populations at risk, and development of new therapies is not a commercial priority for the major pharmaceutical companies of the world. Thirdly, despite the many initiatives to develop an effective anti-malaria vaccine, none have succeeded to date. This is largely attributed to the complexity of the malaria parasites, their life-cycle, interaction with the human host, and their sophisticated strategies for evading the host immune responses. Drug cure is therefore the mainstay for malaria control, although problems of resistance and cost render it at best a 'holding strategy'. This leaves malaria eradication as a distant memory of the 'roll back malaria' campaigns of the last century, and malaria control under the jurisdiction of only those governments with the money, resources, and long-term perspective required to attempt it.

Figure 1.1: Geographical distribution of malaria for the year 2002 (Snow *et al.*, 2005) P. falciparum *endemicity distribution within the global limits of risk. Endemicity classes: light green, areas in which the childhood infection prevalence is less than 10%; medium green, areas where infection prevalence is between 11% and 50%; dark green, areas with an infection prevalence of greater than 50%. Unclassified areas (yellow) represent 6% of total area at risk. All other areas are outside the transmission limits geographically or the population density is deemed below that required for transmission. Figure adapted from Snow* et al, *2005.*

1.2. Malaria: the parasite

1.2.1. Phylogeny

Malaria parasites are classified into the genus *Plasmodium*, family Plasmodiidae, phylum Apicomplexa (Levine, 1988). In a more recent classification system *Plasmodium* is included in one of six major clusters, Chromalveolata. This cluster groups the alveolata (including ciliates, the dinoflagellates, and the Apicomplexa) with cryptophytes, haptophytes, and stramenopiles (including brown algae, the diatoms, many zoosporic fungi, and opalinids, amongst others) (Adl *et al.*, 2005). This classification recognises the shared ancestry of *Plasmodium* with ancient photosynthetic organisms, accounting for the presence of the vestigial chloroplast known as the apicoplast/plastid.

The two most common human malaria species, *P. vivax* and *P. falciparum,* are thought to have diverged approximately 200,000 to 300,000 years ago, based on phylogenetic analysis of the cytochrome b protein from the mitochondrial genome (Escalante *et al.*, 1998). The authors concluded that the genus *Plasmodium* is polyphyletic, with *P. falciparum* and *P. reichenowi* forming a separate lineage to other primate malarial parasites, and sharing a common ancestor with avian parasites e.g. *P. gallinaceum* (see figure 1.2).

Figure 1.2: Phylogenetic relationship among the 17 Plasmodium species inferred from the gene encoding cytochrome b. The tree was estimated using the Neighbour-Joining (NJ) method. Bootstrap values are provided as percents over 1000 replications. The tree shows the location of the root ↑ as estimated by the DNAMLK algorithm from PHYLIP, which assumes a molecular clock. Figure taken from (Escalante et al., 1998).

Figure 1.3: Life-cycle of P. falciparum *(adapted from a drawing by J. Langhorne).*

The parasite undergoes sexual development, replication, and growth within the mosquito host, and asexual replication and growth within the human host. Green arrows indicate parasite protein exposure to human-host-immune elements.

1.2.2. Life-cycle of *P. falciparum*

The malaria parasite has a complex life-cycle involving both an invertebrate mosquito vector and a vertebrate host (figure 1.3). Infection of the human host with *P. falciparum* begins with injection of motile sporozoites into the sub-cutaneous tissue and occasionally directly into the bloodstream via the bite of a female *Anopheline* mosquito.

1.2.2.1. Invasion of hepatocytes

Once in the bloodstream, the sporozoites are rapidly transported to the liver, where they invade hepatocytes. Sporozoites pass through several hepatocytes before invasion is followed by parasite development and replication (Mota *et al.*, 2001). The asexual multiplication hepatoschizont-stage forms approximately 20,000—40,000 haploid liver-stage merozoites, over seven days. After release from the hepatocytes, the merozoites are capable of invading red blood cells (RBCs), in the next stage of the life-cycle.

1.2.2.2. Erythrocytic (asexual) cycle

The asexual blood or erythrocytic-stage begins with the released merozoites invading RBCs, in the case of *P.falciparum* both normocytes and reticulocytes. Each *P. falciparum* or *P. vivax* merozoite undergoes a process of growth and asexual multiplication to produce around 20 daughter merozoites per infected RBC over a period of 48 hours.

Parasite growth within the iRBC progresses through a series of distinct stages, the first of which is the ring-stage at which the parasite begins to metabolise haemoglobin. As the ring-stage parasite grows, it exports its own proteins beyond the confines of the parasite, and the parasitophorous vacuole in which it develops, and into the cytosol and the surface plasma membrane of the iRBC. The parasite continues to grow forming the trophozoite-stage with its characteristic haemozoin pigment. Transcription of *var* starts as early as 9 hours into the cycle with *Plasmodium falciparum* erythrocyte membrane protein 1 (PfEMP1) reaching the iRBC surface at 16-20 hours post-invasion (Kriek *et al.*, 2003).

PfEMP1 contains specific endothelial cell-binding domains, which enable the parasites to withdraw from normal blood circulation in order to avoid splenic clearance. Once sequestered, development into the fully mature schizont form occurs, where nuclear divisions result in a species-dependent number of daughter merozoites. Identification of the different human malaria species is also facilitated by the absence of mature forms of *P. falciparum* in peripheral blood. The iRBC then bursts, dispersing the merozoites, which are then competent to reinvade new RBCs.

1.2.2.3. Invasion of RBCs

The blood-stage merozoite on contact with a RBC re-orientates so that the apical end can make a close contact with the RBC surface (see figure 1.4). The apical tip contains the apical complex which consists of three sets of secretory structures: 1) the micronemes, which contain adhesins and molecules linking host cell-surface to the underlying motor complex; 2) the rhoptries, containing lipids and proteins, contributing to parasite vacuole formation, and also similar to micronemal proteins contributing to RBC surface binding, *e.g.* RhopH complex; and 3) the dense granules, containing proteins of the parasitophorous vacuole membrane (PVM) that enable traffic between the parasite, within the parasitophorous vacuole, and host cell (reviewed in *(Kats et al., 2006)*).

Figure 1.4: Three-dimensional organisation of a P. falciparum *merozoite, with the pellicle partly cut away to show the internal structure (image taken from L. Bannister* et al *(Bannister & Mitchell, 2003)). The apical complex organelles are shown including the micronemes, rhoptries, and dense granules. The surface location of* $MSP1_{19}$ *is indicated as merozoite coat.*

Proteins, such as merozoite surface protein 1 (MSP1) and apical membrane antigen 1 (AMA1), are released from these organelle structures. $MSP1_{19}$ coats the merozoite surface, whilst AMA1 is released from the micronemes and is involved in the apical end reorientation (Bannister *et al.*, 2003). It has been suggested that the location of these important receptor-engaging molecules within organelles may protect the parasite from antibody-mediated neutralisation, as the ordered release from apical organelles after contact with the RBC may limit their exposure to antibody (Miller *et al.*, 2002).

The parasite vacuole is formed primarily of host-cell plasma membrane, but sorting of host membrane proteins occurs such that most transmembrane proteins are excluded but detergent-resistant membranes remain (*i.e.*, Duffy receptor, GPI-anchored proteins, including parasite-derived proteins such as exported protein 1(EXP1)) (Lauer *et al.*, 2000).

This period of exponential asexual parasite growth and replication is responsible for all the symptoms of malaria and continues until the parasite is controlled (through drug intervention, the host's innate and adaptive immune responses, unavailability of fresh RBCs, or death of the overwhelmed host). The synchronous nature of the parasite's development and simultaneous rupture of the iRBCs, releasing large amounts of parasite material, is thought to result in induction of the host's cytokine response and induction of cyclical fevers (every 48 hours for *P. falciparum*).

1.2.2.4. Sexual cycle

The parasite's sexual development begins during the blood-stage with differentiation of male (micro-) and female (macro-) gametocytes from a small proportion of infecting merozoites; these are subsequently taken up in the mosquito's blood meal. Environmental triggers such as the temperature drop within the invertebrate host, and specific chemicals such as xanthurenic acid (Billker *et al.*, 1998), trigger the exflagellation of male gametes

giving rise to 8 micro-gametocytes, each containing a haploid nucleus, which fuse with the female haploid nucleus to form a zygote (diploid)-stage in the mosquito mid-gut. The zygote is then able to invade the gut-wall epithelium, where it develops into an oocyst between the epithelium and basal-membrane. Large numbers of sporozoites are formed, which then mature during their migration to the mosquito salivary glands. The mature sporozoites are then ideally placed for injecting into a new host when the mosquito takes its next blood meal, thus completing the cycle.

1.3. Malaria – the disease

Humans living within malaria endemic areas (see figure 1.1) will be intermittently re-infected with *P. falciparum*. The course and outcome of the resultant disease will depend upon the age, genetics, and infection history of the patient. No disease symptoms are experienced during the initial (approximately 7 days) liver-stage infection, whereas a variety of clinical symptoms occur during the asexual blood-stages, ranging from mild, asymptomatic parasitaemia in immune adults, to acute disease with clinical symptoms including 48-hour cyclical fevers, muscle-aches, and head-aches to life-threatening severe malarial anaemia, metabolic acidosis, and coma that occurs in young children and non-immune adults. In addition to young children and non-immune adults, pregnant women are at increased risk from *P. falciparum* infection, where malaria infection of the placenta is associated with inter-uterine growth retardation and premature delivery leading to neonatal mortality (Steketee *et al.*, 2001), maternal anaemia (reviewed by (Menendez *et al.*, 2000)), and higher mortality for the primigravidae ((Brabin, 1983), reviewed by (Shulman & Dorman, 2003)).

The degree of clinical symptoms suffered is mainly dependent on the level of immunity acquired through previous infections. Older children and adults thus often suffer from asymptomatic or mild malaria, whereas young children suffer from severe malaria, the

syndromes of which include cerebral malaria, severe anaemia, and respiratory distress (Marsh *et al.*, 1995). Severe malaria is now understood to be a multi-system disorder similar to sepsis syndromes and affecting multiple organs of the body (reviewed by (Mackintosh *et al.*, 2004)). The strongest indicator of death in severe malaria is metabolic acidosis, which leads to the clinical symptoms of respiratory distress (English *et al.*, 1995; Marsh *et al.*, 1995; Taylor *et al.*, 1993). Cerebral malaria is characterised by impaired consciousness, confusion, or un-arousable coma; the mortality levels resulting from this syndrome vary (Kwiatkowski *et al.*, 1993; Marsh *et al.*, 1995; Molyneux, 1989; White *et al.*, 1985) but are associated with the depth of the coma (Marsh *et al.*, 1995; Molyneux, 1989; Taylor *et al.*, 1988). Many studies have searched for specific linkage of parasite molecules with typical disease patterns.

In addition, malaria is in part an immune-mediated disease. The initial systemic pro-inflammatory cytokine response leads to fever, nausea, headaches, and other clinical symptoms; therefore inflammatory mediators are also implicated in the pathogenesis of severe malaria.

1.3.1. The relationship between age and disease

Immunity to infection by *P. falciparum* is probably never complete: even adults who remain in areas of high-transmission throughout their lives may be parasitised (Trape & Rogier, 1996). This is in contrast with other, mainly viral, pathogens where a single infection or immunisation can result in long-lived sterile immunity.

Babies below the age of 6 months are protected from infection by a number of factors: maternal malaria-specific protective antibodies acquired initially through the placenta and later transmitted through breast milk (Kassim *et al.*, 2000), foetal haemoglobin, and reduced contact with infective mosquitoes (Hogh *et al.*, 1995; Sehgal *et al.*, 1989; Snow *et al.*, 1998).

However, disease prevalence then rises to a peak in young children, before resistance to severe life-threatening infections develops. In areas where malaria is endemic, resistance to the severest forms of *P. falciparum* is nearly complete by the age of 5 years. In areas of most intense transmission, risk from severe malaria is greatest between the ages of 1 and 2 years (Snow *et al.*, 1997). In contrast, clinical immunity to mild malaria is acquired slowly, and is not usually effective until early adolescence.

In areas of low transmission, resistance to severe (non-cerebral) malaria requires a greater number of infections before becoming protective, thus immunity is acquired over a broader age range, and the peak prevalence occurs later in childhood (Reyburn *et al.*, 2005; Snow *et al.*, 1997; Snow & Marsh, 2002). Thus the prevalence of severe malaria, mild malaria, and parasite prevalence give characteristic age-dependent curves (figure 1.5).

Cerebral malaria exhibits a different age-related profile to that of the other manifestations of severe malaria disease. Incidence of cerebral malaria peaks at a later age than for other main severe syndromes such as severe anaemia. The incidence of cerebral malaria peaks at a mean age of 45 months in the Gambia (Brewster *et al.*, 1990), and 40 months in coastal Kenya (Marsh & Snow, 1997).

In summary, this suggests that in regions of high transmission, immunity to severe disease is acquired earlier than in low-transmission regions. Cerebral malaria is therefore less common, and severe anaemia becomes a more important factor in severe life-threatening malaria.

Figure 1.5: The theoretical relationship between parasitaemia, mild, and severe (non-cerebral) malaria with age in endemic areas. The age-pattern of asymptomatic parasite prevalence and the period prevalence of both mild and severe clinical malaria are shown in relation to maximum prevalences recorded. Based upon a figure from Marsh and Kinyanjui (Marsh & Kinyanjui, 2006), which uses Kilifi population indices of immunity to malaria data.

1.4. Immunology of malaria

The observation that a semi-immune status to severe life-threatening malaria is induced during childhood in endemic areas suggests iRBC surface antigens are present to which naturally acquired immunity to malaria is induced and effective, so that by adulthood malarial disease is reduced to mild and often asymptomatic parasitaemia. However, the continuation of mild malaria infections into adulthood suggests this immunity is not sterile, possibly due to the presence of polymorphic immune targets. Indeed, it has been suggested that it is the additive effects of the gradual acquisition of immunity to these polymorphic targets that results in a repertoire of antibodies against the local parasite population. The age of acquisition of these antibodies inversely correlates with the transmission rates (Bull *et al.*, 1998). Thus given an infinite number of polymorphic variants of immune targets, only a semi-immune status can ever be achieved.

In order to make effective use of information on these important immune targets, we need to know what they are, how they may vary, and their mechanism(s) of protection. To make a study of immune processes during malarial disease, it is necessary to make use of non-human malaria models, and to utilise prospective studies of human malaria infections from early last century. In addition, assessments of genetically inheritable traits that correlate with protection are important indicators of these mechanisms, and will be discussed first here.

1.4.1. Genetic resistance to malaria

P. falciparum has evoked huge selective pressure upon human populations for thousands of years. It is estimated that the divergence of the human *P. falciparum* parasite from *P. reichenowi* or a *P. reichenowi*-like parasite occurred between 4 and 4.75 million years ago, a time-frame consistent with the divergence of *Homo* and *Pan*, which is estimated between 4 and 5 million years ago (Horai *et al.*, 1995). Therefore this highly virulent

parasite has been exerting a positive selective force for various protective genetic traits by causing mortality in pre-reproductive age groups.

Two basic forms of genetically inheritable protection exist (table 1.1): firstly, those that affect the RBC's ability to provide the parasite with a suitable 'home' (for instance, polymorphisms in genes encoding haemoglobins, specific RBC enzymes, or RBC proteins), and, secondly, those genetic traits which result in improved efficiency of the immune system for specifically targeting this intra-cellular obligate pathogen. This requires polymorphisms in the many immune-response genes.

Table 1.1) Genetic traits that affect immunity to malaria

Components	Trait	Gene/ Allele	Effect/mechanism
Factors affecting RBCs			
Thalassaemias	α-thalassaemia		Protection is limited to the anaemic form of malarial disease (Wambua *et al.*, 2006) Reduced CR1 expression therefore protective through reduced rosetting (Cockburn *et al.*, 2004)
	β-thalassaemia		Partially due to early removal of iRBC through an innate mechanism (Ayi *et al.*, 2004)
Haemoglobinopathies	Haemoglobin S (sickle cell disease)	HbS	Partially due to early removal of iRBC through an innate mechanism (Ayi *et al.*, 2004) but the protective effect increases with age (Williams *et al.*, 2005), and may be also due to an accelerated acquisition of immunity to PfEMP1 (Cabrera *et al.*, 2005)
	Haemoglobin C	HbC	(Mockenhaupt *et al.*, 2004; Modiano *et al.*, 2001) Possible inhibition of parasite growth (Fairhurst *et al.*, 2003; Friedman *et al.*, 1979; Pasvol *et al.*, 1982; Rihet *et al.*, 2004) May also protect through failure of HbC cells to display PfEMP1 on iRBC surface
	Haemoglobin E	HbE	Prevalence and severity of complications reduced in adult carriers with malaria, admitted to hospital in Thailand (Hutagalung *et al.*, 1999)
Cells surface molecules	CR1 (CD35)	CR1	S1 (a-) RBCs are unable to form rosettes with *P. falciparum* iRBCs (a virulence factor in *P. falciparum* malaria) (Chen *et al.*, 1998; Rowe *et al.*, 1997)
	Duffy blood-group negativity		Duffy blood-group negativity is completely protective against disease caused by the *P. vivax* parasite (Arevalo-Herrera *et al.*, 2005)
	Gerbich-negative blood group	*GYPCΔex3*	Confers protection against parasite invasion via *P. falciparum* merozoite erythrocyte-binding antigen 140 (EBA-140) and glycophorin C (Maier *et al.*, 2003; Thompson *et al.*, 2001)
	Ovalocytosis (Southeast Asian)	*SLC4A1Δ27*	Deletion in gene encoding RBC membrane protein band 3 is protective against cerebral malaria (Allen *et al.*, 1999; Genton *et al.*, 1995) Possible protection against subset of parasites causing severe disease, or enhanced CD36 binding reducing cerebral cytoadhesion (Cortes *et al.*, 2005; Newbold *et al.*, 1997; Turner *et al.*, 1994)

Factors affecting immunity			
Cells surface molecules	HLA	HLA-Bw53	Associated with reduced risk of severe malaria (Hill *et al.*, 1991)
	IFN-γ receptor	IFNGR1-56	Heterozygous individuals protected from cerebral malaria (Koch *et al.*, 2002)
	IFN-α receptor	IFNAR1	17470-G/G and L168V-G/G genotypes associated with protection from cerebral malaria (Aucan *et al.*, 2003)
	CD36 (scavenger receptor)	CD36	Promoter polymorphisms associated with protection from cerebral mal mutations leading to reduced expression associated with increased ri of severe malaria; nonsense mutation associated with protection fro severe malaria (Aitman *et al.*, 2000; Omi *et al.*, 2003; Pain *et al.*, 200
	CD40L	CD40L 726C	X-linked; marked reduction in risk for severe malaria in homozygous males (Sabeti *et al.*, 2002)
	KIR	KIR3DL2	Association with malaria specific IFN-γ production by NK cells (Artavanis-Tsakonas *et al.*, 2003)
	CD31	CD31/PECAM	The frequency of the 125 V/V 563 N/N genotype was significantly high in cerebral malaria patients as compared with severe cases without cerebral malaria (Kikuchi *et al.*, 2001)
Cytokines	TNF	TNF2	Promoter polymorphism that affects OCT1 binding increases susceptibility to cerebral malaria (Knight *et al.*, 1999; McGuire *et al.*, 1994)
	IL-4	IL-4-524T	Increased malaria-specific antibody levels (Luoni *et al.*, 2001)
	IL-12p70	IL-12B	Promoter polymorphism leading to decreased IL-12 production associated with increased mortality in Tanzanian but not Kenyan children (Morahan *et al.*, 2002)
Serum factors	Mannose-binding lectin deficiency	MBL	Low serum Mannose-binding lectin levels associated with increased risk of severe malaria (Luty *et al.*, 1998)
Enzymes	Inducible nitric oxide synthase	NOS2 (iNO)	NOS2A-1659T associated with increased susceptibility to cerebral malaria.
			NOS2A-954C and NOS2A-1173T associated with protection from clinical malaria and severe anaemia, respectively (Burgner *et al.*, 2003; Hobbs *et al.*, 2002; Kun *et al.*, 2001)
	Glucose-6-phosphate dehydrogenase deficiency	G6PD	Protective mechanism may work through early phagocytosis of iRBC (at early ring-stage). Due to IgG and complement deposition possibly due to accelerated oxidative membrane damage as a result of impaired anti-oxidant defence in G6PD deficient cells (Cappadoro *et al.*, 1998)
	Pyruvate kinase	Pklr	Protects mice against *P. chabaudi chabaudi* infection (Min-Oo *et al.*, 2003)

This table was modified from (Stevenson & Urban, 2006; Williams, 2006).

1.4.2. Innate immune responses control acute asexual blood-stage parasitaemia

In the absence of an immune response, exponential growth of the parasite during the erythrocytic-stage would continue until all available RBCs were infected, and death follows as an inevitable consequence. However, this initial acute phase is controlled to a greater or lesser extent, depending on genetic traits, by innate immunity. Innate immune responses are normally sufficient to reduce the initial peak parasitaemia preventing death of the host, but are not sufficient for clearance of the parasite and hence a chronic infection follows. This works in the parasite's favour, as the chronic stage of infection allows a prolonged period in which transmission to the mosquito vector can occur.

Innate responses are also key in the initiation and direction of the subsequent acquired immune response, and the malaria parasite (and other protozoa) have developed multiple strategies for subverting the innate defences of the host and redirecting the development of the acquired response (reviewed in (Sacks & Sher, 2002)).

1.4.3. Rodent immune responses to malaria infection

Rodent *Plasmodium* infections are used to model human *Plasmodium* infections, and although there are differences between human and mouse immune systems, different aspects of human malaria have been replicated, dependent upon the genetic strain of the rodent host and the infecting *Plasmodium* species. In particular, the immune response to blood-stage parasites has been extensively studied using *P. chabaudi chabaudi* AS, with either C57BL/6 or BALB/c mice. Here the immune response is divided into two stages, the first of which being the acute phase with the first wave of parasitaemia, which is controlled, in resistant mice strains, by antibody-independent (innate) mechanisms. This first peak of parasitaemia is followed by the chronic infection stage, which requires $CD4^+$ T cells and antibody-mediated (adaptive) mechanisms for complete clearance of the parasite.

1.4.3.1. Innate immune responses

The innate immune system is crucial in malaria immunity. For instance, in the absence of natural killer (NK) cells, *P. c. chabaudi* AS infections show a higher peak parasitaemia during the acute phase than in wild type mice (Mohan *et al.*, 1997). In addition, the early production of interferon-γ (IFNγ) from NK and also possibly γδ T cells is essential to avoid a lethal infection in mice infected with various *Plasmodium* species (De Souza *et al.*, 1997; Mohan *et al.*, 1997).

The innate immune system is linked with the adaptive system through the stimulation of toll-like receptors (TLR) on antigen-presenting cells (APCs) by pathogen antigen molecule patterns (PAMPs). TLRs are expressed on the surface or endosomes of NK cells, macrophages, and dendritic cells (DCs). APCs are then induced to produce cytokines, and, in the case of DCs, present antigen to T-cells. Upon infection of naïve mice, APCs produce IL-12 thus initiating the adaptive immune response. IL-12 is an essential cytokine mediating effects through IFNγ and tumour necrosis factor (TNF), leading to induction of IFNγ, and T_H1 cell differentiation, and thus is essential for the development of acquired cell-mediated and antibody-mediated immunity to intracellular parasites.

1.4.3.2. Acquired immune responses

As briefly mentioned above, the control and clearance of a chronic malaria infection requires protective $CD4^+$ T-cell-dependent mechanisms. Evidence from *P. c. chabaudi* AS infections indicates mice lacking or depleted of $CD4^+$ T-cells during the acute phase of an infection are not able to control and clear the parasite (Langhorne *et al.*, 1990; Suss *et al.*, 1988). In contrast, depletion of CD8+ or δγ T-cells before infection only leads to a slight parasitaemia increase and delay in parasite clearance (Seixas *et al.*, 2002). The early pro-inflammatory response leads to induction of IgG2a, IgG2b, and IgG3 sub-

classes of antibodies in mice (reviewed in (Okamura *et al.*, 1998; Purkerson & Isakson, 1992)), and it is the antibody response that is responsible for final clearance of the parasite.

Despite such overwhelming and/or longstanding evidence that antibody is protective we still do not know the mechanism of protection. Several mechanisms have been proposed and partially demonstrated:

1) Antibody-mediated phagocytosis by macrophages (Shear *et al.*, 1979), although FcγRII receptor-deficient and wild type mice are equally capable of resolving a *P. yoelii yoelii* or *P. c. chabaudi* infection (Langhorne *et al.*, 2002; Rotman *et al.*, 1998).

2) Complement-dependent antibody-mediated cytolysis of *Plasmodium* -infected mouse erythrocytes and merozoites (Gabriel & Berzins, 1983; Krettli *et al.*, 1976).

3) Opsonising and neutralising antibodies inhibiting iRBC sequestration (Pleass & Holder, 2005).

4) Invasion-inhibiting antibodies through neutralisation of merozoites or inhibition of merozoite surface protein-1 (MSP-1) processing (Blackman *et al.*, 1994; Guevara Patino *et al.*, 1997).

All four mechanisms probably participate in the antibody-mediated parasite clearance to a variable degree, dependent on the *Plasmodium* spp. and the infected host.

1.4.4. Human immune responses to malaria infection

Data from the rodent models is complemented by data obtained in humans through retrospective analyses of data collected by the U.S. Public Health Service between 1940 and 1963, when malaria-induced fevers were used to treat neurosyphilis. The treatment course with a primary *P. falciparum*, *P. ovale*, *P. malariae*, *P. vivax* infection and with/or without a secondary infection was followed in patients, and suppressive, but non-curative anti-malarial treatments were given where necessary.

1.4.4.1. Innate immune responses

Analysis of the clinical records of repeated infections in non-immune neurosyphilis patients that were treated with malaria induced fevers showed that the density of parasitaemia at which parasite growth was controlled was highly predictable in an individual, and independent of the *Plasmodium* strain or species. The authors concluded that this data is best explained by the induction of innate immune mechanisms (Molineaux *et al.*, 2002). Thus parasite growth can be modulated very early in the course of infection. The initiation of innate immune responses is crucial for the subsequent triggering of the adaptive responses, and pro-inflammatory cytokines including IFN, 1L-12p70, and IL-18 (normally made by innate cells) were increased in the serum at the first appearance of iRBCs in the blood of malaria naïve individuals experimentally infected with *P. falciparum* (Hermsen *et al.*, 2003).

1.4.4.2. Acquired immune responses

Immunity to malaria is both stage- and species-specific: re-infection is the norm, and sterile immunity does not occur, unlike with viral pathogens. Clinically protective immune responses require repeated exposures to infection over an individual's lifetime (see also section 1.3.1).

Evidence that humans develop naturally acquired immunity is derived from retrospective examination of patient data, where, on re-inoculation with either a homologous or heterologous strain, humans were susceptible but experienced fewer high-intensity fever episodes and lower asexual and gametocyte parasite counts. This suggests the development of acquired immunity within a single infection (Collins & Jeffery, 1999a; Molineaux *et al.*, 2002). Interestingly, only a primary infection of *P. malariae*, but not *P. ovale* or *P. vivax*, was shown to protect against a secondary *P. falciparum* infection (Collins & Jeffery, 1999b). It was suggested that *P. malariae* shares common antigens that are able to induce protective immunity. However, this may also be a reflection of the

greater role that the acquired immune response plays in the control of *P. malariae* infection, which has a slower development and later peak parasitaemia than *P. ovale* or *P. vivax*.

A crucial point is that although antibodies can be strain-specific, at some level it is possible to use antigens from one strain to induce immunity to heterologous strains, and therefore an anti-malaria vaccine is theoretically possible. The main target of antibodies has emerged as the parasite-encoded variant-surface antigens (VSA) found on the surface of the iRBC.

The protective effect of anti-malaria antibodies was first demonstrated in the 1960s. γ-Globulin transferred from immune adults into non-immune children with severe clinical malaria in the Gambia brought about a reduction in parasitaemia and alleviation of disease symptoms (Cohen *et al.*, 1961). Subsequent studies showed that this antibody immunity was strain-transcending, protecting children exposed to malaria parasites from different geographical locations (McGregor *et al.*, 1966; Sabchareon *et al.*, 1991). However, the persistence of parasite and length of time it takes to acquire protective immunity against mild malaria indicates that the parasite's clonal VSA may prevent the development of a fully protective antibody response.

A study by Marsh and Howard in 1986 showed that sera obtained from 10 Gambian children during the acute phase of infection were unable to agglutinate iRBCs from the corresponding infection, but that convalescent sera, obtained 3—4 weeks later, contained antibodies recognising those same parasites but not recognising heterologous parasites (Marsh & Howard, 1986). In contrast, sera from adults living in the same area were able to agglutinate all or the majority of the 10 parasite isolates. Thus as people get older they accumulate a repertoire of strain-specific antibodies that recognise VSA on the surface of iRBCs. Subsequently, more extensive studies have evaluated these targets of the antibody response and identified the highly polymorphic VSA PfEMP1 as key targets.

Convalescent sera from children infected by *P. falciparum* agglutinate homologous parasites, but frequently do not show reactivity to heterologous parasites (Bull *et al.*, 1998). Thus only those parasites expressing VSA corresponding with a gap in the host's antibody repertoire are able to maintain infection.

1.5. Molecular aspects of malaria disease

1.5.1. Parasite immune targets in the human host

As indicated by the green arrows in the life-cycle (figure 1.3), there are several points during the parasite's life-cycle at which it may be vulnerable to immune antibody attack. Multigene families, an immune evasive mechanism, encode many of the exposed parasite proteins on the iRBC and merozoite surfaces. In the case of the iRBC-stage, PfEMP1 (which is one of the important immune targets on the iRBC surface) can undergo clonal antigenic variation (reviewed by (Kyes *et al.*, 2001). Clonal antigenic variation of PfEMP1 is crucial to the parasite as a means of prolonging chronic infection, and evading the host antibody response. A brief discussion of the pre-erythrocytic-stage immune-targets will be followed by discussion of the merozoite and iRBC surface as targets of immunity.

1.5.1.1. Sporozoites and pre-erythrocytic-stages as a target for immunity

Briefly, immunity may be directed at the sporozoite from the point it is injected into the skin and its migration through the blood to intra-hepatocytic schizont development. There is a very short window in which antibodies may potentially protect against the sporozoite, either by opsonisation of the sporozoite or prevention of hepatocyte invasion. Anti-sporozoite and liver-stage targets include the immunodominant circumsporozoite protein (CSP), liver-stage antigen-1 (LSA1), and thrombospondin-related adhesive protein (TRAP), among others (Calle *et al.*, 1992; Esposito *et al.*, 1988; John *et al.*, 2003; Kumar

et al., 2006). Interestingly, the best induction of protective immunity is through immunisation with attenuated sporozoites (Nardin *et al.*, 1999). However this is in contrast to naturally induced anti-sporozoite immunity, which does not immediately induce sterile protection.

1.5.1.2. Merozoites as a target for immunity

Invasion of RBCs is a key moment in the parasite's life-cycle, requiring a complex cascade of events, starting with initial attachment, re-orientation, and invasion of the RBC (described in section 1.2.2.3). Proteins necessary for all these processes are exposed on the merozoite surface or secreted onto the merozoite's surface upon contact with the RBC. However, the timing between merozoite release and re-invasion is short, and therefore antibodies are the main source of protective immunity against merozoites. Antibodies may protect through blocking invasion by opsonisation, inducing complement-mediated damage, preventing processing of merozoite invasion proteins, or blocking RBC-binding interactions.

A monoclonal antibody-screen of *P. falciparum* parasites isolated from different geographical locations has provided evidence for considerable antigenic diversity, and most of the strain-specific determinants were shown to be associated with merozoite surface proteins (McBride *et al.*, 1982). Therefore fine specificity of the antibody, in addition to the antigen in question, is relevant in determining whether antibodies correlate with protection from malaria (reviewed by (Jennings *et al.*, 2006; Marsh & Kinyanjui, 2006)).

Merozoite proteins vary using two basic mechanisms: 1) they may exist as different allelic forms of the same gene whereby a parasite has one copy of a gene which varies from parasite to parasite, resulting in polymorphic proteins found in different parasite clones (for example, MSP-1), (Anders *et al.*, 1993); or 2) merozoite proteins may be the

products of multigene families, such as the two classes of ligand-binding invasion proteins found in the merozoite apical organelles. These are the family of reticulocyte binding protein homologues (RBPs) and the family of erythrocyte binding proteins/ligands (EBLs). The RBP superfamily includes, the *P. yoelii* 235kDa rhoptry proteins (Py235) (Holder & Freeman, 1981). *P. vivax* reticulocyte binding proteins (PvRBP 1 and 2) (Galinski *et al.*, 1992), and the *P. falciparum* rhoptry protein homologues (PfRH1, PfRH2a, PfRH2b, PfRH3, PfRH4 and PfRH5) (Cowman & Crabb, 2006; Kaneko *et al.*, 2002; Rayner *et al.*, 2000; Rayner *et al.*, 2001; Stubbs *et al.*, 2005; Taylor *et al.*, 2001; Triglia *et al.*, 2001a; Triglia *et al.*, 2005; Tsuboi *et al.*, 1994). EBL homologues include the Duffy Binding Protein (DBP) of *P. vivax* and *P. knowlesi*, the *P. falciparum* EBA175, BAEBL (EBA140), EBL-1, JESEBL (EBA181) and PEBL (EBA165) (Camus & Hadley, 1985; Lobo *et al.*, 2003; Peterson & Wellems, 2000; Triglia *et al.*, 2001b). Therefore merozoites have the potential to vary antigenically in order to evade antibody opsonisation and other cellular immune mechanisms.

1.5.1.3. The surface of the iRBC as a target for immunity

As the parasite grows and matures within the iRBC, it inserts parasite-derived proteins, or alters host-cell proteins, which are then exposed on the iRBC plasma membrane. The iRBC surface proteins are here referred to as VSA and are, in the majority, the product of multigene families. There are three main multigene families in *P. falciparum*; one of these is the prime target of anti-VSA antibodies, PfEMP1. However, the products of the other two extensive multigene families, *rif* and *stevor*, may also be expressed on the iRBC surface. A fourth, much smaller, family encoding SURFINs is co-transported with PfEMP1 and RIFINs to the iRBC surface (Winter *et al.*, 2005). In addition, a number of hypothetical proteins may also be expressed on the iRBC surface. The multigene families of *P. falciparum* are described later (see section 1.6).

1.5.2. Identification of parasite proteins and novel immune targets

1.5.2.1. Genome projects

Significant progress in the field of comparative genomics has been made in recent years. This is due to the extensive sequencing and availability of several human and other malarial parasite genomes (www.sanger.ac.uk/Projects/Protozoa/). These include the *P. falciparum* 3D7 whole genome, 1x coverage of a second laboratory clone *P. falciparum* IT, and, most interestingly, substantial coverage (8x) of a Ghanaian field isolate parasite clone. The *P. falciparum* 23-megabase nuclear genome consists of 14 chromosomes, encodes about 5,300 genes, and is the most (A + T)-rich genome sequenced to date (Gardner *et al.*, 2002).

Sequencing of several rodent malaria genomes (including *Plasmodium berghei, Plasmodium chabaudi, Plasmodium yoelii*) has allowed the identification of approximately 4500 orthologues shared between the rodent malarias and *P. falciparum* (Kooij *et al.*, 2005). Conversely, 575 *P. falciparum*-specific genes and gene families were identified in the sub-telomeric regions, plus 168 other *P. falciparum*-specific genes, located at the boundaries of conserved (syntenic) regions (Kooij *et al.*, 2005). Clustering of *P. falciparum* sub-telomeric genes revealed that nearly 50% of these genes belong in just 12 distinct gene families, including the *var*, *rif*, and *stevor* families, plus families with various or unknown functions Pf-*fam-a* through Pf-*fam-i* (Carlton *et al.*, 2005). However the majority of these *P. falciparum*-specific genes were predicted to play a role in host-parasite interactions such as invasion, adhesion, and antigenic variation (Carlton & Carucci, 2002). Therefore comparative genomics has facilitated the identification of hypothetical and other parasite proteins that are potential therapeutic targets.

1.6. Clonal antigenic variation and multigene families

Clonal antigenic variation is a mechanism employed by extra-cellular pathogens such as African trypanosomes to escape immune clearance, but is also used by the intracellular malaria parasite. In the case of malaria parasites, multigene families are generated by gene recombination during transmission through the mosquito vector. In turn, the variation with time of multigene-encoded antigens allows the parasite to replicate in an infected human host, utilising antigenic variation as a means of immune evasion. The resultant chronic infection then enables the parasite to increase its potential for mosquito transmission and further gene recombination.

Another mechanism for the generation of multigene families is gene duplication. This ensures retention of the gene's original function, whilst allowing the potential for new functions. Recombination and duplications in sub-telomeric chromosomal regions are important in the generation and diversity of large multigene families in *P. falciparum*. Pseudogenes, with the potential for chromosome crossover events, may provide an additional store of diversity to be accessed through telomeric recombination.

1.6.1. Location of multigene families in chromosome ends

A clone of *P. falciparum*, 3D7 has been completely sequenced (Gardner *et al.*, 2002). This has revealed a number of multigene families, the vast majority of which are located in sub-telomeric regions of the parasite's 14 chromosomes. These include the *var*, *rifin*, *stevor*, Pf*60*, and *P. falciparum Maurer's cleft 2 transmembrane (PfMC-2TM)* multicopy families (Baruch *et al.*, 1995; Carcy *et al.*, 1994; Cheng *et al.*, 1998; Sam-Yellowe *et al.*, 2004; Smith *et al.*, 1995; Su *et al.*, 1995). There are also several hundreds of hypothetical proteins within the sub-telomeric regions as yet not identified as belonging to particular gene families (Gardner *et al.*, 2002).

Location in the sub-telomeric regions is significant as there is conservation of gene order in these regions (Bowman *et al.*, 1999; Gardner *et al.*, 2002; Lavazec *et al.*, 2006). Multigene family genes are located sub-telomerically after 20—40kb of non-coding sequences, consisting of a mosaic of telomere-associated repetitive elements (TAREs1-6) (figure 1.6) (de Bruin *et al.*, 1994; Delves *et al.*, 1989; Gardner, 1999). TAREs are implicated in the formation of chromosome clusters in the nuclear periphery and hence gene-transcriptional regulation. It has been shown recently that transcription of specific *var* genes is dependent on the separation of a chromosome end away from its cluster, a change in chromosome structure and telomere-associated proteins (PfSir2) (Duraisingh *et al.*, 2005; Freitas-Junior *et al.*, 2005; Ralph *et al.*, 2005). This is, however, a highly localised change, as other genes located close-by on the same chromosome do not necessarily become actively transcribed at the same time.

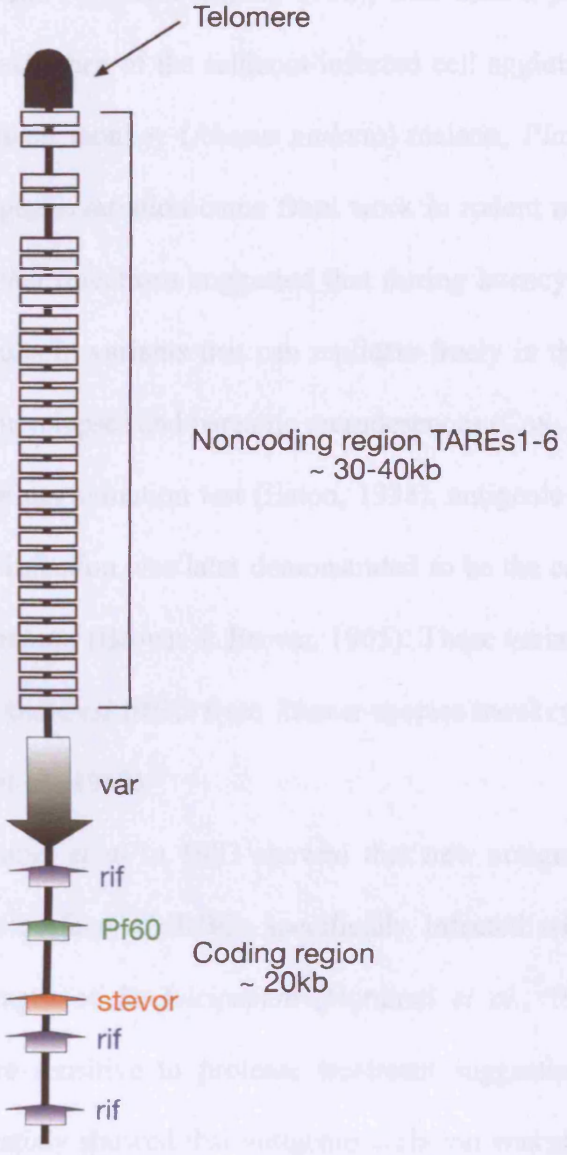

Figure 1.6: Detailed structure of P. falciparum *chromosome ends*

Showing typical ordering of multigene family genes in the sub-telomeric coding regions.

1.6.2. Antigenic variation and the discovery of parasite-derived proteins on the surface of the *P. falciparum* iRBC

The first evidence for parasite-derived proteins in schizonts as targets of acquired immunity was found by Eaton (Eaton, 1938), who used a parasite agglutination test to demonstrate the existence of the schizont-infected cell agglutination (SICA)-var proteins in the highly virulent monkey (*Rhesus mulatta*) malaria, *Plasmodium knowlesi*. Indirect evidence for antigenic variation came from work in rodent malarias. A study of relapse *Plasmodium berghei* infections suggested that during latency parasites undergo biologic variation that results in variants that can replicate freely in the previously immune host-mouse, resulting in relapses and parasitic recrudesences (Cox, 1958).

Using the parasite agglutination test (Eaton, 1938), antigenic variation of proteins at the schizont-stage of infection was later demonstrated to be the cause of chronic *P. knowlesi* infections in *R. mulatta* (Brown & Brown, 1965). These variant antigens were present on the surface of *P. knowlesi* iRBC from *Rhesus*-species monkeys, as detected by the SICA assay (Barnwell *et al.*, 1982).

A study by Hommel *et al* in 1983 showed that new antigenic determinants were also detectable on the surface of iRBCs specifically infected with the trophozoite/schizont developmental stages of *P. falciparum* (Hommel *et al.*, 1983). These new antigenic determinants were sensitive to protease treatment suggesting that they were proteins. Importantly, this study showed that antigenic variation was also possible not only across strains but within a cloned population, and immune pressure, in the form of passive transfer of immune serum, could also induce antigenic variation in *P. falciparum* (Hommel *et al.*, 1983).

These strain-specific surface antigens were metabolically labelled with radioactive amino acids, indicating that they were of parasite origin rather than altered host components (Leech *et al.*, 1984). Importantly, the parasite iRBC surface proteins, present in knob-like

structures, may be responsible for cytoadherence between iRBC and endothelium (Luse & Miller, 1971; Schmidt *et al.*, 1982; Udeinya *et al.*, 1981).

Expression of a single protein denoted PfEMP1 (*P. falciparum* erythrocyte membrane protein 1) immunoprecipitated by immune sera was correlated with the ability of immune sera from *Aotus* monkeys, infected repeatedly with one of four strains of *P. falciparum*, to block *in vitro* cytoadherence of iRBCs and agglutinate iRBCs infected with homologous but not heterologous parasites (Howard *et al.*, 1988).

The genes for the PfEMP1 proteins were eventually cloned and the large and extremely diverse *var* multigene family described in *P. falciparum* (Baruch *et al.*, 1995; Smith *et al.*, 1995; Su & Stevenson, 2002). To date, three large multigene families that are potentially on the iRBC surface have been described in *P. falciparum*. The PfEMP1 and RIFIN families together with other iRBC surface proteins (including AE1/band 3, a RBC membrane anion transporter modified by P. falciparum infection, *clags*, PfMC-2TM, and SURFINs) are here briefly described. This is then followed by a detailed description of the final major gene family STEVOR, the main subject of this thesis.

1.6.3. *P. falciparum* erythrocyte membrane protein 1 (PfEMP1)

var genes encode the PfEMP1 proteins (Smith *et al.*, 1995; Su *et al.*, 1995). The sequenced *P. falciparum* 3D7 clone has 59 *var* gene copies found sub-telomerically (and occasionally centrally) in all 14 chromosomes (Gardner *et al.*, 2002); however, *var* gene repertoires are thought to be strain–specific. PfEMP1 variants are large proteins (approximately M_r ~220-350kDa). PfEMP1 are iRBC surface-membrane proteins as determined by lactoperoxidase-catalyzed radio iodination (^{125}I) (Leech *et al.*, 1984), trypsin treatment sensitivity (0.1μg/ml) (Hommel *et al.*, 1983; Leech *et al.*, 1984), and antibody immunoprecipitation of intact iRBC (Leech *et al.*, 1984). They are anchored in the iRBC plasma membrane as determined by detergent solubility (Leech *et al.*, 1984).

PfEMP1s are highly diverse but share similar organisation as single transmembrane-spanning proteins. Each member consists of a large 5' exon with high sequence-variability separated from a smaller highly conserved 3' exon by a transmembrane domain. The 3' exon encodes the acidic terminal segment (ATS), presumed to anchor PfEMP1 to knob-like structures on the iRBC surface, while the N-terminal end is extra-cellular, and contains 2 to 5 copies of a motif denoted DBL (Duffy-binding-ligand). The nomenclature of the DBL motifs is based on numbering them in the order from the gene's 5' end, and to denote their sequence type by Greek letters α - ε, (x) (i.e. Common organisation of *var* results in DBL1(α), DBL2 (β),...DBL5(ε)).

A second motif common to all PfEMP1s is the cysteine-rich inter-domain region (CIDR), of which there are one or two copies (termed α and β or 1 and 2). The first CIDR, CIDR-1(α), is found immediately after DBL1α in most *var* genes. The detailed domain structure of PfEMP1 is illustrated in figure 1.7.

Specific domains of PfEMP1 interact with specific host endothelial cell receptors *e.g.* CD36 or ICAM-1 (intercellular adhesion molecule 1), which endow the parasite with the ability to bind to endothelial cells (Baruch *et al.*, 1995; Smith *et al.*, 1995). Binding to endothelial receptors enables parasites to sequester out of peripheral circulation, thereby escaping splenic clearance of iRBC, and thus facilitates chronic infections that give gametocytes time to develop. This is especially important to *P. falciparum* parasites where the gametocytes have a particularly long developmental period before appearing in peripheral circulation (minimum 7 days) (Lensen *et al.*, 1999; Sinden & Smalley, 1979). Early-stage gametocytes express PfEMP1 and their sequestration is dependent on binding to the CD36 host endothelial receptor (Hayward *et al.*, 1999; Piper *et al.*, 1999b). Parasite-binding properties (such as to ICAM-1 in the brain microvasculature) have been correlated with the variation in *var* repertoire between parasite strains, and could explain

the serious disease morbidity and slow development of natural immunity to *P. falciparum*.

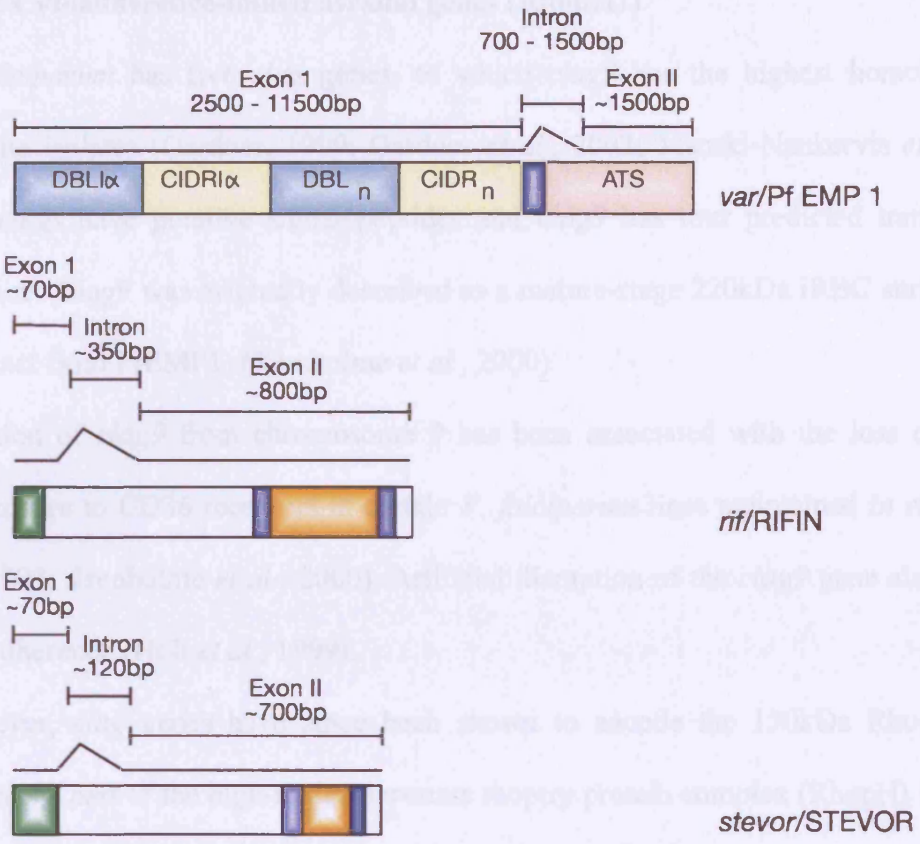

Figure 1.7: Representative structures of the var, rif, *and* stevor *genes as well as the encoded* PfEMP1, RIFIN, *and STEVOR proteins.* var *genes are between 3.9 and 13 kb in size. The encoded* PfEMP1*s are composed of different numbers (n) of Duffy-binding-like (DBL) and cysteine-rich interdomain region (CIDR) domains. All* var *genes have an intron relatively close to the 3' end, and all* PfEMP1*s have a transmembrane region (dark blue) followed by an intracellular acidic terminal segment (ATS) (pink).*

rif *and* stevor *genes as well as their encoded RIFIN and STEVOR proteins are similar in structure. Exon I of both genes only encode a hydrophobic signal peptide sequence (green). Their introns are different lengths, and are relatively close to the 5' end. Two predicted transmembrane sequences (dark blue) are located in the middle as well as close to the C-terminus of RIFIN and STEVOR, and a region of extreme polymorphism is enclosed (orange). Figure is adapted from a review by Rasti* et al., *(Rasti et al., 2004).*

1.6.4. Cytoadherence-linked asexual genes (RhopH1)

P. falciparum has five *clag* genes, of which *clag9* has the highest homology across parasite isolates (Gardner, 1999; Gardner *et al.*, 2002; Manski-Nankervis *et al.*, 2000). The *clags* have putative signal peptides and *clag9* has four predicted transmembrane domains. Clag9 was originally described as a mature-stage 220kDa iRBC surface-protein (distinct from PfEMP1) (Trenholme *et al.*, 2000).

Deletion of *clag9* from chromosome 9 has been associated with the loss of ability to cytoadhere to CD36 receptors in certain *P. falciparum* lines maintained *in vitro* (Day *et al.*, 1993; Trenholme *et al.*, 2000). Artificial disruption of the *clag9* gene also abolished this adherence (Holt *et al.*, 1999).

However, *clag* genes have since been shown to encode the 150kDa RhopH1protein, which is a part of the high-molecular-mass rhoptry protein complex (RhopH) found in the merozoite rhoptry organelles (Kaneko *et al.*, 2001; Kaneko *et al.*, 2005; Ling *et al.*, 2004). Thus the clag-variant proteins may provide the RhopH complex with multiple functions, potentially including a cytoadhesive role, dependent on the exact clag protein combination in its composition (Ling *et al.*, 2004).

1.6.5. Surface-associated interspersed genes (SURFINs)

In *P. falciparum*, SURFINs encoded by 10 *surf* genes are located in "an amorphous cap at the parasite apex" during the merozoite-stage (Winter *et al.*, 2005). These proteins are also expressed on the iRBC surface of mature parasites: A SURFIN was cleaved by trypsin off the surface of *P. falciparum* 3D7 live iRBC (Winter *et al.*, 2005).

1.6.6. *P. falciparum* Maurer's cleft two transmembrane proteins (PfMC-2TMs)

PfMC-2TMs are transcribed during the trophozoite-stage of the erythrocytic cycle (Sam-Yellowe *et al.*, 2004). Genes are located sub-telomerically, and PfMC-2TM proteins were

located in the Maurer's clefts. This family has a signal peptide and Pexel/VTS motifs characteristic of parasite proteins within the iRBC cytosol. 13 members of the PfMC-2TM family share amino acid conservation throughout with the exception of a 17 amino acid HVR between the two predicted transmembrane domains.

1.6.7. Human anion-exchange protein 1 (AE1 or band 3)

Unlike the other proteins associated with the iRBC membrane, AE1 (otherwise known as band 3) is not of parasite origin, but it is included here as it constitutes a major modification of the iRBC membrane. Modified AE1 enables the parasite iRBC to interact with other host cells in a similar fashion to parasite-derived iRBC surface proteins. Normal AE1 is a major membrane protein of RBCs, with two main functions: maintenance of RBC structure, and transport of carbon dioxide from the intra-cellular to the extra-cellular space. Parasite growth modifies the AE1 protein, so that normally unexposed parts are exposed on the iRBC surface. By the late parasite-stages, these exposed regions result in an increase in iRBC adhesiveness (Crandall & Sherman, 1994b).

Peptides designed on human-band 3 epitopes were able to block iRBC adhesion to C32 amelanotic melanoma cells in a dose-dependent manner, as did antibodies to these sequences. These cytoadherence blocking band 3 peptides were termed Pfalhesin (Crandall & Sherman, 1994a). When Pfalhesin peptides were infused into *Aotus* or *Saimiri* monkeys infected with *P. falciparum*, large numbers of trophozoites and schizonts were observed in peripheral blood 24 hours post-infusion, suggesting that these peptides delayed or reversed sequestration (Crandall *et al.*, 1993). The endothelial cell receptors for Pfalhesin have been identified as thrombospondin (TSP) and CD36 (Crandall *et al.*, 1994; Eda *et al.*, 1999).

Interestingly, parasite merozoite-binding ligands $MSP1_{42}$ and $MSP1_{19}$ have been shown to recognise and bind to extra-cellular regions of normal AE1 in a sialic acid-independent parasite-host interaction (Goel *et al.*, 2003).

Both normal and modified AE1 forms therefore function as a major point of interaction between the parasite and host, as a binding ligand on RBCs at the merozoite invasion-stage, and a sequestration ligand in post-24hours trophozoite /schizont-stages, where modification of this major RBC protein by the parasite growth leads to increased iRBC cytoadherence to CD36 receptors and TSP resulting in iRBC sequestration. In addition to its other normal functions, this ubiquitous membrane transport protein also provides signals marking up senescent cells for removal by the immune system in mammals, thus the parasite has the potential to interfere with the regulation, aging processes and removal of iRBCs (Kay *et al.*, 1990; Low *et al.*, 1985).

1.6.8. Repetitive interspersed family of genes (RIFINs)

The *rif* gene family was identified as an interspersed repetitive gene sequence (*rif*), with 149 copies in the 3D7 genome (Gardner *et al.*, 2002). RIFINs encode variable size (27-45kDa) proteins transcribed and expressed in the trophozoite-stage (figure 1.7). The proteins have an N-terminal semi-conserved domain with the majority of cysteines, while the C-terminal contains two predicted transmembrane domains and a highly polymorphic region (Cheng *et al.*, 1998; Kyes *et al.*, 2001). RIFINs were initially linked to rosetting although this is a role now fulfilled by the complement receptor 1 (CR1) binding domain to PfEMP1 (Fernandez *et al.*, 1999; Helmby *et al.*, 1993; Stanley & Reese, 1986). The two transmembrane domains are thought to create a polymorphic loop present on the iRBC surface consistent with a role in antigenic variation (Fernandez *et al.*, 1999; Kyes *et al.*, 1999). However recent work by Khattab and Klinkert used green fluorescent protein (GFP)-chimeric molecules to track a RIFIN through the iRBC, and found the RIFIN

localised to the Maurer's clefts (MC), with the polymorphic region exposed to the iRBC cytosol (Khattab & Klinkert, 2006). Maurer's clefts are flattened vesicular structures localised beneath the iRBC surface membrane (Bannister & Mitchell, 2003).

Antibodies in hyper-immune sera from adults recognise RIFIN proteins, indicating that, like PfEMP1, they are immunogenic, exposed, and induce malaria-specific IgG antibodies. The concentration of anti-RIFIN antibodies has been correlated with time taken for parasite clearance suggesting they confer some protection against malaria (Abdel-Latif *et al.*, 2002; Abdel-Latif *et al.*, 2003; Abdel-Latif *et al.*, 2004).

1.6.9. Sub-telomeric variable open reading frame (STEVORs)

The sub-telomeric variable open reading frame (*stevor*) multigene family is the third largest family in *P. falciparum* and is the subject of this study. Genomic sequencing of laboratory lines predicted the *stevor* family to consist of 33 copies in *P. falciparum* 3D7, 30 copies in *P. falciparum* W2 and 34 copies in *P. falciparum* Dd2 parasites (Cheng *et al.*, 1998). Originally identified and used as a DNA probe, to distinguish between *P. falciparum* isolates, *stevors* have similarities to the *rif*s, however they are two clearly distinguishable gene families. *Stevors* are smaller 1kb genes compared with *rif* genes which are 1.3kb on average (Limpaiboon *et al.*, 1990). Like the *rif* genes, *stevors* are found on all 14 chromosomes, however unlike the *vars*, none is located centrally on the chromosomes (Gardner *et al.*, 2002).

Stevor proved a sensitive target for PCR, and has been used for clinical purposes (detecting 0.01 parasites in 1µl of blood) (Filisetti *et al.*, 2002), giving distinctive multiple banding patterns in Southern blots capable of distinguishing *P. falciparum* parasite clones (Limpaiboon *et al.*, 1990; Prescott *et al.*, 1994).

The two-exon structure of *stevor* and *rif* was confirmed by Cheng *et al*, 1998 (figure 1.7) (Cheng *et al.*, 1998). The first short exon, approximately 50—75bp in length, encodes a

start codon and predicted canonical signal sequence. Analysis showed the AT-rich intron starts with a GT and ends in a poly-T sequence before a consensus TAG splice site. The second exon, shorter in *stevor* than *rif*, encodes several conserved regions and a highly polymorphic region flanked by two predicted transmembrane domains. This region is predicted by Kyes *et al* to be an external 'hyper-variable loop' and is considerably longer in RIFIN (170 amino acids) than STEVOR (70 amino acids) (Cheng *et al.*, 1998; Kyes *et al.*, 2001).

STEVOR is a transmembrane, integral-membrane protein, which has been located in Maurer's clefts in the iRBC cytosol (Cheng *et al.*, 1998; Kaviratne *et al.*, 2002; Kyes *et al.*, 1999; Przyborski & Lanzer, 2005). STEVOR is located in the Maurer's clefts during the trophozoite-stage of a laboratory *P. falciparum* line (3D7), which is grown continuously in *in vitro* cultures (Kaviratne *et al.*, 2002). Polyclonal mouse and rabbit antibodies against conserved STEVOR N- and C-terminal peptide sequences were used to demonstrate STEVOR expression in blood-stage parasites. An approximately 37kDa protein was recognized in Western blots of asexual 3D7 parasite lysate. These same antibodies were used in immunofluorescence assays, and in the 3D7 strain co-localised the STEVOR proteins in the Maurer's clefts with *P. falciparum* Skeletal Binding Protein-1 (PfSBP1) and truncated *P. falciparum* Erythrocyte Membrane Protein-3 (PfEMP3) antibodies (Blisnick *et al.*, 2000; Kaviratne *et al.*, 2002; Waterkeyn *et al.*, 2000). Like other Maurer's cleft structural components, STEVOR reportedly remains associated with the iRBC ghost after schizont rupture and merozoite release, indicating stable STEVOR-Maurer's clefts associations (Kaviratne *et al.*, 2002). This is in contrast to the iRBC surface location of the other multigene families: PfEMP1 and RIFINS.

1.6.9.1. STEVOR in gametocyte-stages

STEVOR has also been shown to be present in gametocyte-stages (McRobert *et al.*, 2004). In late-stage gametocytes STEVOR appears to be associated with the iRBC membrane. However, this is *via* a Maurer's cleft-independent pathway as gametocytes lack Maurer's clefts. Identical STEVOR proteins are transcribed and expressed in *P. falciparum* 3D7 asexual and gametocyte parasites (McRobert *et al.*, 2004; Sharp *et al.*, 2006). In addition, truncated STEVORs are found in gametocytes (Sutherland, 2001). The population of truncated STEVORs may be important as they lack the second predicted transmembrane domain and therefore would be arranged differently within the membrane (Sutherland, 2001). They could also be redundant transcripts. However, a smaller protein band with sizes corresponding to the truncated transcript was detected by Western blot only in gametocyte parasite lysates (McRobert *et al.*, 2004).

As mentioned previously, early-stage gametocytes express PfEMP1 and sequestration is dependent on binding to the CD36 host endothelial receptor (Day *et al.*, 1998; Hayward *et al.*, 1999; Piper *et al.*, 1999a). However gametocyte-stages II–IV, which also adhere to endothelium, use a CD36-independent adhesion mechanism (Rogers *et al.*, 2000). STEVOR is suggested as one potential candidate for this adhesion mechanism.

1.6.9.2. STEVOR in sporozoite-stages

There is also evidence for the presence of STEVOR in sporozoite-stages. Proteomic analysis of total sporozoite extracts indicated the presence of a single STEVOR protein (Florens *et al.*, 2002). In addition, the presence of STEVOR in sporozoites has been demonstrated by immunofluorescence within cytoplasmic vesicles (McRobert *et al.*, 2004). However, presence in sporozoites is not unique to the STEVOR multigene family, as PfEMP1 and RIFIN peptides were also found within the sporozoite-stage (Florens *et al.*, 2002), and transcriptome data detected twenty-five *rifin* genes, four *stevor* genes, and a single common *var* detected in sporozoites (Le Roch *et al.*, 2003).

1.7. Proteins targeted by *P. falciparum* to the host iRBC cytosol and surface

All the protein families described above belong with a catalogue of proteins that are predicted to be trafficked into the iRBC cytosol. They are grouped according to criteria describing architecture, for example size (~300 amino acids) and a 2-transmembrane topology.

Recent work suggests that combinations of signals are important for the transport of parasite-proteins into the iRBC cytosol, to the Maurer's clefts and iRBC surface:

1) Canonical (Burghaus & Lingelbach, 2001; Waller *et al.*, 2000) or unconventional hydrophobic N-terminal signal sequences target the protein to the parasite endoplasmic reticulum (Lopez-Estrano *et al.*, 2003; Wickham *et al.*, 2001).

2) An eleven-amino acid-vacuolar transit sequence/ pentameric sequence-protein export element (VTS/PEXEL) motif: RxLxE/Q, identified in the N-terminal domain of exported proteins, is required for transport across the PVM (Hiller *et al.*, 2004; Marti *et al.*, 2004). PfEMP1 lacks this exact motif, but an N-terminal conserved motif with similar features is thought to function as its translocation motif: AKHLLDRLG (Marti *et al.*, 2004) or FFRWFSEWSE (Hiller *et al.*, 2004).

3) Only one transmembrane domain is required for STEVOR, an integral-membrane protein (Przyborski *et al.*, 2005), and for PfEMP1, which, despite the transmembrane domain, traffics as a soluble protein within a chaperoned complex, to associate with the Maurer's clefts (Knuepfer *et al.*, 2005b; Papakrivos *et al.*, 2005). These signals are present in many of the proteins exported into the iRBC cytoplasm defined as the "secretome" (Hiller *et al.*, 2004; Marti *et al.*, 2004).

Proteins move *via* the Maurer's clefts to the iRBC surface. PfEMP1, the best characterised of the parasite-derived proteins that are expected on the iRBC surface, is known to be exported *via* Maurer's clefts (Haeggstrom *et al.*, 2004). Another parasite-derived protein associated with the iRBC surface and Maurer's clefts, PfEMP3, is thought to be important for the modification of the iRBC surface by insertion of PfEMP1 into knobs on the iRBC surface (Knuepfer *et al.*, 2005a; Waterkeyn *et al.*, 2000). Knob-associated histidine-rich protein (KAHRP), which contains the conserved *P. falciparum* PEXEL/VTS motifs (Hiller *et al.*, 2004; Marti *et al.*, 2004), is also transiently associated with the Maurer's clefts before being redistributed to knobs on the cytoplasmic face of the iRBC (Lopez-Estrano *et al.*, 2003; Wickham *et al.*, 2001).

Several parasite proteins reside in the Maurer's clefts: these include PfSBP1 (an established Maurer's-cleft marker (Blisnick *et al.*, 2000)), the Maurer's cleft two-transmembrane domain proteins (Pf MC 2-tm) (Sam-Yellowe *et al.*, 2004), the membrane-associated histidine-rich protein 1 (MAHRP1) (Spycher *et al.*, 2003), and a number of novel proteins identified through proteomics analysis (Vincensini *et al.*, 2005). In addition STEVOR is exported and remains integral to these membranous structures (Kaviratne *et al.*, 2002).

1.7.1. Maurer's clefts as a protein transport organelle

Evidence exists for classical secretory transport of proteins in the iRBC. Interestingly, several Maurer's-cleft-associated proteins (including PfEMP3, REX1, PfSec31p, and PfSar1p) show structural similarity to vesicle-tethering proteins (Hawthorne *et al.*, 2004; Waterkeyn *et al.*, 2000). In addition, the Maurer's-cleft proteins PfSec31p and PfSar1p are *P. falciparum* homologues of COPII proteins, which mediate vesicle transport, and are evidence that the parasite exports proteins for vesicle-mediated protein transport into the iRBC cytosol (Adisa *et al.*, 2001; Albano *et al.*, 1999), suggesting that Maurer's clefts

are probably the parasite's answer to the protein-trafficking and -sorting problem posed by living within a de-nucleated cell lacking a protein-transport system. In this case, Maurer's clefts would provide the parasite with a location within which protein complexes are assembled before being transported to the iRBC surface. Indeed targeted gene disruption of PfSBP1, (an integral Maurer's-cleft protein with a cytoplasmic C-terminal, and Maurer's cleft lumen N-terminal), prevented iRBC adhesion due to loss of PfEMP1 expression on the iRBC surface (Cooke *et al.*, 2006). Functional complementation of the PfSBP1-deleted parasites with a chimeric SBP1 gene restored the wild-type phenotype, and thus PfSBP1 crucially functions in the transfer of PfEMP1 from the Maurer's clefts to the iRBC surface.

Crucially, parasite proteins use Maurer's clefts to get to the iRBC surface. STEVOR co-localises along with the surface-expressed multigene families, RIFINs and PfEMP1, to these structures. This raises the question of whether STEVOR also goes to the surface of the iRBC as its final destination within the blood-stage cycle. Therefore the key is to locate STEVOR more specifically in iRBCs.

1.8 Justification and objectives

Analysis of data obtained from the treatment of neurosyphilis with malaria fevers suggested that although the immunity generated by infection was protective for homologous parasites, an important component of protective immunity is 'strain' specific. Parasite heterogeneity and specificity of the resulting immune response is a plausible explanation of the need for prolonged exposure to multiple parasites, in order to achieve both anti-parasite and clinical immunity to malaria. Parasites vary through polymorphisms in the putative target antigens for protective immune responses, either through the existence of alternative allelic forms in the case of many key merozoite antigens, or through the existence of multiple homologous genes and the mechanism of

clonal antigenic variation, in the case of important iRBC surface proteins. The emerging evidence of protective responses being directed against such polymorphic and variant epitopes implies that it is unlikely that immune status will ever be defined by any single response. This has serious implications for the future planning of vaccine components and current trials have generally not accounted for this variation. Therefore a fuller knowledge of the potential parasite genotypic and phenotypic variation is necessary before an effective vaccination strategy can be attained.

A substantial body of information has been gathered on the iRBC surface protein PfEMP1, which has revealed certain common *var* genes, which the parasites use initially unless prevented by a specific protective immune response. The *stevor* multigene family is the third next largest gene family in the *P. falciparum* genome, and as such, it is of interest to determine whether a similar hierarchy of common variants exists between different parasite genomes. Initially it will be necessary to determine if the *stevor* family is a common feature of *P. falciparum* parasites, as current knowledge only extends to the laboratory line 3D7. Field parasite isolates are of particular interest given the expectation that multigene families are positively driven by immune responses.

Currently, it is not known whether STEVOR proteins are exported to the surface of the iRBC, which would make them key immune targets. In addition, it is likely that STEVOR proteins may play important roles in the biology of the parasite and pathogenesis of malaria. Therefore a more extensive study of the localisation of these proteins, particularly in field-isolate parasites, is necessary. As has already been discussed, evidence exists for expression of STEVOR in several different-stages of the life-cycle, which may suggest that STEVOR has multiple functions. However, it also suggests that similar antigenic surfaces will be presented to the immune system enabling a multi-stage targeting immune response. These studies aim to gain a more intimate knowledge of the

biology of the parasite and its interactions with the human host with specific regard to STEVOR.

1.8.1. Specific objectives

1) To assess the newly available genomic sequence data for *stevor* to identify the global STEVOR repertoires in available parasite genomes.

2) To determine if *stevor* is transcribed and expressed in all parasites (different parasite isolates from laboratory and field).

3) To compare the expression profiles of STEVOR across different laboratory parasite isolates and field parasites.

4) To make a detailed assessment of the location of STEVOR within the erythrocytic-stage parasites, including gametocytes.

5) To determine if STEVOR is expressed on the iRBC surface.

Chapter 2) Materials and Methods

2.1. Media, solutions and buffers

All chemicals and reagents were of analytical grade and purchased from BDH chemicals Ltd, UK, or Sigma, UK, unless otherwise stated. Compositions of media solutions and buffers are given in the text.

2.1.1. Parasite media

RPMI 1640 complete medium (with 10% Albumax) (Gibco) for laboratory parasite lines

RPMI 1640 with 10% AB serum supplemented (see below) for Kilifi parasite isolates

RPMI 1640 complete medium (without Albumax) (Gibco) for washes *etc*

2.2. Parasites

The parasites used in this study were well-characterised laboratory strains or were blood samples isolated from in Africa. See table 2.1 for list of all parasite clones used for *in vitro* culture and their origin.

The African study parasites were acquired at Kilifi district hospital, situated 60km north of Mombasa on the Kenyan coast. More than 10% of the children under the age of 5 years who reside within the Kilifi district are admitted into hospital each year. The area has prolonged seasonal *P. falciparum* transmission following the long and short rains, transmitted by the *Anopheles gambiae s.l.* complex (Mbogo *et al.*, 1993).

Parasites were obtained from the KEMRI-Wellcome Trust, Kilifi, Kenya. Blood was taken from patients in the Kilifi general district. Lymphocytes were removed from blood samples prior to preservation in liquid nitrogen.

2.2.1. Parasite culture of *P. falciparum* laboratory lines

All media used for parasite culture were first warmed to 37 °C. All centrifugation steps were carried out at 25 °C.

Laboratory parasite lines were cultured in fresh human RBC (supplied by National UK Blood Donation Service) in RPMI 1640 complete medium (with Albumax) (supplemented with 2mM glutamine (NIMR media service)) (Trager & Jensen, 1976). The flasks were maintained in a low oxygen environment (88% Nitrogen with 5% Oxygen and 7% Carbon dioxide). Medium and gas were changed daily, and cultures maintained at below 30% parasitaemia in approximately 2% haematocrit.

Parasitaemia was monitored by microscopy; thin blood films were fixed in methanol onto glass slides, and stained with Giemsa stain (diluted in water). The slides were examined at 100X with an oil objective on a light microscope.

Table 2.1) The origins of *P. falciparum* clones used for *in vitro* culture

Clone	Parent isolate	Geographical origin	Reference
3D7	NF54	Amsterdam airport - Netherlands (unknown origin)	(Walliker *et al.*, 1987)
A4	IT04	Brazil	(Roberts *et al.*, 1992)
C10	1776	Malaysia	(Ang *et al.*, 1996)
D10	FCQ-27	Papua New Guinea	(Chen *et al.*, 1980)
Dd2	W2-MEF	Indochina	(Oduola *et al.*, 1988)
FcB1		Colombia	(Schrevel *et al.*, 1994)
T9/96	T9	Thailand	(Thaithong *et al.*, 1984)

2.2.2. Induction of gametocytes during *P. falciparum* 3D7 culture

In order to induce gametocyte production, *P. falciparum* 3D7 stock culture was increased to 4-6% haematocrit with fresh RBC (personal communication Muni Grainger). The culture was monitored by thin blood smears over approximately 18 days for the

development of gametocytes. During this period, no new RBCs were added to the flask but medium and gas were changed daily.

2.2.3. Recovery of *P. falciparum* Kilifi parasite isolates from frozen stock

Cryovials of between 500µl and 1ml infected-blood were removed from liquid nitrogen and thawed rapidly at 37°C (by enclosing the cryovial in a fist). Samples were gradually returned to isotonicity, using a three-step process. First, 200µl sodium chloride (12% solution) was added drop-wise with agitation over 2 minutes, (to a 1:5 saline to sample volume ratio). This was followed by 5mls (5 volumes) sodium chloride (1.8% solution) added with agitation over 5 minutes, finally 5mls sodium chloride (0.9% solution) was added likewise. The blood was centrifuged at 561xg, 5 minutes at 24°C and the supernatant removed.

2.2.4. *In vitro* culture of *P. falciparum* isolates from Kilifi

The parasites (iRBCs) were cultured in RPMI 1640 media supplemented with 10% AB human serum (Kilifi General Hospital, Kenya), 2mM L-glutamine (Gibco), 37.5mM HEPES (Gibco), 20mM Glucose, 2µg/ml Gentamycin (Gibco), pH 7.2 in a reduced oxygen environment (see above for exact gas mixture). No fresh RBCs were added to the cultures, and the parasites were maintained in culture for approximately 30 hours, or allowing for delayed growth, until they reached late trophozoite/schizont-stages. Parasite samples were divided into two for later processing for gDNA and RNA (see below).

2.2.5. Schizont purification and synchronisation

Parasites were first washed in RPMI 1640 medium (without Albumax), and resuspended at 20% haematocrit. The parasites were layered gently on top of 5mls 70% isotonic Percoll (in PBS pH7.2) (Amersham Biosciences) in RPMI 1640 (without Albumax), in 20ml universal tubes. The gradient was spun at 1000xg, for 10 minutes, without brake. The resultant schizont layer was removed and resuspended 1:1 in RPMI 1640 (without Albumax). The schizonts were washed by centrifugation at 815x*g*, 3 minutes and the supernatant containing residual Percoll was removed.

The schizont pellet could then be used for snap freezing etc, or the parasites added back into culture with fresh RBC for reinvasion and synchronisation of the culture.

To synchronise the culture, approximately 2 hours after reinvasion of merozoites into RBC, or once ring-stages were visible by thin blood film, 5% sorbitol (NIMR media service) was added 1:1 for twelve minutes in a 37°C water bath, to remove stages older than 24 hours post-invasion (Hoppe *et al.*, 1991). The culture was then washed in RPMI 1640 (without Albumax) to remove contaminating sorbitol, centrifuged at 815xg, for three minutes, and the supernatant removed. The remaining sorbitol-treated iRBCs were replaced back in culture with fresh RBCs and RPMI 1640 (with Albumax).

2.2.6. Parasite purification on a MACS column (miltenyibiotec)

Synchronised parasites were purified on a MACS column (20ml) placed in a magnetic field to remove all uninfected RBC and ensure parasites for protein extraction were high purity (Taylor *et al.*, 2002). Haemozoin within the iRBCs is bound by the magnet allowing all other cells to be washed off the column. The column was washed with distilled water to remove all traces of ethanol and equilibrated with RPMI 1640 (without Albumax) before the parasite culture was applied to the column. The column was washed with a further 2 column volumes of RPMI 1640 (without Albumax), before the column

was removed from the magnetic field and the bound parasites eluted into a new tube. Parasites for protein extraction were then centrifuged (815x*g*, 3 minutes) and aliquots of the pellet snap frozen in an ethanol/ dry ice bath prior to storage at –80°C.

2.2.7. Purification of *P. falciparum* 3D7 gametocytes on a Percoll gradient

A discontinuous Percoll gradient was used to purify the gametocytes from culture. Solutions of 90% (2ml), 60% (2ml), 54% (4ml), 45% (2ml), 30% (2ml) Percoll were layered carefully in 15ml Falcon tubes, before adding the gametocyte enriched cultures at 20% haematocrit on top. The gradients were then centrifuged at 815x*g*, 6 minutes without brake. The top layer containing parasite debris was removed, and the gametocyte-containing fraction, between the 54 and 45% gradient layers, was collected.

The purity of the gametocytes was approximately 6-16%.

2.3. Preparation and manipulation of parasite DNA and RNA

2.3.1. Preparation of parasite genomic DNA (gDNA)

P. falciparum iRBC, which had been cultured for more than 30 hours (to late trophozoite stage of development) were centrifuged 560x*g* 5 minutes. The pellets were stored at -80°C in screw top cryovials. A Phenol /Chloroform extraction method was used for larger (greater than 500µl) iRBC pellets (Beck, 2002). The DNeasy® kit (Qiagen) protocols 1 and 2 (see manufacturer's handbook) were used for small (less than 500µl) blood samples. DNA was resuspended in nuclease-free water (50µl).

2.3.2. Preparation of parasite RNA

Corresponding *P. falciparum* iRBC, at late trophozoite developmental stage (positive for expected *rif/stevor* transcription, which had been cultured for more than 30 hours were centrifuged 560xg for 5 minutes, then iRBC pellets (approximately 100µl) for RNA extraction were stored at -80°C in 1ml (10 pellet volumes) pre-warmed (37°C) Trizol® LS reagent (Gibco Invitrogen) in screw top cryovials. Kyes *et al* developed the extraction method, used for analysis of the *var* and *rif* multigene family expression patterns (Kyes *et al.*, 2000). RNA was resuspended in nuclease-free water (20µl).

2.3.3. Primer design for *stevor* specific PCR/RT-PCR

The primers were assessed using multiple sequence alignments to ensure that the chosen sequences were in regions conserved within the *stevor* gene family, but not in other genes (for example the *rif* gene family). A combination of two sets of primers in a nested PCR was used. Cheng designed the RepF1, RepF2 and RepR internal-PCR primers (table 2.2) (Cheng *et al.*, 1998). The RepF1/2 primers were redesigned to remove an opal stopcodon (TGA) replacing it with (TGC). The smf1/smr1 external primers were from (Kaviratne *et al.*, 2002). All primers were synthesised by Eurogentic/Oswel (Southampton, UK) or Research Biolabs (Singapore). The use of a nested-PCR protocol for RT-PCR was problematic, due to amplification of contaminating gDNA, therefore a *stevor*-specific single step amplification was designed, facilitated by the complete genome sequence (Gardner *et al.*, 2002), using the primers JBSTEVORF1 and JBSTEVORR1 (table 2.2).

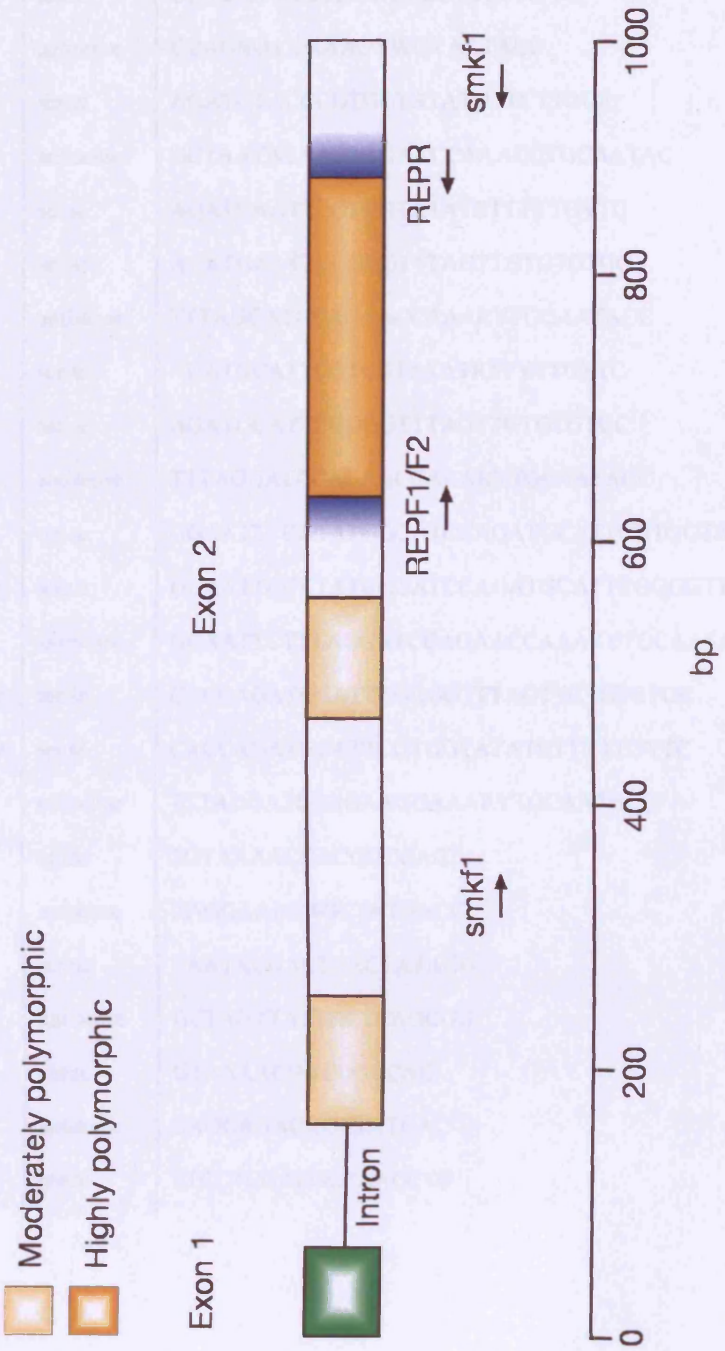

Figure 2.1: Schematic of stevor showing primer location

Table 2.2) Primer sequences

Primer name	Direction	Primer Sequence (5' -3')	Tm (°C)
smf1	sense	GAYSCAGAACTCAARGAAATWATTG	46.42
smr1	antisense	GCAGMACCAAAGYWGYAATACC	47.9
JBSTEVORF1	sense	AGATGTACCCGTGGTATATGTTCTTGCA	54.96
JBSTEVORR1	antisense	GCTAATATAAGTAGAACCAAAGCTGCAATAC	54.44
RepF1	sense	AGATGAATTCGTGGTATATRTTYTTGYTC	55.84
RepF2	sense	AGATGAATTCGGGGTTTAGTTGTGTGTGC	63.86
RepR	antisense	TTTAGGATCCAGAACCAAARYTGCAATACC	62.21
TARepF1	sense	AGATGCATTCGTGGTATATRTTYTTGYTC	53.13
TARepF2	sense	AGATGCATTCGGGGTTTAGTTGTGTGTGC	61.42
TARepR	antisense	TTTAGGATCCAGAACCAAARYTGCAATACC	56.9
pET24RepF1	sense	GGAATTCCATATGGGATCCAGATGCATTCGTGGTATATRTTYTTGYTC	62.5
pET24RepF2	sense	GGAATTCCATATGGGATCCAGATGCATTCGGGGTTTAGTTGTGTGTGC	65.5
pET24RepR	antisense	GGAATTCTTTAGGATCCAGAACCAAARYTGCAATACC	58.3
TOPORepF1Jane	sense	CACCAGATGCATTCGGGGTTTAGTTGTGTGTGC	60.6
TOPORepF2Jane	sense	CACCAGATGCATTCGTGGTATATRTTYTTGYTC	56.2
RepRTOPO	antisense	TTTAGGATCCAGAAGGAAARYTGCAATACC	53.8
M13 Forward	sense	TGTAAAACGACGGCCAGT	42.9
M13 Reverse	antisense	CAGGAAACAGCTATGACC	42.9
T7 promoter	sense	TAATACGACTCACTATAGG	39.5
T7 terminator	antisense	GCTAGTTATTGCTCAGCGG	46
M13 Forward	sense	GTAAAACGACGGCCAG	50
M13 Reverse	antisense	CAGGAAACAGCTATGAC	50
TrxFus forward	sense	TTCCTCGACGCTAACCTG	56

2.3.4. Polymerase chain reaction (PCR) amplification of *stevor* genes' hyper-variable region

The target region of *stevor* genes was amplified from gDNA using PCR. PCR reactions were carried out in both Eppendorf Mastercycler gradient, and standard machines (Eppendorf, Hamburg, FRG). A combination of heated lid, plate sealers (Eppendorf), and/or 50µl mineral oil was used to prevent sample evaporation. See table 2.2 for primer sequences.

Separate primer sets were designed for 3 vector systems used for product sequencing (Figure 2.2): A) pCR2.1 B) pCRII C) pET-24a (+) and D) pET102/D-TOPO vectors. The pCR2.1/pCRII system utilises a one-step cloning strategy that does not require addition of restriction sites to the primers. The pET-24a (+) and pET102/D-TOPO systems were each designed to include a restriction or ligation site at the end of the resultant product. The Magnesium chloride concentration (2mM-4mM), and primer annealing temperatures were optimised for the different reactions.

The production of PCR products for sequencing was further optimised by the use of a proof reading polymerase *Pfu* enzyme (Stratagene). The 5' to 3' –DNA polymerase and 3'- to 5' –exonuclease activity results in a six-fold increase in fidelity of DNA synthesis compared to *Taq* DNA polymerase (Stratagene product information). A brief incubation step with *Taq* polymerase for 10 minutes at 72°C following PCR with the proof reading enzyme added the 3' A-overhang necessary for cloning into the pCR2.1/pCRII systems.

Figure 2.2: Plasmid vector maps

A) pCR2.1 (invitrogen)

B) pCRII (invitrogen)

C) pET-24a (+) (Novagen)

D) pET102/D-TOPO (invitrogen)

E) pET-24a (+) S1 insert (Novagen)

F) pET-24a (+) S2 insert (Novagen)

Vector maps obtained from manufacturer's product protocols.

A)

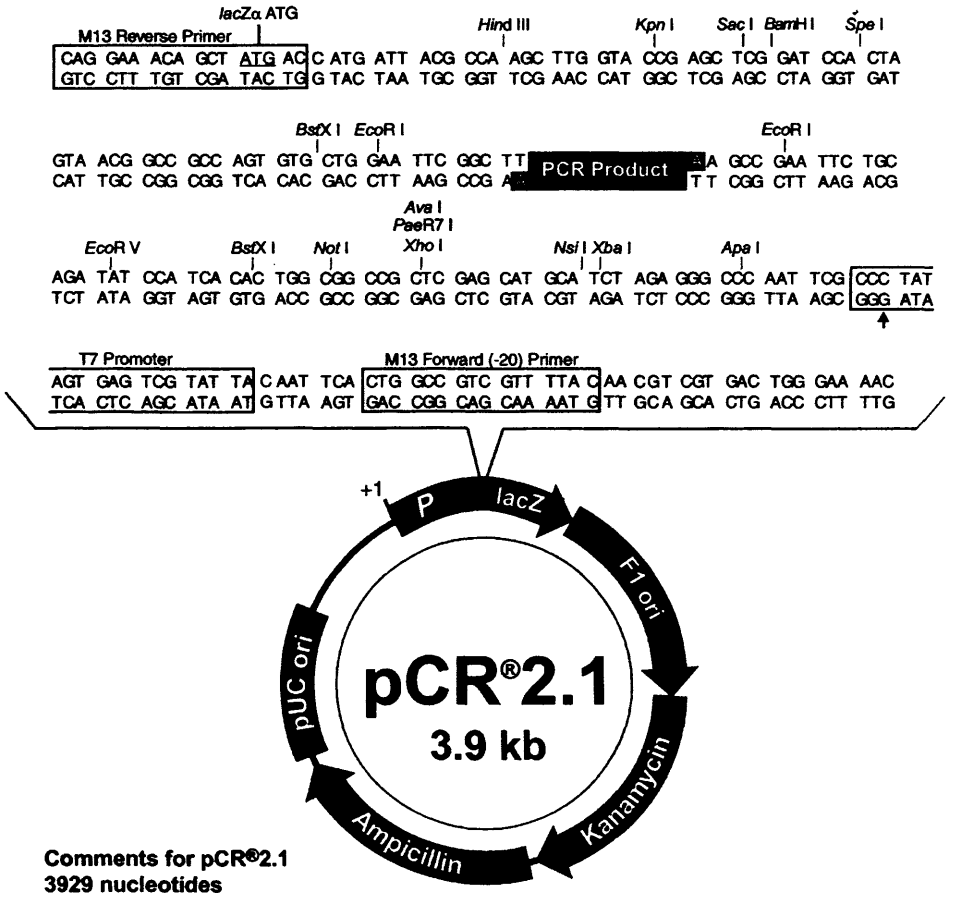

Comments for pCR®2.1
3929 nucleotides

LacZα gene: bases 1-545
M13 Reverse priming site: bases 205-221
T7 promoter: bases 362-381
M13 (-20) Forward priming site: bases 389-404
f1 origin: bases 546-983
Kanamycin resistance ORF: bases 1317-2111
Ampicillin resistance ORF: bases 2129-2989
pUC origin: bases 3134-3807

B)

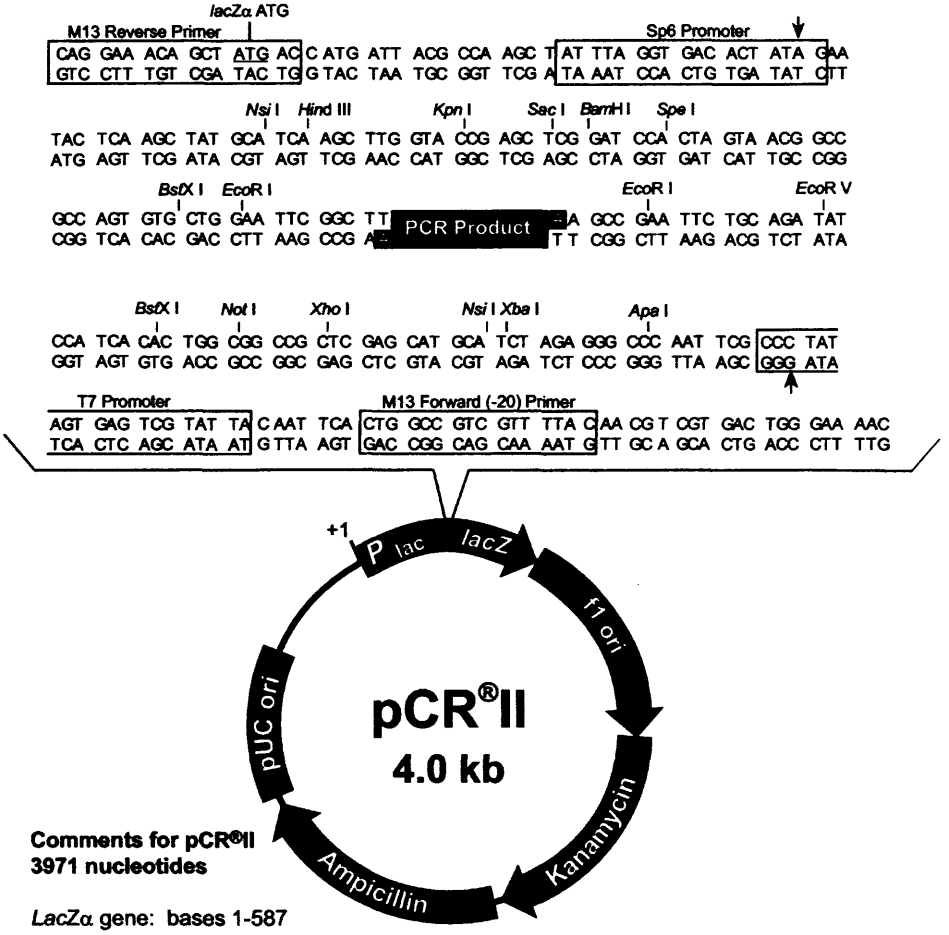

Comments for pCR®II
3971 nucleotides

LacZα gene: bases 1-587
M13 Reverse priming site: bases 205-221
Sp6 promoter: bases 239-256
Multiple Cloning Site: bases 269-381
T7 promoter: bases 404-423
M13 (-20) Forward priming site: bases 431-446
f1 origin: bases 588-1025
Kanamycin resistance ORF: bases 1359-2153
Ampicillin resistance ORF: bases 2171-3031
pUC origin: bases 3176-3849

C)

pET-24a(+) sequence landmarks	
T7 promoter	311-327
T7 transcription start	310
T7•Tag coding sequence	207-239
Multiple cloning sites	
(*BamH* I - *Xho* I)	158-203
His•Tag coding sequence	140-157
T7 terminator	26-72
lacI coding sequence	714-1793
pBR322 origin	3227
Kan coding sequence	3936-4748
f1 origin	4844-5299

The maps for pET-24b(+), pET-24c(+) and pET-24d(+) are the same as pET-24a(+) (shown) with the following exceptions: pET-24b(+) is a 5309bp plasmid; subtract 1bp from each site beyond *BamH* I at 198. pET-24c(+) is a 5308bp plasmid; subtract 2bp from each site beyond *BamH* I at 198. pET-24d(+) is a 5307bp plasmid; the *BamH* I site is in the same reading frame as in pET-24c(+). An *Nco* I site is substituted for the *Nde* I site with a net 1bp deletion at position 238 of pET-24c(+). As a result, *Nco* I cuts pET24d(+) at 234, and *Nhe* I cuts at 229. For the rest of the sites, subtract 3bp from each site beyond position 239 in pET-24a(+). *Nde* I does not cut pET-24d(+). Note also that *Sty* I is not unique in pET-24d(+).

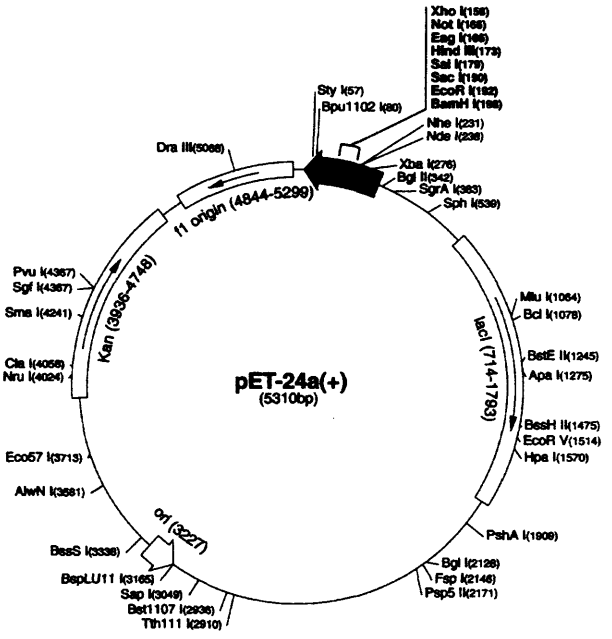

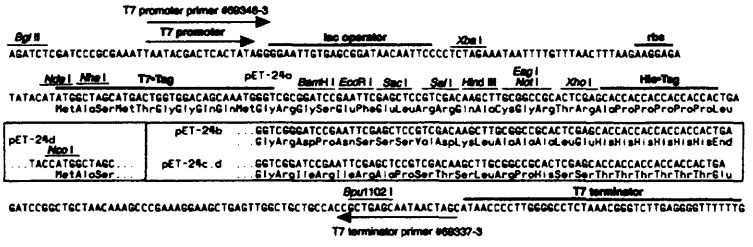

D)

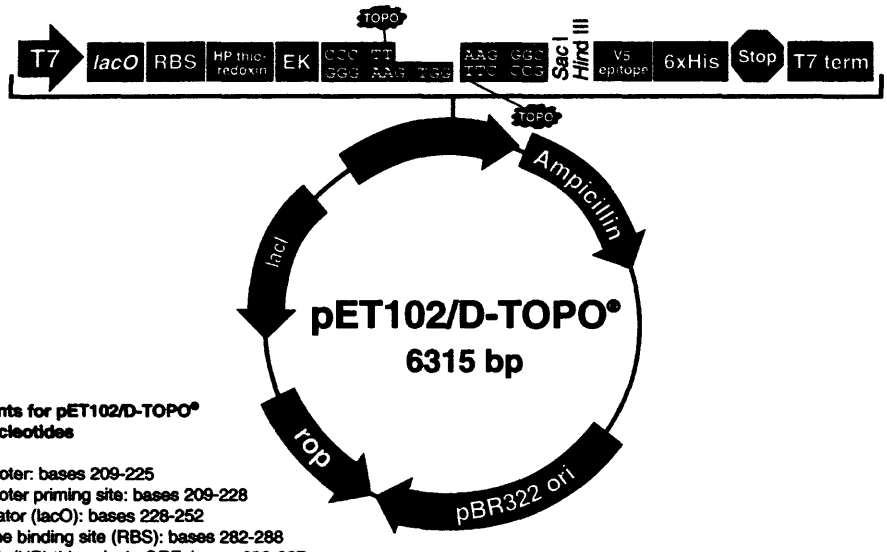

Comments for pET102/D-TOPO®
6315 nucleotides

T7 promoter: bases 209-225
T7 promoter priming site: bases 209-228
lac operator (lacO): bases 228-252
Ribosome binding site (RBS): bases 282-288
His-patch (HP) thioredoxin ORF: bases 298-627
TrxFus forward priming site: bases 607-624
EK recognition site: bases 643-657
TOPO® recognition site 1: bases 670-674
Overhang: bases 675-678
TOPO® recognition site 2: bases 679-683
V5 epitope: bases 700-741
Polyhistidine (6xHis) region: bases 751-768
T7 reverse priming site: bases 822-841
T7 transcription termination region: bases 783-911
bla promoter: bases 1407-1505
Ampicillin (*bla*) resistance gene (ORF): bases 1506-2366
pBR322 origin: bases 2511-3184
ROP ORF: bases 3552-3743 (complementary strand)
lacI ORF: bases 5055-6146 (complementary strand)

E)

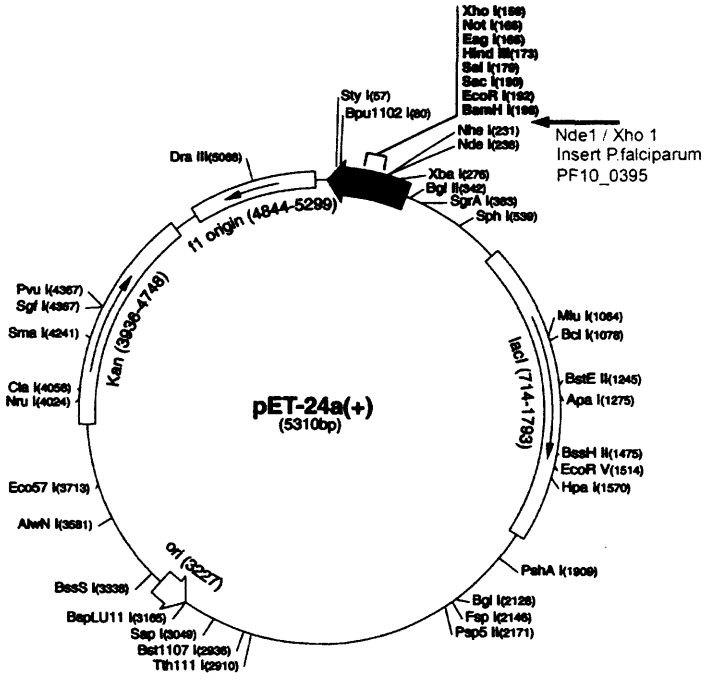

>*PF10_0395*

TATGCAAAATAAGCATTATAACATAAGCCTCATACAAAACAACACGCAAG
GAACAACGATAAAATCAAGATTATTAGCACAAACCCAAAATCATAATCCA
CATTATCATAATGATCCAGAACTCAAAGAAATAATTGATAAATTAAACGA
TGAAGCAATAAAAAAATACCAAAAAACCCATGATCCATATAAACAATTG
AAAGAAGTAGTAGAAAAAAACGGAACCAAAATTAGAGGCGGAAATTCTG
CAGAACCTATGTCAACGATAGAAAAAGATTTATTGGAAAAATATGAAGAC
GTGTTTGGTGACAAAAATCATGCTATGTTAAAATCAGGTAGGTACCCAAA
TGATGATGACGAATCGGATGATTCATCTTCATGTGGATGTACTGATATTAA
TAATGCAGAATTAGAAAAAACAAAAGGAAGAGATAAGTATTTAAAACAC
TTAAAAGGGAGATGTACCCTCGA

F)

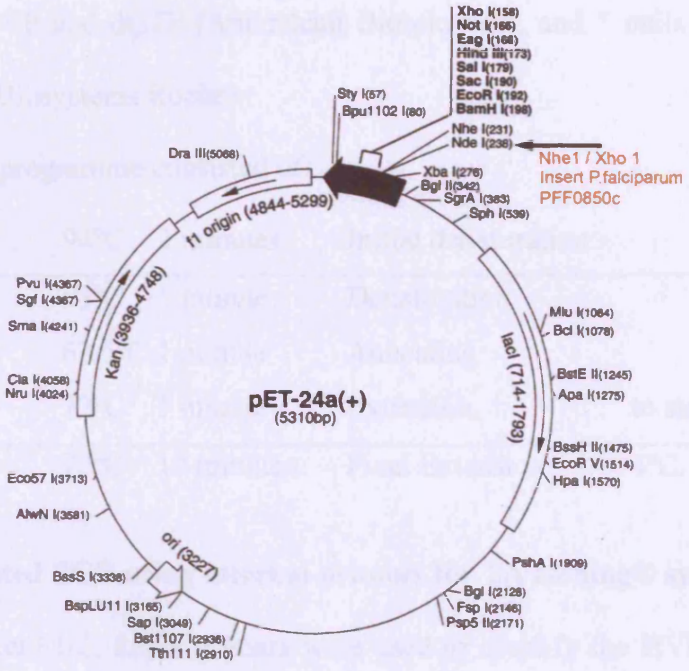

>PFF0850c

CTAGCATGCATAATGAAAATTGTCAAAATAACCAATATAATATAAG
CCTCATAAAAAACAACACACAAAGAACAACGATAAAACCAAGACTCTTA
GCACAAACCAAAAACCATAATCCACATTATCATAATGATCCAGAACTCAA
AGAAATGATTGACAAATTGAACAAAGAAGCAATAAAAAAATACCAAAAA
ATTCATGAACCATATGAACAATTGCAAGAATTAGTAGAAAAAAAAGGAA
CAAAACCTGTAGGTGAACATGGTACAGAACCTATGTCAACGATAGAAAA
AGAATTATTGGAAACATATGAAAAAATGTTTGGTGACAAAAAGGATATTA
TGTTAAAATCGGGTATGCCCCCAAATGATGATGACAGATCAGACAAGTCA
ATAACATGTGAATGCACTGATATTAATAATCCAGACTTAACAAAAGCAAA
AAGCAAGGATAAGTATTTAAAACGCTTAAAAGAGTCGAG

2.3.5. PCR using external primers

Reactions were performed in 50µl volumes, or divisions thereof (25µl/12.5µl) containing approximately 100ng gDNA template, 10 pmoles of each primer: Smf1/Smr1 (Eurogentic), 5µl 10X PCR buffer without $MgCl_2$ (100mM Tris-HCl, 500mM KCl) (Applied Biosystems Roche), 2mM Magnesium chloride (Roche), 200µM each of dATP, dCTP, dTTP and dGTP (Amersham Biosciences), and 5 units AmpliTaq™ polymerase (Applied Biosystems Roche).

The PCR programme consisted of:

Step 1	94°C	3 minutes	Initial denaturation	
Step 2	93°C	1 minute	Denaturation	
Step 3	62.5°C	1 minute	Annealing	
Step 4	72°C	1 minute	Extension,	to step 2 for 35 cycles
Step 5	72°C	10 minutes	Final Extension	4°C.

2.3.6. Nested PCR using internal primers for TA cloning® system

Internal RepF1/2, RepR primers were used to amplify the HVR from the external PCR products. Reaction volumes were 25µl or divisions there of, containing 2µl external PCR product, 5 pmoles RepF1 and RepF2, 10 pmoles RepR, 2.5µl 10X PCR buffer, 3mM $MgCl_2$, 200µM each of dATP, dCTP, dTTP and dGTP and 2.5 units AmpliTaq™ polymerase.

The PCR programme consisted of:

Step 1	94°C	3 minutes	Initial denaturation	
Step 2	93°C	30 seconds	Denaturation	
Step 3	45°C	50 seconds	Annealing	
Step 4	70°C	30 seconds	Extension,	to step 2 for 40 cycles
Step 5	72°C	10 minutes	Final Extension	4°C.

2.3.7. PCR using pET-24a (+) vector primers for sequencing STEVOR HVR

Nested PCR conditions using pET-24a (+) specific primers were as above. PCR products were digested with *BamH1* and *EcoR1* restriction enzymes as per the manufacturer's protocols (New England Biolabs) (see restriction digests below).

2.3.8. PCR using pET102/D-TOPO vector primers for sequencing STEVOR hyper-variable regions

Forward primers RepF1TOPO and RepF2TOPO, and reverse primer RepRTOPO were used to amplify the same HVR but were designed for the pET102/D-TOPO vector. Optimum PCR conditions were assessed and found to be as follows: Reactions were performed in 50µl volumes containing 1µl external PCR product. Each reaction contained 25 pmoles of each forward primer and 50 pmoles of reverse primer, 5µl 10X PCR buffer without $MgSO_4$ (Fermentas), 3mM $MgSO_4$, 200µM each of dATP, dCTP, dTTP and dGTP, and 1.25units *Pfu* DNA polymerase (Fermentas).

PCR conditions were adjusted for the new enzyme as follows:

Step 1	95°C	4 minutes	Initial denaturation	
Step 2	94°C	30 seconds	Denaturation	
Step 3	45°C	50 seconds	Annealing	
Step 4	70°C	1.5 minutes	Extension,	to step 2 for 40 cycles
Step 5	72°C	10 minutes	Final Extension	4°C.

Blunt-ended PCR products were suitable for cloning directly into the pET102/D-TOPO vector.

2.3.9. Preparation of RNA for Reverse Transcriptase (RT)-PCR

2.3.9.1. DNase digestion of contaminating DNA

2µl RNA (500-1000ng/µl) in water were incubated with 1unit Deoxyribonuclease I (DNase I) (amplification grade, Invitrogen), 1.5µl 10X DNase I Reaction buffer, 40 units Recombinant RNasin Ribonuclease inhibitor (Promega, Madison, USA) plus water up to 15µl.

The Eppendorf mastercycler was programmed as follows:

15 minutes at 37°C	Incubation
15 minutes at 55°C	Followed by addition of a further 1 unit DNase I
15 minutes at 37°C	Incubation
10 minutes at 65°C	Enzyme inactivation
Hold at 4°C	Addition of 1µl EGTA 20mM pH8.0
	(RQ1 stop solution, Dnase digestion kit, ProMega)
5 minutes at 65°C	Enzyme inactivation
Hold at 4°C	

2.3.9.2. cDNA (First strand) synthesis

Two tubes containing 5µl DNase digested RNA (see above), 3µg random primers (Invitrogen), 10mM dNTPs (Amersham), up to 8µl in water were incubated 5 minutes at 65°C then kept on ice. A total of 11µl reaction mixture (4µl of 5X First-Strand-Buffer (250mM Tris-HCl, pH8.3, 375mM KCl, 15mM $MgCl_2$) (Invitrogen), 4µl of 25mM $MgCl_2$ (Roche), 2µl 0.1M DTT (Invitrogen), and 1µl (40units) RNasin (Promega) were added to each tube. The contents were mixed and spun briefly before incubating 2 minutes at 25°C and returning onto ice.

1µl (200units) superscript™ II Reverse Transcriptase (RT) (Invitrogen) was added to the RT positive tube, whilst 1 µl water was added to the RT negative control tube.

The reactions were then incubated as follows:

10 minutes at 25°C
50 minutes at 42°C
15 minutes at 70 ° C
Hold at 4°C

After a brief (30 second) centrifugation at 10000x*g*, the reactions were then amplified using *stevor*-specific primers in a nested PCR (see above). Presence of a product in the RT negative control tube was indicative of contaminating DNA and the RT-PCR, or RNA extraction and RT-PCR, repeated until this was clean.

2.4. Separation of DNA, RNA, and PCR products by agarose gel electrophoresis

DNA and RNA were separated by electrophoresis in 1% multi purpose agarose (Roche) in 1X Tris (0.089 M), Boric acid (0.089 M), 2mM EDTA (TBE) buffer. Smaller PCR products (<1kb) were separated by electrophoresis in 2.5% Metaphor agarose (Cambrex Biosciences, Rockland, USA) in 1X TBE. Gels contained 0.25 μg /ml Ethidium bromide to enable UV visualization. RNA gels also contained 5mM Guanidine thiocyanate. All gels were run in 1X TBE buffer.

2.4.1. Nucleic acid quantification and fragment size comparison

Nucleic acid concentration was estimated by comparison with molecular markers run adjacently on an Ethidium bromide-stained agarose gel. A λ*Hind III* molecular mass marker (Biorad) or the Hyperladder 1 (Bioline) bands of known concentration and size were used for comparison. Biorad 1kb/100 bp, or Amplisize 50 -2000bp molecular rulers were used to determine DNA fragment size.

2.5. Restriction digests

Purified DNA vector and PCR products were prepared for ligation by restriction digestion. Plasmids extracted from transformed bacteria were screened by restriction enzyme digestion to verify the presence of the insert. Table 2.3 shows the enzymes used and their respective buffers as recommended by manufacturers.

Table 2.3) Enzymes for restriction digests and their buffers

Enzyme	Buffer
Eco R1 (Promega, UK)	Multicore (Promega, UK)
Eco R1 (Roche Diagnostics, UK)	H (Roche Diagnostics, UK)
Eco R1 (NE Biolabs)	Unique (NE Biolabs)
Bam H1 (Promega, UK)	Multicore (Promega, UK)
Bam H1 (Roche Diagnostics, UK)	B (Roche Diagnostics, UK)
Bam H1 (NE Biolabs)	Unique (NE Biolabs)

pET-24a (+) vector DNA was digested for 4 hours, whilst PCR products were incubated from 4-12 hours with the required number of enzyme units at 37°C. If a change of restriction enzyme buffer was required, a buffer exchange was facilitated through G50 microspin columns (Amersham). pET-24a (+) plasmid was digested sequentially with EcoR1 and BamH1 restriction enzymes according to manufacturer's instructions (NE Biolabs). The double digested plasmid was then treated with calf intestinal alkaline phosphatase (Promega) before ethanol precipitation using 7.5M ammonium acetate.

2.5.1. Cleaning of PCR and RT-PCR products

The QIAquick PCR purification kit (Qiagen, Hilden, Netherlands) was used according to manufacturer's directions to remove primer dimers. The reactions were eluted into 50µl

dH_2O. Amersham Microspin G-50 columns were used as per manufacturer's instructions, to remove small DNA fragments following restriction enzyme digestions.

2.6. Ligation

Purified PCR products for sequencing were cloned into the pCR®2.1 or pCR® II vectors (Invitrogen) according to manufacturer's protocols. Ligation occurs via a 3' single deoxyadenosine on the end of the PCR product combining with the linearised vector's single 3' deoxythymidine residue. Approximately 13ng of PCR product was ligated with 50ng TA vector, (typically 2µl nested PCR product).

The pET102/D-TOPO plasmid required blunt-ended PCR product inserts generated using *Pfu* DNA polymerase (Fermentas). Plasmid specific primers were used to generate translatable PCR products and cloning carried out according to Novagen's pET system manual.

2.7. Transformation of DNA constructs

Ligation reactions were transformed into One Shot™ competent cells (*Escherichia coli* INVαF' or TOP10F') (Invitrogen) provided with the relevant vector kits using manufacturer's protocols. Colonies from LB agar Ampicillin or Kanamycin plates were picked into 3ml LB broth containing 50µg/ml Ampicillin or 30µg/ml Kanamycin, and grown at 37°C with agitation.

2.8. Small-scale preparation of plasmid DNA (minipreps)

Plasmid DNA was isolated using either the QIAprep spin SNAP Miniprep® Kit (Invitrogen), or the Wizard ® *Plus* Miniprep kit in combination with the Vac-Man® vacuum manifold (Promega) according to the manufacturer's protocols (The Wizard ® *Plus* Miniprep kit was later identified as unsuitable for further sequencing procedures).

The QIAgen Maxiprep® kit was used according to manufacturer's protocol to isolate larger quantities of pET-24a (+) vector.

2.9. Automated DNA Sequencing

Following DNA expansion, purification, and confirmation a *stevor* insert was present, the DNA was then, quantified by spectrophotometry, pelleted and dried before sequencing. Three systems have been used for sequencing reactions:

a) The BigDye® Terminator Cycle Sequencing Ready Reaction kit (Perkin-Elmer, Applied Biosystems, Warrington, USA) was used according to manufacturer instructions. The reaction is carried out using approximately 600ng of pCR®2.1 or pCR® II DNA (vector plus insert) per sample with either M13 forward or reverse primers in the Eppendorf Mastercycler. Unincorporated dye terminators are removed by ethanol precipitation. Samples were resuspended in 3µl loading dye 16.5% v/v Blue Dextran/ EDTA (Applied Biosystems) in formamide (Amresco, Solon USA), followed by electrophoresis and data collection on the ABI PRISM™ 377 DNA sequencer (Perkin - Elmer).

b) The BigDye® reactions were also used with T7 primers and pET-24a (+) DNA, or TrxFus forward or T7 reverse primers with pET102/D-TOPO DNA. Sequencing was performed at the National Neuroscience Institute, Singapore (commercial service).

c) The MegaBACE system (Amersham Biosciences) was used. The ABI PRISM® BigDye® Terminator v1.1 Cycle Sequencing kit (Applied Biosystems) cycle sequencing mix was used according to the manufacturer's protocols. Samples were ethanol precipitated before addition of MegaBACE™ loading solution (Amersham Biosciences) and loading onto a MegaBACE 96-capillary machine.

2.10. Bioinformatics

2.10.1 Sequence alignment analysis (hyper-variable loop)

A fragment of approximately 280 base pairs (bp) was successfully isolated through PCR and RT-PCR amplification; however due to the variant nature of the hyper-variable loop, sequences varied in length, coding for a maximum of 82 amino acids. Clones have been obtained from multiple PCR reactions to reduce PCR bias, and were sequenced in forward and reverse directions; differences in the degenerate primer regions were disregarded. *P. falciparum* 3D7, IT and Ghanaian isolates, and *P. reichenowi stevor* sequences were obtained from BLAST and Tools-oligo searches within the http://www.plasmodb.org site.

Editing of nucleotide and amino acid (translated) sequences was carried out using the Autoassembler®, Chromas®, DNAstar (2001) freeware programmes. The sequences from different parasite sources and different amplification reactions were aligned by using ClustalX® (Higgins & Sharp, 1988), and Bioedit7.0.1® softwares (Hall, 1998). Multiple alignments and their corresponding chromatograms were edited manually for discrepancies in mistaken nucleotide assignment by automated sequencing method. BLAST analysis, version 4.4 from www.plasmodb.org was used in order to confirm that DNA sequences were the result of the amplification of *stevor* exon-2 hyper-variable loop locus (now accessible at http://v4-4.plasmodb.org/plasmodb/servlet/sv?page=blast).

2.10.2 Phylogenetic analysis

Phylogenetic trees showing genetic distance were constructed using the following programmes: Molecular Evolutionary Genetics Analysis (MEGA) 2.1 or 3.0®, PAUP version 4.0 (Kumar *et al.*, 2004; Swofford, 2003), and Tree view® (Page, 1996). These programmes enable the construction of trees using tree-building models: neighbour-joining, maximum parsimony and maximum likelihood, taking into account the observed

nucleotide frequency, substitution rate and transition/transversion ratio, based on Nei genetic distance estimates (Kumar *et al.*, 2004). The bootstrap analysis (Felsenstein, 1988) was used in order to statistically assign support to hypotheses of phylogenetic relationship among sequences estimated by the methods mentioned above.

Further protein structural prediction analysis was done using PIX multi-programme analysis web tool. This was available from the human genome mapping project site (www.hgmp.mrc.ac.uk/Registered/Webapp/pix). Protein structure predictions based upon protein alignments were made using the web-based tool from http://www.predictprotein.org.

2.11. Source of protein expression constructs

The pET-24a (+) vector constructs (figure 2.2E and F) containing the N-terminal semi-conserved fragments (amino acids 26-182) of PF10_0395 (S1) and PFF0850c (S2) were kind gifts from Peter Preiser (Nanyang Technological University, Singapore).

2.11.1. Transformation of competent *E. coli* bacterial cells for plasmid maintenance

In each case, a 50µl aliquot of *E. coli* DH5α cells (sub-cloning efficiency) was thawed on ice. 0.1µl of DNA was added to the cells and mixed gently. The mixture was incubated on ice for 30 minutes. The mixture was then incubated for 20 seconds in a 42°C water bath and then quickly placed back on ice for a further 2 minutes. 950µl of pre-warmed LB medium containing 30µg/ml Kanamycin was added and the mixture shaken at 225rpm for 1 hour in a 37°C incubator. The cells were centrifuged at full speed (13000 x g) in a bench top centrifuge for 30 seconds and 800µl media removed. The remainder (50µl and 100µl) was plated out on two pre-warmed Kanamycin plates to ensure well-spaced colonies on at least one plate. The plates were then incubated overnight at 37°C.

2.11.2. Transformation of competent *E. coli* bacterial cells for protein expression

Initial protein expression protocols (performed in Singapore) using standard BL21 *E. coli* had resulted in insoluble protein only. Therefore, two different *E. coli* cell lines were tested in order to maximise the possibility of obtaining soluble proteins, BL21-CodonPlus® (DE3)-RIL (Stratagene), and Rosetta-gami 2 (DE3) pLysS (Novagen). The BL21-CodonPlus® (DE3)-RIL competent cells have functional expression of the rare tRNA genes and this rare codon usage makes these cells more suitable for enhanced expression of eukaryotic proteins that contain codons rarely used in *E. coli*. The Rosetta-gami 2 (DE3) pLysS cells combine this feature with additional enhanced disulphide bond formation. 25µl and 100µl aliquots, respectively, were thawed on ice and 1µl DNA gently stirred in. Cells were incubated 5 minutes on ice, before heat-shock for 30 seconds at 42°C, followed by 2 minutes on ice. 200µl of pre-warmed SOC medium was then added and the mixture was shaken at 225rpm in a 37°C incubator for 1 hour. 50µl or 150µl of the transformation reaction was then plated out on pre-warmed Kanamycin (50µg/ml) LB or Kanamycin (50µg/ml) plus Chloramphenicol (34µg/ml) agar plates. The plates were incubated overnight at 37°C.

2.11.3. Storage of transformed bacterial cells

For immediate use, single colonies of bacteria were picked and grown overnight in 5ml LB media containing 50µg/ml Kanamycin. Longer-term cultures were stored at -80°C after the addition of Glycerol, to 15% (V/V), to overnight culture medium.

2.12. Expression of recombinant proteins

The His-tag® expression system allows the target protein to be detected on Western blots using commercially available specific and sensitive reagents. In addition, fusion to the His-tag enables the protein product to be affinity purified on nickel–nitrilotriacetic acid (Ni-NTA) agarose (Qiagen) columns, where the His-tag is bound with high affinity to 2

ligand-binding sites of the nickel ion immobilised and coupled to sepharose® CL-6B. See Figure 2.2C vector map pET24-a (+) illustrating the main features of this expression system, and E and F showing insert details.

Initially, small-scale experiments were done in order to optimise conditions for the two proteins. After optimisation of the procedure, 8 hour BL21-CodonPlus® (DE3)-RIL bacterial cultures were diluted 1:50 with fresh LB media containing Kanamycin 30μg/ml, and grown overnight in a shaking (225rpm) incubator at 37°C. A 20L culture was then inoculated 1:40 with the overnight culture, and cultures incubated in a fermenter (Bioflo 4000500, New Brunswick) until an OD_{600} reached 0.6. A sample of material was taken (0 hours), before IPTG was then added to a final concentration of 0.5mM. The cells were cultured for a further 2 (S1) or 3 (S2) hours, before the cells were pelleted by centrifugation (20000 x g) in a Powerfuge (Carr) at 4°C. The cell pellet (approximately 60g) was then resuspended thoroughly in 150ml cold lysis buffer (50mM NaH_2PO_4; 300mM NaCl; 10mM imidazole; 5mM β-mercaptoethanol; pH8.0) plus complete protease inhibitor tablets (EDTA-free) (Roche); lysozyme 1000U/ml; IGEPAL CA630 0.2%; and DNase 1 (Roche). The mixture was then subjected to mechanical breakage using pressure (20-24000 psi) in a cell disrupter (constant systems) at 4°C. The lysed cell suspension was pelleted by centrifugation at 13000rpm (Beckman J2-MC) at 4°C for 20 minutes. Supernatants were collected on ice, and pellets were frozen at –80°C. All following steps were maintained at 4°C. 3.5ml of 50% Ni-NTA agarose slurry was used per column (Econo-pac disposable chromatography columns, Biorad), and drained through gravity flow, before being equilibrated with cold lysis buffer. The supernatants were passed over the columns and the flow-through collected. The columns were then washed sequentially with 3 different buffers: Wash 1-lysis buffer (as above); Wash 2-high salt buffer (1M NaCl; 50mM NaH_2PO_4; 10mM imidazole; 5mM β-mercaptoethanol; pH8.0); Wash 3-increased imidazole buffer (50mM NaH_2PO_4; 300mM NaCl; 30mM

imidazole; 5mM β-mercaptoethanol; pH8.0). Each wash was tested for protein content by the Bradford test, 10µl wash sample was added to 1ml Bradford reagent (Biorad) and the colour change (brown-blue) observed. The wash volume was dependent on the Bradford test showing proteins were no longer present in the wash flow through. Each wash was carefully collected into a clean tube and a small sample from the final stage of each wash kept separately for later analysis. Finally the proteins were eluted off the column in elution buffer (50mM NaH_2PO_4; 300mM NaCl; 300mM imidazole; 5mM β-mercaptoethanol; pH8.0). Again, the volume of elution buffer used was dependent on the result from the Bradford assay, typically 6-8mls. Protein samples needed to be concentrated before further purification steps. The fractions were concentrated to <5ml using vivaspin 20ml spin columns with a MW cutoff of 5000kDa (Sartorius, UK). These were pre-rinsed with water to remove trace Sodium azide, and centrifuged at 4000xg at 4°C.

2.13. Purification of recombinant proteins by gel filtration

The proteins were further purified by low-pressure chromatography on the Fast Protein Liquid Chromatography (FPLC) (Amersham's AKTAPrime system, UK) over a 16/60 superdex 75 prep grade column with 1XPBS tissue culture grade (pH7.2) as the mobile phase. The fractions corresponding to the peaks of interest in the FPLC elution profile were pooled and concentrated as described previously. The peak containing the protein of interest and its purity were assessed by SDS-PAGE, Coomassie blue staining and anti-His tag Western blot detection. Protein concentrations were assessed by spectrophotometry (absorbance over the range 240.1-360nm).

2.14. Peptide design

Peptides were designed against conserved regions of STEVOR based on translated and aligned *P. falciparum* 3D7 *stevor* genes. Three peptides were synthesised using the NIMR peptide synthesis service. Peptide 1 sequence: CNPHYHNDPELKEII corresponds to amino acids 57-71 of the alignment. Peptide 2 sequence: CEPMSTLEKELLETYE corresponds to amino acids 110-124. Peptide 3 corresponds to the C-terminal tail of the protein, sequence: RRRKNSWKHECKKHLC corresponds to amino acids 296-312 of the alignment. All peptides have an N or C-terminal cysteine to facilitate conjugation to a carrier protein.

A control peptide (A20/B) sequence: CTEEQLRSSQRRDVPRT was used as a rabbit anti-sera control. This peptide sequence was blasted against the plasmodb EST databases (www.plasmodb.org), but no sequence match identified.

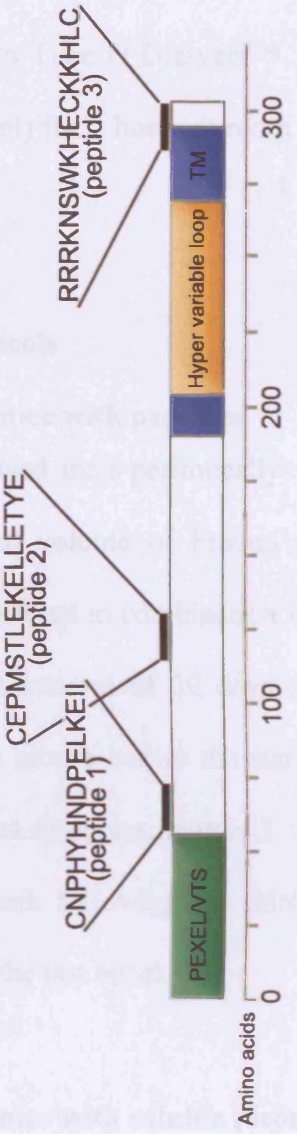

Figure 2.3: Schematic of STEVOR showing peptide locations

2.15. Production of specific anti-sera

2.15.1. Peptides

Peptide immunogenicity was increased by combining with a carrier protein: Reduced peptides were conjugated to Imject® Maleimide Activated Mariculture Keyhole Limpet Hemocyanin (KLH) (Pierce, Illnois, USA) according to manufacturer's instructions. Solutions were transferred to Tube O Dialyzer™ vials (GenoTech). The solutions were dialysed twice in PBS (500ml) for 2 hours at room temperature, followed by overnight at 4°C (1L PBS).

2.15.2. Immunisation protocols

2.15.2.1. Immunisation of mice with peptides

BALB/c mice were immunised intra-peritoneally with 50μg peptide-KLH conjugate in 100μl of PBS and an equal volume of Freund's complete adjuvant (Sigma). The 3 identical boosts were administered in combination with Freund's incomplete adjuvant and administered at a minimum interval of 30 days (maximum 176 days). Normal mouse serum was taken from each mouse before the start of the immunisation schedule. Post-immunisation bleed 1 was taken approximately 1 week following the second boost, post immunisation bleed 2, 1 week following the third boost, and the terminal bleed taken approximately 1 week after the last boost.

2.15.2.2. Immunisation of mice with soluble recombinant proteins

BALB/c mice were immunised intra-peritoneally with 50μg recombinant protein in 200μl (100μl in each of 2 sites) PBS plus MPL + TDM adjuvant system (Sigma) followed by 3 boosts, at intervals of between 2 and 5 weeks. The final bleed was taken 2.5 weeks after the final boost, and blood from 2 mice was pooled per heparin tube for extraction of

serum. Blood was allowed to clot slowly at room temperature, before overnight incubation at 4°C and serum separation.

2.15.2.3. Immunisation of rabbits with peptides

2 New Zealand White rabbits (female or male) were immunised per peptide; All work was carried out by Harlan Sera-Lab., Loughborough, UK. 200μg of peptide-KLH conjugate was given sub-cutaneously using Freund's complete adjuvant for immunisation and incomplete Freund's adjuvant for 3 boosts. Pre-immunisation bleeds were taken at day 0 followed by the initial immunisation. Boosts were at 14 day intervals followed by post-immunisation bleed 1 one week after the second boost (day35). A third boost at day 42 was followed one week later by the terminal bleed. An additional test bleed 2 (rabbits 8606 and 8607 only) was required, and taken after the third boost and prior to the terminal bleed.

2.15.2.4. Source of rabbit serum immunised with insoluble recombinant proteins

2 rabbits were immunised per STEVOR S1 and S2 proteins; all work was carried out by ProSci incorporated, CA, USA.

2.16. Testing for peptide/recombinant protein specific antibodies by enzyme-linked immunosorbent assay (ELISA)

Anti-sera were tested for the presence of peptide, or recombinant protein-specific antibodies. Rabbit sera were also tested for reactivity with the A20/B negative control peptide, and KLH or His-tagged positive control proteins (Calbiochem-Behring). Briefly, 5μg peptide/ protein in 50μl PBS per well was coated in 96-well, flat bottom Polysorb plates (NUNC, Roskilde, Denmark) and incubated overnight at 4°C in 100% humidity.

Antigen was then removed by 'flicking'/inverting plates, and 200µl blocking buffer (PBS plus 1% (w/v) Bovine Serum Albumin Fraction V (Sigma), 0.3% Tween 20 (BDH), 0.05% NaN_3) was incubated for 1 hour (minimum) at 37°C, to block non-specific binding. Wells were then washed 8 times in ELISA wash buffer (0.9% NaCl, 5mM K_2HPO_4, 5mM KH_2PO_4, 0.025% (v/v) Tween 20, pH 7.0-7.2). Serial dilutions of the anti-sera in blocking buffer (50µl per microwell) were incubated at 37°C for 1 hour, before discarding well contents and washing as described previously. The bound antibodies were detected using a secondary antibody step of alkaline phosphatase conjugated anti-mouse or rabbit IgG (Sigma) 50µl per well, diluted 1:10000 in PBS. Secondary antibodies (table 2.4) were incubated at 37°C for 1 hour before discarding and washing as before. The substrate *p*-nitrophenylphosphate-sodium (PNPP) salt (Sigma) 1mg/ml in diethanolamine buffer (4.85% (v/v) diethanolamine pH9.8, 0.2M $MgCl_2$ $6H_2O$, 0.1% NaN_3) was added 50µl per well. The reaction was developed in the dark at room temperature. Readings were taken using a MRX microplate reader (Dynex Technologies, Billingshurst, UK) at OD 405 (reference filter 492) with Revelation 3.04 software (1997).

Table 2.4) Secondary antibodies used to detect rabbit and mouse immunoglobulins

Host	Specificity	Conjugate	Dilution	Manufacturer	Catalogue number
Goat	Rabbit IgG (whole molecule)	Alkaline phosphatase	1 in 10000	Sigma	A-3687
Goat	Mouse IgG (H+L)	Alkaline phosphatase	1 in 1000	Southern Biotech	1031-04
Goat	Mouse IgG (γ-chain specific)	Alkaline phosphatase	1 in 1000	Southern Biotech	1030-04
Goat	Rabbit IgG	Alkaline phosphatase	1 in 2000	Dako	D0487
Goat	Mouse IgG (γ-chain specific)	FITC	1 in 200	Sigma	F-8264
Goat	Rabbit IgG (whole molecule)	FITC	1 in 200	Sigma	F-0382
Goat	Mouse IgG (γ-chain specific)	FITC	1 in 200	Southern Biotech	1030-02
Swine	Rabbit IgG	FITC	1 in 200	Dako	F0205
Goat	Mouse IgG (whole molecule)	TRITC	1 in 200	Sigma	T-5393
Goat	Rabbit IgG (whole molecule)	TRITC	1 in 200	Sigma	T-6778
Goat	Mouse IgG (γ-chain specific)	TRITC	1 in 200	Southern Biotech	1030-03
Goat	Mouse IgG (H+L)	Horse radish peroxidase	1 in 2000	Biorad	170-6516
Goat	Rabbit IgG (H+L)	Horse radish peroxidase	1 in 2000	Biorad	170-6515
Goat	Mouse IgG	Horse radish peroxidase	1 in 1000	Dako	P0447
Swine (Human absorbed)	Rabbit Ig	Horse radish peroxidase	1 in 1000	Dako	P0399
Goat	Rabbit Ig	Horse radish peroxidase	1 in 1000	Dako	P0448

2.17. Affinity purification of peptide-specific rabbit antibodies

Antibodies were affinity purified on peptides, which had been coupled to 1ml NHS-activated Sepharose columns (Amersham Bioscience), according to the manufacturer's instructions. The column was washed with 6 ml of a cold HCl solution (1mM HCl, ice cold) at a flow rate of half a drop per second. Two to five milligram of reduced peptide were dissolved in 1 ml coupling buffer (0.2M NaHCO3, 0.5M NaCl, pH 7-9) and slowly administered to the column. The peptide was coupled for 30 min at room temperature. The column was deactivated with three repeats of 5 ml solution A (0.5M Ethanolamine, 0.5M NaCl, pH 8.3) and 5 ml solution B (0.1M Acetate, 0.5M NaCl, pH 4) and finally washed with 5 ml phosphate buffer and stored in storage buffer (50mM NaH_2PO_4, 0.1% NaN3, pH7).

Anti-serum was centrifuged for 10 min at 12,000g to remove precipitates. The serum was diluted 1/5 in PBS and administered to the column repetitively four times at a flow rate of half a drop per second. Non-specific antibodies and contaminants were washed off with 5-10 volumes of PBS. Bound antibodies were eluted with 5 times 1 ml elution buffer (0.2M Glycine, 0.15M NaCl, pH 2.7) and captured in 1.5 ml tubes containing 200 ml of neutralizing buffer (1M TrisHCl, pH 8.2). Antibody-containing elutions were pooled, concentrated with Vivaspin 20000 (MWCO 10,000, Vivascience) and dialyzed against PBS. Purified antibodies were stored at –20°C. The affinity purifications were tested and controlled on ELISA.

2.17.1. Measuring protein concentration

Protein concentrations were measured with the BCA protein assay (#23223, Pierce, Rockford, IL) according to the manufacturer's instructions. Components A and B were mixed in a ratio of 50:1. The reaction was carried out in flat-bottomed 96-well plates where each well contained 200 µl of the pre-mixed BCA reagents and 25 µl of the

protein. Concentrations of BSA (diluted in the same buffer as the protein samples) ranging from 0-1 mg / ml were in included as a standard. The plates were covered and incubated at 37° C for 30 min. The optical density at 565 nm was measured on the ELISA reader, and the protein concentration calculated by comparison with BSA as standard curve.

2.18. Separation of parasite extracts into soluble and membrane-bound protein fractions

2.18.1. Method 1: Hypotonic lysis (personal communication Irene Ling)

Parasitised RBC or RBC pellets ($1x10^7$cells) were lysed in 4 volumes of hypotonic lysis buffer at 4°C (10mM Tris pH8, 5mM EDTA, 5mM EGTA, complete protease inhibitors (Boehringer)). The samples were then sonicated 30 seconds and centrifuged at 100 000xg, for 1 hour. Supernatants were removed from the pellet. Soluble non-membrane proteins including haemoglobin remained in the soluble fraction (S), whereas non-soluble, membrane-bound proteins remain in the pellet (P) with membrane fragments.

Both fractions were resuspended in Nupage™ LDS loading buffer (4X) (Invitrogen), with 10% 1M DTT, vortexed and centrifuged 14000x*g*, 6 minutes at 4°C. The supernatants were aspirated off, divided into aliquots and stored at -70°C.

Before finally loading onto protein gels, the supernatants were heated at 90°C for 3 minutes.

2.18.2. Method 2: Hypotonic lysis and carbonate extraction of proteins

(figure 2.4) (Papakrivos et al., 2005)

Schizont parasitised or RBC 50µl pellets were lysed in 1 ml hypotonic lysis buffer (as above), incubated on ice 30 minutes, and mixed with a syringe and needle. The samples were centrifuged 100,000x*g* for 30 minutes, and separated into supernatant and pellet

fractions. The pellet was processed in 1ml carbonate buffer (0.1M sodium carbonate pH11.0 plus complete protease inhibitors), resuspended using a syringe and needle, then both pellet and soluble protein fractions were centrifuged again. The final pellet was resuspended in PBS (pH7.2), whilst the carbonate soluble fraction needed to be dialysed (Vivaspin mini spin columns, Sartorius) to decrease pH prior to SDS-PAGE. The 3 fractions are referred to as soluble (S), carbonate (C) and pellet (P).

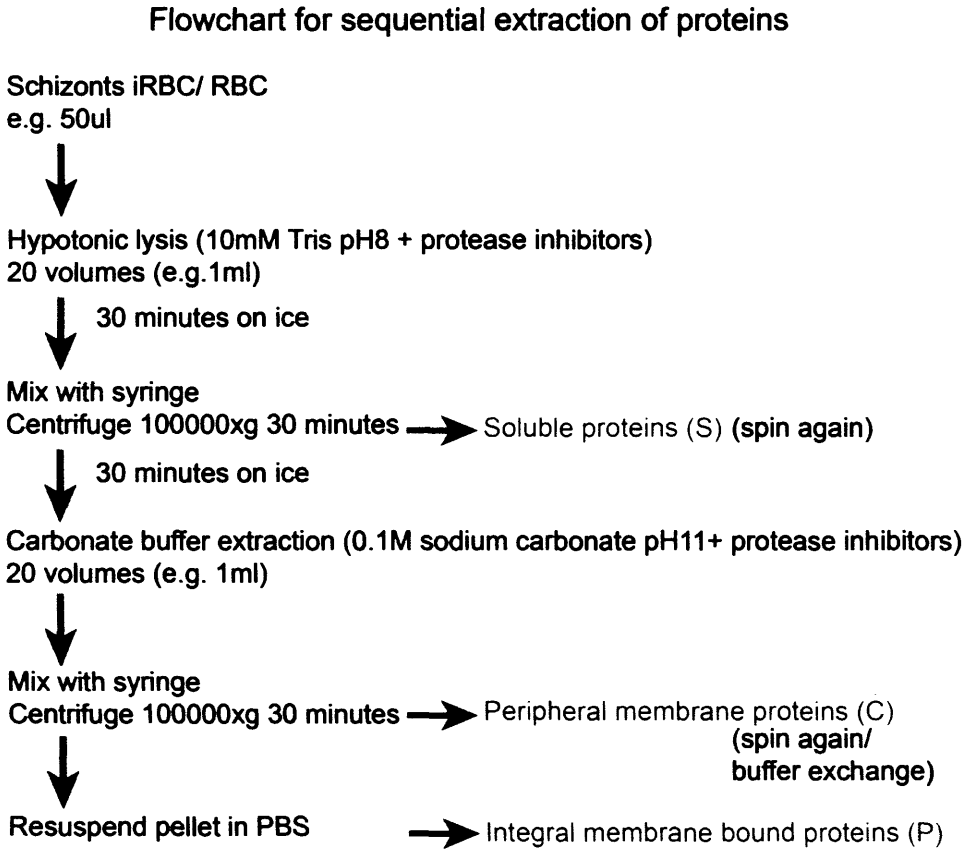

Figure 2.4: Flowchart showing sequential separation of iRBC proteins

2.19. Protein separation by SDS-PAGE

Samples (prepared as above) were loaded onto a NuPAGE™ 10 or 12% Bis-Tris Gel (1.0mm X 10/15 well) (Invitrogen). Proteins were run alongside 7µl 1X SeeBlue Plus2® pre-stained standard (Invitrogen).

Marker sizes (kDa):

188	
98	orange
62	
49	
38	
28	
17	red
14	
6	
3	

Gels were run in NuPAGE® 1X MES SDS buffer (Invitrogen) plus NuPAGE® antioxidant as per manufacturer's directions. Proteins were stained first by Coomassie brilliant blue R-250 staining solution (Biorad), before destaining in Coomassie R-250 1X solution (Biorad), as per manufacturer's instructions, until proteins became visible.

2.20. Detection of STEVOR by Western blot analysis

Proteins were electrophoretically transferred (1 hour at 30 Volts constant) from the gel onto Hybond C membrane (Amersham Biosciences) in NuPAGE ™ 1x transfer buffer (Invitrogen) containing 10% methanol and NuPAGE ™ antioxidant (Invitrogen). The membrane and bound proteins were incubated overnight at 4°C with agitation, in blocking buffer (PBS plus 5 % (w/v) skimmed milk powder (Marvel, Wirral, UK) and 0.05%

Tween 20). The membrane was washed three times for 10 minutes (all subsequent steps were at room temperature with agitation) in PBS with 0.05% Tween 20.

Primary antibodies/anti-STEVOR sera were diluted in PBS plus 1% BSA, 0.05% Tween 20, and strips of membrane were incubated with antibodies for 1 hour. The strips were then washed separately, 7 times for 5 minutes in PBS plus 0.05% Tween 20.

Secondary horse radish peroxidase-conjugated antibodies specific for either mouse or rabbit IgG (table 2.4), were used at 1 in 1000-2000 in PBS plus 0.05% Tween 20. After incubation for 1 hour, membrane strips were washed thoroughly 6 times, for 10 minutes in PBS/ Tween, followed by a 30-minute wash in PBS only.

The peroxidase was detected using Pierce 'Supersignal® west pico chemiluminescent substrate according to manufacturer's protocol. The membrane was exposed (various exposure lengths) to Kodak® Biomax MR single emulsion film and the film developed.

2.21. Localisation of STEVOR using indirect immunofluorescent assay (IFA)

Thin blood smears were made following late trophozoite/schizont development in cultures. Slides were fixed in 4°C acetone for 2 to 5 minutes, wrapped in foil and kept in sealed bags at -20°C with silica gel. Slides were allowed to reach room temperature before unwrapping. Wells were marked (on topside) using immunopen™ (Calbiochem), and permanent marker (underside).

A blocking step of 30 minutes with 20µl per well PBS, 3% BSA, and 0.05% NaN_3 was carried out prior to binding with anti-sera.

Primary antibodies (table 2.5) were diluted in PBS plus 1% BSA, and 0.05% NaN_3, (10µl per well), were added to the slides and incubated in a humid chamber for 1 hour at 37°C. The slides were washed in PBS three times for 5 minutes. After blotting off excess PBS, the appropriate secondary antibody (10µl per well) was added and incubated 30 minutes-1 hour at 37°C. All antibodies were added at separate incubation steps. The above

incubation and wash steps were repeated for subsequent primary antibody or secondary conjugated-antibody combinations. Slides were then dipped for 5 seconds in 4, 6-diamindino-2-phenylindole (DAPI) 2μg/ml in PBS to stain the parasite DNA. Finally, the slides were washed three times each for 5 minutes in PBS, before thoroughly air-drying. The wells were covered with a drop of Citifluor AF1 (Citifluor, London, UK) and coverslip. The edges were sealed with nail polish and slides stored in dark at 4°C. Slides were viewed on a fluorescence microscope: (100X oil objective) Deltavision (Applied Precision Inc) and camera (Roper Scientific) using SoftWoRx Explorer 1.0 software; or LSM 510 Confocal microscope (63X or 100 X oil objectives) (Zeiss) using LSM510 META software.

2.21.1. Percentage measurement from IFA slides of STEVOR expressing iRBC

Total parasites determined by DAPI staining to be mature schizont-stages were counted in the relevant wells, before switching the microscope to FITC staining in order to count the number of schizonts expressing STEVOR. The percentage of parasites expressing STEVOR was calculated as follows:

$$\frac{\text{Number of STEVOR positive parasites}}{\text{Total number of schizonts}} \times 100\%$$

Table 2.5) Primary antibodies used for STEVOR (co-) localisation studies

Host species	Antibody specificity	Dilution	Source
Mouse (B28)	PfSBP1	1 in 200 (IFA)	C. Braun-Breton, France
Rabbit W49/W50	Human RBC ghosts	1 in 1000 (FACS)	A.A. Holder NIMR, UK
Rabbit (Al) 3085	$MSP1_{19}$	1 in 1000 (IFA/FACS)	I. Ling NIMR, UK
Rabbit 1E1	$MSP1_{19}$	1 in 500 (IFA)	I. Ling NIMR, UK
Mouse 4E10 (mAb)	RhopH2	Use neat culture supernatant (IFA)	I. Ling NIMR, UK
Mouse	STEVOR peptide 1	1 in 2000 (Western)	NIMR, UK
Mouse	STEVOR peptide 2	N/a	NIMR, UK
Mouse	STEVOR peptide 3	N/a	NIMR, UK
Rabbit (8225/8226)	STEVOR peptide 1	1 in 20-80 (IFA)	Harlan Seralab, UK
Rabbit (8606/8607)	STEVOR peptide 2	1 in 20 (FACS)	Harlan Seralab, UK
Rabbit (8432/8433)	STEVOR peptide 3	1 in 20 (FACS)	Harlan Seralab, UK
Mouse	STEVOR PF10_0395 (S1)	1 in 100 (IFA)	NIMR, UK
Mouse	STEVOR PFF0850c (S2)	1 in 100 (IFA)	NIMR, UK
Rabbit (5003/5004)	STEVOR PF10_0395 (S1)	1 in 500 (Western) 1 in 200 (IFA)	P.R. Preiser, Singapore
Rabbit (5005/5006)	STEVOR PFF0850c (S2)	n/a	P.R. Preiser, Singapore

2.22. Localisation of STEVOR using Flow cytometry (FACS)

Cells ($1x10^7$) were first washed in sterile PBS (containing 0.5% BSA, 5 mM EDTA pH8.0 and 0.01% NaN_3) and pelleted by centrifugation at 800xg for 2 minutes. The cells were then incubated for 45 minutes with anti-sera (table 2.5), washed 3 times as described above, and incubated with the appropriate secondary FITC conjugated anti-IgG antibody (table 2.4), for 45 minutes. Unbound antibody was removed by washing 3 times as above, and the parasite DNA was labelled with Hoechst 33342 dye (50 µl at 10µg/ml in PBS) for 20 minutes.

After final 3 washes (as above), the cells were fixed in 1% paraformaldehyde in PBS. All antibody labelling was carried out in FACS tubes or 96-well microtitre plates (V-bottomed).

Flow cytometry was carried out on BD™ LSR (BD Biosciences) using Cell Quest software (Becton Dickinson, San Jose, CA, USA). Subsequent analysis was done using FlowJo version 6.2.1 software (Tree Star Inc, USA).

2.22.1. Live FACS and immunofluorescence studies of the iRBC surface

To make a thorough study of the localisation of STEVOR, it was necessary to study the surface of unfixed iRBC.

Two visualisation methods were used following identical staining protocols:

Parasite isolates were studied when the majority of parasites were ideally in late schizont-stage. The iRBCs were pelleted from culture by centrifugation at 800xg for 3 minutes the pellet was washed thrice with PBS plus 0.1% BSA wash buffer. Parasitaemia was then diluted with uninfected RBC to 5%, and the pellet resuspended at 5% haematocrit.

10µl of the iRBC/RBC suspension was placed per well in a round-bottomed 96-well plate, and 2.5µl of test serum (various dilutions) added to give a final test serum dilution of 1:5. Anti-sera to internal iRBC proteins were included in the assay to control for the

possibility of leakiness of the iRBC surface membrane. The reaction mixture was incubated for 1 hour at room temperature following which the cells were washed thrice with wash buffer, centrifuging between each wash to remove the wash medium. After washing, the cells were re-suspended in 50µl of secondary anti-mouse or rabbit IgG antibody, diluted in 0.1%BSA/PBS and containing 10µg/ml Ethidium bromide. After incubation for 30 minutes at room temperature, the cells were washed as previously.

Cells (100000) were collected on a FACscalibur™ using Cell Quest software (Becton Dickinson, San Jose, CA, USA) and analysed as above, or were examined by fluorescence microscopy by placing a drop of cells on a glass slide mixed with 50µl Citifluor AF1. Fluorescence staining of the cell surface was visualised with a fluorescence microscope: (100X oil objective) Deltavision (Applied Precision Inc) and camera (Roper Scientific) using SoftWoRx Explorer 1.0 software.

Chapter 3) Introduction: Bioinformatic analysis

The *stevor* multigene family was originally identified using a DNA probe, 7H8/6, containing a single full-length open reading frame originating from the *P. falciparum* Malayan Camp strain (Limpaiboon *et al.*, 1990). This probe hybridised downstream of the telomeric rep20 repetitive sequences on most of the 14 chromosomes (Oquendo *et al.*, 1986), as seen by multiple bands on Southern blots of gDNA. This hybridisation pattern varied between *P. falciparum* clones, suggesting the existence of variable *stevor* repertoires between parasites. This was later confirmed by the amplification of variable numbers of *stevor* genes in different parasite clones as detailed in chapter 1 (Cheng *et al.*, 1998).

The work of Cheng *et al.,* 1998 defined the sub-telomeric location, two-exon structure and multi-copy nature of the *stevor* gene family prior to publication of the complete *P. falciparum* genome and its annotation (Gardner *et al.*, 2002). When the sequence of the complete *P. falciparum* 3D7 genome was available, 28 *stevor*s were identified, along with a number of pseudogenes and gene truncations (Gardner *et al.*, 2002). Two larger multigene families were also annotated, including 59 *var* and 149 *rifs*. These three multigene families are arranged in two basic arrangements, on 24 of the chromosome ends, each gene cluster starting with a *var* gene (see table 3.1 and figure 1.6).

Table 3.1) Telomeric multigene family arrangements (Gardner *et al.*, 2002)

Importantly, *rif* and *var* are found in centrally located clusters, whilst *stevor* genes are exclusively found at telomeric ends.

The first exon is 66bp in length, encodes a secretory signal sequence and is conserved between gene family members. *Stevor*'s second exon is approximately 1kb in length and includes the most variable region. This HVR allows the differentiation of unique *stevor* genes whereas the N- and C-terminal regions are conserved or semi-conserved between *stevors*. *Stevor*s and *rifs* (along with other variant antigen families) share architectural similarities, in particular, being characterised by the presence of two transmembrane domains. However *stevor*s and *rifs* differ in that the HVR of *rif* is up to 300bp longer than the equivalent region in *stevor*. In both protein families, predicted transmembrane-spanning regions flank the HVR. Kyes *et al.*, 2001 predicted the HVR formed a loop on the iRBC surface, exposing it to the immune system and placing the remainder of the N-terminal and C-terminal within the iRBC cytoplasm (Kyes *et al.*, 2001). Immunologically distinct variant proteins exposed to the immune system on the iRBC surface are driven to diversify by cross-reactive immune responses (Recker *et al.*, 2004). Thus, the host positive pressure drives gene diversification of these protein-domain surface-targets. However nothing is known about the natural immune response to STEVOR, and indeed given the presence of a N-terminal signal sequence and two transmembrane domains, the classic protein secretion pathway would place the loop on the intracellular side of the iRBC membrane (Bock *et al.*, 2001).

Recent studies using microsatellite markers and extensive sequencing of *P. falciparum* isolates from different regions worldwide have identified single nucleotide polymorphisms (SNPs) and insertion-deletion (indels) polymorphisms. These are the main mechanisms generating polymorphism in *P. falciparum*, with indels providing at least as much polymorphism as SNPs (Volkman *et al.*, 2007a). SNPs were estimated to occur at a frequency of one every 446 bases across the genome (Volkman *et al.*, 2007b),

with an overall pairwise nucleotide diversity (π) $=1.16 \times 10^{-3}$. However, most of the variation (nucleotide diversity) occurs in small regions of high diversity corresponding with the genes in the gene ontology categories containing surface molecules involved in cytoadherence and antigenic variation (Ashburner *et al.*, 2000). In this regard, the individual genes with the greatest diversity were *var*, *rif*, and *stevor* genes (from $\pi = 1 \times 10^{-3}$ to $\pi = 6.1 \times 10^{-2}$).

African parasites are suggested to be the common ancestors of *P. falciparum* parasites worldwide in part because of their higher diversity (Wootton *et al.*, 2002). However there are important differences between the parasite genomes worldwide: Linkage disequilibrium was found to extend over much shorter distances in African parasite genomes, than Asian (Volkman *et al.*, 2007b). In addition, there is evidence, based on 137 genotyped SNPs, for different clades with substantial parasite population differentiation, between the African, Asian or American continental groups.

A study of *var* gene sequences in 12 Kilifi parasite-isolates, showed these African parasites had a comparable number of *var* genes to the fully sequenced *P. falciparum* 3D7 clone (Bull *et al.*, 2005). The 3D7 *var* genes were grouped into six types based on specific sequence features, and the Kilifi *vars* had a similar type distribution. A total of 878 non-identical *var* sequences were identified from these 12 parasite isolates with virtually no overlap between sequences from different isolates reported. A second study of *var* sequences from Amazonian parasite isolates indicated the expected repertoire size was again similar to the fully sequenced *P. falciparum* 3D7 genomic repertoire, and that the Amazonian *var* genes were most similar to *vars* isolated from other American isolates (Albrecht *et al.*, 2006). This study also estimated significant repertoire overlaps between the *rif* and *stevor* repertoires of the Amazonian isolates with the *P.falciparum* 3D7 genome. However, it is not known if field isolates will contain a similar number of *stevor*

to the *P. falciparum* 3D7 clone. Additionally a more extensive study of *stevor* from isolates worldwide is required in order to estimate global repertoire size.

Comparisons of long-term laboratory-adapted parasite cultures with recent isolates showed laboratory-adapted parasites are not significantly more or less divergent than recent isolates (Volkman *et al.*, 2007b). However, the *P. falciparum* isolate 3D7 was shown to have accumulated DNA in culture through insertions at a rate of +1nucleotide/kb (Jeffares *et al.*, 2007).

Nucleotide substitutions can either be synonymous, where no change occurs to the amino acid sequence of the protein, or non-synonymous, when the amino acid changes. Thus rapidly evolving proteins can be predicted using the ratio of non-synonymous (d_N) versus synonymous (d_S) nucleotide substitutions, where pressure to evolve results in a high d_N / d_S value. This ratio was used in an analysis of the *P. reichenowi* genome with *P. falciparum* 3D7 genome. Those genes, which had evolved furthest, as judged by significant excess of non-synonymous polymorphisms (amino acid changes), were those whose function is grouped in merozoite invasion or early ring formation (Jeffares *et al.*, 2007). In particular, predicted membrane-spanning proteins and exported proteins were also found to have evolved significantly more rapidly. This finding corresponds with a different study, which found that membrane-associated proteins accounted for more than 85% of all polymorphisms (Volkman *et al.*, 2002). In addition, rapidly evolving genes are characterised by their low expression levels and high expression duration i.e. expressed in multiple stages of the lifecycle (Jeffares *et al.*, 2007).

Var, *rif*, and *stevor* genes all meet the criteria for rapidly evolving proteins (as demonstrated by the high rate of amino acid evolution). This evolution is predicted to be as a result of strong immune-mediated diversifying selection (Mu *et al.*, 2005; Trimnell *et al.*, 2006).

Extensive sequencing of other *P. falciparum* parasites including a Ghanaian clinical isolate (8x coverage), the IT isolate (current sequencing and 1x coverage), and the closely-related parasite *P. reichenowi* (partial genome shotgun sequencing), now facilitate the further exploration of the *stevor* multigene family in these parasites (www.sanger.ac.uk/Projects/Protozoa/).

Objectives

1) **Characterisation of *stevor* through comparison with *rifs***
2) ***Stevor* expression, a comparison of laboratory and field parasite isolates**
3) **Characterisation of *stevor* sequence diversity, and comparison of laboratory and field parasite isolates**
4) **Predicting protein function using RIFIN based studies as a model**

Results

3.1. Characterisation of *stevor* through comparison with *rifs*

The *rifs* and *stevors* have recently been classified as a super family, due to structural similarities between the two gene families (Cheng *et al.*, 1998). Before comparing the genomic structure of these two gene families, it was important to identify the distinct and conserved regions. This was carried out using an alignment of STEVOR and RIFIN amino acid sequences taken from the annotated *P. falciparum* 3D7 plasmodb database (Bahl *et al.*, 2003; Gardner *et al.*, 2002).

Bootstrap consensus trees were generated at bootstrap values of 99% and STEVOR and RIFIN families were classified as two distinct sub-groups (figure 3.1a). In addition, when the two families are aligned before performing a profile alignment at 84% consensus, the RIFINs form two sub-groups (figure 3.1b, purple and green) defined by the presence of a consensus peptide sequence, KEL (X_{15}) IPTCVCR approximately 100 amino acids from the N-terminus in one of the RIFIN sub-groups.

Interestingly, this additional 25 amino acid insert results in the addition of two cysteines in the RIFIN proteins, which are also present in STEVORs (figure 3.2 arrows 1 and 2). A total of 6 cysteines are conserved between the STEVORs and RIFINs (black arrows 1-6). RIFINs usually contain 10 cysteines in total, whereas STEVORs contain 8 cysteines. Both STEVOR and RIFIN have the highest number of cysteines within the N-terminal region of the protein, and despite the HVR size difference both HVRs contain between 2 and 4 cysteines in this region. The major difference in cysteine distribution lies in STEVORs having two cysteines in the extreme C-terminal domain not present in RIFINs. This may be indicative of differences in orientation and/or function between the two groups of proteins, as cysteines can facilitate di-sulphide bonds, which are important for tertiary structure.

Figure 3.1: 26 STEVOR and 114 RIFIN amino acid sequences were aligned in Clustal X® and bootstrapped. Bootstrapping is a test of reliability of the phylogenetic analysis; multiple random sampling (500 sets) from the original dataset creates pseudo-datasets of an identical size to the input dataset. New trees are then generated from the pseudo-datasets, and the frequency with which a branch remains in an identical position gives the bootstrapping value for that particular branch. Consensus neighbour joining un-rooted phylogenetic trees were constructed in MEGA3, and bootstrapped to evaluate the validity of the phylogeny.

A) 99% consensus B) Radiation-format tree showing all branches. Groupings were identified manually STEVOR pink squares, RIFIN purple squares (sub-type 1) and green squares (sub-type 2).

A

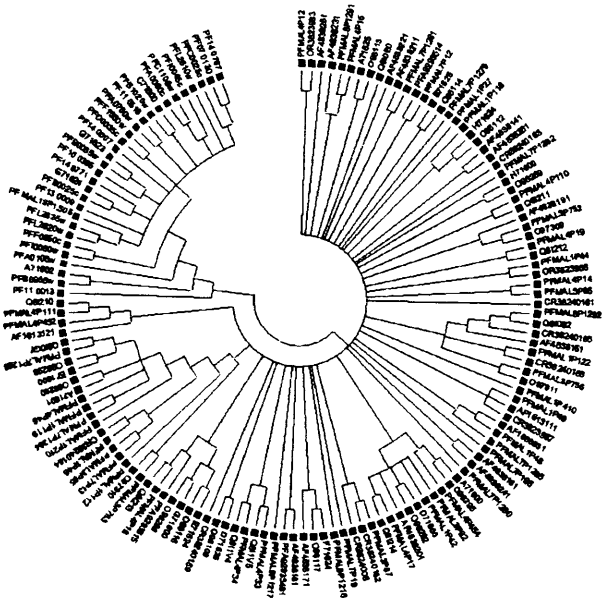

B

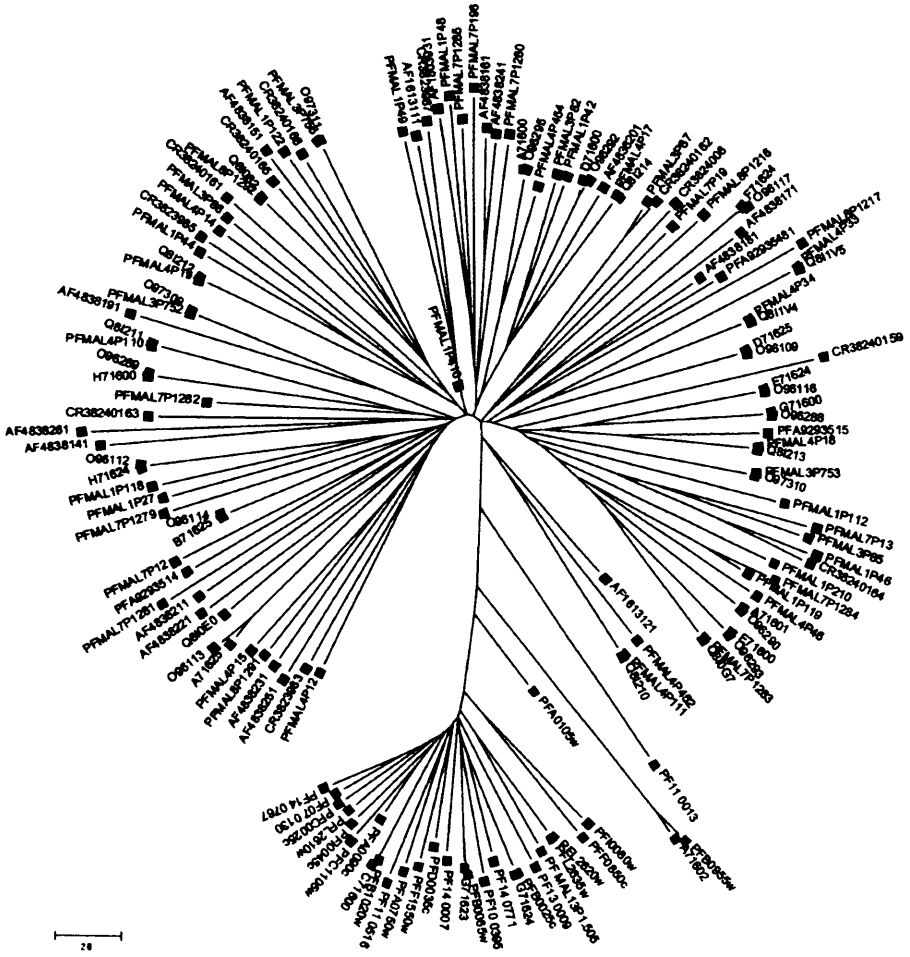

Figure 3.2: Schematic of conserved features in STEVOR and RIFIN proteins

N-terminal signal sequences are shown in grey including a canonical signal sequence (encoded by exon 1) and Plasmodium exported element/vacuolar transport signal (PEXEL/VTS) sites. Predicted transmembrane domains are shown in black (TM1/2). Putative apical organelle targeting motifs (YLIL/YIWL) are identified in the C-terminal region following the TM2. Percentage similarity data are taken from a review from (Kyes et al., 2001).

Cysteines are marked (C): Black arrows indicate those cysteines that are conserved in at least 75% of proteins. Dark grey arrows indicate cysteines conserved in at least 50% of proteins. Light grey arrows indicate cysteines conserved in less than 25% of proteins. Cysteines 1-6 are highly conserved at a structurally equivalent site in both STEVORs and the majority of RIFINs. Proteins are shown to scale (1cm equals 16 amino acids). Amino acid position is based on an alignment of the complete P. falciparum *3D7 STEVOR and RIFIN repertoires (www.plasmodb.org).*

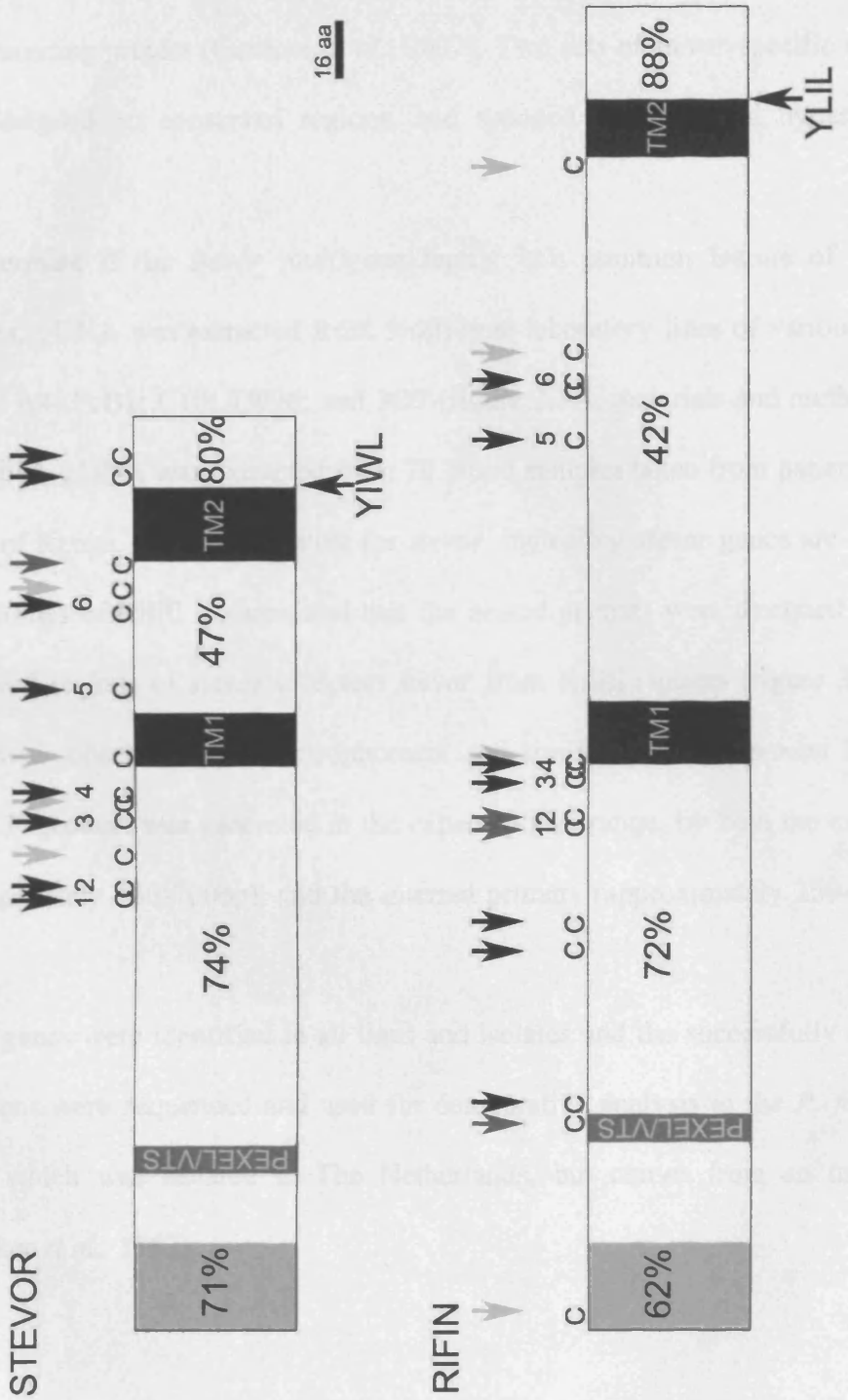
16 aa
STEVOR
RIFIN
PEXEL/VTS
TM1
TM2
74%
47%
80%
71%
72%
42%
88%
62%
YIWL
YLIL
1 2 3 4 5 6

3.2. DNA analysis of the *P. falciparum stevor* multigene family comparing laboratory strains and Kilifi isolates

A detailed study of *stevor* in the *P. falciparum* clone 3D7 was possible using data from the sequencing project (Gardner *et al.*, 2002). Two sets of *stevor*-specific nested primers were designed on conserved regions, and spanned the predicted hyper-variable loop region.

To determine if the *stevor* multigene family is a common feature of *P. falciparum* parasites, gDNA was extracted from 5 different laboratory lines of various geographical origins: A4; FcB1; C10; T9/96; and 3D7 (figure 3.3A, materials and methods table 2.1). In addition, gDNA was extracted from 70 blood samples taken from patients in the Kilifi region of Kenya. All were positive for *stevor*, indicating *stevor* genes are also present in the genomes of Kilifi isolates, and that the nested primers were designed to sufficiently conserved regions of *stevor* to detect *stevor* from Kilifi isolates (figure 3.3B). Multiple bands were observed after electrophoresis, and similar to *P. falciparum* 3D7 more than one PCR product was generated in the expected size range, by both the external primers (approximately 550-700bp), and the internal primers (approximately 250-350bp) (figure 2.1).

Stevor genes were identified in all lines and isolates and the successfully amplified PCR amplicons were sequenced and used for comparative analysis to the *P. falciparum* 3D7 clone, which was isolated in The Netherlands, but comes from an unknown origin (Walliker *et al.*, 1987).

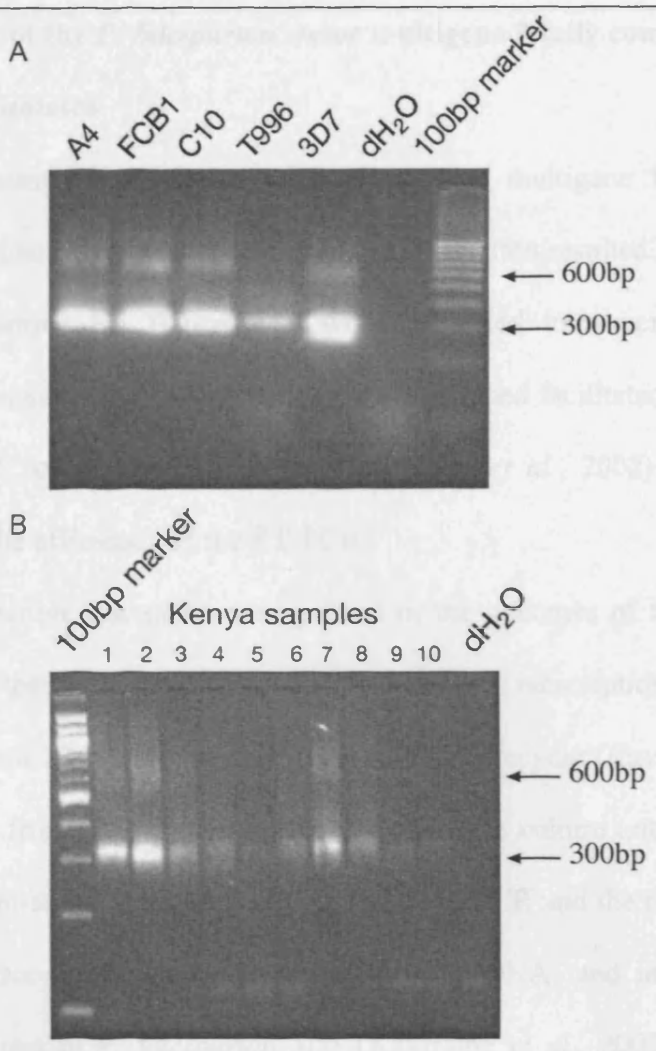

Figure 3.3: Agarose gel showing PCR products obtained from laboratory parasite and from Kilifi parasite isolates' gDNA

Gel electrophoresis of nested stevor PCR products from genomic (g)DNA extracted from A) 5 representative P. falciparum *laboratory clones: A4; FcB1; C10; T9/96; and 3D7 or B) 10 representative parasite isolates from Kilifi. 5µl of each product was loaded onto a 2.5% agarose gel. Results show two amplicons in the expected size ranges, products carried over in the nested PCR-step from the external PCR (approximately 600bp) with primers smf1 and smr1, and internal PCR products (approximately 300bp) from primers RepF1/2 and RepR. 100bp marker (Fermentas). dH_2O = negative control containing sterile water instead of template DNA.*

3.3. RNA analysis of the *P. falciparum stevor* multigene family comparing laboratory strains and Kilifi isolates

RT-PCR for measuring transcription of *P. falciparum* multigene families is difficult because of contamination by gDNA. Here, nested PCR often resulted in the amplification of gDNA (see sample K5 figure 3.4), which required improvement for RT-PCR. Therefore an additional single step primer set was designed facilitated by the publication of the complete *P. falciparum* 3D7 genome (Gardner *et al.*, 2002). This modification greatly improved the efficiency of the RT-PCR.

Following confirmation that *stevor* was present in the genomes of the Kilifi isolates, I wanted to confirm that these parasites transcribed *stevor*. Transcription of *stevor* has been shown to occur from 22 hours onwards in the asexual lifecycle (Kaviratne *et al.*, 2002); therefore parasites from the Kilifi isolates were grown in culture until they reached late trophozoite/schizont-stages, before RNA isolation, RT-PCR and the resulting cDNA was sequenced. As observed following amplification of gDNA, and in concordance with previous observations in *P. falciparum* 3D7 (Kaviratne *et al.*, 2002), several RT-PCR products were observed after electrophoresis (figure 3.4), indicating that more than one *stevor* transcript is present in both *P. falciparum* laboratory and Kilifi parasite populations at one time.

Figure 3.4: Agarose gel showing RT-PCR products from RNA extracted from laboratory and Kilifi parasite-isolates

Gel electrophoresis of nested stevor RT-PCR products from RNA extracted from A) 4 P. falciparum *laboratory clones 3D7, T9/96, FcB1 and D10, or B) 12 representative* P. falciparum *Kilifi isolates. 5µl of each product was loaded onto a 3% Metaphor agarose gel. Results show two amplicons, products carried over from the external PCR (approximately 600bp) with primers smf1 and smr1, and internal PCR products (approximately 300bp) from primers RepF1/2 and RepR. (+) Sample contained reverse transcriptase. Negative control (-) contained sterile water in place of enzyme. 100bp marker (Fermentas). dH2O = negative control containing sterile water instead of template RNA +/- reverse transcriptase.*

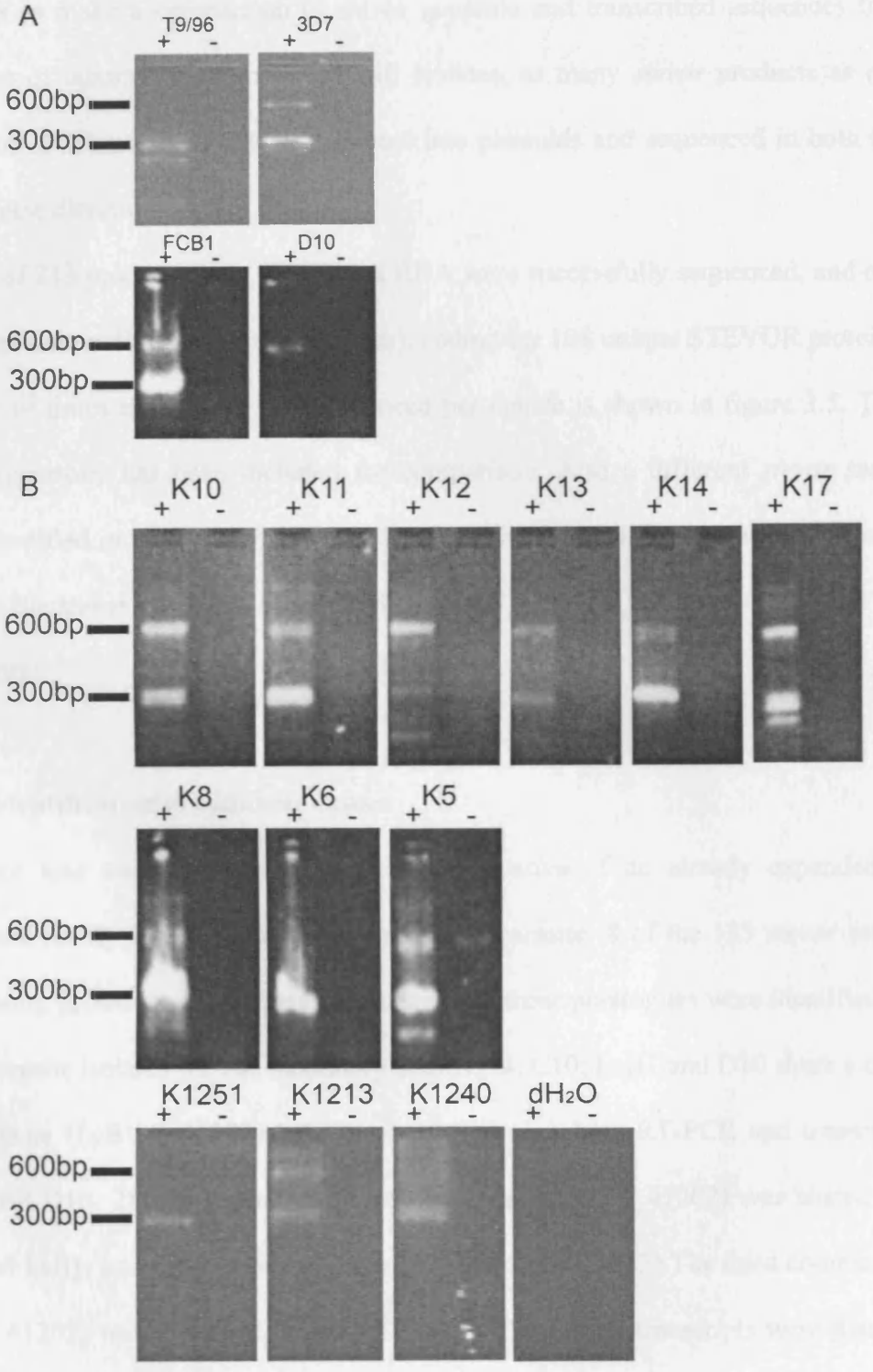
A
T9/96
+ -
3D7
+ -
600bp
300bp
FCB1
+ -
D10
+ -
600bp
300bp
B
K10
+ -
K11
+ -
K12
+ -
K13
+ -
K14
+ -
K17
+ -
600bp
300bp
K8
+ -
K6
+ -
K5
+ -
600bp
300bp
K1251
+ -
K1213
+ -
K1240
+ -
dH2O
+ -
600bp
300bp

3.4. Characterisation of *stevor* sequence diversity, and comparison of laboratory and field parasite isolates

In order to make a comparison of *stevor* genomic and transcribed sequences from the genomes of laboratory strains and Kilifi isolates, as many *stevor* products as possible from both PCR and RT-PCR were ligated into plasmids and sequenced in both forward and reverse directions.

A total of 213 products from gDNA and RNA were successfully sequenced, and of these, 133 were unique DNA sequences (alleles), coding for 108 unique STEVOR proteins. The number of times each allele was sequenced per isolate is shown in figure 3.5. The 3D7 *stevor* repertoire has been included for comparison. Also 6 different *stevor* sequences were identified in the *P. falciparum* 3D7 isolate from the NIMR that were different from those in the *stevor* repertoire of the published 3D7 genome (3D7_1-3_41202 and 3D7_1-3_181202).

3.4.1. Identification of common *stevors*

Evidence was sought for common stevors indicative of an already expanded stevor multigene family in the *P. falciparum* ancestral parasite. 8 of the 133 *stevor* sequences were found in more than one parasite isolate, 4 of these paralogues were identified in 3 or more parasite isolates. 1) The laboratory strains A4; C10; FcB1 and D10 share a common *stevor* gene (FcB1_2_41202), which was also detected by RT-PCR and transcribed in FcB1 and D10. 2) The second common *stevor* gene (A4_1_41202) was shared by A4, C10 and FcB1, and again was transcribed in the FcB1 clone. 3) The third common *stevor* (A4_4_41202) was identified in A4; C10 and T9/96 but no transcripts were detected by RT-PCR. 4) The fourth common *stevor* (A4_4_41202) was identified in A4; C10 and T9/96 isolates. Interestingly, although these four genes were found in multiple clones from the laboratory parasites, they were not detected in any of the Kilifi isolates.

The four other paralogues were each shared by just two isolates, two were shared only by laboratory lines: T9/96 or A4, with 3D7: 1) T9/96+14_190903 identical to 3D7_2_41202, or 2) A4_1_170105 identical to 3D7_1_181202. 3) A Kilifi isolate sequence, K1640_1_BD141105 is identical to PFL2610w from the *P. falciparum* 3D7 genome and is the only *stevor* shared between a laboratory line and a Kilifi isolate. A large number of *stevor* sequences were found in the Kilifi isolates, but only one *stevor* sequence was found present in more than one isolate. This particular sequence was transcribed in both the parasites K11 and K14: 4) sequences K11+_1111104 and K14+_2_111104.

Figure 3.5: Number of times each stevor *allele was identified per parasite isolate.*

The stevor *HVRs were amplified, cloned and sequenced from parasite DNA and RNA. Graphs A and B) Clones derived from DNA have solid coloured bars those from RNA are indicated by hatched coloured bars (Graph C shows transcribed (+) sequences only). Parasite isolates are shown in different colours below the graph. The sequence name is denoted along the x-axis, each sequence has a unique identifier consisting of the parasite isolate (+ if amplified from RNA), clone number and date. The number of clones per sequence is shown on the y-axis.* P. falciparum *3D7 genomic* stevor *sequences are included for comparison (solid black).*

A)

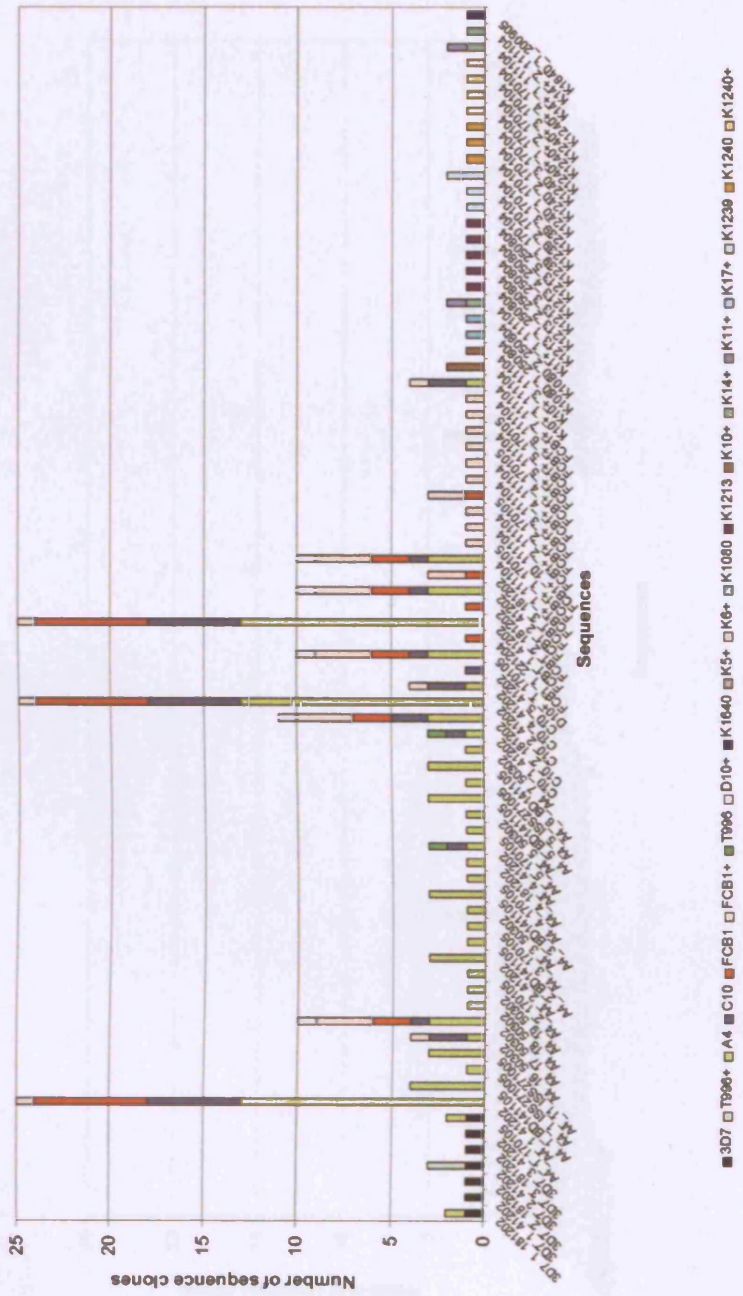
Number of sequence clones
25
20
15
10
5
0
Sequences
3D7 T996+ A4 C10 FCB1 FCB1+ T996 D10+ K1640 K5+ K6+ K1080 K1213 K10+ K14+ K11+ K17+ K1239 K1240 K1240+

B)

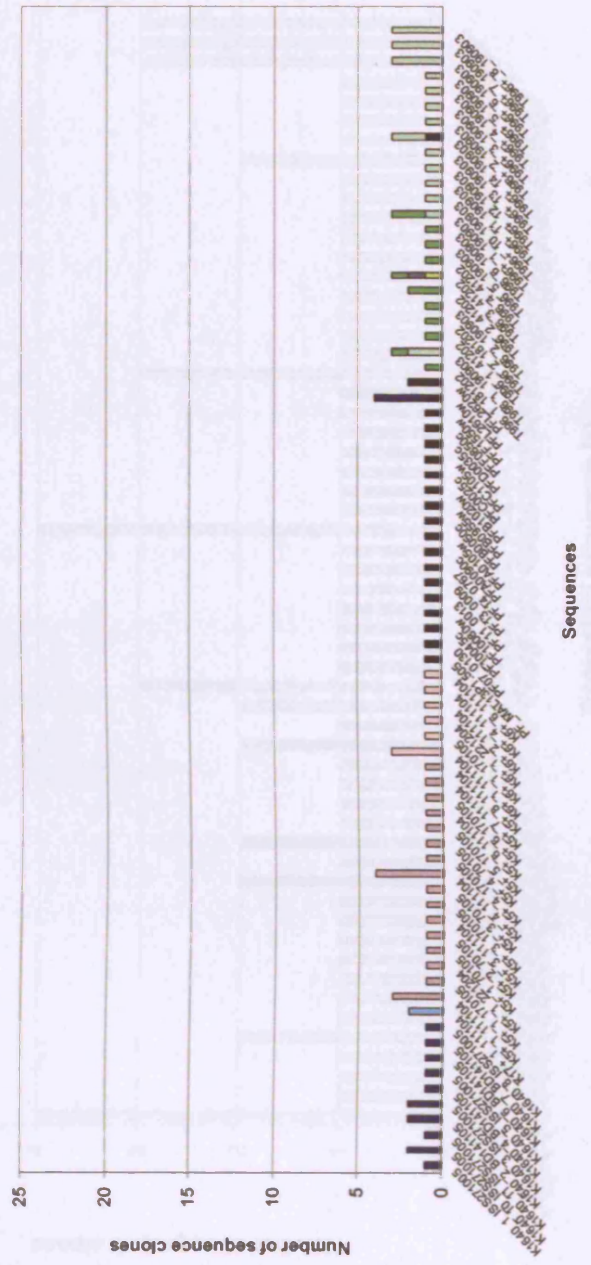

C)

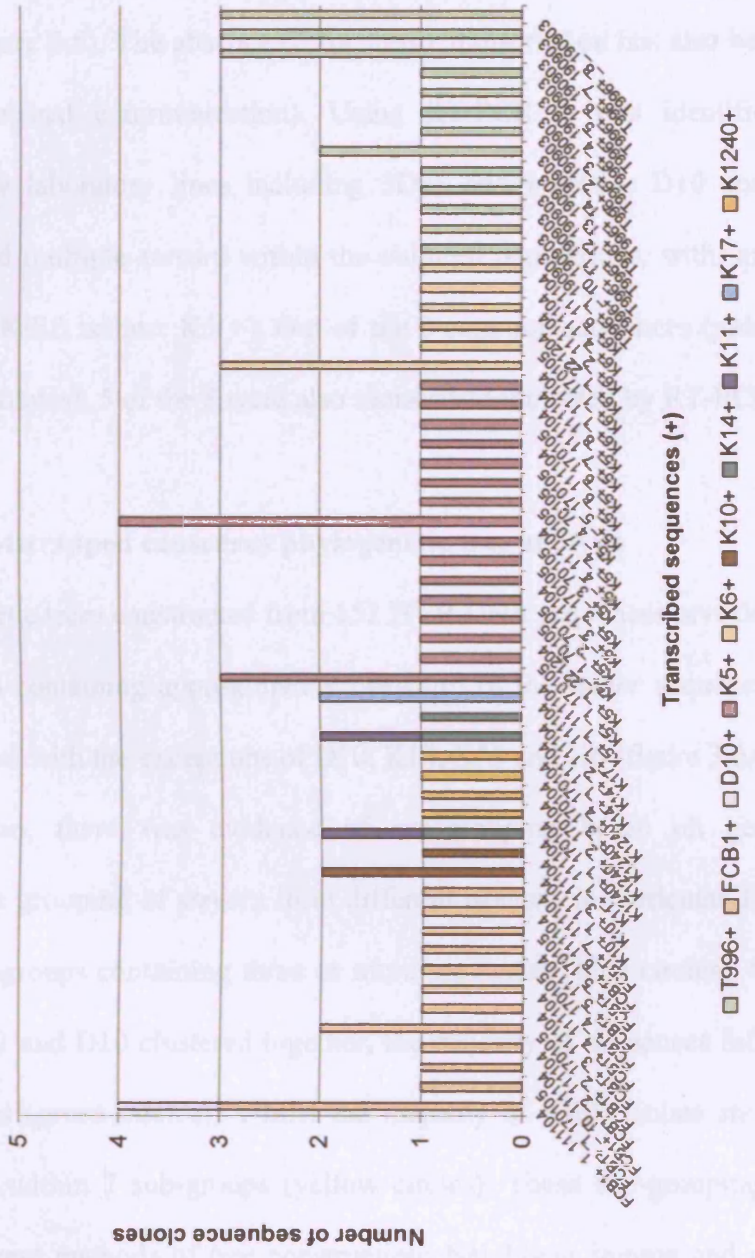
Number of sequence clones
0
1
2
3
4
5
Transcribed sequences (+)
T996+
FCB1+
D10+
K5+
K6+
K10+
K14+
K11+
K17+
K1240+

3.4.2. Repertoire of transcribed *stevor* genes

Interestingly, *stevor* was transcribed in all *P. falciparum* strains shown, with the exception of the parasite clone A4, which did not transcribe *stevor,* as no RT-PCR products were detectable, however, the A4 genome contains at least 15 different *stevor* genes (figure 3.5). The absence of A4 *stevor* transcription has also been observed by Sue Kyes (personal communication). Using RT-PCR it was identified that several *P. falciparum* laboratory lines including 3D7; T9/96; FcB1; D10 and 16 Kilifi isolates transcribed multiple *stevors* within the cultured populations, with up to 10 *stevor* genes from one Kilifi isolate: K5(+). Out of the 8 common sequences (present in two or more parasite isolates), 5 of the 8 were also transcribed (detected by RT-PCR).

3.4.3. Bootstrapped consensus phylogenetic tree analysis

Phylogenetic trees constructed from 152 HVR DNA sequences revealed overall, one large sub-group containing approximately one-third of the *stevor* sequences, with all isolates represented with the exceptions of D10, K14, K11 and K6 (figure 3.6A).

In addition, there was evidence of sub-grouping based on geographical regions, significant grouping of *stevor*s from different isolates, in particular T9/96 *stevors* formed three sub-groups containing three or more sequences (blue circles). Sequences from A4, C10, FcB1 and D10 clustered together, the majority of sequences falling within just four sub-groups (green circles). Whilst the majority of Kilifi isolate *stevor* sequences were contained within 7 sub-groups (yellow circles). These sub-groupings are present using two different methods of tree construction: Neighbour joining and minimum evolution, and are conserved at 95% significance bootstrap values. The complete *P. falciparum* 3D7 *stevor* repertoire is included in the tree for comparison, and these are distributed throughout the entire trees (pink).

Figure 3.6: Unrooted A) neighbour-joining and B) minimum evolution 95% consensus phylogenetic trees of 152 HVR stevor *alleles*

Trees are based upon a nucleotide alignment of the HVRs and condensed to show only those branches with a bootstrap value of 95% significance and above. Sequences are colour coded according to originating isolate: Kilifi-yellow; T9/96-dark blue; 3D7-pink; A4 and C10-green; FcB1-light blue; D10-light green.

Orange open-circle around a branch point indicates the major stevor *sub-grouping, blue open-circles highlight T9/96 sub-groups, green open-circles highlight sub-groupings including FcB1, C10 and A4 sequences, yellow open-circles highlight Kilifi sequence sub-groupings.*

A
Neighbour joining

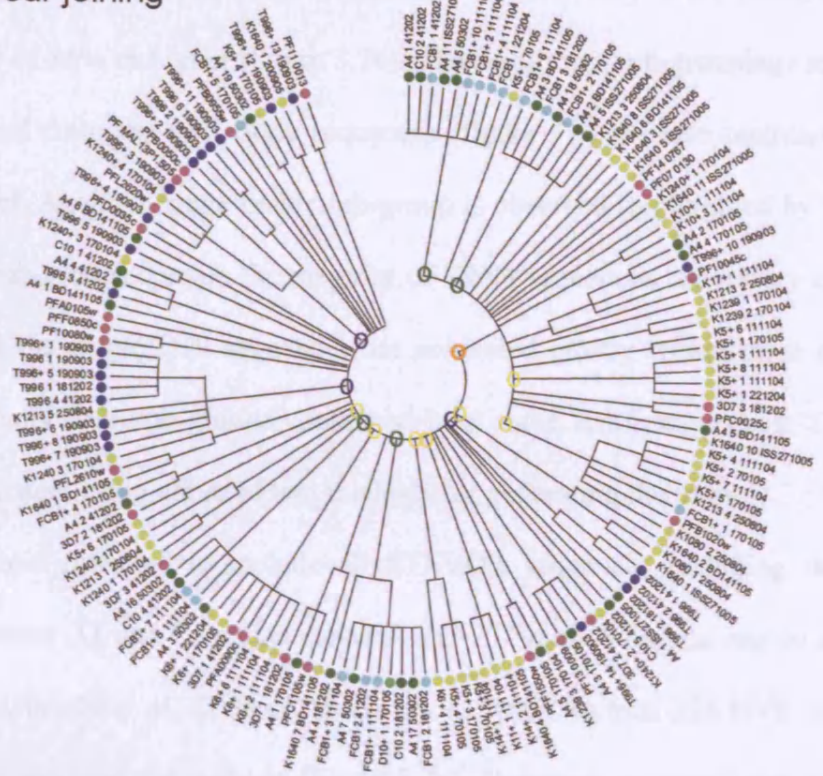

B
Minimum evolution

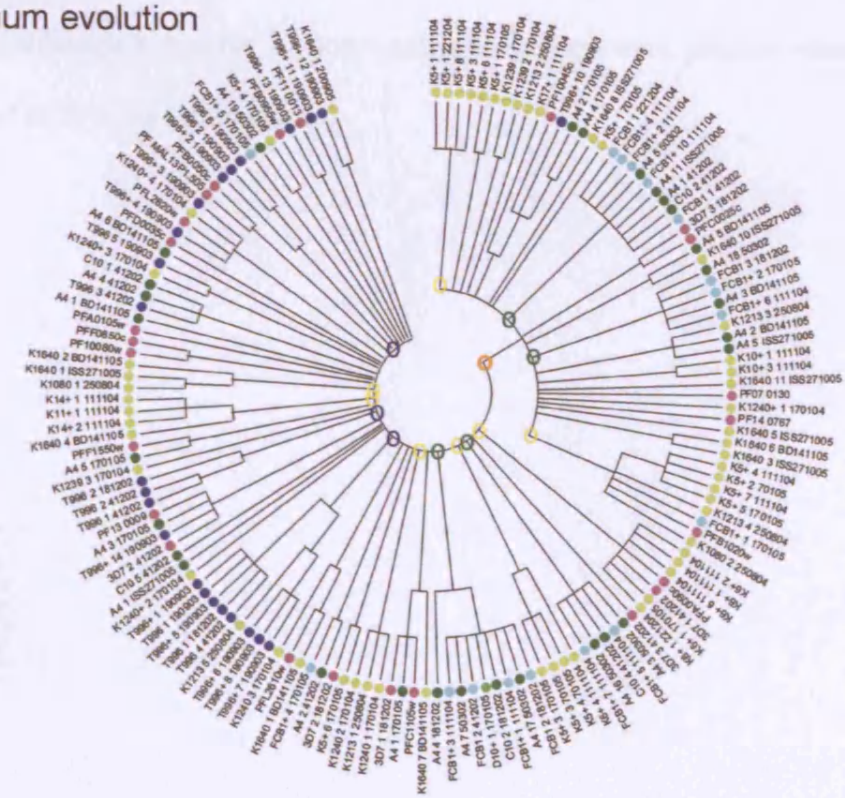

Phylogenetic trees of 108 unique STEVOR amino acid sequences reveal firstly a trend for sequences of the same geographical region to be more closely related, seen most clearly in figure 3.7a. These trees were then condensed to show only those branches with a bootstrap value of 85% or higher (figure 3.7b). The significant sub-groupings seen within the trees inferred from the nucleotide sequences (figure 3.6) are also maintained at the amino acid level. Again, a single major sub-group is observed (highlighted by an orange circle). Three sub-groups contain the majority of T9/96 sequences, laboratory clones A4, C10, FcB1 and the single D10 sequences are contained mostly within three other sub-groups, and finally four sub-groups contain at least three Kilifi sequences. These sub-groups are consistent using either of two methods for generating the trees.

This analysis was extended to include all STEVOR sequences including those from published databases (IT and Ghanaian isolates) and 75 South American region sequences obtained from Albrecht *et al.,* 2006 (Albrecht *et al.*, 2006). In total 226 HVR amino acid sequences were used for the analysis (figure 3.7c). However, no significant sub-groups were present, although a number of non-significant groups were present when the tree was condensed at 50% bootstrap values.

Figure 3.7: Unrooted phylogenetic trees using neighbour-joining and minimum evolution methods A) showing all branches and B) 85% condensed trees using 108 amino acid sequences C) 50% condensed tree using 226 amino acid sequences.

Trees are based upon an alignment of the HVRs then condensed to show only those branches with a bootstrap value of 85% or 50% significance and above. Sequences are colour coded according to originating isolate: Kilifi field isolates-yellow; T9/96-dark blue; 3D7-pink; A4 and C10-green; FcB1-light blue; D10-light green, IT-black, Ghanaian field isolate-red.

Orange open-circle indicates a major stevor *sub-group, blue open-circles highlight T9/96 sub-groups, green open-circles highlight sub-groupings including FcB1, C10 and A4 sequences, yellow open-circles highlight Kilifi sequence sub-groupings.*

A

Neighbour joining

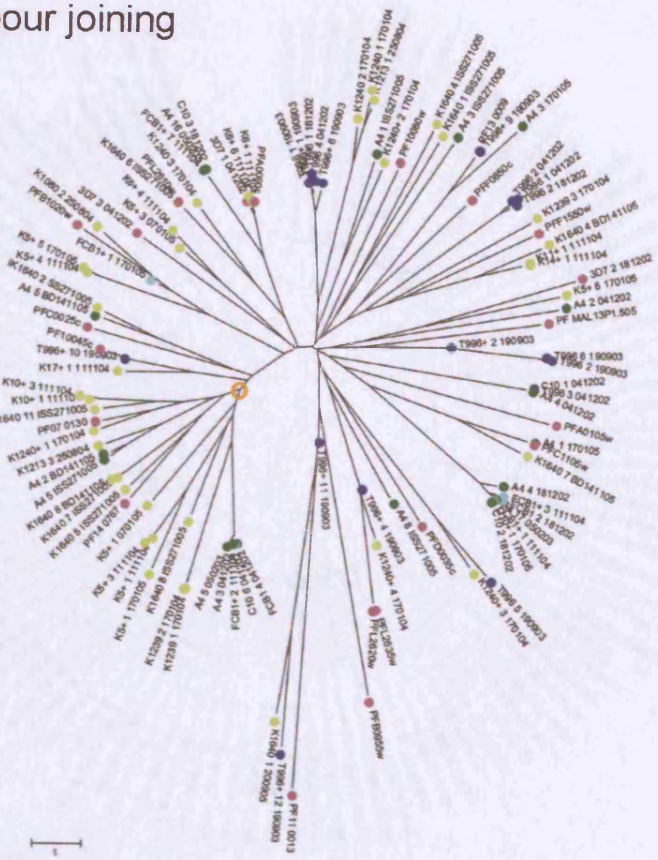

Minimum evolution

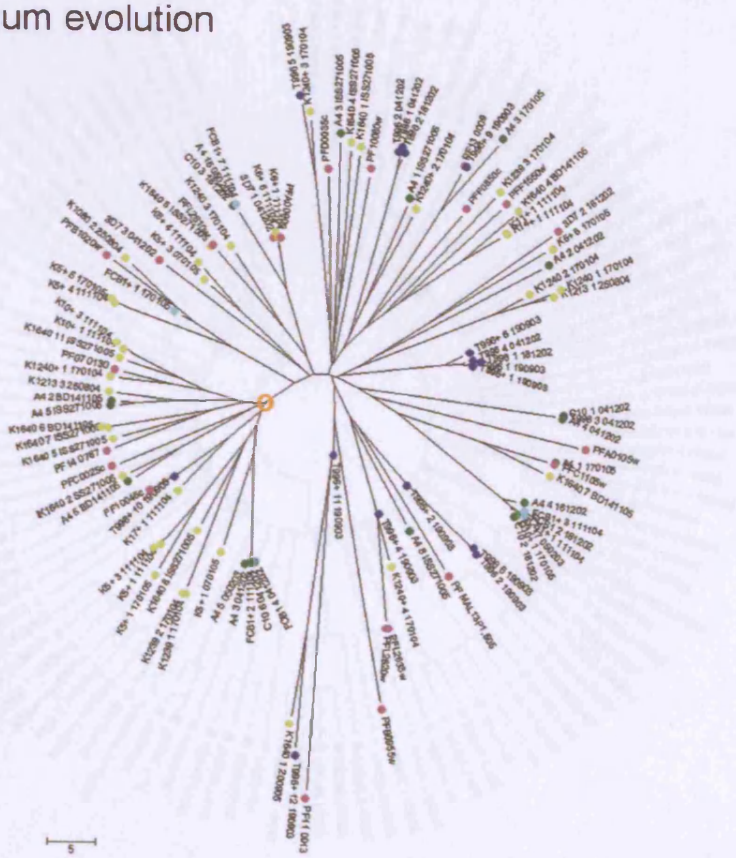

B

Neighbour joining

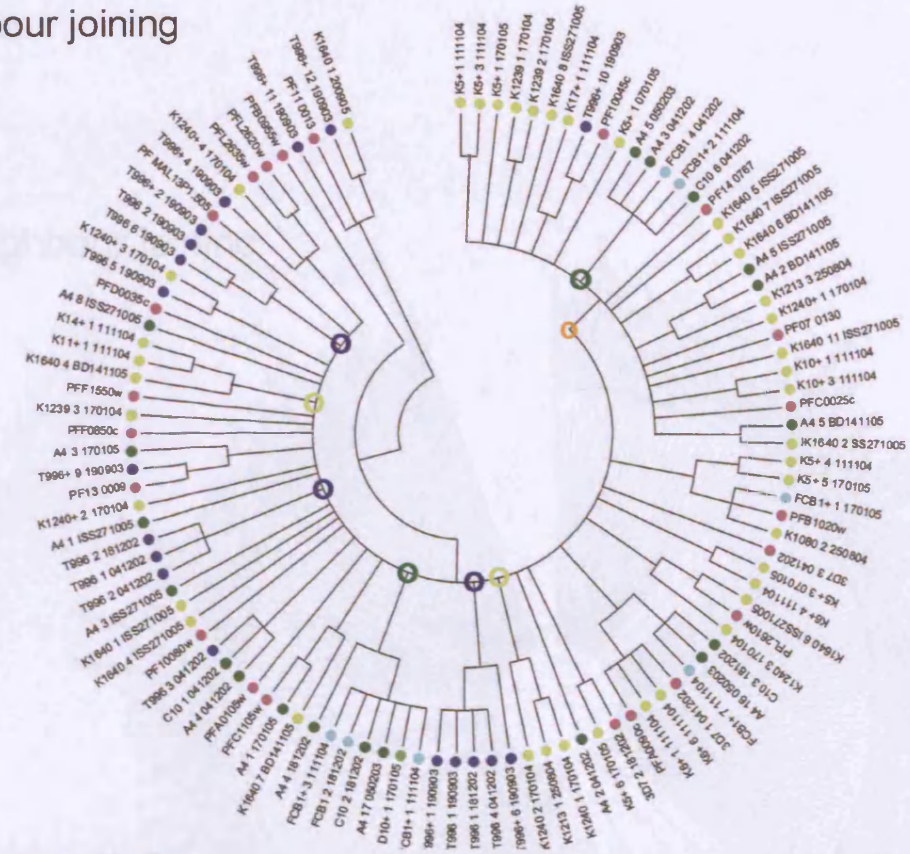

Minimum evolution

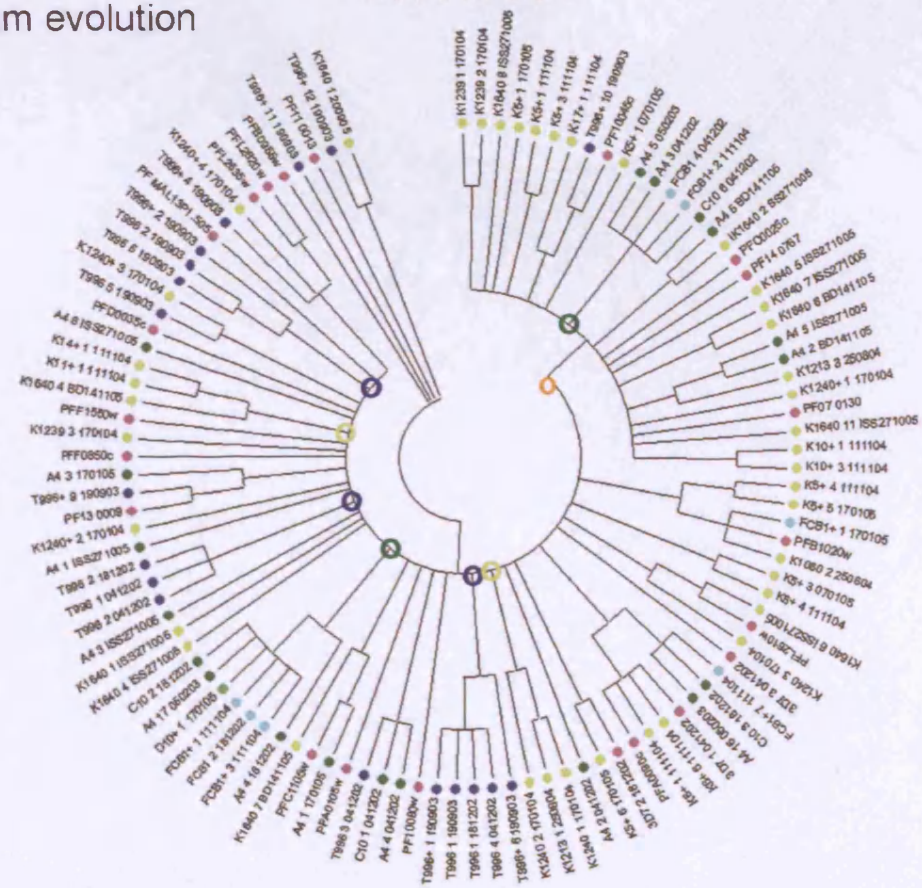

C
Neighbour joining

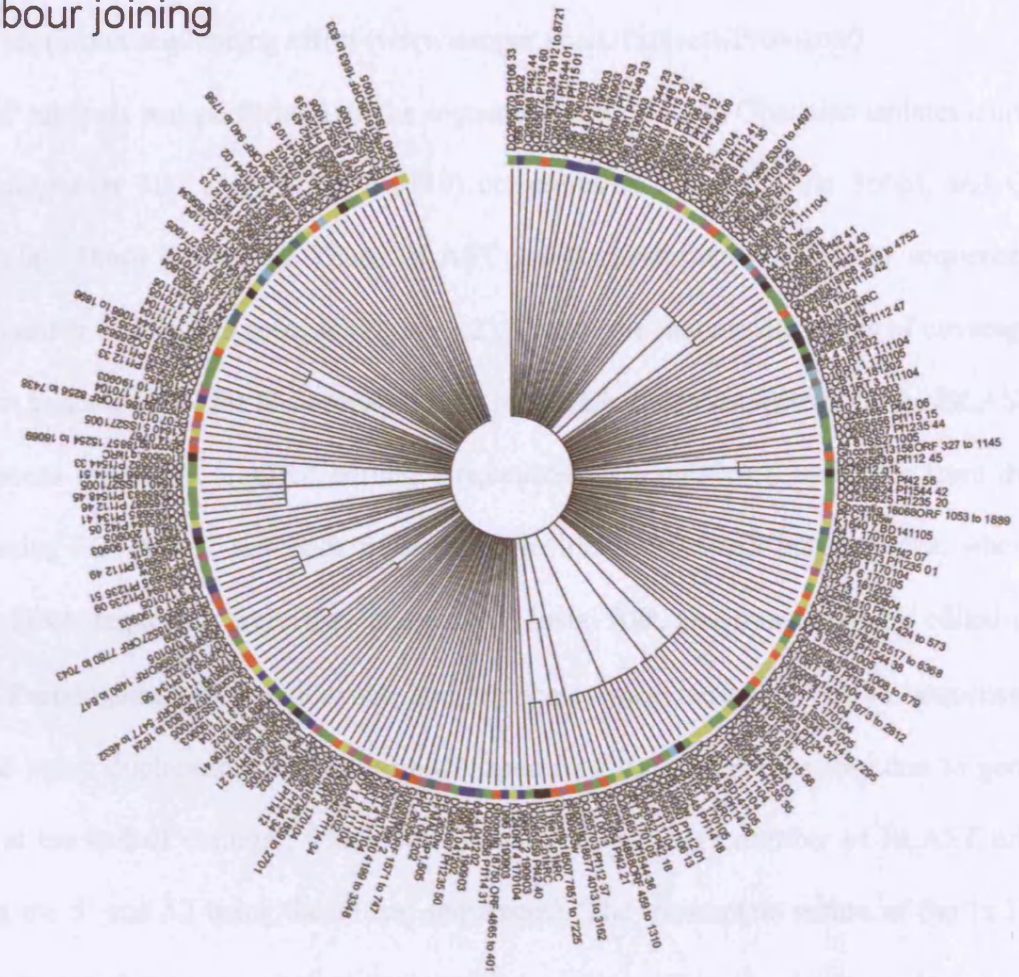

To determine the size of the *stevor* multigene family in isolates other than *P. falciparum* 3D7, data for *stevor* genes have been gathered from the genomes of 3 sequenced *P. falciparum* isolates: 3D7, Ghanaian, and IT (table 3.2). *Stevor* sequence data was derived from the *P. falciparum* genome project (www.plasmodb.org) and Wellcome Trust Sanger Institute protozoan sequencing effort (www.sanger.ac.uk/Projects/Protozoa/).

A BLAST analysis was performed on the sequences of the IT and Ghanaian isolates using the *P. falciparum* 3D7 *stevor* (PF07_0130) conserved N-terminal (first 36bp), and C-terminal (last 38bp) sequences. These BLAST searches returned only *stevor* sequences and the number of hits was recorded (table 3.2). Due to the incomplete status of coverage of the two genomes, (1x for IT compared with 8x for Ghanaian respectively), the BLAST hit sequences recovered required editing. Sequences were recovered manually from the contigs using 3D7 *stevor* sequence information to identify the full-length genes, where possible. DNA sequences were then aligned in Clustal X®, and translated and edited in BioEdit. Pseudogenes, short sequences, and duplicates were removed. The IT sequences contained many duplications and incomplete open reading frames (possibly due to gene location at the end of contigs), which was reflected by the high number of BLAST hits (41 using the 5' and 52 using the 3' end sequences). The incomplete nature of the 1x IT coverage means that many smaller unassembled contigs are in the database. Increased coverage would allow these to be assembled into fewer (larger) contigs, directly reducing the number of incomplete open reading frames.

Table 3.2) *Stevor* identification in genomic databases

Database searched	BLAST hits 5' (36bp)	BLAST hits 3' (38bp)	STEVOR minus short /edited	STEVOR minus pseudogenes	STEVOR minus duplicates
Ghanaian	13	38	26	25 (full-length)	25
IT	54	107	99	41 (5') 52 (3')	17

26 *stevor* sequences were identified in the Ghanaian isolate genome, two of these nucleotide sequences resulted in the same amino acid sequence STEVOR. 26 genes are comparable with the 28-stevor genes in the *P. falciparum* 3D7 genome. A total of 17 unique *stevor* sequences were identified in the IT genome, none of which gave the same amino acid sequence. Therefore a total of 25 Ghanaian, and 17 IT-isolate STEVOR-sequences were used in the analysis.

3.5. Other malaria genomic data: *P. reichenowi* and *P. gallinaceum*

A simian malaria *P. reichenowi,* the most closely related parasite species to *P. falciparum*, had a total of 8 *stevor* sequences, all of which were found in the *P. reichenowi* database following BLAST searching using the degenerate internal primer sequences (RepF1/2 and RepR, table 2.2). All sequences were translatable and between 651-672bp in length and therefore on average 300 nucleotides shorter than *P. falciparum* 3D7 *stevor*.

In a tree based on the exon 2 sequences only, *P. reichenowi stevor* genes cluster together in two groups (orange circles) and were distributed throughout the tree (figure 3.8). This suggests *P. reichenowi stevors* are more similar to each other than to *P. falciparum stevors*. They are shorter missing the most N-terminal end of exon 2, indicating the N-

terminal region is not functionally conserved between *P. falciparum* and *P. reichenowi*. This could also be due to the genome coverage of the *P. reichenowi* clone and greater coverage may reveal full-length *stevors*.

Although the *P. falciparum* origin has been suggested along with *P. reichenowi* to share a common ancestor with avian parasites (Escalante *et al.*, 1998), no *stevors* were detected in the *P. gallinaceum* genome using the same BLAST search methods.

Figure 3.8: 95% Consensus neighbour joining and minimum evolution un-rooted phylogenetic trees of stevor *exon 2 were constructed using all available* stevor *sequences, and bootstrapped to evaluate the validity of the phylogeny. An alignment was made using* P. reichenowi *(black) and* P. falciparum *(3D7-pink; Dd2-grey; D10-green)* stevor *sequences, which have dissimilar N-terminal sequences.*

A
Neighbour joining

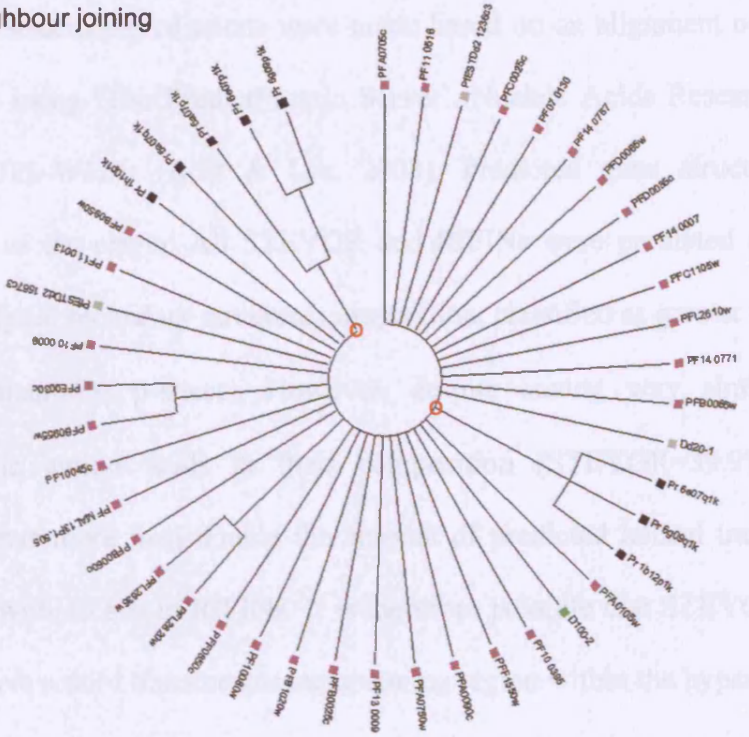

B
Minimum evolution

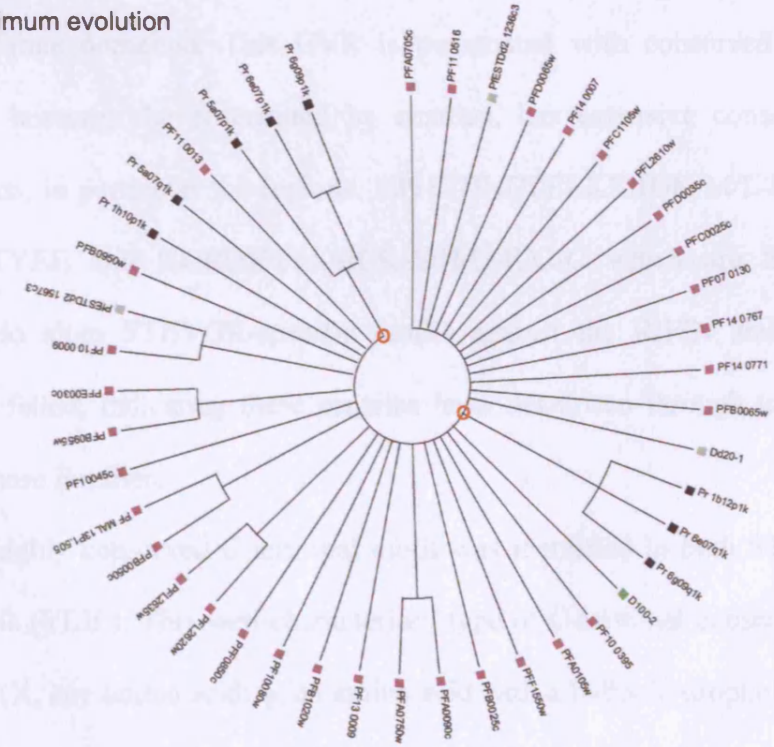

3.6. Secondary structure and motif prediction

Secondary structure predictions were made based on an alignment of 24 STEVORs and 89 RIFINs using 'The PredictProtein Server'. Nucleic Acids Research 32 (Web Server issue): W321-W326. (Rost & Liu, 2003). Predicted gene structure was consistent regardless of the origin. All STEVOR and RIFINs were predicted as globular proteins with 'all-alpha' secondary structure composition, classified as greater than 45% α-helices, and less than 5% β-sheets. However, despite having very similar percentages of hydrophobic amino acids in their composition (STEVOR=39.9% RIFIN =41.2%) STEVOR has more than double the amount of predicted helical transmembrane 29.4% compared with 13.8% in RIFINs. It is therefore possible that STEVOR proteins, but not RIFINs, have a third transmembrane-spanning region within the hyper-variable loop.

Diversity of the majority of *stevor* sequences studied from all isolates was confined almost exclusively to the approximately 70 amino acid HVR (between the two predicted transmembrane domains). This HVR is punctuated with conserved residues such as cysteines, however the N-terminal by contrast, has extensive conserved stretches of amino acids, in particular the regions: NPHYHNDPELKEIIDK-M/L-NEE, EPMST-I/L-EKELLETYEE and KGRDKYLKHLK-E/H/G-R/G-C which are STEVOR specific. Attempts to align STEVOR-specific motifs against the RIFIN amino acid sequence alignment failed, indicating these proteins have not arisen through transfer of domains between these families.

A single highly conserved C-terminal motif was identified in both STEVORs (YWLY) and RIFINs (YLIL). This well-characterised type of C-terminal consensus motif consists of YXXϕ (X, any amino acid; ϕ, an amino acid with a bulky hydrophobic side chain) and acts as a sorting signal (Marks *et al.*, 1996). It is located in both protein families at the C-terminal end of the most C-terminal transmembrane domain (TM2) (figure 3.2).

Although not included in the regions used for the phylogenetic analysis, the C-terminal of STEVOR also includes a highly conserved motif consisting of HECKKHLC, this contrasts with the RIFIN C-terminus, which does not contain cysteines. However, overall both the RIFIN and STEVOR C-termini are positively charged consisting in the majority of highly conserved lysines and arginines. In T.gondii, transmembrane micronemal proteins use a tyrosine-based sorting motif and an acidic patch of residues in the C-terminal tail (Di Christina et al., 2000). These features are also found on several *P. falciparum* micronemal proteins. However, in the case of the micronemal protein erythrocyte binding antigen 175 (EBA-175) neither the tyrosine signal nor the acidic patch are necessary for micronemal targeting. Instead, an unknown signal within the cysteine-rich region directs EBA-175 to the micronemes and then unknown features located within the cytoplasmic tail enable EBA-175 to function as an invasion ligand (Gilberger et al., 2003).

Rhoptry protein targeting is Brefeldin-A sensitive indicating that proteins pass through the ER and Golgi (Howard and Schimdt., 1995 and Noe et al., 2000). Rhoptry protein targeting in *T. gondii* relies on a tyrosine-based motif, as described above, YXXϕ, many *P. falciparum* rhoptry proteins do contain a C-terminal tyrosine-based motif, although nothing is known of the requirements for rhoptry targeting. Rhoptry targeting in *T. gondii* also relies on the packaging of transmembrane proteins into clathrin-coated vesicles by an interacting of the C-terminal tyrosine motif with the μ1 subunit of the adaptor protein complex-1 (AP-1) clathrin-coat complex (Ngo et al., 2003). All homologous components that are necessary for this targeting mechanism are present in *P. falciparum*, but whether they function in rhoptry targeting is unknown (Gardner et al., 2002).

Discussion

In order to characterise *stevor* gene diversity and to form a framework for studies of parasite isolates from endemic areas, a phylogenetic analysis was performed on all available *stevor* sequences. I sought to establish whether *stevor* was indeed present in the genomes of all *P. falciparum* parasites, and whether *stevor* was transcribed in these same parasites. PCR and RT-PCR methods were used followed by extensive sequencing from the HVR of *stevors* from multiple laboratory lines and Kilifi isolates. Evidence was sought for the presence of globally conserved *stevor* genes, consistent with the hypothesis of an ancestral parasite with an already expanded *stevor* multigene family.

The *stevor* multigene family was found in all *P. falciparum* isolate genomes. The copy-number per genome for the Ghanaian isolate (26) is consistent with that of the *P. falciparum* 3D7 isolate, which has 28 copies. The 17 *stevors* in the IT genome, on the other hand, was considerably lower. However, it is likely that there are more *stevor* sequences, which have been missed due to the incomplete status of the sequencing of this genome.

It was interesting to note that the *P. falciparum* 3D7 clone from the NIMR is not identical to the 3D7 clone sequenced and published (Gardner *et al.*, 2002). Due to the multi-copy nature of the gene family and potential for recombination in the sub-telomeric chromosomal regions, this would not be surprising. When a similar sequencing study of the *yir* multigene family was made, sequences were found to be different to those published by Carlton 2002 (Carlton *et al.*, 2002) (Sandra Koernig personal communication). However the *P. yoelii* 17XNL rodent parasite used for the published genome is different from the *P. yoelii* clone held at the NIMR.

STEVOR and RIFIN are distinct proteins despite sharing architectural similarities. The RIFINs form, in addition, two further sub-groups (Gardner *et al.*, 2002), which are defined by a consensus 25 amino acid sequence present in only one of the RIFIN sub-

groups. The phylogenetic analysis performed in this thesis supports this suggested sub-grouping.

The HVR of STEVOR is highly divergent and there is no evidence of sub-groups from phylogenetic analysis based on this region from 226 amino acid sequences worldwide. In addition, although analysis from a smaller sample of STEVORs suggested sequences from the same isolate cluster together, when this analysis was extended this clustering was no longer evident. Overall, the Kilifi isolates appear to be more closely related to each other than any of the other laboratory parasites, and no common *stevors* were found between Kilifi isolates and for example A4 or FcB1. The only exception was a single *stevor* shared between a Kilifi isolate and the 3D7 isolate. The *stevor* found in two Kilifi isolates (K11 and K14) may either be due to an overlap in *stevor* repertoire of the two infecting parasites, or homologous parasites infecting both patients. The most highly conserved *stevor* is in fact a pseudogene fragment also present in the *P. falciparum* 3D7 genome (PFA0105w), and several other isolates including the Ghanaian isolate.

There are conserved genes (paralogues) identified in different *P. falciparum* isolates from different global locations for example: A4, C10 and FcB1 in particular, contain several closely related *stevors*. These data are evidence therefore that the ancestral *P. falciparum* parasite genome already had multiple *stevor* genes. That may subsequently have diversified further within the different *P. falciparum* isolates. Since I identified 8 *stevors* in *P. reichenowi* this suggests that the ancestral multigene *stevor* family existed before the split of *P. reichenowi* from *P. falciparum*. It is likely that more than 8 *stevors* are present within the *P. reichenowi* genome (Chris Janssen, personal communication) however it has not been possible to obtain *P. reichenowi* DNA or RNA for further analysis.

Stevors were not detected in *P. gallinaceum:* Therefore the *stevor* multigene family has arisen in this particular branch of the primate malarias (figure 1.2), and is unlikely to be shared by other human malarias or the rodent malarias, such as in the Plasmodium

interspersed repeats (pir) super-family, as suggested by Janssen 2004 (Janssen *et al.*, 2004).

Similar to the *var* genes, each parasite also has an extensive repertoire of *stevor* genes. Transcription of particular *stevor* genes is not up-regulated at a the gametocyte stage of the lifecycle (Sharp *et al.*, 2006). By contrast, a defined subset of *var* genes (type Ups C), are specifically transcribed in the gametocyte-stages, and independently of the *var* type transcribed by the asexual-stage parasite-population (Sharp *et al.*, 2006).

The RT-PCR data suggest that multiple *stevors* are transcribed in a parasite population. However, the presence of multiple transcripts does not necessarily imply more than one *stevor* is translated and expressed at a time in a single parasite, or rule out the possibility that different *stevors* may be expressed in different life cycle-stages. Therefore *stevors* may also be subject to clonal phenotypic variation.

As it has been suggested that particular regions of *stevor* may be exposed to the host immune system, we analysed the HVR. The diversity observed is almost exclusively specific to the region between the two predicted transmembrane domains. Data on the hyper-variable loop regions from other two-transmembrane-protein families e.g. SURFINs, give evidence that the loops are exposed on the surface of the iRBC, thus it is likely that this region of STEVOR is also exposed on the iRBC surface. However it has not been determined whether STEVOR is expressed on the iRBC surface, which would imply that the diversity observed in the loop region is driven by positive selection, and amplification of *stevor* genes is a direct result of the parasites' need to avoid antibodies.

However, the hydrophobic nature of this region and higher percentage of helical trans-membrane predicted in STEVOR compared with RIFINs may also be more consistent with three transmembrane domains. This would potentially result in surface-exposure of both the HVR and N-terminal regions. It is possible that the N-terminus is functionally constrained, for example, due to coding for a specific binding domain. Since *stevor*

expression is late in the erythrocytic cycle, it would be unlikely to reach the iRBC-surface before the development of the schizont. At this late stage of intra-erythrocytic development STEVOR could potentially be important for adhesion to RBCs, making parasites more effective in rosetting, similar and in addition to PfEMP1 function during the trophozoite-stage. This could enable faster access of the merozoites to new RBC.

A tyrosine-based motif found conserved in all STEVOR (YWLY) and RIFIN proteins (YLIL), raises the interesting possibility that STEVOR may be found in the merozoite apical organelles, in addition to its presence in sporozoites, sexual and asexual erythrocyte-stages. This location would not be unique to the STEVOR family as in addition, the much smaller SURFIN family of proteins are expressed both on the iRBC surface and at the apical tip of merozoites (Winter *et al.*, 2005).

Tyrosine-based motifs of this type are known in mammalian cells and also *Toxoplasma gondii*, another intracellular Apicomplexan parasite with specialised secretory organelles, to direct targeting of transmembrane proteins to sub-cellular locations e.g. rhoptries (Hoppe *et al.*, 2000). A similar motif is also conserved in the C-terminus of a sub-set of the *P. yoelii yir* multigene family (Sandra Koernig personal communication).

In summary, the *stevor* multigene family is found consistently in the genome of all the *P. falciparum* isolates tested, and considerable diversity between isolates is observed, although some orthologues were found. In all isolates, except one (A4), *stevor* genes were transcribed and in any population there were multiple genes transcribed. Phylogenetic analysis did not reveal any STEVOR sub-groups, unlike *rifins* where 2 distinct sub-groups were verified. STEVOR are also not a further sub-grouping of the RIFINs. Several potentially important architectural differences were found to exist between the STEVOR and RIFIN multigene families, including a very different cysteine distribution, predicted helical transmembrane percentage and hydrophobicity distribution within the hyper-

variable loop region. Finally, the STEVOR proteins may be expressed and located on both the iRBC surface and in merozoite apical organelles.

In conclusion, the HVR of the STEVOR gene family is highly divergent both within and between isolates. The question now is what is the driving force of this gene diversification. One reason for the loop to show no sign of conservation is an absolute lack of function, however studies have shown the evolutionary rate of the loop is higher than that of the genome overall average, this strongly suggests the second possibility; that the genes are under positive selective pressure. It has been clearly shown for several other *Plasmodium* genes that regions encoding exposed loops are driven to diversify by immune pressure (Conway *et al.*, 2000; Escalante *et al.*, 1998). Of course immune pressure can only be exerted upon genes that are translated, expressed in exposed locations and that are the target of immune responses that lead to reduced parasite fitness. While it has clearly been shown that isolates transcribe *stevor*, the number of *stevors* transcribed per parasite is unknown, as is the location and topology of the protein product.

Chapter 4) Introduction: Generation of antibody reagents for detecting STEVOR

Proteins belonging to the *P. falciparum* multigene family, STEVOR, are variant proteins. In order to study the expression of STEVOR in the iRBC, it will be necessary to have antibody reagents that detect as many STEVOR variants as possible. Therefore the most useful antibodies, for localisation and expression studies, will be those specific for the conserved or semi-conserved regions of these homologous proteins. We have firstly identified those conserved STEVOR-specific regions (see chapter 3), before generating antibodies that detect the maximum number of STEVOR proteins.

Proteins belonging to the *P. falciparum* multigene family, STEVOR, share conserved composition. They have an N-terminal region (amino acids 1-53), which contains highly conserved motifs (PEXEL/VTS) and is known to have protein targeting properties (Hiller *et al.*, 2004; Marti *et al.*, 2004). This N-terminal region is involved in directing the trafficking of STEVOR proteins into the iRBC cytosol and to the Maurer's clefts (Przyborski *et al.*, 2005). Adjacent to the N-terminal is a conserved/semi-conserved region, of approximately 130 amino acids, which is then followed by the first potential transmembrane domain (TM1). This region has 74 percent similarity between *P. falciparum* 3D7 *stevor* sequence pairs, likewise 71 percent similarity was found between sequence pairs within the initial signal sequence (amino acids 1-24) (Kyes *et al.*, 2001), suggesting that the conservation of residues seen could be due to functional restraints (figure 4.1). In contrast, the level of similarity between sequence pairs in the subsequent approximately 70 amino acid HVR, is only 47%, which suggests that this region may be under strong immune pressure or non-functional. The antigenic diversity generated in this region may have a role in immune-evasion or other parasite-survival functions that are yet to be revealed.

Figure 4.1: Schematic of conserved features in STEVOR and RIFIN proteins showing location of peptides and recombinant proteins

Peptides 1-3 and recombinant proteins are marked with red bars. N-terminal signal sequences are shown in grey including a canonical signal sequence (encoded by exon 1) and Plasmodium *exported element/vacuolar transport signal (PEXEL/VTS) sites. Predicted transmembrane domains are shown in black (TM1/2). Apical organelle targeting motifs (YIWL) are identified in the C-terminal following the TM2. Percentage similarity data is taken from a review from (Kyes et al., 2001).*

The positions of all cysteines are indicated (C), Black arrows indicate those cysteines that are conserved in at least 75% of proteins. The dark grey arrows indicate cysteines conserved in at least 50% of proteins. The light grey arrows indicate cysteines conserved in less than 25% of proteins. Numbers 1-6 show those cysteines highly conserved at a structurally equivalent site in both STEVORs and the majority of RIFINs. Proteins are shown to scale (1cm equals 16 amino acids). Amino acid position is based on an alignment of the complete P. falciparum *3D7 STEVOR and RIFIN repertoires (www.plasmodb.org).*

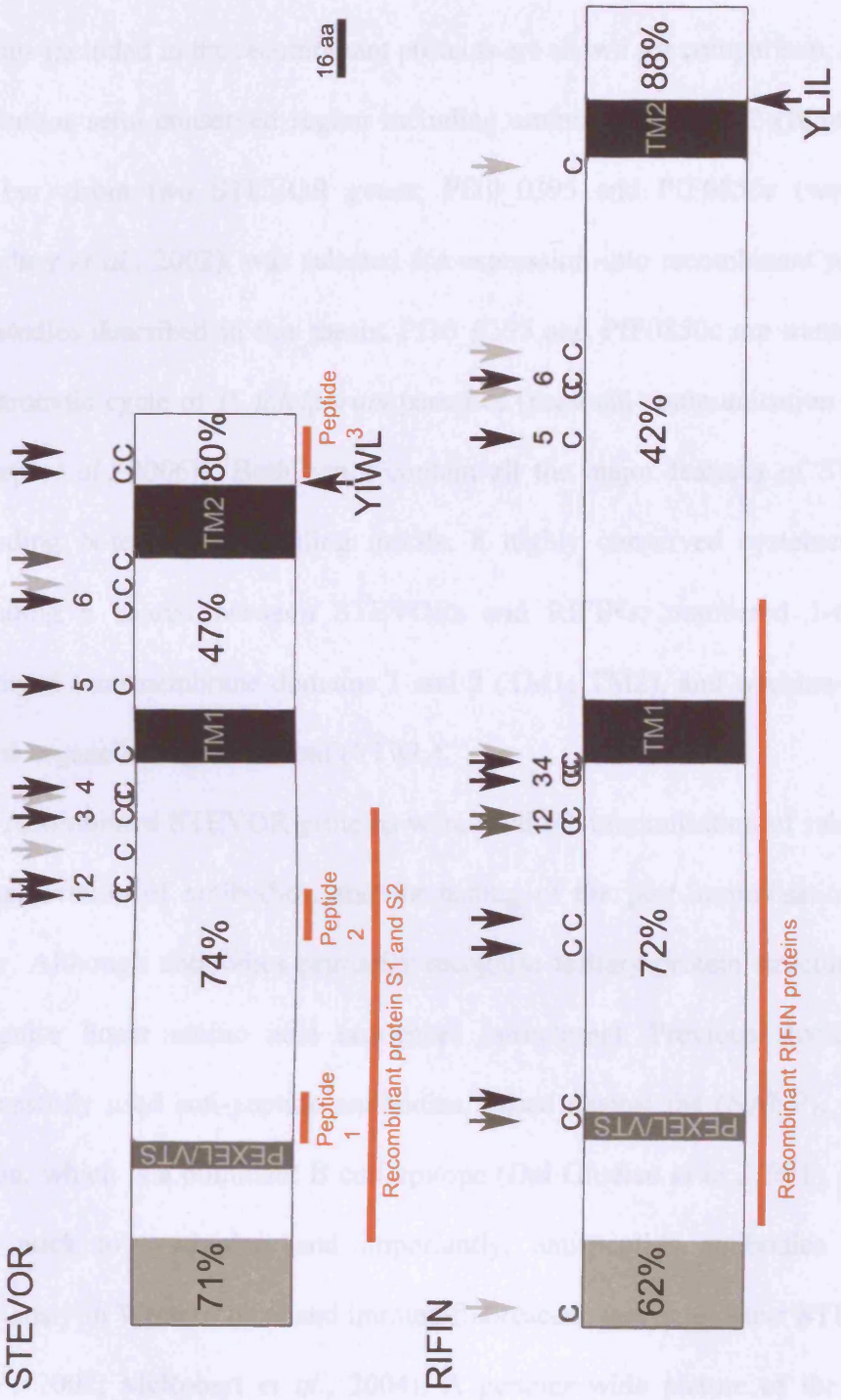
STEVOR
RIFIN
16 aa
PEXELVTS
TM1
TM2
71%
74%
47%
80%
62%
72%
42%
88%
YIWL
YLIL
Peptide 1
Peptide 2
Peptide
Recombinant protein S1 and S2
Recombinant RIFIN proteins

Interestingly, studies using recombinant RIFIN proteins that express the N-terminal (130 amino acid) region and also include a proportion of the HVR, showed anti-RIFIN antibodies are produced in natural infections (Abdel-Latif *et al.*, 2002) (figure 4.1, RIFIN, regions included in the recombinant proteins are shown for comparison, red bar).

A similar semi-conserved region including amino acids 26-182 (figure 4.1. STEVOR, red bar) from two STEVOR genes: Pf10_0395 and PfF0850c (www.plasmodb.org) (Gardner *et al.*, 2002), was selected for expression into recombinant proteins for use in the studies described in this thesis. Pf10_0395 and PfF0850c are transcribed during the erythrocytic cycle of *P. falciparum* parasites (personal communication Colin Sutherland (Sharp *et al.*, 2006)). Both genes contain all the major features of STEVOR proteins: including N-terminal signalling motifs, 8 highly conserved cysteines (Black arrows, including 6 shared between STEVORs and RIFINs, numbered 1-6 in figure 4.1), predicted transmembrane domains 1 and 2 (TM1; TM2), and tyrosine-based C-terminal apical organelle targeting motif (YIWL).

The recombinant STEVOR proteins were used for immunisation of rabbits and mice for the generation of antibodies, and for testing of the post-immunisation sera in ELISA assay. Although antibodies primarily recognise tertiary protein structures, they can also recognise linear amino acid sequences (structures). Previous studies on CSP have successfully used anti-peptide antibodies, raised against the $(NANP)_3$ repetitive peptide region, which is a dominant B cell epitope (Del Giudice *et al.*, 1991). Peptides are easy and quick to synthesise, and importantly, anti-peptide antibodies have been used previously in Western blots and immunofluorescent assays to detect STEVOR (Kaviratne *et al.*, 2002; McRobert *et al.*, 2004). A genome-wide picture of the complete *stevor* multigene family is now available for different *P. falciparum* clones, and has been used in this project to assess the conservation of the peptides used for antibody generation (Gardner *et al.*, 2002), (see short red bars, peptides 1-3, shown in figure 4.1). Therefore

for the studies described in this thesis, both anti-peptide and anti-recombinant protein antibodies were generated for the identification of STEVOR in blood-stage parasites from multiple laboratory strains, and Kilifi field isolates.

The objectives of this chapter were:

1) **To utilise *stevor* sequence information and determine which peptides and fragments of STEVOR to use in the generation of antibody reagents.**
2) **To determine how many STEVORs they will represent.**
3) **To raise and test anti-sera to be used later in immunofluorescence studies.**

Results

4.1. Selection and design of STEVOR peptides

3 peptides from different regions of STEVOR originally described by Kaviratne *et al*, were analysed for conservation within the *stevor* family, re-synthesised and used to immunise rabbits and mice. The peptides were originally based on an alignment of six STEVOR sequences from www.plasmodb.org (Kaviratne *et al.*, 2002). With the completion of the *P. falciparum* 3D7 genome sequencing, and partial sequencing of other clones (Gardner *et al.*, 2002), it is now possible to make a more comprehensive assessment of the *P. falciparum* STEVOR family repertoire to ensure that the peptides were designed to highly conserved regions and therefore that antibodies would detect a wide repertoire of STEVOR proteins as shown in table 4.1.

Peptides 1 and 2 are in close proximity to one another on the N-terminal side of the HVR, whereas peptide 3 is located within the highly conserved C-terminal end of STEVOR (figure 4.1). These regions were proposed to be on the internal cytoplasmic side of the iRBC membrane and therefore unlikely to be exposed on the iRBC surface (Cheng *et al.*, 1998).

It was observed that peptide 3 (IWLY) RRRKNSWKHECKKHLC included 4 amino acids (in brackets) that constituted part of the hydrophobic predicted transmembrane region (figure 4.1), which may render anti-peptide antibody recognition within the native STEVOR protein difficult. It is possible that this linear epitope would not be accessible to antibodies in its natural tertiary configuration, due to the predicted proximity to the membrane.

Peptide 1 is clearly the most conserved in both *P. falciparum* 3D7 and the Ghanaian isolate STEVORs (see chapter 3), whereas peptide sequences 2 and 3 were present and conserved in around 50% or less of STEVOR genes, and were overall less conserved in the Ghanaian genome than in the 3D7 genome (see table 4.1). This suggested that the

anti-peptide 1 antibody would identify the majority of STEVORs, if expressed, whereas anti-peptide 2 and 3 antibodies would recognize a more limited range of STEVORs. There were no other regions sufficiently conserved to be useful as peptides.

Table 4.1) Percentage of STEVOR genes with 100% identity to the peptide sequences used for the generation of STEVOR-specific antibodies.

Peptide	3D7 (1)	Ghanaian isolate (2)
Peptide 1	78.5% (22/28)	77.78% (21/27)
Peptide 2	42.86% (12/28)	22.22% (6/27)
Peptide 3	53.57% (12/28)	44.44% (12/27)

1) Available from www.sanger.ac.uk/Projects/P_falciparum/ via GeneDB or PlasmoDB.

2) Available from www.sanger.ac.uk/Projects/P_falciparum/ via *P. falciparum* Blast server.

4.2. Expression and purification of recombinant STEVOR proteins

STEVOR fragments (S1 (containing PF10_0395 amino acids 28-182), and S2 (containing PFF0850c amino acids 26-182), see figure 4.1) were cloned into pET24a+ expression vector constructs as described in materials and methods chapter 2. Competent *E. coli* bacteria strain BL21 were transformed with the vectors and cultures expanded. Expression within the BL21 strain host resulted in the expression of insoluble proteins, which could be solubilised in 8M urea. Therefore, protease deficient *E. coli* BL21 RIL and Rosetta-gami cells were transformed with the vectors containing S1 or S2. These bacterial host strains are manipulated to allow functional expression of the rare tRNA genes making them more suitable for the high A/T percentage of the *P. falciparum* genome, and the Rosetta-gami cells additionally have enhanced disulfide bond formation, to maximise solubility of the expressed proteins. Both host cell types allowed expression of soluble S1 and S2 proteins.

After transformation and induction with IPTG the bacterial cells were harvested and sonicated, and the recombinant proteins were purified from the sonicated extract using a Ni-NTA column, as described in materials and methods.

A bacterial growth time-course (from 0-5 hours) was used to determine optimal timing for maximal expression and minimal degradation of the STEVOR proteins (figure 4.2). Bacterial samples were taken hourly following induction with IPTG, insoluble (i) and soluble (s) protein fractions from each time point were analysed on an SDS-PAGE gel. Western blotting using an anti-His tag antibody revealed proteins of the expected size (S1: 18.49kDa /S2: 19.47kDa) in insoluble and soluble fractions following induction of protein expression. A small amount of S1 and S2 protein was seen already in Western blot at 0 hours (figure 4.2 C): This was probably due to mis-regulation and leaky expression of the proteins.

STEVOR protein, S1 and S2, were present in both the insoluble and soluble fractions, and an additional smaller product of approximately 9kDa was present in the soluble fraction. S1 expression was maximal at 2-3 hours, and S2 expression was maximal at 2-4 hours, after which time the level of protein expression declined. A much larger polypeptide of around 49kDa, in the protein blots, reacted with the anti-His tag antibody. These are most likely due to non-specific binding of the anti-His tag antibody, or to insufficient protein reduction and protein dimerisation.

Equal volumes of culture were processed at each time-point. However these are only roughly equivalent, as the bacterial cultures were continually growing throughout the 5 hours, therefore bacteria were at a greater density at 5 hours than at 1 hour (At 0 hours OD_{600}: 0.6).

Figure 4.2: SDS-PAGE and Western blot analysis of a time course of recombinant STEVOR protein expression in BL21 RIL host cells

A time-course from 0 hours to 5 hours post-induction with IPTG was followed hourly for both S1 (A, and B), and S2 (C and D). Bacterial culture insoluble (i) and soluble (s) fractions were separated on 4-12% BisTris gels in MES SDS running buffer under reducing conditions. See Blue molecular marker was used for size identification (kDa). Arrows mark expected molecular weight of recombinant proteins. A control His-tagged protein of approximately 60kDa was used as a positive control for the Western blot (lanes marked C).

Proteins were either visualised specifically in Western blot (A, and C) by chemiluminescence using anti-His tag antibodies, detected via a secondary anti-mouse IgG HRP-conjugated secondary antibody, or stained with Coomassie blue stain (B and D).

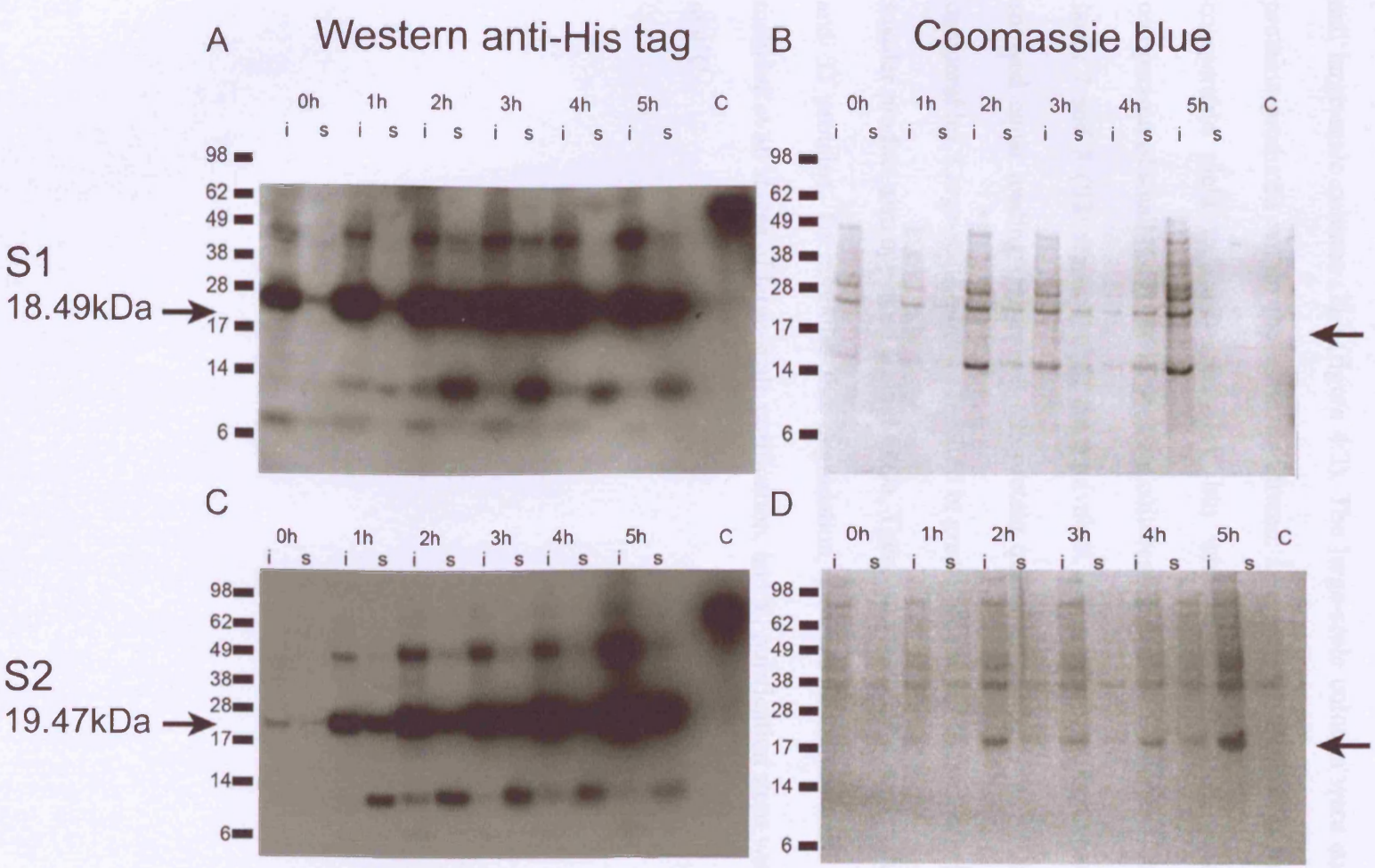
A
Western anti-His tag
B
Coomassie blue
0h 1h 2h 3h 4h 5h C
i s i s i s i s i s i s
98
62
49
38
28
17
14
6
S1
18.49kDa
C
D
S2
19.47kDa

Using the optimum induction time of 2 (S1) or 3 (S2) hours, large-scale bacterial cultures were set up. A comparison of protein production was made, between small-scale (100ml) and large-scale cultures (2L) (figure 4.3). The large-scale cultures were successful with proteins produced within the same timeframe. Large-scale (ls) protein induction gave comparable yield to small-scale (ss), but with more breakdown products. For a comparison of small-scale and large-scale cultures: (figure 4.3 (A) lanes 3 and 4 (S1), and lanes 7 and 8 (S2) respectively). An equivalent gel stained with Coomassie blue stain showed equal loading (figure 4.3 (B) protein quantities are low, but visible bands are comparable). Large-scale cultures resulted in greater quantities of the 9kDa protein, and a smaller product also appeared around 6kDa. These may be breakdown products of the S1 and S2 proteins. To minimise this degradation, protease inhibitors were subsequently included at all stages of large-scale purification, and all purification steps were carried out at 4°C.

Figure 4.3: SDS-PAGE and Western blot analysis of a trial 2L large-scale culture of STEVOR S1 and S2 expression

Proteins were separated on a 4-12% BisTris SDS gel in MES SDS running buffer under reducing conditions, before either (A) detection of recombinant protein's 6-Histidine tag, using commercially available anti-His tag antibodies, visualised by chemoluminescence, via a secondary anti-mouse IgG antibody conjugated to HRP, or (B) staining of proteins with Coomassie blue stain. Lanes (1-4) BL21 RIL transformed with construct S1 soluble fraction, lanes (5-8) BL21 RIL construct S2 soluble fraction. The arrows in A and B show the expected size of the recombinant proteins.

Lane contents: lanes 1; 5) 0 hour culture small-scale, lanes 2; 6) 0 hour culture large-scale, lanes 3; 7) 2 hours post-IPTG induction small–scale culture, lanes 4; 8) 2 hours post-IPTG induction large-scale cultures for comparison. See Blue molecular marker was used for size identification (kDa). All strips shown are from the same gel and were developed at the same time.

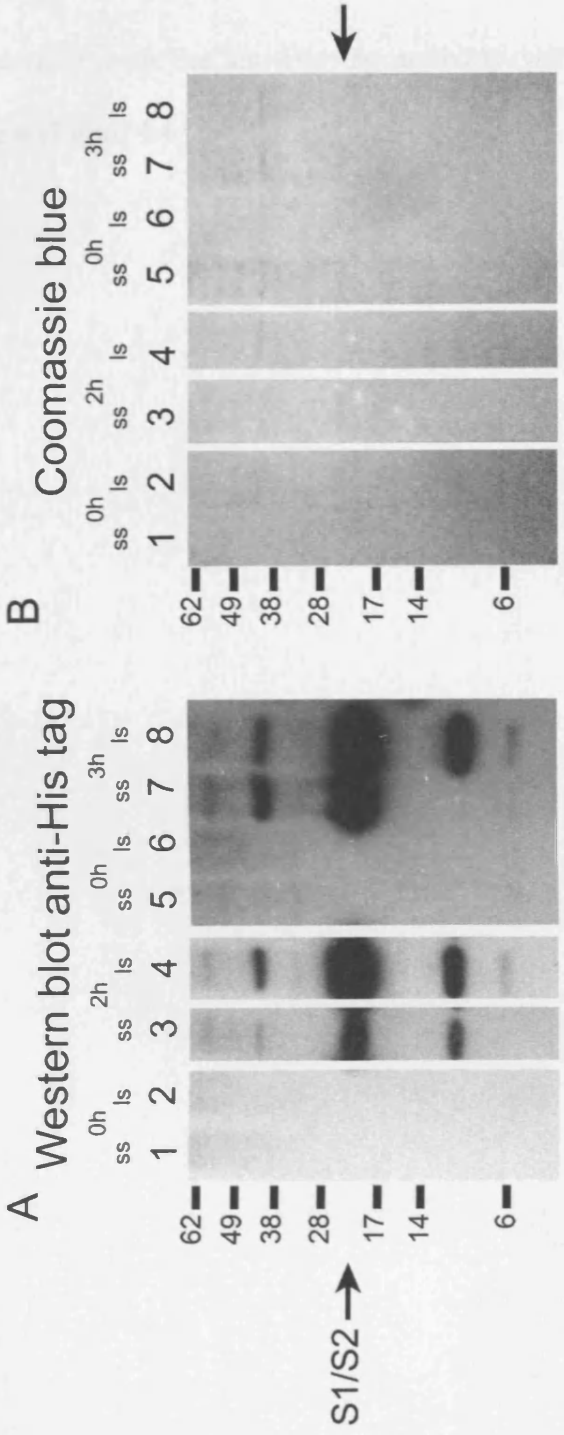
A
Western blot anti-His tag
B
Coomassie blue
0h
2h
3h
ss
ls
1 2 3 4 5 6 7 8
62
49
38
28
17
14
6
S1/S2

Small-scale purification on Ni-NTA was successful (figure 4.4 A and B), however in addition to the S1 protein expected size, a smaller 9kDa protein which reacts with the anti-His tag antibody, was also purified on the column. Other larger (e.g. 45kDa) proteins observed to cross-react with the anti-His tag antibody were removed by the Ni-NTA purification process (figure 4.4 lane 4).

Figure 4.4: SDS-PAGE and Western blot analysis of small-scale protein purification on Ni-NTA matrix

Full-length S1 protein was purified on Ni-NTA matrix along with the smaller 9kDa protein fragment (indicated by arrows in A and B). Proteins were separated on a 4-12% BisTris SDS gel in MES SDS running buffer under reducing condition before either (A) detection of recombinant protein's 6-Histidine tag, using commercially available anti-His tag antibodies, visualised by chemoluminescence, via a secondary anti-mouse IgG antibody conjugated to HRP, or (B) staining of proteins with Coomassie blue stain. See Blue molecular marker was used for size identification (kDa).

Lane contents: (1) unbound flow-through from Ni-NTA incubation from small-scale purification, (2) Ni-NTA beads post-incubation with S1-bacterial culture supernatant, (3) wash, (4) fraction eluted off matrix by high imidazole concentration buffer.

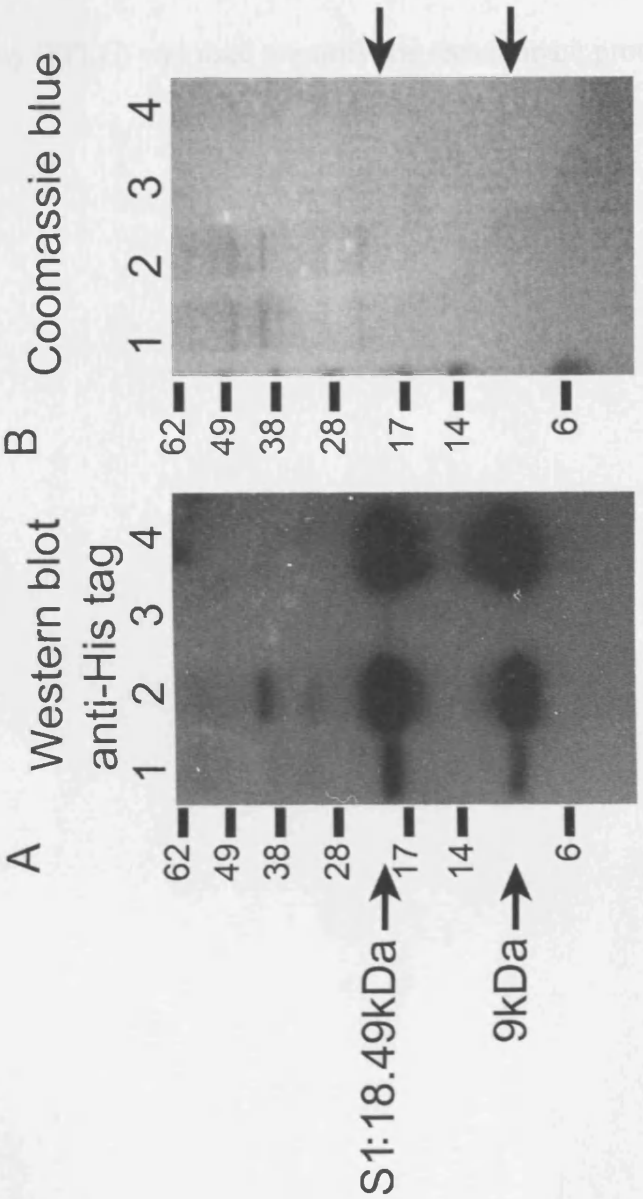
A
Western blot
anti-His tag
1 2 3 4
62
49
38
28
17
14
6
S1:18.49kDa
9kDa
B
Coomassie blue
1 2 3 4
62
49
38
28
17
14
6

A representative protein gel and Western blot showing the results of the large-scale purification of S1 and S2 are shown in figure 4.5. With both constructs, purification using the His-tag on Ni-NTA matrix was not completely successful, and a number of non-His tagged contaminating proteins were present in the eluted fraction (compare figure 4.5 lane E; A with B, or C with D). Therefore gel filtration using Fast Protein Liquid Chromatography (FPLC) was used to purify the recombinant proteins further.

Figure 4.5: SDS-PAGE and Western blot analysis of large-scale purification of S1/S2 using the His-tag, on Ni-NTA matrix

Proteins were run on a 4-12% Bis-Tris gel in MES SDS running buffer under reducing conditions. Proteins are visualised in A, and C, using an anti-His tag antibody, detected via a secondary anti-mouse IgG-HRP conjugated antibody using chemoluminescent substrate, and in B, and D, all proteins are stained using Coomassie blue stain. See Blue molecular marker was used for size identification (kDa).

S1 (A and B) and S2 (C and D) non-induced (0 hours) cultures, protein samples from wash 1 (W1): lysis buffer, wash 2 (W2): high salt buffer, wash 3 (W3): increased imidazole buffer, and eluted (E) fractions post-Ni-NTA matrix column.

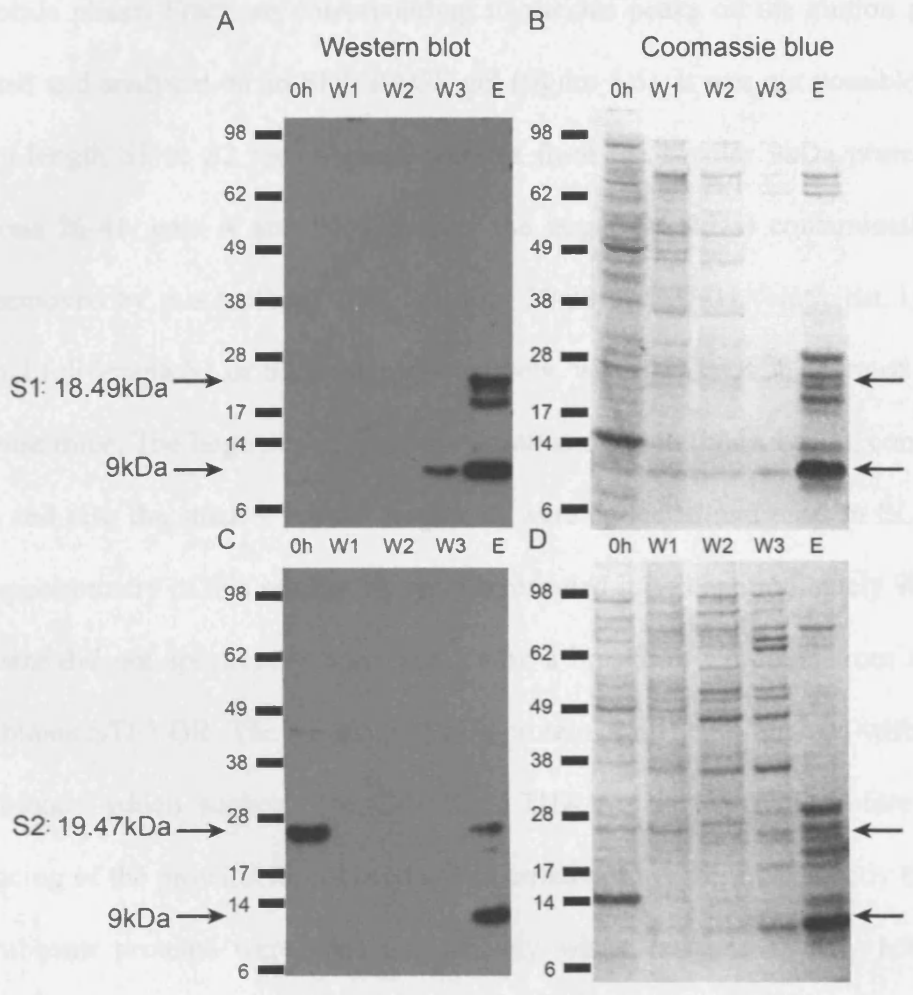
A
Western blot
B
Coomassie blue
0h W1 W2 W3 E
98
62
49
38
28
17
14
6
S1: 18.49kDa
9kDa
C
D
S2: 19.47kDa
9kDa

4.2.1. Chromatographic purification of S1 and S2 STEVOR fragments

The proteins eluted from the His-tag purification column were concentrated to a volume of 3-5ml and purified further by size exclusion on Superdex 75 using FPLC, with PBS as the mobile phase. Fractions corresponding to various peaks on the elution profile were collected and analysed on an SDS-PAGE gel (figure 4.6). It was not possible to separate the full-length S1 or S2 recombinant proteins from the smaller 9kDa protein fragment (fractions 26-41, gels A and B). However the larger (>28kDa) contaminating proteins were removed by this method. The fractions 30-33 and 27-31 (black bar 1) containing maximal full-length S1 or S2 protein respectively, were pooled, concentrated and used to immunise mice. The large peaks, fractions 34-40 and 32-40 (black bar 2), containing full-length and also the smaller protein fragment, were collected and used in ELISA assays. Mass spectrometry of this smaller S1 species revealed it was approximately 9kDa, but the exact size did not specifically correspond with a breakdown product from a full-length recombinant STEVOR. The S1 and S2 9kDa protein consistently reacted with an anti-His tag antibody which suggests the C-terminal (His-tag) is intact. Therefore N-terminal sequencing of the proteins would need to be carried out to determine exactly their origin. Recombinant proteins were used immediately where possible as they both exhibited precipitation on freezing, and therefore were stored a short time at 4°C.

Figure 4.6: Chromatographic purification of S1 and S2 recombinant protein, on Superdex 75

A) Profile of proteins from the purified S1 protein after FPLC, black bars 1 (fractions 30-33) and 2 (fractions 34-40) were collected and pooled. B) Purified S2 protein profile black bars 1 (fractions 27-31) and 2 (fractions 32-40) were collected and pooled. S1 fractions 20, 26, 29, 32, 34, 36 and S2 fractions 20, 26, 29, 32, 34, 36 41, were run on 12% Bis-Tris gel in MES SDS running buffer under reducing conditions and stained with Coomassie blue. See Blue molecular marker used for size comparison (kDa).

A S1

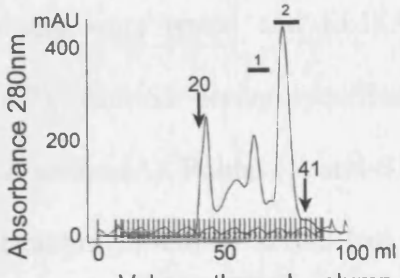

Volume through column (elution fractions)

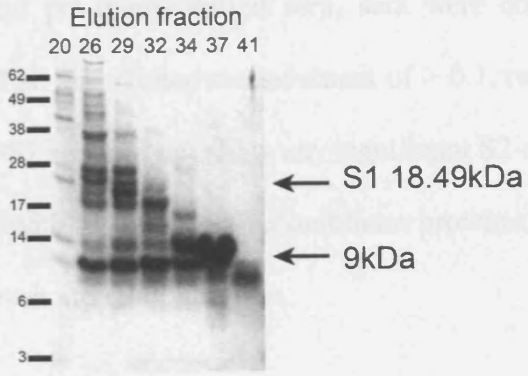

B S2

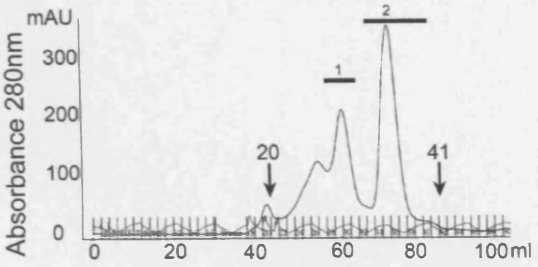

Volume through column (elution fractions)

4.3. Verification of rabbit anti-STEVOR S1 and S2 sera

Rabbits were immunised by ProSci Inc., CA, USA as described in materials and methods. Post-immunisation sera were tested and ELISA screening assays performed by the company (figure 4.7). Anti-S1 serum specifically recognised insoluble recombinant protein S1 in ELISA assays (A). Rabbit (1) anti-S1 serum showed an ELISA titre positive at 1: 25000, whilst rabbit (2) anti-S1 serum had antibody at a 1:14500 dilution. This is normalised against the rabbit pre-immunisation sera, sera were considered to contain specific antibody if they had an absorbance measurement of > 0.1, read at 405nm optical density (OD). However anti-S2 sera did not show any significant S2-specific binding (B). The two rabbits immunised with insoluble S2 recombinant protein did not show a clear antibody-specific response even at 1:1000 dilution.

Figure 4.7: ELISA to measure levels of anti-STEVOR S1 and S2 antibodies in sera from immunised rabbits: S1, but not S2-specific antibodies were detected in post-immunisation sera.

2 rabbits were immunised per recombinant protein: Post-immunisation sera were tested for the presence of anti-S1 or S2 antibodies (solid lines): Antibodies to STEVOR S1 (A), and S2 (B). Pre-immunisation sera from each rabbit, collected before the start of the immunisations, was included as a negative control (dotted lines). The endpoint is calculated relative to the pre-immunisation background and sera considered only to contain specific antibody at an absorbance above 0.1 (measured at OD 405 (horizontal dashed line on graph)). ELISAs were carried out by ProSci incorporated, CA, USA.

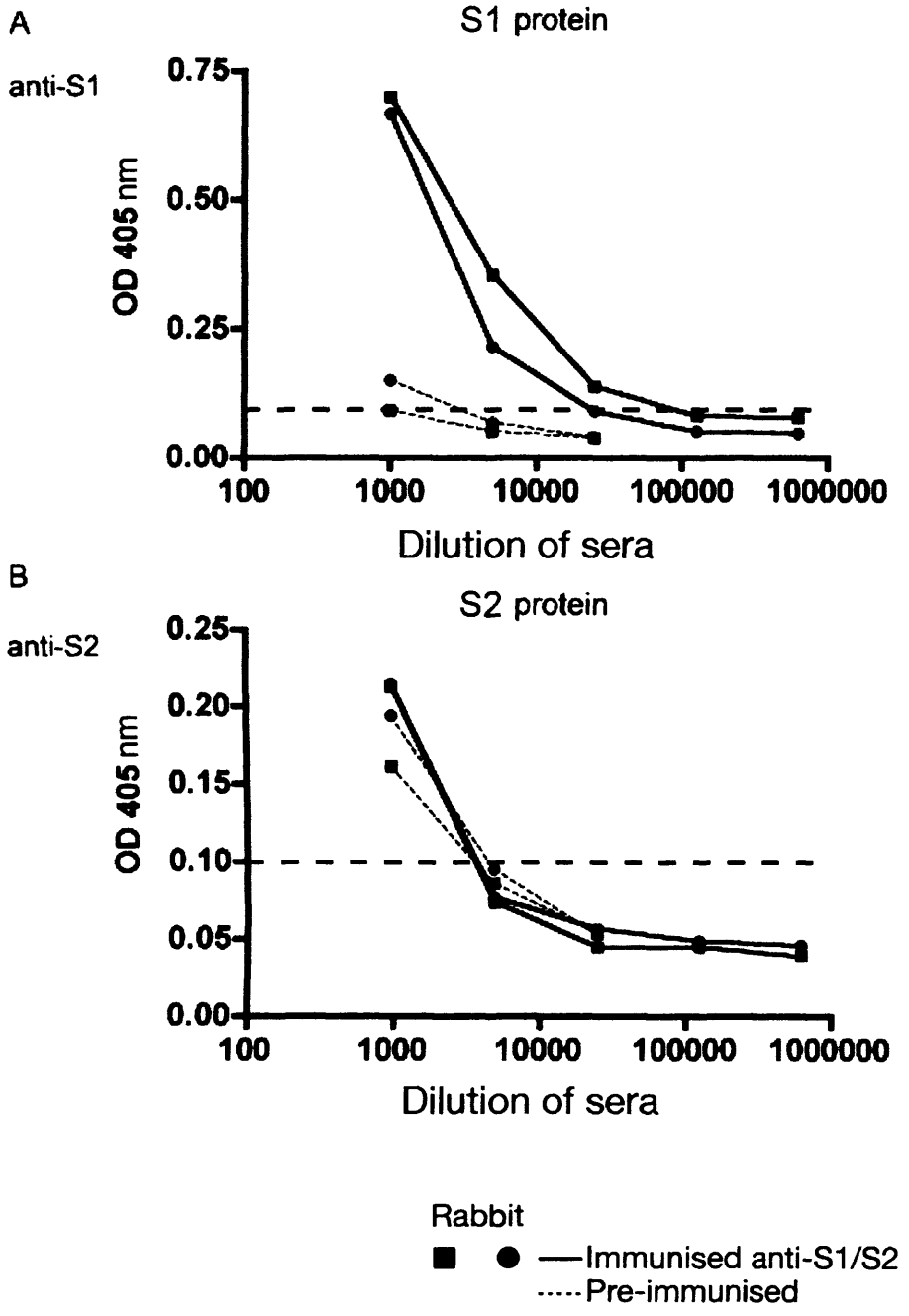
A
S1 protein
anti-S1
OD 405 nm
0.75
0.50
0.25
0.00
100
1000
10000
100000
1000000
Dilution of sera
B
S2 protein
anti-S2
OD 405 nm
0.25
0.20
0.15
0.10
0.05
0.00
100
1000
10000
100000
1000000
Dilution of sera
Rabbit
—Immunised anti-S1/S2
Pre-immunised

4.4. Generation of mouse anti-STEVOR S1 and S2 specific antibodies

BALB/c mice were immunised with soluble recombinant STEVOR S1 and S2 proteins, as described in materials and methods. Initially, anti-S1/S2 sera were tested in ELISAs on the recombinant proteins, and S1 and S2-specific antibodies were detected in post-immunisation sera. (figure 4.8). Sera from 3 mice were tested from a 1 in 5, to a 1 in 2560 dilution, at which they still showed specific reactivity to the recombinant proteins above the background (pre-immunisation sera baseline). All post-immunisation sera showed a similar profile, relative to each other, in response to the recombinant proteins.

A control His-tagged protein of approximately 20kDa was used to test for specificity and the anti-His antibody component of the responses. Anti-S2 sera showed minimal response to this irrelevant His-tagged protein (B, open symbols, tested at the two highest sera concentrations); however anti-S1 sera reactivity was not as STEVOR-specific, with only 1 serum showing specificity for S1 recombinant protein (A, solid symbols), over and above that seen in response to His-tagged protein controls (open symbols). Control wells of diluents in place of sera, no peptide coat, and no secondary antibody were included and were negative (data not shown).

Although these anti-sera bound recombinant protein in ELISAs, they were unable to recognise any proteins in Western blots of SDS-PAGE gels of S1 and S2 run under reducing or non-reducing conditions.

Figure 4.8: ELISA to measure levels of anti-STEVOR S1 and S2 antibodies in sera from immunised mice.

Post-immunisation sera from 3 mice are shown A) anti-S1 recombinant protein B) anti-S2 recombinant protein. Sera were titrated in 2-fold serial dilutions starting at 1:5 The end-point is calculated relative to the pre-immunisation serum (NMS, dotted line) diluted identically to the immune sera, and is shown for comparison. Sera were tested on an approximately 20kDa His-tagged irrelevant protein control, at 1:5 and 1:10 sera dilutions, and the results shown as open symbols. The ELISA reader was set to take measurements at an optical density (OD) 405nm.

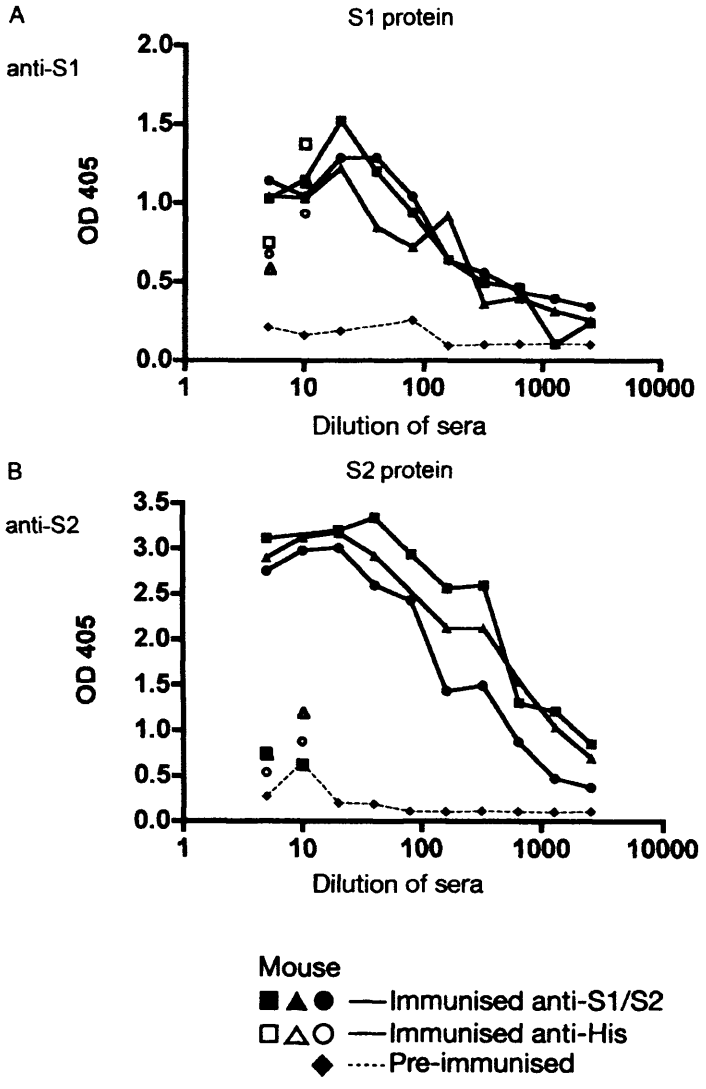
A
S1 protein
anti-S1
OD 405
2.0
1.5
1.0
0.5
0.0
1
10
100
1000
10000
Dilution of sera
B
S2 protein
anti-S2
OD 405
3.5
3.0
2.5
2.0
1.5
1.0
0.5
0.0
1
10
100
1000
10000
Dilution of sera
Mouse
■▲● —Immunised anti-S1/S2
□△○ —Immunised anti-His
◆ ·····Pre-immunised

4.4.1. ELISA assays to measure the antibody titre of mouse peptide-specific sera

The presence of antibodies to the different STEVOR peptides was determined by ELISA as described in materials and methods, and peptide 1 and 3-specific antibodies were detected in post-immunisation sera (figure 4.9). Post-immunisation sera (solid lines) from 4 mice immunised with peptide 1 (A), contained peptide-specific antibodies at titre 1 /10000, for mice 1/2/4, after which it indistinguishable from the pre-immunisation sera background (dotted lines). Mouse 3 showed a 10-fold higher antibody response than the other animals, discernible from background at a titre 1/100000.

Post-immunisation sera from 5 mice immunised with peptide 3 (B) contained peptide-specific antibodies with titres of approximately 1/10000, compared with the pre-immunisation sera (dotted lines). Mouse 5 anti-sera (circle solid lines) contained 10 fold less detectable antibody than the other 4 mice, but its pre-immunisation sera also had the lowest background (circle dotted lines). Control wells of diluents in place of serum, no peptide coat, and no secondary antibody were included and all were negative (data not shown).

Post-immunisation sera containing anti-peptide 1 and 3-specific antibodies were used for expression and co-localisation studies. Animals immunised with peptide 2 did not show specific anti-peptide antibodies, following completion of the immunisation schedule, and therefore were not used for further analysis (data not shown).

Figure 4.9: ELISA to measure levels of anti-STEVOR peptide antibodies in sera from immunised mice. Post-immunisation sera from A) four mice immunised with peptide 1, and B) five mice were immunised with peptide 3, were tested for the presence of anti-peptide antibodies (solid lines). The sera were titrated using 10-fold serial dilutions starting at 1:100. Pre-immunisation serum from each mouse, collected before the start of the immunisations, was included as a negative control (dotted lines). The endpoint is calculated relative to the pre-immunisation background, and sera considered positive only when readings were above the absorbance (OD 405nm) of identically diluted pre-immunisation sera. The assay was done in duplicate wells and the average value plotted.

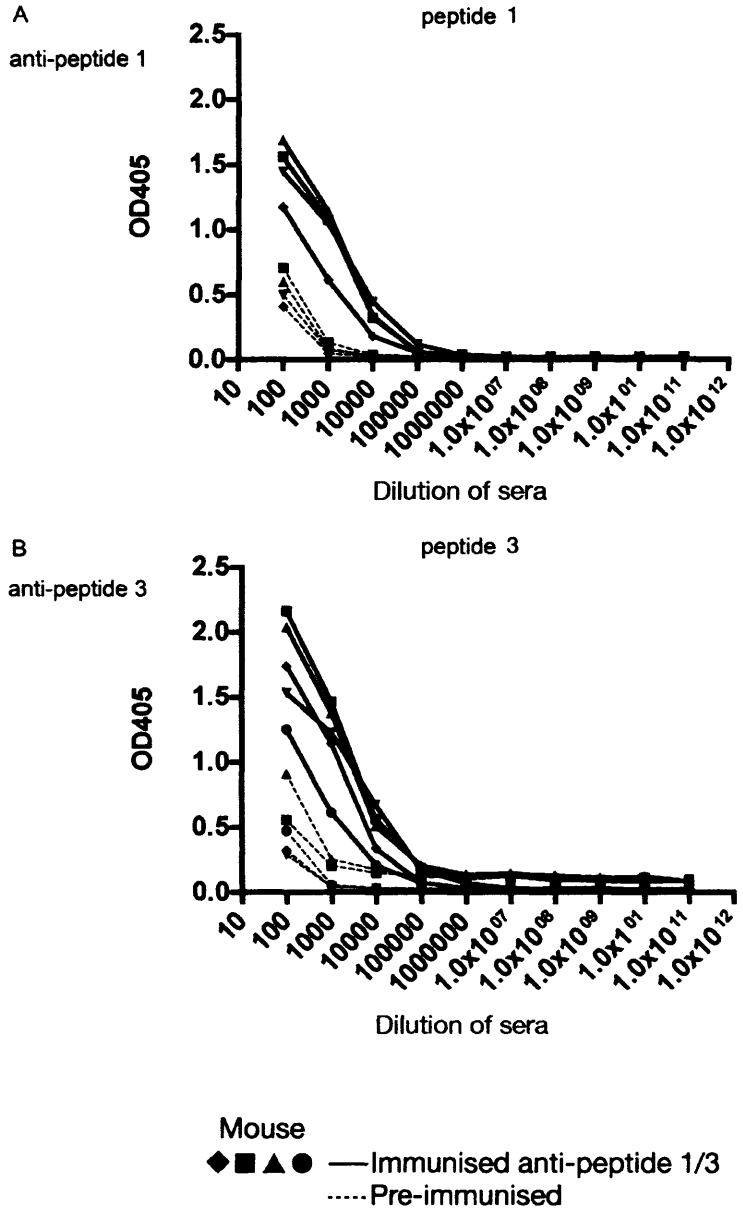
A
anti-peptide 1
peptide 1
OD405
2.5
2.0
1.5
1.0
0.5
0.0
10
100
1000
10000
100000
1000000
1.0x10^07
1.0x10^08
1.0x10^09
1.0x10^01
1.0x10^11
1.0x10^12
Dilution of sera
B
anti-peptide 3
peptide 3
OD405
2.5
2.0
1.5
1.0
0.5
0.0
10
100
1000
10000
100000
1000000
1.0x10^07
1.0x10^08
1.0x10^09
1.0x10^01
1.0x10^11
1.0x10^12
Dilution of sera
Mouse
◆■▲● —Immunised anti-peptide 1/3
·····Pre-immunised

4.5. Generation and verification of rabbit anti-peptide sera

Rabbits were bled and preliminary bleeds tested in ELISA assays to determine whether anti-peptide antibodies were present (data not shown). Seven days after the final boost (3^{rd}), the host rabbits were bled out. Plasma was prepared as described in materials and methods, and tested in ELISA assays on the specific peptide and on an irrelevant peptide control (figure 4.10).

Rabbits immunised with peptide 1 (A) and peptide 3 (C) produced high titres of specific antibodies, (1:4000-1:400000), with anti-peptide 1 sera showing the highest titre. However rabbits immunised with peptide 2 had no peptide-specific antibody response. This was not a technical problem with immunisation, since anti-KLH antibodies were present, up to 1:4000000 titre (B). Indeed, the problem also occurred with peptide 2 immunisations of mice. This peptide may not have coupled successfully to the carrier protein: The peptide was not hydrophobic and was very hydroscopic (Peter Fletcher, personal communication), but may still be a problem. Secondly this peptide may simply be non-immunogenic.

All anti-sera showed negative results when tested on an irrelevant-peptide control. Additional ELISA control wells of diluents in place of sera, no peptide coat, and no secondary antibody were included and in all cases negative.

Figure 4.10: ELISA to measure levels of anti-STEVOR peptide 1/2/3 or anti-keyhole limpet haemocyanin (KLH) antibodies in sera from immunised rabbits

Two rabbits were immunised with A) peptide 1 B) peptide 2 and C) peptide 3, serum was tested for the presence of anti-peptide antibodies either using the correct peptide or an irrelevant peptide control. Rabbits (anti-peptide 2) were also tested for anti-KLH antibodies (B). The sera were titrated using 10-fold serial dilutions starting at 1:40. The end-point was calculated relative to the pre-immunisation serum from each rabbit, collected before the start of the immunisations, and was included as a negative control, diluted identically to the immune sera. The assay was done in duplicate wells and the average value plotted.

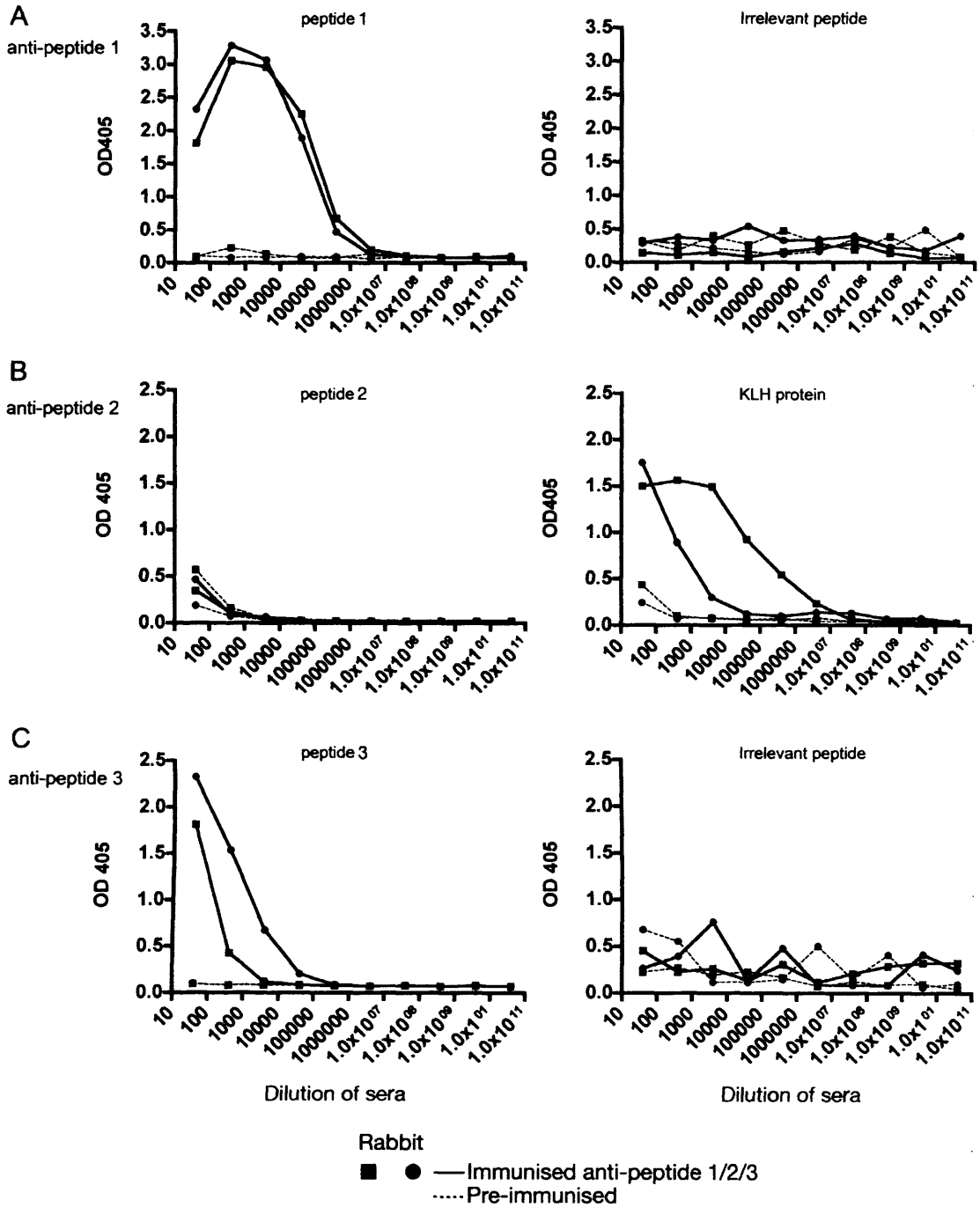
A
anti-peptide 1
peptide 1
Irrelevant peptide
OD405
OD 405
B
anti-peptide 2
peptide 2
KLH protein
C
anti-peptide 3
peptide 3
Irrelevant peptide
Dilution of sera
Dilution of sera
Rabbit
—Immunised anti-peptide 1/2/3
Pre-immunised

4.5.1. Affinity purification of rabbit anti-sera on peptide immunogen

Previous work in the lab has shown that rabbit sera used in FACS, IFA, etc tends to give high background staining. This is possibly due to natural antibodies in sera that cross-react on human proteins, and also due to binding of rabbit antibodies to human FcR (Alexander *et al.*, 1979).

To reduce the antibody binding to e.g. human antigens, affinity purification of the rabbit anti-peptide sera was carried out using NHS-activated sepharose ™ high performance Hi TRAP ™ columns covalently coupled to the STEVOR peptides (via the primary amino groups). Sera from 2 rabbits, one specific for peptide 1, and one for peptide 3, which showed the highest reactivity to peptide by ELISA, as well as a serum from 1 rabbit immunised with a control peptide (anti-A20/B) were purified on their respective peptides. 1ml of each rabbit serum was diluted 1:5 and passed over the respective column, washed and eluted in 6 elutions. For anti-peptide 1 serum, all 6 elutions contained anti-peptide 1-specific antibodies (tested in ELISA assays on the respective peptide and control irrelevant peptide), and all were pooled. Anti-peptide 3 serum-elution fractions 3-5 were pooled, and anti-A20/B serum-elution fractions 1-3 were pooled. The amounts of peptide-specific IgG recovered from 1ml of each serum are shown in table 4.2.

Table 4.2) Purification of peptide-specific antibodies

Anti-sera	**Volume of serum passed over column**	**Amount of peptide–specific IgG recovered**	**Final concentration to give positive result in ELISA assay**
Anti-peptide 1	1ml	251μg	1:2560 dilution
Anti-peptide 3	1ml	68 μg	1:2560 dilution
Anti-peptide A20/B	1ml	406 μg	1:2560 dilution

Antibodies were visualised by Coomassie blue staining on a protein gel run under reducing conditions to determine purity and check for degradation (figure 4.11). Antibody

(either anti-peptide 1 or A20/B) heavy chain (approx 60kDa) and light chain (approx 25kDa) are marked with arrows, antibodies were not fully reduced on the gel therefore larger bands (approx 170kDa) are also marked with an arrow. Multiple products, possibly due to degradation of the heavy chain are seen below 60kDa. The dialysed and concentrated eluted fractions were used subsequently in Western blot assays, immunofluorescence assays and in flow cytometry assays of gametocytes (see chapter 5).

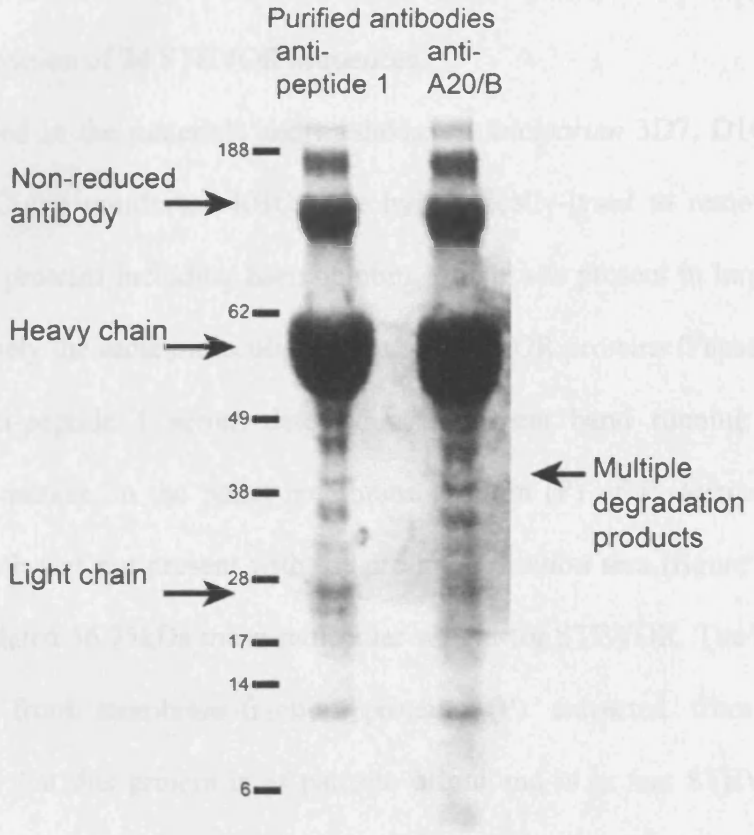

Figure 4.11: SDS-PAGE and Coomassie blue stained gel showing purified rabbit antibodies

Proteins were run on a 12% Bis-Tris gel in MES SDS running buffer under reducing conditions. Anti-peptide 1 and A20/B purified antibodies are reduced into heavy and light chains (marked with arrows). See Blue molecular marker was used for size comparison (kDa)

4.6. Western blot analysis of mouse anti-peptide sera

Western blot analysis was performed to determine whether the mouse anti-STEVOR sera recognised proteins of the predicted 30-40kDa in *P. falciparum* iRBC protein extracts (Cheng *et al.*, 1998). STEVOR mean molecular weight equals 36.75kDa, based on amino acid composition of 24 STEVOR sequences.

As described in the materials and methods, *P. falciparum* 3D7, D10 and A4 schizont-stage iRBC and uninfected RBC were hypotonically-lysed to remove all soluble non-membrane proteins including haemoglobin, which was present in large amounts and has approximately the same molecular weight as STEVOR proteins (Papakrivos *et al.*, 2005).

Mouse anti-peptide 1 serum detected a prominent band running above the 28kDa molecular marker, in the pellet membrane fraction (P) of *P. falciparum* 3D7 schizont iRBC, which was not present with the pre-immunisation sera (figure 4.12). This is close to the predicted 36.75kDa mean molecular weight for STEVOR. The corresponding band is absent from membrane-fraction proteins (P) extracted from uninfected RBC, suggesting that this protein is of parasite origin and is in fact STEVOR. Other weaker bands are visible above and below the band of interest, but these are observed in all protein fractions from both infected and uninfected RBCs, and were present with mouse pre-and post-immunisation sera.

Figure 4.12: SDS-PAGE and Western blot assay of P. falciparum *3D7 protein extracts using mouse anti-peptide antibodies*

Proteins were run on a 10% Bis-Tris gel in MES SDS running buffer under reducing conditions. Mouse antibodies were detected by anti-mouse IgG-HRP conjugated secondary antibody, and visualised using chemiluminescence. See Blue molecular marker was used for size comparison (kDa).

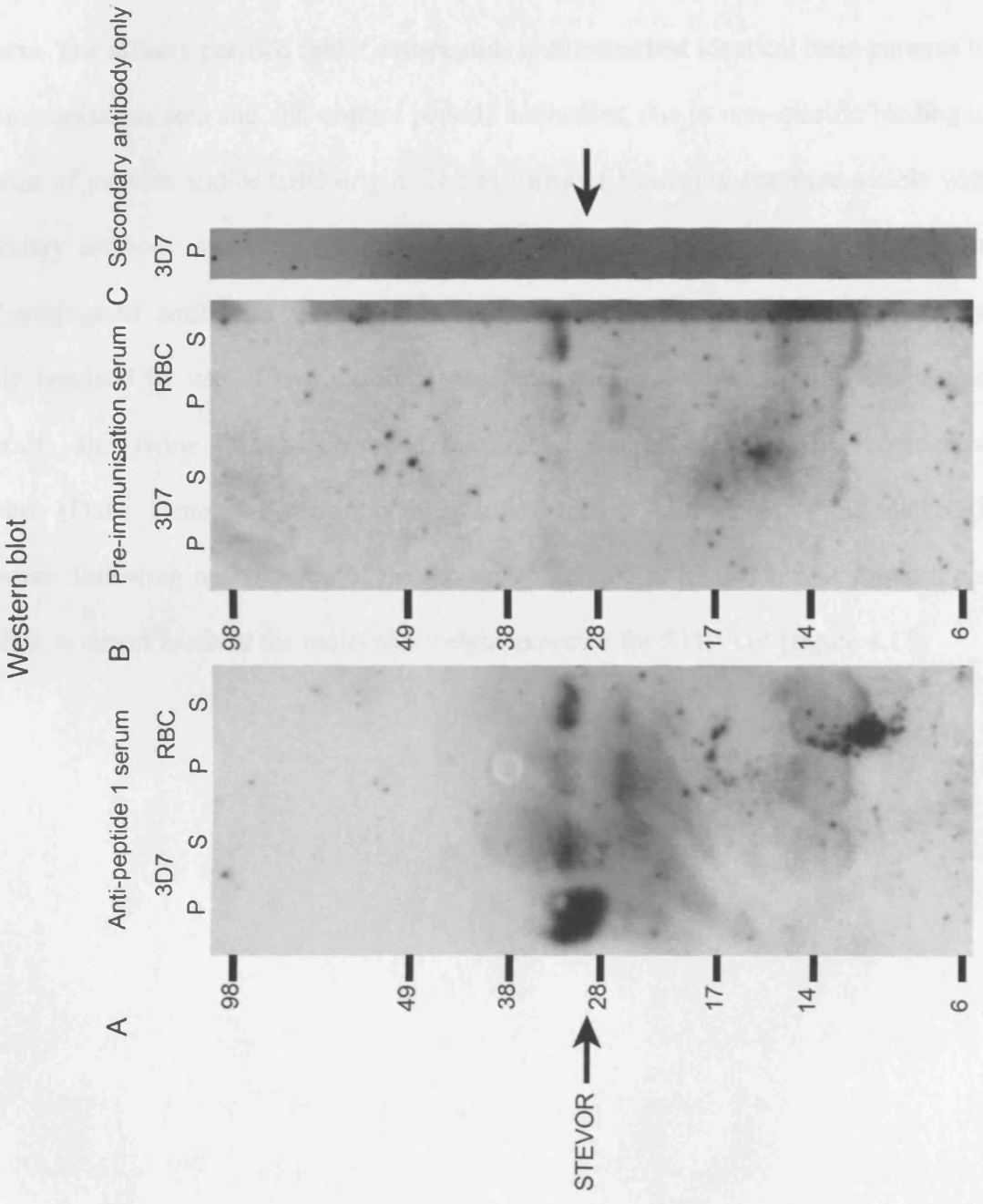
Western blot
A
Anti-peptide 1 serum
3D7
P
S
RBC
P
S
B
Pre-immunisation serum
3D7
P
S
RBC
P
S
C
Secondary antibody only
3D7
P
98
49
38
28
17
14
6
STEVOR

4.7. Affinity purified rabbit anti-peptide sera tested on parasite extracts by Western blot

No parasite-specific proteins were detected using the rabbit anti-peptide antibodies, as no difference was detected in binding of post- versus pre-immunisation antibodies to parasite extracts. The affinity purified rabbit anti-peptide antibodies had identical band patterns to pre-immunisation sera and anti-control peptide antibodies, due to non-specific binding to proteins of parasite and/or RBC origin. The majority of bands present were visible with secondary antibody alone, therefore a range of secondary anti-rabbit-immunoglobulin HRP-conjugated antibodies were tested. Problems with the secondary reagents were finally resolved by use of two excellent products, goat anti-rabbit Ig HRP-conjugated antibody, and swine (human absorbed) anti-rabbit immunoglobulin HRP-conjugated antibody (Dako, Denmark) (see antibody overview table 2.4, in materials and methods). However, following optimisation of the secondary antibodies by titration, it was still not possible to detect bands at the molecular weight expected for STEVOR (figure 4.13)

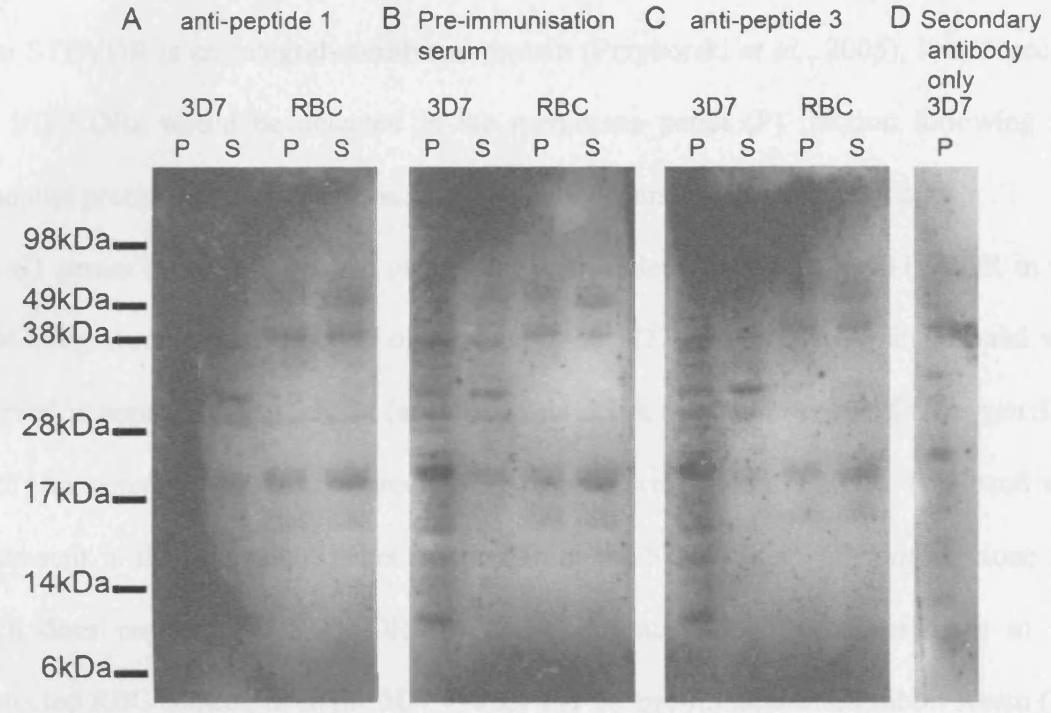

Figure 4.13: SDS-PAGE and Western blots of rabbit anti-peptide 1 or 3 affinity purified antibodies on P. falciparum *3D7 iRBC and uninfected RBC protein samples.*

A) anti-peptide 1 affinity purified antibodies B) pre-immunisation sera C) anti-peptide 3 affinity purified antibodies D) Secondary anti-rabbit IgG antibody only, were tested on iRBC and uninfected RBC protein samples split into soluble (S) and pelleted membrane (P) fractions. See Blue molecular marker was used for size comparison (kDa).

4.8. Specificity of rabbit STEVOR S1 protein sera tested on parasite extracts by Western blot

The anti-S1 sera with high antibody titres to the STEVOR recombinant protein, S1, were tested in Western blot assays using extracts of *P. falciparum* schizont iRBC (figure 4.14). Since STEVOR is an integral-membrane protein (Przyborski *et al.*, 2005), it is expected that STEVORs would be detected in the membrane pellet (P) fraction following the sequential protein extraction as described in materials and methods (figure 2.4).

Anti-S1 serum detected a protein of the expected molecular weight for STEVOR in the pellet-integral-membrane fraction of *P. falciparum* 3D7 iRBC only. A single band was observed at approximately 35kDa (arrow) in this pellet fraction (P) of *P. falciparum* 3D7 iRBC (A), corresponding to the predicted molecular weight of STEVOR. This band was not present in the equivalent pellet fraction from the STEVOR *P. falciparum* clone A4 which does not express STEVOR (personal communication Sue Kyes), nor in the uninfected RBC control, or in the 3D7 extract and the pre-immunisation rabbit serum (B). The Coomassie blue stained gel (C), shows equal loading of parasite material and RBC control proteins.

One non-specific band at 36kDa, two above and below 14kDa, and a fourth at approximately 3kDa are visible, these are most prominent in the soluble (S) protein fractions. A 14kDa band was also very obvious in the soluble fractions in the Coomassie blue stained gel (C); these bands were recognised by both pre- and post-immunisation sera. This may be due to cross-reactivity of rabbit antibodies with human normal RBC proteins. Preliminary Western blots using protein extraction method 1, as described in materials and methods, were unsuccessful and therefore the extended fractionation method 2 was used.

Figure 4.14: SDS-PAGE and Western blots using rabbit- anti-S1 sera on P. falciparum *A4/3D7 iRBC and uninfected RBC protein samples.*

P. falciparum *3D7 (STEVOR-positive) and A4 (STEVOR-negative) clones were fractionated into 3 protein populations: soluble proteins (S), carbonate-peripherally membrane-associated proteins (C), and pellet-integral-membrane proteins (P). An uninfected RBC control was treated identically. Anti-S1 rabbit serum detected STEVOR as an approximately 35kDa protein (A, marked by arrow). Rabbit pre-immunisation sera did not detect STEVOR (B). A secondary swine anti-rabbit IgG HRP-conjugated antibody and chemiluminescence was used to visualise the result on photographic film. An identical protein gel was stained with Coomassie blue stain to allow comparison of protein sample loading (C).*

Proteins were separated on a 12% Bis-Tris gels in MES-SDS running buffer under reducing conditions. See Blue molecular marker was used for protein size comparisons (kDa).

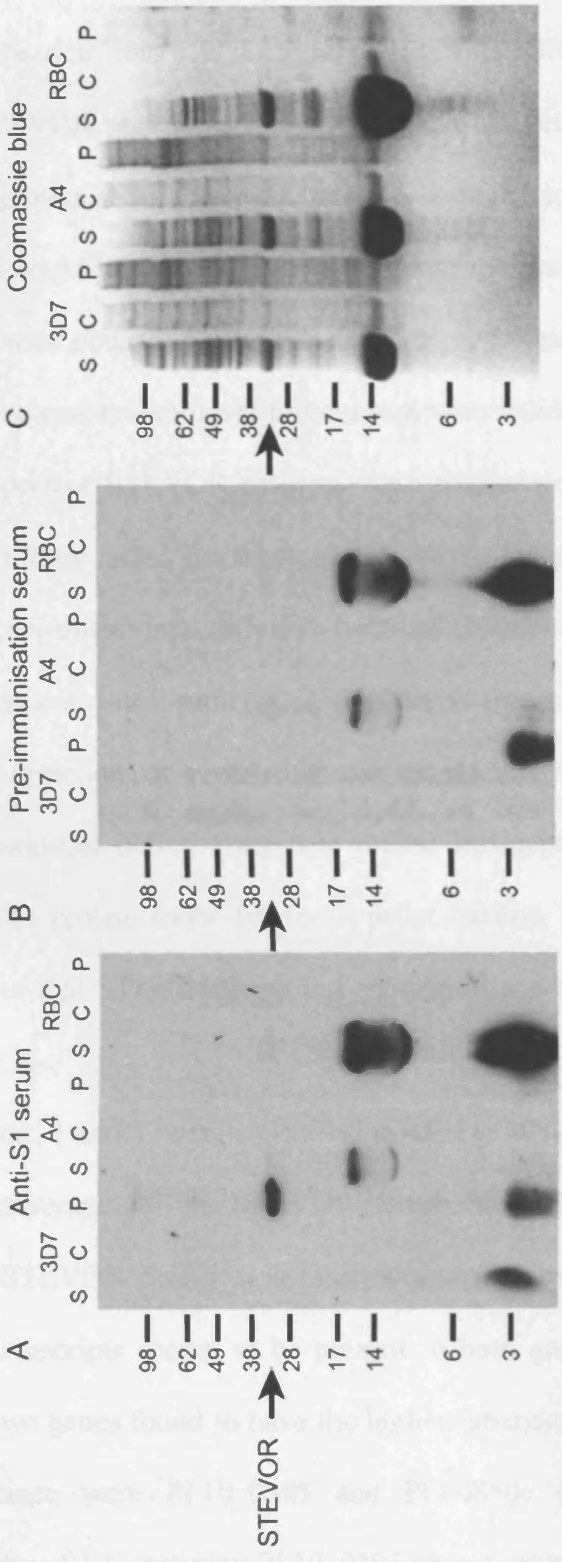
A
Anti-S1 serum
B
Pre-immunisation serum
C
Coomassie blue
3D7
A4
RBC
S C P S C P S C P
98
62
49
38
28
17
14
6
3
STEVOR

Discussion

This chapter describes the development of a panel of mouse and rabbit antibody reagents that will allow the detection and localisation of STEVOR proteins in *P. falciparum* parasites. The STEVOR proteins are highly variable in certain regions and the peptide and recombinant protein sequences were therefore designed to avoid these regions, so that antibody reagents could be developed that recognise the maximal number of STEVORs possible within a wide range of parasite lines, clones or isolates.

All anti-peptide and anti-recombinant protein sera were validated by ELISA to determine whether their respective STEVOR antigens were recognised specifically. Positive and specific sera were then tested by Western blot on *P. falciparum* blood-stage proteins, which had been separated into different fractions: Soluble proteins; carbonate buffer soluble membrane-associated proteins, and pelleted integral-membrane proteins. This method enabled detection of protein of the expected size (mean: 36.75kDa) in *P. falciparum* 3D7 schizont iRBC, using both mouse anti-peptide 1 antibodies, and rabbit anti-recombinant S1 protein antibodies in the pellet fraction, thus supporting the evidence of Przyborski *et al* that STEVOR is an integral-membrane-bound protein (Przyborski *et al.*, 2005).

The peptide regions, 1 and 3, were conserved in 45% to 80% of STEVORs, and therefore gave sufficient coverage of the STEVOR family to make useful reagents. The *P. falciparum* 3D7 STEVOR family was recently assessed by quantitative RT-PCR, and common major transcripts shown to be present in both gametocytes and their asexual progenitors, the two genes found to have the highest abundance compared to total *stevor* transcript abundance were PF10_0395 and PFF0850c (Sharp *et al.*, 2006). The recombinant proteins S1 (containing PF10_0395 amino acids 28-182) and S2 (containing PFF0850c amino acids 26-182) therefore will detect the major STEVOR proteins expressed in *P. falciparum* 3D7 asexual and sexual blood-stage parasites. In addition, the

recombinant proteins cover conserved regions of the protein (including peptide regions 1 and 2) and these antibodies are therefore expected to cross-react with other STEVOR variants.

Recombinant protein work in malaria is notoriously difficult with the majority of proteins insoluble in *E. coli* protein expression systems (Mehlin *et al.*, 2006). In addition, STEVOR is a transmembrane protein, and overall is hydrophobic and highly likely to be insoluble: The two predicted transmembrane regions and hydrophobic HVR were therefore left out of the recombinant constructs. In order to improve solubility, STEVOR N-terminal fragments were expressed in specialist host bacterial cell lines, and soluble protein was obtained. This was however at a relatively low efficiency of, on average 1mg per litre of culture despite optimisation of culture procedures. Preliminary circular dichroism data from the two recombinant proteins revealed alpha-helical structure (data not shown), this is consistent with secondary structure predictions for STEVOR (see chapter 3), suggesting the recombinant proteins had, in part, the expected secondary-structure configuration.

The recombinant protein constructs containing the STEVOR sequences do not represent the entire N-terminal semi-conserved domain (figure 4.1), missing both the canonical signal sequence at the N-terminus, and 7 amino acids prior to the first predicted transmembrane domain (TM1). The solubility and conformation of the recombinant proteins may have been improved by the inclusion of these additional 7 amino acids at the C-terminus of both recombinant proteins (amino acids 183-189), as this would have included an important, positionally conserved, cysteine (see figure 4.1; black arrow number 4), and incorporated a total of four conserved cysteines from within the N-terminal region.

Limitations of peptides

Disappointingly, despite removal of "non-specific" binding antibodies, in Western blot assays none of the rabbit anti-peptide antibodies detected proteins of the molecular weight of STEVOR. There were severe background problems in the Western blot assays, with cross-reactivity of the anti-peptide rabbit and mouse antibodies to various soluble proteins, solved as described above, in addition to various cross-reactive secondary antibody reagents. The problem with separating the "problematic cross-reactive soluble proteins" away from STEVOR is that when using these sera on iRBC in other assays IFA etc, it is not possible to separate away these same cross-reactive proteins. Therefore removal of non-specific antibodies was used to try and improve the sensitivity of the rabbit anti-peptide sera. Rabbit anti-peptide antibodies were affinity purified successfully, but this was not sufficient for recognition of STEVOR proteins within parasite extracts by Western blotting.

The anti-peptide sera may also have been unsuccessful in Western blot assays because the antibodies detect linear (peptide), rather than tertiary structural epitopes, and the linear forms are unavailable for antibody binding in the context of the endogenous proteins. STEVOR is expected to have some structural complexity, predicted as a globular protein with approximately 60% alpha helical structure by secondary structure predictions from PHDsec and PHDhtm programs (see chapter 3)(Rost & Sander, 1993; Rost *et al.*, 1995). The peptides were designed to highly conserved regions of STEVOR, the reason these regions are conserved may be that they are structurally confined and therefore hidden in the native protein structure.

Indeed, the converse may also be true in the case of the mouse anti-soluble recombinant proteins, whereby antibodies directed to tertiary structural epitopes do not then recognise the reduced form of the protein in the Western blot assay. Immuno-precipitations were carried out to determine if these antibodies would bind STEVOR protein successfully in

the liquid phase, as opposed to in a membrane-bound state: However specific bands were not detected by the post-immunisation sera (data not shown). It is highly likely that the vast majority of the soluble protein produced was not in the correctly folded configuration; therefore antibodies recognising non-native epitopes consequently do not recognise reduced endogenous STEVOR by these methods.

Advantage of recombinant proteins

The anti- recombinant S1 antibodies recognised STEVOR-sized proteins in Western blot assays. Optimised Western blot assays were successful with the rabbit-anti-S1 recombinant protein sera, and STEVOR was detected as a 35kDa band in the pellet fraction from *P. falciparum* 3D7 iRBC, but not in the A4 iRBC fraction. This provides further evidence for the non-expression of STEVOR in the A4 parasite clone, and suggests that under cultured *in vitro* conditions the *stevor* multigene family is non-essential. This may also explain why anti-peptide 3 antibodies did not recognise STEVOR in Western blot assays, as low expression levels of the STEVOR multigene family in the cultured laboratory parasites (see chapter 5, table 5.1), in combination with only approximately 50% of STEVOR sequences being recognised by the anti-peptide 3 sera (see table 4.1), may have meant STEVOR was below the detection level for these reagents. Indeed anti-peptide 3 antibodies would not recognise, (having two amino acid mismatches), the *stevor* gene PF10_0395 the major transcript found in *P. falciparum* 3D7 blood-stage parasites (Sharp *et al.*, 2006).

Conclusions

In conclusion, we have a number of rabbit and mouse antibody reagents, which recognise up to 80% of the *P. falciparum* 3D7 STEVOR multigene family, and approximately the same proportion of STEVORs from a Ghanaian field isolate. These specifically recognise

STEVOR peptides, and recognise an integral membrane protein of similar molecular weight to STEVOR in the pellet fraction from *P. falciparum* 3D7 iRBC in Western blot assays. Therefore they will be useful tools for fully evaluating the expression and localisation of STEVOR within a range of *P. falciparum* clones and isolates.

Table 4.3) Summary of anti-STEVOR antibody reagents

		ELISA		Western blot	
Reagent	**Host**	**Result**	**Figure**	**Result**	**Figure**
S1	Rabbit	+	4.7	+	4.14
S2	Rabbit	-	4.7	n.d.	_
S1	Mouse	~	4.8	-	p177 (data not shown)
S2	Mouse	+	4.8	-	P177 (data not shown)
P1	Rabbit	+	4.10		4.13
P2	Rabbit	-	_		n.d.
P3	Rabbit	+	4.10		4.13
P1	Mouse	+	4.9		4.12
P2	Mouse	-	_		n.d.
P3	Mouse	+	4.9		4.12

Chapter 5) Introduction: Co-localisation of STEVOR

The presence of STEVOR-proteins in several parasite life-stages has lead to the suggestion that STEVOR may have multiple functions. Transcription of STEVOR during the later-stages of the blood-stage cycle (from 22 hours post-invasion) (Kaviratne *et al.*, 2002; Sharp *et al.*, 2006), following that of the *rif* and *var* gene families (Kyes *et al.*, 2000), raises the possibility that STEVOR is functionally required post-expression of these two families. Therefore the final destination of STEVOR will most likely be found at the late schizont-stage, just prior to or at, rupture and merozoite release. Interestingly, another smaller gene family encodes SURFINs which are found both on the surface of the iRBC and at the apical tip of merozoites (Winter *et al.*, 2005). Therefore given the timing of STEVOR expression it potentially could also be located in merozoites. The late stages of the erythrocytic cycle were thus the major focus in this chapter.

STEVOR within asexual-stages

Current knowledge of STEVOR location within the iRBC is based almost entirely upon immunofluorescence studies with anti-peptide antibodies on fixed *P. falciparum* 3D7 iRBC, which locate STEVOR in the Maurer's clefts during trophozoite and schizont-stages (Kaviratne *et al.*, 2002). STEVOR was found to co-localise with anti-PfSBP1 antibodies, and also with anti-truncated PfEMP3 antibodies, both of which stain proteins located in, or exported to the Maurer's clefts.

A second study of STEVOR export within 3D7 trophozoites transfected with GFP-fusion constructs, observed full length STEVOR is exported to the Maurer's clefts where it was shown to co-localise with PfSBP1 and PfEMP1 (Przyborski *et al.*, 2005).

The polymorphic nature of STEVOR's HVR, together with the high copy numbers of homologous *stevor* genes in the *P. falciparum* genomes, suggests that STEVOR is an immune target. Evidence exists that multigene families including *var* and potentially *rif*

commonly encode VSAs. This suggests that the iRBC surface is a reasonable location to expect to find STEVOR. Whether STEVORs, RIFINs, of indeed another family of two transmembrane paralogues, PfMC-2TM, reach the iRBC surface is not known.

This iRBC surface prediction is inconsistent with evidence from studies of STEVOR and RIFIN using transfections and GFP-tagged recombinant proteins to investigate protein localisation and orientation, which indicate that both STEVORs and RIFINs reside in the Maurer's clefts in late stage iRBCs (Khattab & Klinkert, 2006; Przyborski *et al.*, 2005). Selective permeabilisation experiments to determine the orientation of STEVORs within the Maurer's cleft, place the HVR within the Maurer's cleft lumen (Przyborski *et al.*, 2005). In contrast, the longer HVR of the RIFIN protein was exposed to the iRBC cytosol (Khattab & Klinkert, 2006). Thus the final destination and orientation of these proteins is somewhat contradictory. What their functions are and how they are related to one another is also unknown.

Other surface immunofluorescence techniques, such as flow cytometry allow a direct-examination of the surface of individual iRBCs, which means that blood containing a low percentage of late stages (as low as 0.05%) can be tested without prior purification and concentration, suitable in particular for field parasite isolates where parasitaemia may be low. In addition, heterogeneous samples, containing more than one serotype, can be identified by the relative percentage of fluorescent and non-fluorescent pigment-containing cells (Hommel *et al.*, 1983). Therefore it was possible using reagents described in chapter 4, to examine live (unfixed) iRBCs for STEVOR surface expression.

STEVOR within gametocytes

Transcription, expression and location of STEVOR is different in gametocytes to in asexual-stages: 1) truncated *stevor* transcripts are present in gametocytes; and a missing second transmembrane domain could lead to a different orientation of STEVOR in the

membrane (Przyborski *et al.*, 2005; Sutherland, 2001). 2) STEVOR is expressed in late stage gametocytes and is associated with the iRBC membrane, and not within Maurer's clefts (McRobert *et al.*, 2004). 3) Export to the iRBC membrane is Maurer's clefts independent, since these structures are not present in late stage gametocytes. Maurer's cleft PfSBP1 staining was only transiently observed in day 6 gametocytes with no evidence of STEVOR co-localisation (McRobert *et al.*, 2004). All these facts suggest that STEVOR may be located in the surface membrane of gametocyte iRBC, and potentially orientated in a different membrane-bound state, to that in the asexual-stages. Consequently regions to which peptides 1, 2 or 3 were designed could be exposed on the surface of unfixed gametocytes. Mediation of gametocyte sequestration has been suggested as one possible function for STEVOR at this stage, thus if expressed on the surface of gametocytes, STEVOR could function through conserved N-terminal sequences encoding binding domains (Rogers *et al.*, 2000).

Finally, a comparison of transcription of *rif* and *stevor* gene families in *P. falciparum* 3D7 and fresh isolates revealed higher transcription levels in fresh isolates compared with the 3D7 parasite (Daily *et al.*, 2005). In addition a genome-wide comparison of three *P. falciparum* laboratory clones Dd2, 3D7 and HB3, revealed transcriptional differences in polymorphic antigens e.g. encoding *var* and *rifins*, whilst transcription of *stevor* during the intra-erythrocytic-stage was not observed (Llinas *et al.*, 2006). Expression of STEVOR has thus far only been studied in *P. falciparum* 3D7 and it is possible that prolonged culture has affected STEVOR expression. Therefore a more comprehensive study of STEVOR from multiple *P. falciparum* sources is necessary.

Objectives

This chapter describes the investigation of:

What is the final destination of STEVOR within the iRBC

1) **Is STEVOR expressed on the iRBC surface**
2) **Is STEVOR expressed in the apical organelles of merozoites**
3) **Does expression of STEVOR in the laboratory strain *P. falciparum* 3D7 reflect that of other laboratory grown parasites, and, more importantly, fresh field isolates of *P. falciparum*.**

Results

5.1. Detection of STEVOR using affinity purified anti-peptide antibodies

Affinity purified rabbit anti-peptide 1 immunoglobulin (see table 4.2 and figure 4.11) was used to determine STEVOR expression in the *P. falciparum* laboratory strains 3D7, D10, and a representative field isolate from Kilifi: K1657 (figure 5.1).

This anti-STEVOR antibody gave a punctate staining throughout the iRBC, present from the late trophozoite-stage and throughout schizont development. However, in the highly developed segmented schizont-stage parasites the staining pattern of STEVOR was more diffuse both around the parasite nuclei and throughout the iRBC cytosol, potentially associated with the iRBC surface membrane. The amount of STEVOR positive parasites differs marginally between the two lab strains (table 5.1) but the intensity and pattern are similar. The field isolate, K1657 (figure 5.1c) however has a much brighter, stronger staining most visible at late schizont-stage, and a much higher proportion of parasites are STEVOR expressing (table 5.1).

Maurer's cleft staining by PfSBP1 antibodies was punctate throughout the iRBC cytoplasm as described previously (Blisnick *et al.*, 2000), although the majority of Maurer's clefts were often found in the periphery of the iRBC cytosol during the late schizont-stage, compared with earlier trophozoites (figure 5.1b LT/ES compared with LS). This pattern and distribution of Maurer's clefts was consistent regardless of whether parasites were cultured, or parasite's origin.

In both the laboratory strains and in the K1657 field isolate, STEVOR and PfSBP1 antibodies co-localised at late trophozoite and early schizont-stages, but at late schizont-stage the staining patterns of each were distinct, suggesting that the final location of STEVOR was not the Maurer's cleft.

For all isolates, control stains using normal rabbit immunoglobulin or secondary antibody reagents alone were negative. The positive control anti-MSP1-$_{19}$ (FITC) showed

characteristic staining of the merozoite's surface and did not co-localise with Maurer's cleft staining with anti-PfSBP1.

Table 5.1) Percentage of STEVOR positive parasites

P. falciparum clone/ Kilifi field isolate	% STEVOR expressing schizonts	Anti-STEVOR antibody reagent
3D7	3%	Anti-peptide 1
	5%	Anti-S1
D10	7%	Anti-peptide 1
	7%	Anti-S1
A4	0%	Anti-S1
K1657	50%	Anti-peptide 1
K1640	50%	Anti-S1

Figure 5.1: STEVOR immunofluorescence staining of mature (>24hour) blood-stage P. falciparum *A) 3D7 B) D10 and C) representative Kilifi field isolate (K1657) parasites using anti-peptide 1 antibodies.*

*a) An early or late-stage trophozoite (ET/LT), b) a late trophozoite-early schizont-stage (LT/ES), c) late schizont (LS)-stage parasite double-stained with STEVOR anti-peptide 1 rabbit affinity-purified antibodies (green), and Maurer's cleft anti-*PfSBP1 *mouse serum (red). Parasite nuclei are stained with DAPI (1μg/ml) (blue). d) Negative control anti-irrelevant peptide antibodies (green) e) Positive control anti-MSP1-$_{19}$ anti-sera (green) f) Secondary goat anti-rabbit IgG FITC conjugated antibody only (green).*

Goat anti-rabbit IgG FITC conjugated antibody and goat anti-mouse IgG TRITC conjugated antibodies were used as secondary antibodies. Cells were viewed on a Deltavision fluorescence microscope under a 100X oil objective, overall magnification 110X. Images shown represent the vast majority of iRBC viewed in 100 plus fields.

3D7

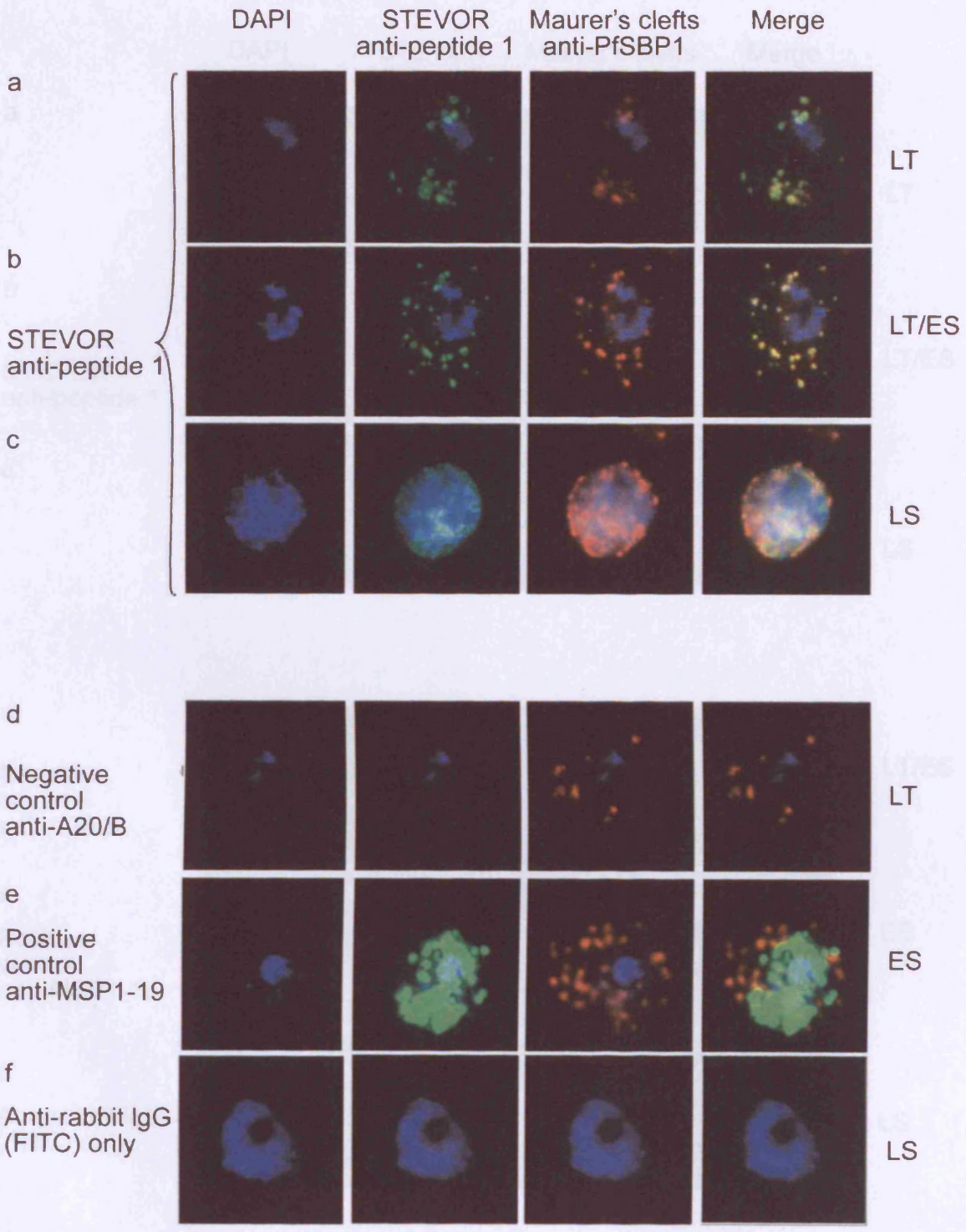
DAPI
STEVOR anti-peptide 1
Maurer's clefts anti-PfSBP1
Merge
a
b
c
STEVOR anti-peptide 1
LT
LT/ES
LS
d
Negative control anti-A20/B
e
Positive control anti-MSP1-19
f
Anti-rabbit IgG (FITC) only
LT
ES
LS

D10

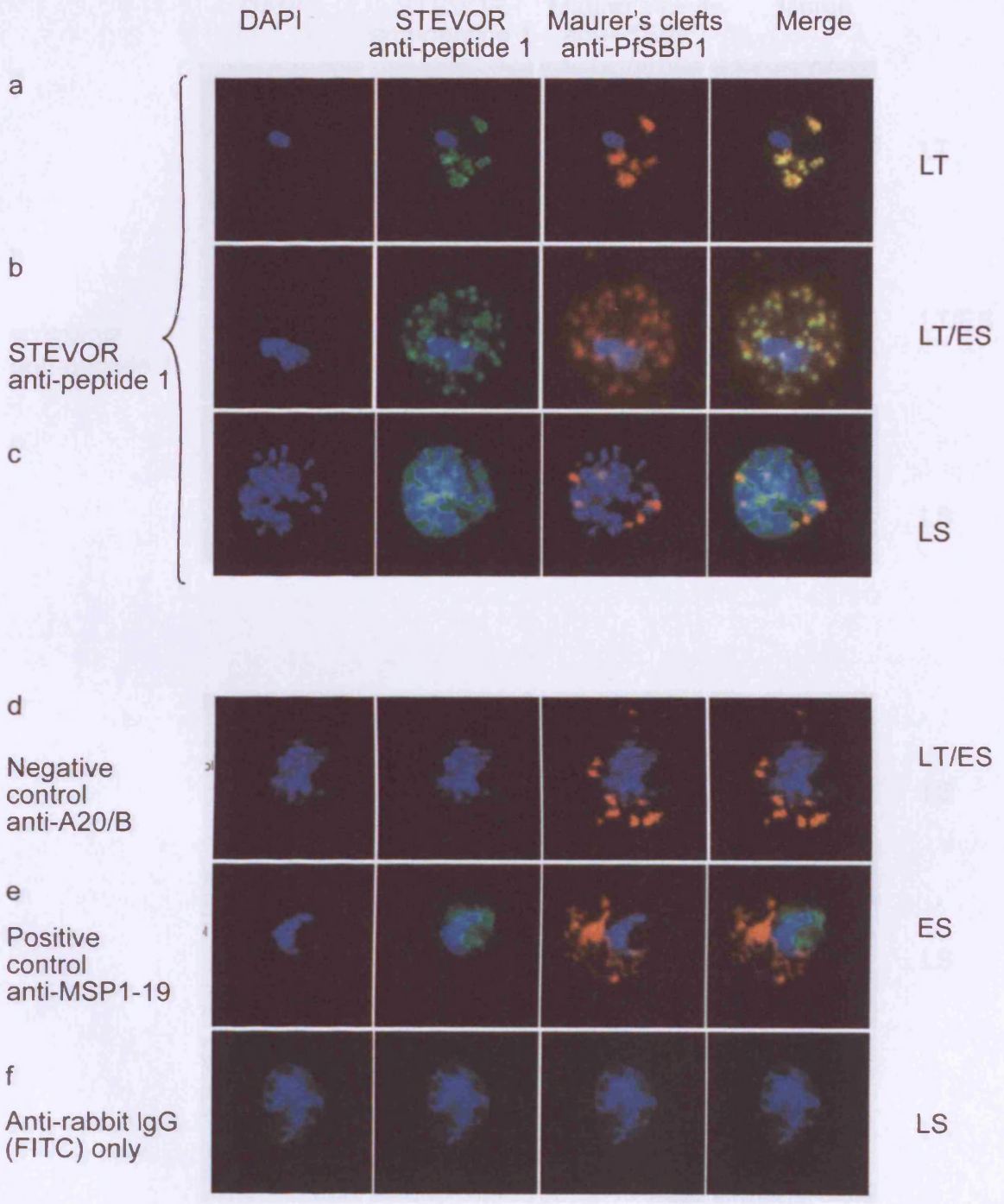
DAPI
STEVOR anti-peptide 1
Maurer's clefts anti-PfSBP1
Merge
a
b
STEVOR anti-peptide 1
c
LT
LT/ES
LS
d
Negative control anti-A20/B
e
Positive control anti-MSP1-19
f
Anti-rabbit IgG (FITC) only
LT/ES
ES
LS

K1657

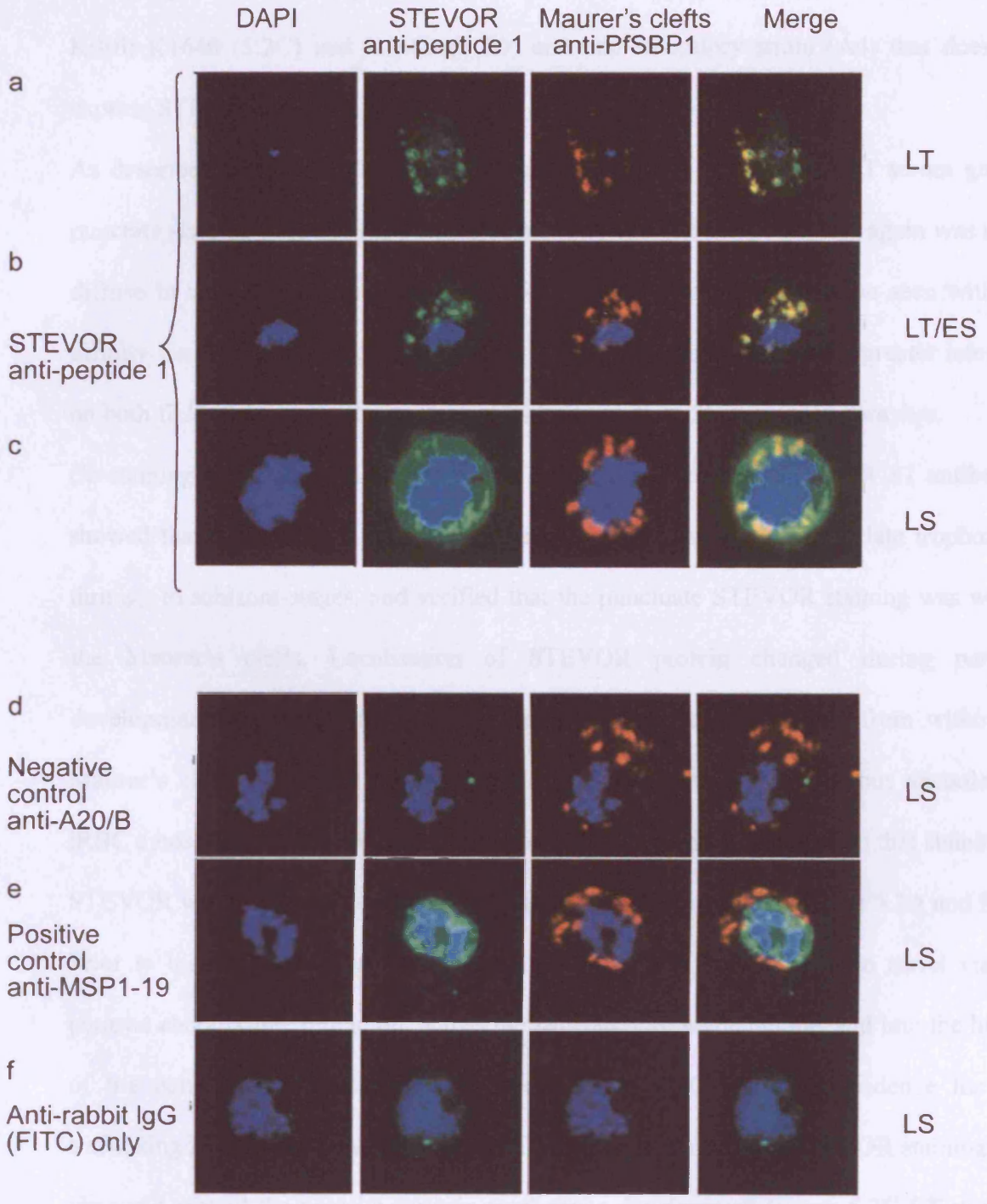
DAPI
STEVOR anti-peptide 1
Maurer's clefts anti-PfSBP1
Merge
a
b
c
STEVOR anti-peptide 1
LT
LT/ES
LS
d
Negative control anti-A20/B
e
Positive control anti-MSP1-19
f
Anti-rabbit IgG (FITC) only
LS
LS
LS

5.2. Location of STEVOR using rabbit anti-recombinant protein S1 anti-sera

Anti-S1 rabbit-serum was used to determine STEVOR expression in the *P. falciparum* laboratory strains 3D7 (figure 5.2A), D10 (5.2B), two representative field isolates from Kilifi: K1640 (5.2C) and K1489 (5.2D) and one laboratory strain (A4) that does not express STEVOR.

As described with the anti-peptide antibodies in section 5.1, the anti-S1 serum gave a punctate staining-pattern in late trophozoite, early and late schizonts, and again was more diffuse in the late schizonts (figure 5.2A-C), identical to the distribution seen with the affinity-purified anti-peptide 1 antibodies. Again, the staining showed a greater intensity on both field isolate parasites compared with that seen on 3D7 and D10 parasites.

Co-staining using antibodies specific for PfSBP1 and the anti-STEVOR S1 antibodies showed that the STEVOR proteins co-localised with Maurer's clefts in late trophozoite through to schizont-stages, and verified that the punctuate STEVOR staining was within the Maurer's clefts. Localisation of STEVOR protein changed during parasite development, from early trophozoites through to late schizont-stages, from within the Maurer's clefts to a more diffuse staining throughout the parasitophorous vacuole and iRBC cytosol in the late schizonts. Analysis of bright field images showed that staining of STEVOR was closely associated with the iRBC surface membrane (figure 5.2A and B).

Prior to localisation within the Maurer's clefts, STEVOR is thought to travel via the parasite endoplasmic reticulum, across the parasite plasma membrane, and into the lumen of the parasitophorous vacuole (Przyborski *et al.*, 2005). Further evidence for this trafficking is provided here using anti-STEVOR S1 antibodies, as STEVOR staining was observed around the parasite early in trophozoite development (figure 5.2C ET-stage (a and b)).

Mouse anti-S1 sera were also generated and tested in IFA for co-localisation with rabbit anti-S1 sera to verify STEVOR staining on iRBC (figure 5.2E). The characteristic

punctuate staining is observed in *P. falciparum* 3D7 with both antibodies indicating the mouse anti-sera are STEVOR-specific. Both antibodies were observed to completely merge when overlaid.

Staining of *P. falciparum* A4 parasites was carried out with anti-STEVOR antibodies, as this clone does not transcribe or express STEVOR proteins (RT-PCR and Western blot assays chapter 3 figure 3.4, and chapter 4 figure 4.13). Staining of all *P. falciparum* A4 schizonts with all anti-STEVOR antibodies was negative.

Figure 5.2: STEVOR immunofluorescence staining of mature (>24hour) blood-stage P. falciparum *A) 3D7, B) D10, and two representative Kilifi field isolates C) K1640, and D) K1489 parasites, using anti-S1 sera. Early trophozoite (ET), late trophozoite (LT), early schizont (ES), or late schizont (LT) iRBC were either double-stained with STEVOR anti-S1 rabbit serum (green), and Maurer's cleft anti-*PfSBP1 *mouse serum (red), or only single-stained with STEVOR anti-S1 serum (green) and bright field images shown.*
E) IFA showing complete co-localisation of rabbit (green) and mouse (red) anti-S1 recombinant protein anti-sera, a) late trophozoite (LT) blood-stage parasite with a single nucleus, b) an early schizont (ES) with the beginnings of multiple nuclei.
Goat anti-rabbit IgG FITC conjugated antibody and goat anti-mouse IgG TRITC conjugated antibodies were used as secondary antibodies. Parasite nuclei are stained with DAPI (1μg/ml) (blue). Cells were viewed on a Deltavision fluorescence microscope under a 100X oil objective, overall magnification 110X. Images shown represent the vast majority of iRBC viewed in 100 plus fields.

3D7

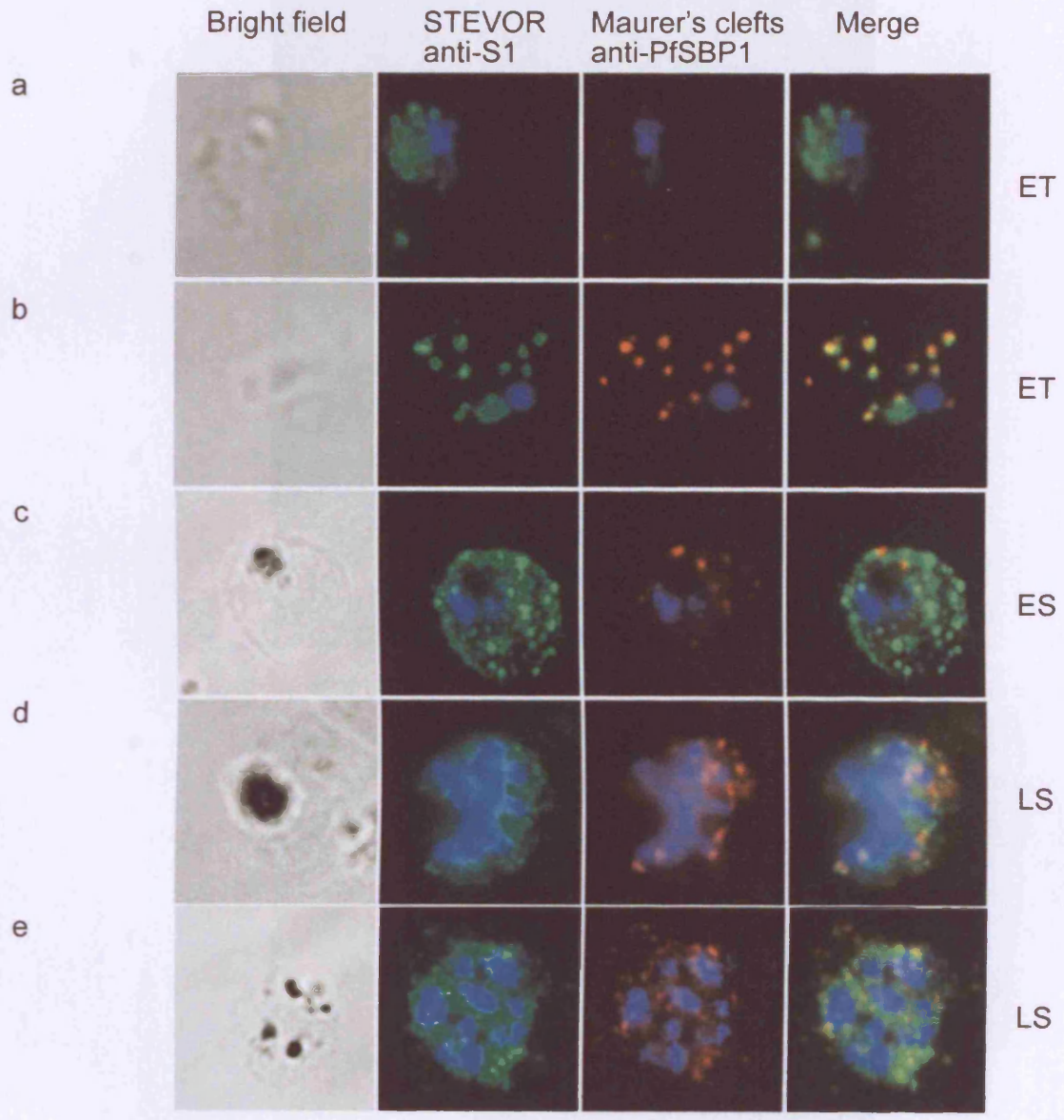
Bright field
STEVOR anti-S1
Maurer's clefts anti-PfSBP1
Merge
a
b
c
d
e
ET
ET
ES
LS
LS

D10

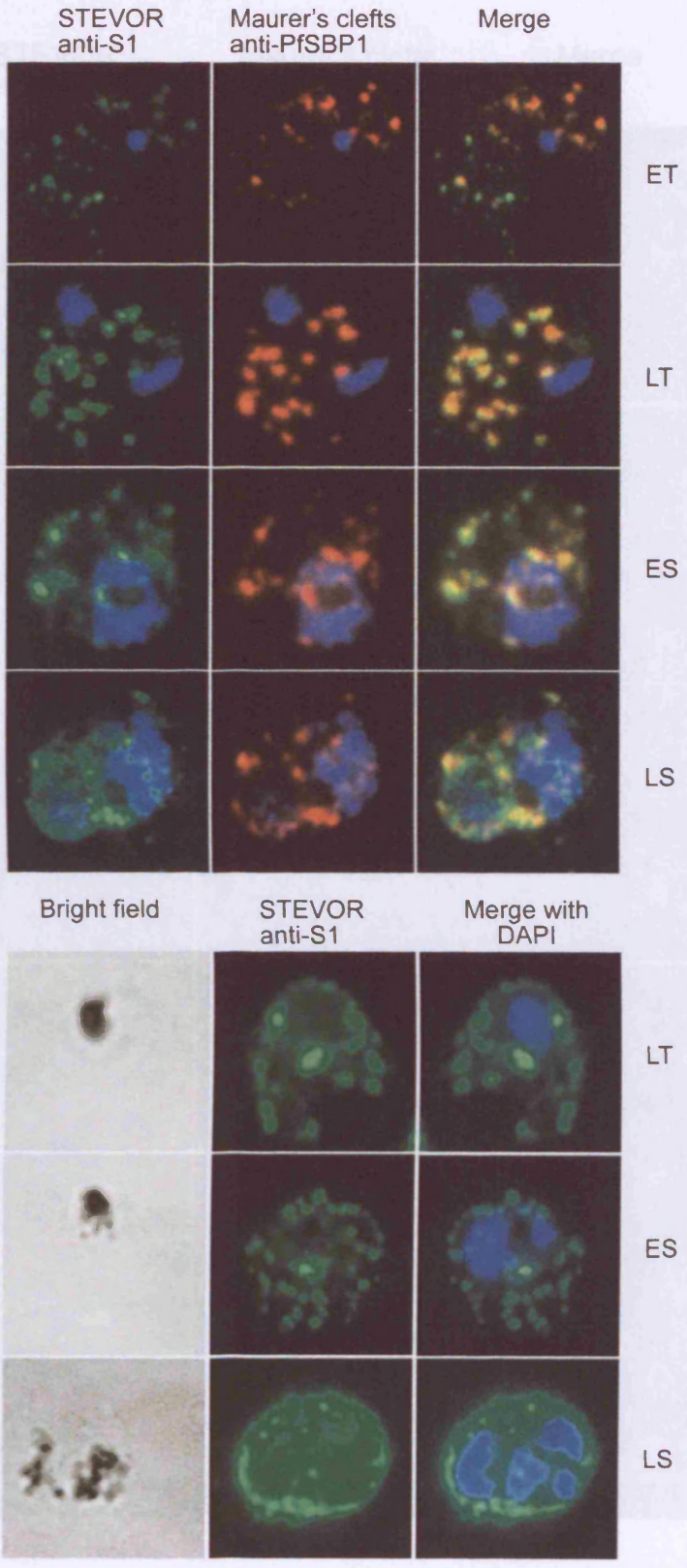
STEVOR anti-S1
Maurer's clefts anti-PfSBP1
Merge
a
b
c
d
ET
LT
ES
LS
Bright field
STEVOR anti-S1
Merge with DAPI
e
f
g
LT
ES
LS

K1640

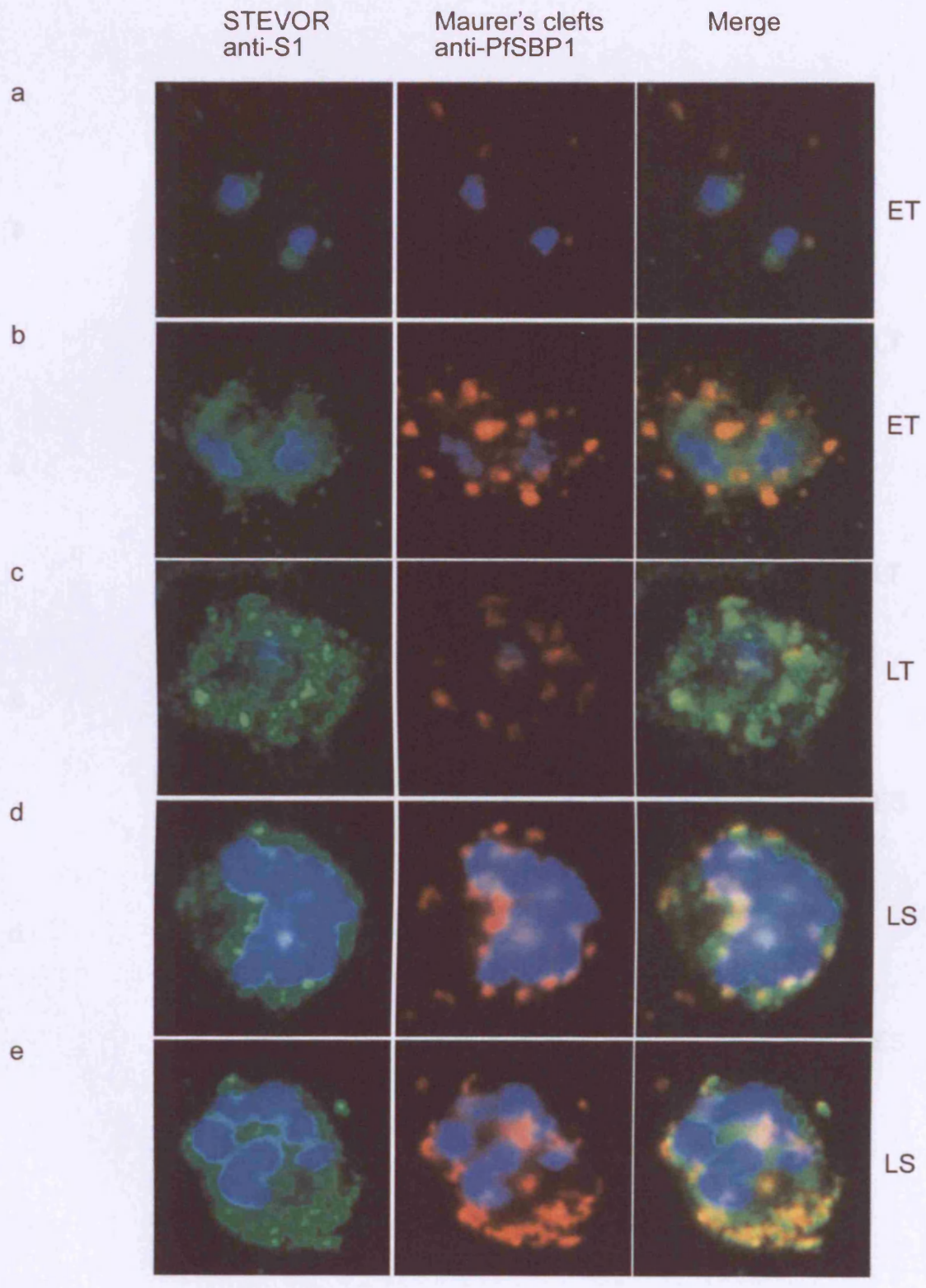
STEVOR
anti-S1
Maurer's clefts
anti-PfSBP1
Merge
a
b
c
d
e
ET
ET
LT
LS
LS

K1489

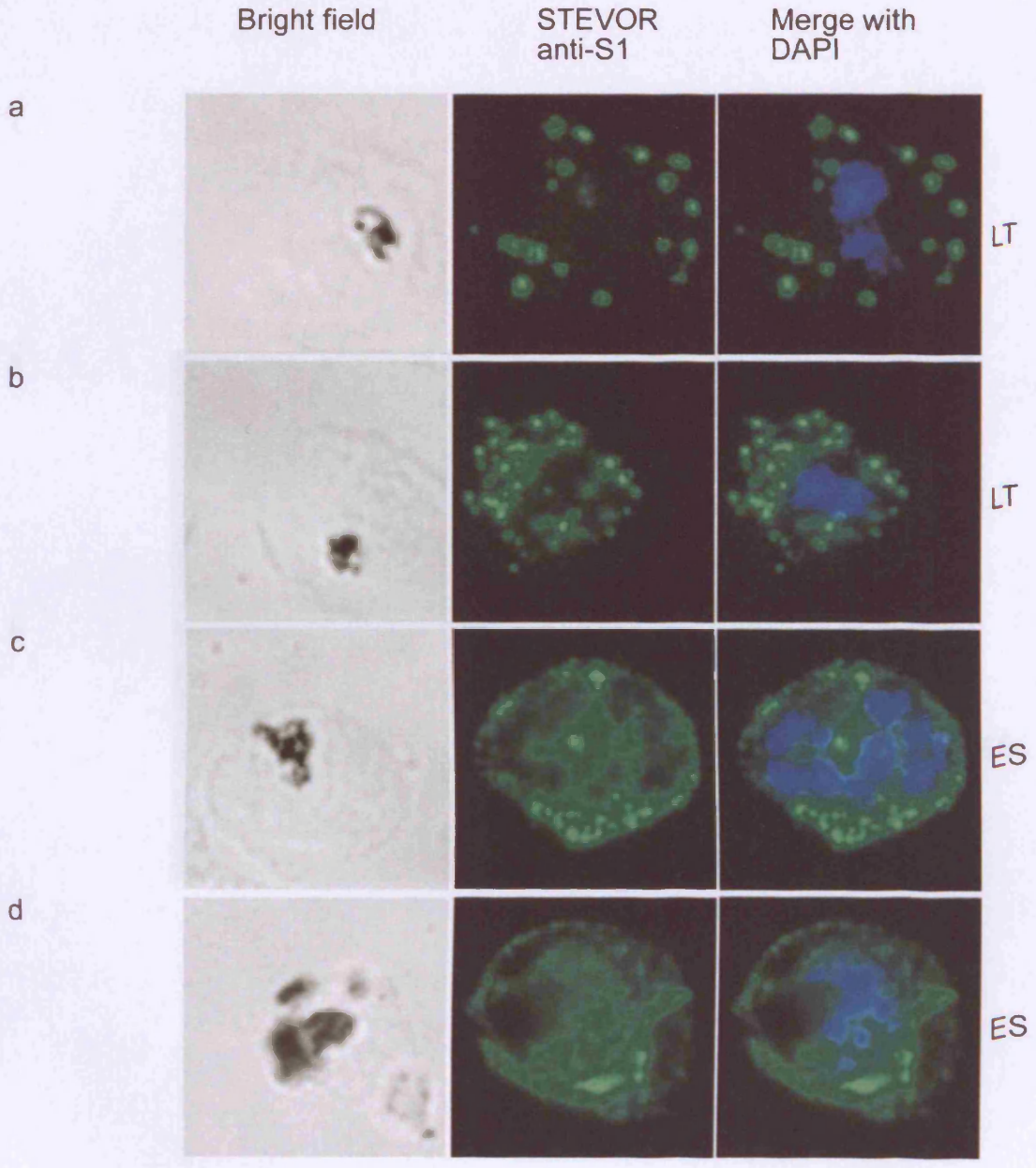

3D7

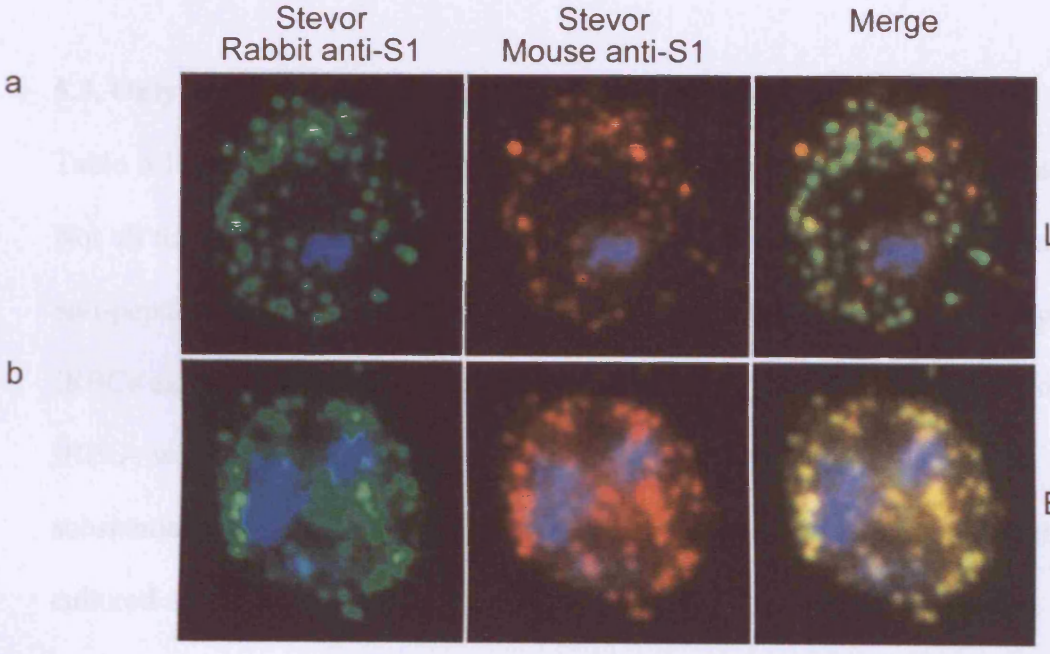

In summary, both affinity-purified anti-peptide 1 antibodies and anti-S1 recombinant protein anti-sera give similar staining-patterns. Importantly STEVOR is seen closely co-localised in the Maurer's clefts throughout late trophozoite and schizont-stages, but not in late schizonts of all STEVOR-expressing parasites studied. All parasites studied showed the same pattern and localisation of STEVOR protein-expression. However STEVOR expression in the Kilifi field isolates looked very different compared with the in vitro laboratory cultured lines. A much higher proportion of the iRBCs expressed STEVOR and the staining was much more intense than those of the laboratory lines.

5.3. Only a sub-population of iRBCs express STEVOR proteins

Table 5.1 summarises the percentage of schizont-stage parasites that express STEVOR. Not all the schizonts in each of the parasite clones tested gave positive staining with the anti-peptide 1 antibodies and the anti-S1 anti-serum, suggesting that only a proportion of iRBCs express STEVOR. In the case of two laboratory lines 3D7 and D10, only 3-7% of iRBC were positively stained. The proportion of positively stained iRBC was substantially higher in the iRBC from field isolates (50%). This difference between cultured strains and field isolates was unlikely to be due to expression of different STEVORs as theoretically the antibody reagents were able to detect a large number of STEVORs from all parasites studied (see chapter 4). By contrast, all *P. falciparum* schizonts counted had Maurer's clefts, judged by the PfSBP1 antibody staining.

In order to assess whether the low percentage of *P. falciparum* 3D7 schizont-stage parasites expressing STEVOR may have been due to preparation of samples at different stages or times in the *in vitro* cycle, slides of purified schizonts undergoing transfer from schizont to reinvasion states were prepared and stained with anti-S1 serum. Previously, parasite samples although cultured to allow trophozoite and late schizont-stages to develop, still contained mixed parasite-stages, as the cultures were not synchronous.

Therefore assessment of STEVOR positive schizonts was difficult due to low numbers of schizonts per viewing field, whereas field isolate samples were synchronous as they were not cultured beyond a single cycle after resuscitation.

However, even in the samples with purified schizont-stages, expression of STEVOR occurred only in a small sub-population of parasites. The percentage of STEVOR positive (3D7) schizonts, using anti-S1 rabbit anti-sera, was found to be 5% only in this purified schizont population, slightly higher than when previously assessed (compared to 3% using anti-peptide 1 rabbit sera).

5.4. Is STEVOR expressed on the surface of RBC infected with asexual-stages?

The peripheral staining pattern of STEVOR on late schizont-stages in *P. falciparum* fixed iRBC suggested that STEVOR may be either associated with the iRBC membrane or is on the surface of the iRBC, similar to VAR and RIFINs (Baruch *et al.*, 1995; Fernandez *et al.*, 1999; Kyes *et al.*, 1999; Smith *et al.*, 1995; Su *et al.*, 1995).

To test this hypothesis, both the affinity-purified anti-peptide antibodies and anti-S1 serum were used to stain live *P. falciparum* in different stages of the intra-erythrocytic life cycle from culture.

5.4.1. Optimisation of staining conditions for flow cytometry

The staining method for flow cytometry of live *P. falciparum* infected-cells was optimised on the *in vitro* culture parasite lines: *P. falciparum* 3D7 and A4. Parasites were grown to late schizont-stage, which was shown in the previous section to be the optimum time in the erythrocytic-stages of 3D7 development, when STEVOR expression was associated with the iRBC membrane.

Hoechst 33342 or Ethidium bromide were used to stain parasite iRBC and thus identify and determine the proportion of iRBC in the sample (figure 5.3). The excitation of

Ethidium bromide with the argon laser (488nm) leads to peak emission at 605nm when bound to DNA in iRBCs (Jagers, 1983; Watson, 1981), but it can also be detected by photomultipliers with band passage filters set at 585nm (FL-2) and >650nm (FL-3) on the FACSCalibur (Vindelol, 1978). Hoechst 33342 exclusively stains DNA: it is excited by a UV laser (355nm) and detected in the UV range (395-415nm) (Hiller *et al.*, 2004). Both methods were titrated to give parasitaemias comparable with counts on Giemsa-stained thin blood films. However, due to health and safety restrictions it was only possible to carry out live-cell flow cytometry on a FACSCalibur thus only Ethidium bromide was suitable for this method.

RBCs and iRBCs were first gated on forward scatter (FCS) and side scatter (SSC), enabling the elimination of debris. Together with cell size (FCS) and granularity/complexity (SSC), both DNA fluorochromes allow the distinction of gametocyte-stages and other single nucleated-stages (rings, trophozoites) from multinucleated schizont-stage iRBC (Hiller *et al.*, 2004). Rabbit anti-human RBC ghost sera (W49/W50) were then used to optimise the method for labelling molecules on the surface of both RBC and iRBC (figure 5.4).

Additionally, the *P. falciparum* laboratory clone A4 was used as a negative control for the expression of STEVOR (Sue Kyes personal communication): Since this clone has been used to study expression of VSA, and reacts well in FACS assays with Kilifi immune sera (Macintosh, 2006). The anti-STEVOR peptide 1 antibodies did not stain the surface of *P. falciparum* A4 iRBC, whereas both RBC and iRBC could be stained with the rabbit anti-human RBC ghost sera (figure 5.5a).

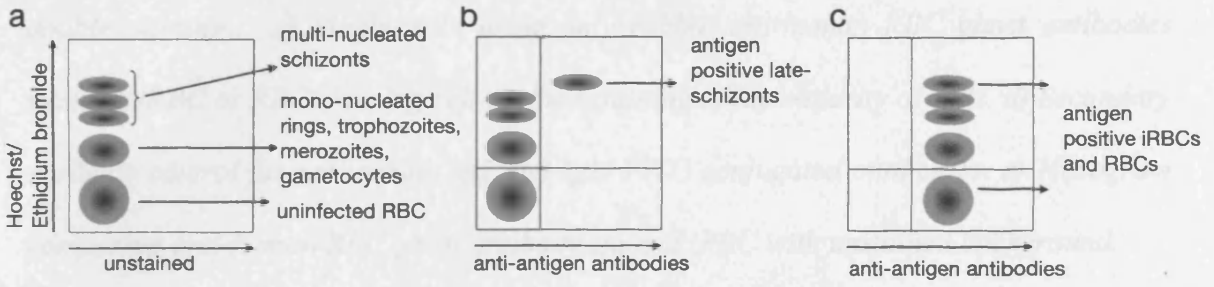

Figure 5.3: Schematic of flow cytometry interpretation

Schematic depiction of Hoechst or Ethidium bromide defined Plasmodium *-stages (uninfected RBC, rings, trophozoites, gametocytes and multi-nucleated schizont iRBC). A)* iRBC *stained with either Ethidium bromide or Hoechst (Upper-left quadrant). Ethidium bromide is acquired in FL-2 (585nm) on FACSCalibur and Hoechst 33342 in FL-4 (395-415nm) on the LSR. B)* P. falciparum *late schizont-stage iRBC positive for surface antigen (Upper-right quadrant) e.g. human anti-iRBC sera. C) All cells stained for surface antigen e.g. W49/50 anti-RBC ghost antibodies.*

Figure 5.4: iRBC surface staining for flow cytometry a) P. falciparum *3D7 iRBC and uninfected RBC were stained with Hoechst 33342 only (Upper-left quadrant) in FL-4 (395-415nm) on the LSR. b) Rabbit anti-human RBC ghost antibodies showing cell-surface staining of both infected and uninfected RBC (distinguished by Hoechst 33342 double-staining). c) Single-stain using only rabbit anti-human RBC ghost antibodies staining iRBC or RBC showing cell-surface staining of the majority of cells. d) Secondary antibody control for anti-rabbit IgG and IgM FITC conjugated antibodies. e) Histogram comparing anti-human RBC ghost antibody stained iRBC with unstained background.*

3D7

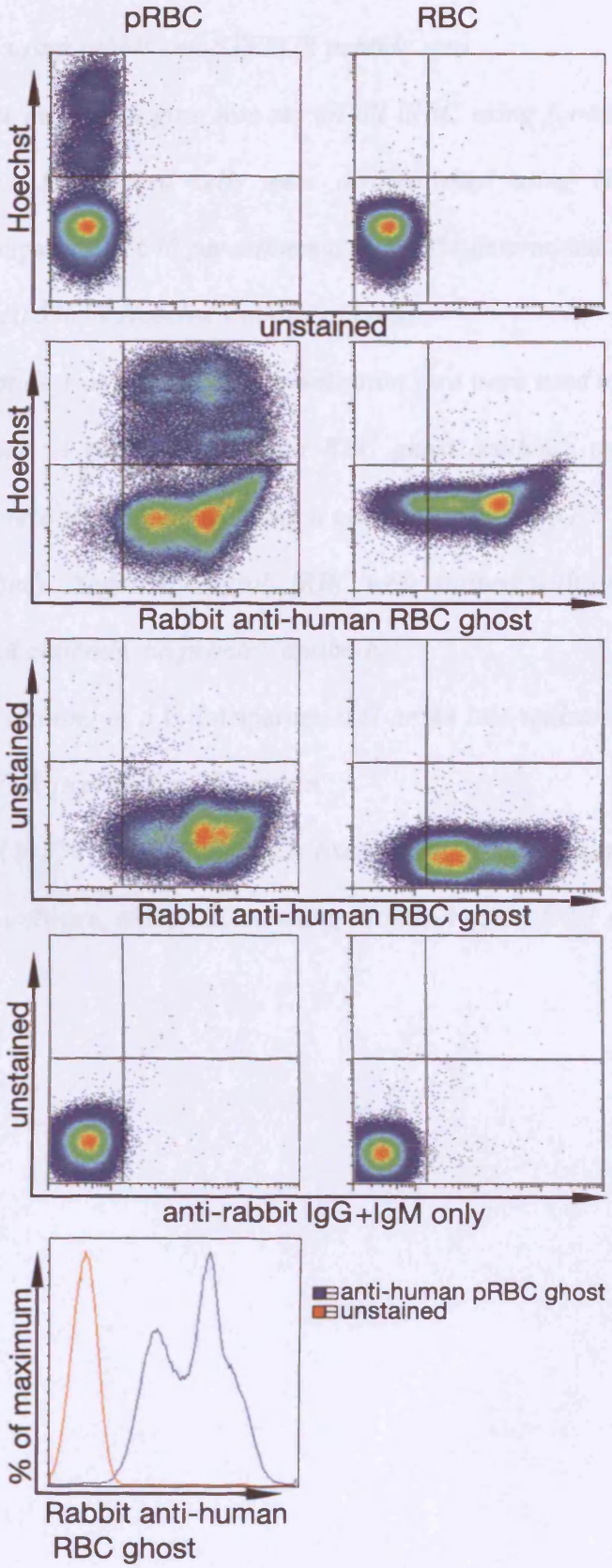
pRBC
RBC
Hoechst
unstained
Hoechst
Rabbit anti-human RBC ghost
unstained
Rabbit anti-human RBC ghost
unstained
anti-rabbit IgG+IgM only
% of maximum
anti-human pRBC ghost
unstained
Rabbit anti-human
RBC ghost

Figure 5.5: FACS cell-surface staining of A) P. falciparum *A4 iRBC and B) Kilifi field isolate (K1640) using rabbit anti-STEVOR peptide sera.*

For the analysis initially a gate was set on all iRBC using forward and side-scatter to eliminate debris. Parasitised cells were distinguished using Hoechst 33342 dye at 10μg/ml (P. falciparum *K1640 parasitaemia was 13% determined by blood smear count, compared with 10.5% by Hoechst staining of cells).*

Rabbit anti-peptide 1 or 2, and pre-immunisation sera were used to stain for STEVOR on the iRBC surface. A rabbit anti-human RBC ghost antibody was used as a positive control. Rabbit sera were detected using a goat anti-rabbit IgG + IgM FITC-conjugated secondary antibody. Negative control: iRBC were stained with only an anti-rabbit IgG FITC conjugated antibody, no primary antibody.

Inset is an IFA staining of a P. falciparum *3D7 or A4 late schizont-stage iRBC using the same anti-STEVOR peptide 1 rabbit serum.*

Cells were fixed in 1% paraformaldehyde fixation buffer before acquiring on a BD™ LSR with CellQuest software, and analysed using FlowJo version 6.2.1 software.

A4

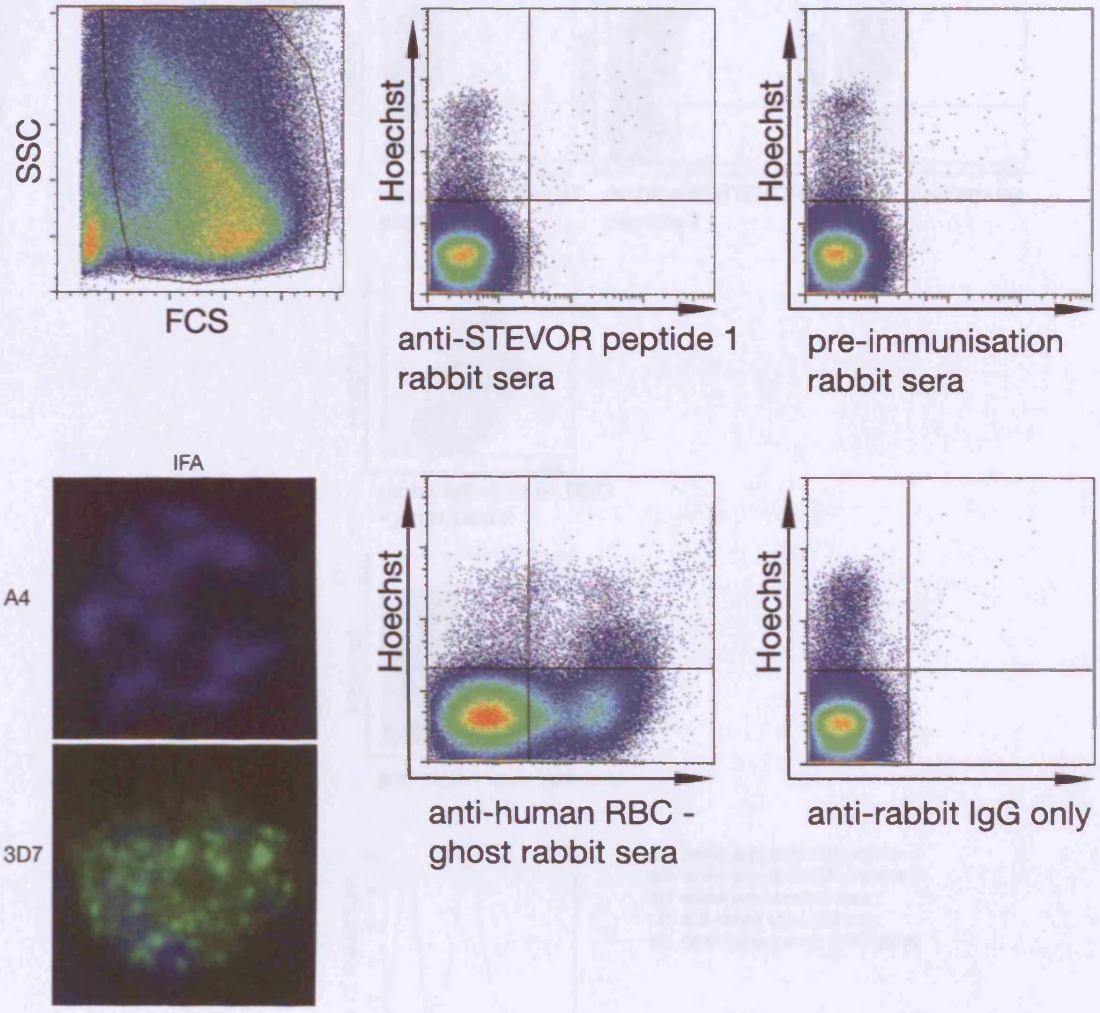
SSC
FCS
Hoechst
anti-STEVOR peptide 1
rabbit sera
Hoechst
pre-immunisation
rabbit sera
IFA
A4
3D7
Hoechst
anti-human RBC -
ghost rabbit sera
Hoechst
anti-rabbit IgG only

K1640

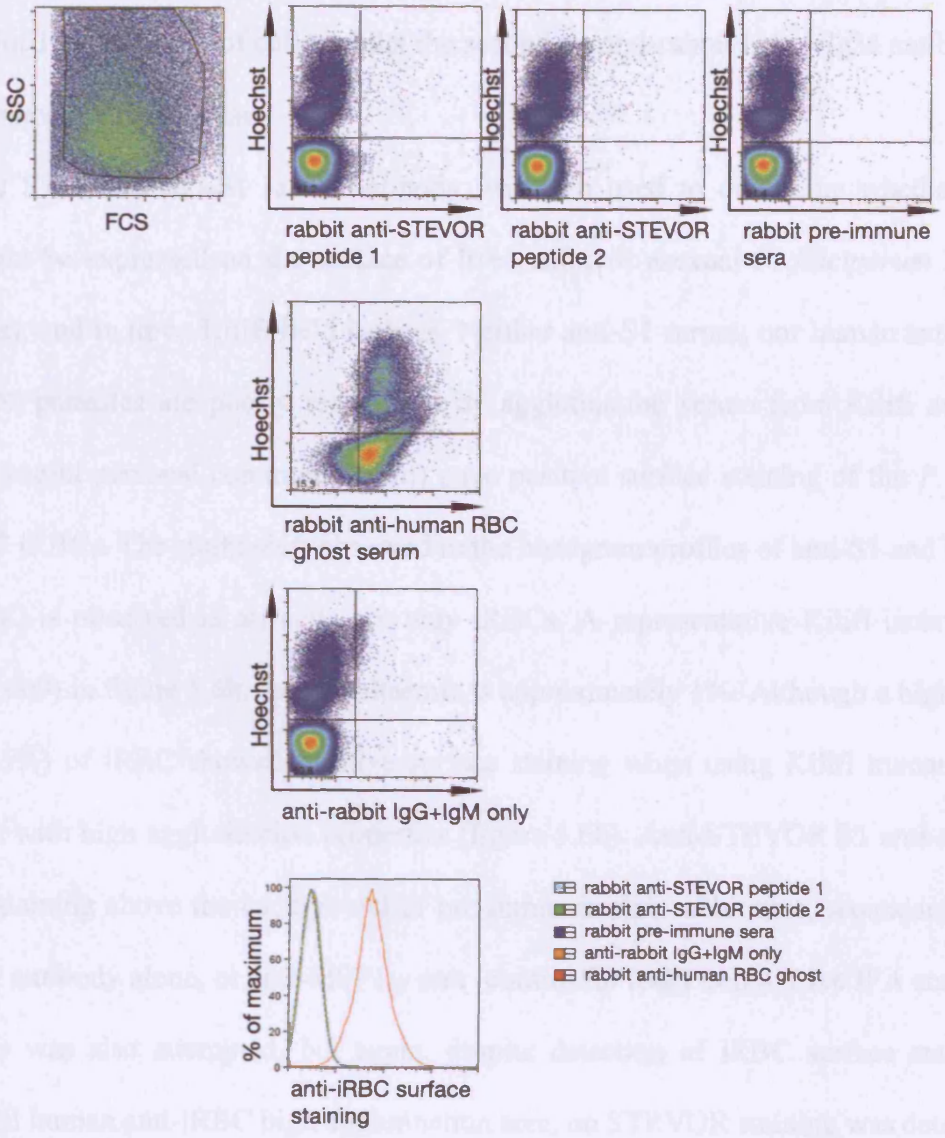
SSC
FCS
Hoechst
rabbit anti-STEVOR peptide 1
Hoechst
rabbit anti-STEVOR peptide 2
Hoechst
rabbit pre-immune sera
Hoechst
rabbit anti-human RBC -ghost serum
Hoechst
anti-rabbit IgG+IgM only
% of maximum
anti-iRBC surface staining
rabbit anti-STEVOR peptide 1
rabbit anti-STEVOR peptide 2
rabbit pre-immune sera
anti-rabbit IgG+IgM only
rabbit anti-human RBC ghost

Eight Kilifi field isolates (parasitaemias 0.88%-13%) were tested over four independent FACS staining experiments using anti-STEVOR peptide sera. In all cases no positive staining was observed above the rabbit pre-immunisation sera background, with either anti-peptide 1, or anti-peptide 2 sera. A representative Kilifi field isolate (K1640) is shown in figure 5.5b. Surface staining using a rabbit anti-human RBC ghost antibody stained the majority of cells, whilst the secondary anti-rabbit IgG + IgM antibody control was negative in all cases.

The STEVOR anti-S1 rabbit antibody was then used to determine whether STEVOR might be expressed on the surface of live (unfixed) asexual *P. falciparum* 3D7 (figure 5.6a), and in three Kilifi field isolates. Neither anti-S1 serum, nor human anti-iRBC sera (3D7 parasites are poorly recognised by agglutinating serum from Kilifi adults (Sam Kinyanjui personal communication)) gave positive surface staining of the *P. falciparum* 3D7 iRBCs. The slight shift observed in the histogram profiles of anti-S1 and human anti-iRBC is observed in all cells not only iRBCs. A representative Kilifi isolate is shown (K1609) in figure 5.6b, the parasitaemia is approximately 1%. Although a high proportion (>95%) of iRBC showed positive surface staining when using Kilifi human anti-iRBC sera with high agglutination properties (figure 5.6b). Anti-STEVOR S1 anti-sera showed no staining above the background of pre-immunisation rabbit sera, secondary anti-rabbit IgG antibody alone, or anti-$MSP1_{19}$ sera (control for leaky cells). Live IFA staining of the cells was also attempted, but again, despite detection of iRBC surface staining using Kilifi human anti-iRBC high agglutination sera, no STEVOR staining was detected on the surface of iRBC using this second technique (data not shown).

Figure 5.6: FACS cell surface staining of A) live P. falciparum *3D7 iRBCs and B) live Kilifi field isolate (K1609) iRBCs using rabbit anti-STEVOR recombinant protein pre- and post-immunisation sera to stain for STEVOR on the iRBC surface.*

For the analysis initially a gate was set on live, parasitised RBC (e.g. 91.3%) using forward and side-scatter to eliminate debris. Parasitised cells were then distinguished using Ethidium bromide (10μg/ml). The majority of parasites (e.g. K1609 ~1.1% iRBC) were schizont multi-nucleated forms, with some single-nuclei rings, and uninfected RBC (e.g. 98.9% RBC).

Positive control staining was carried out using either human anti-iRBC sera or rabbit anti-human RBC ghost sera (W49/50). Controls were performed to differentiate intact (anti-MSP1-19 or anti PfSBP1 negative) and leaky (anti-MSP1-19 or anti PfSBP1 positive) iRBCs.

A histogram of surface staining intensity (% of Maximum) is shown: human anti-iRBC sera/rabbit anti-iRBC ghost serum (red positive control), rabbit anti-S1 post-immunisation sera, rabbit pre-immunisation sera and secondary goat anti-rabbit IgG + IgM FITC conjugated antibody alone.

Cells were unfixed, and acquired on a FACs calibur™ *with CellQuest software, and analysed using FlowJo version 6.2.1 software.*

A) 3D7

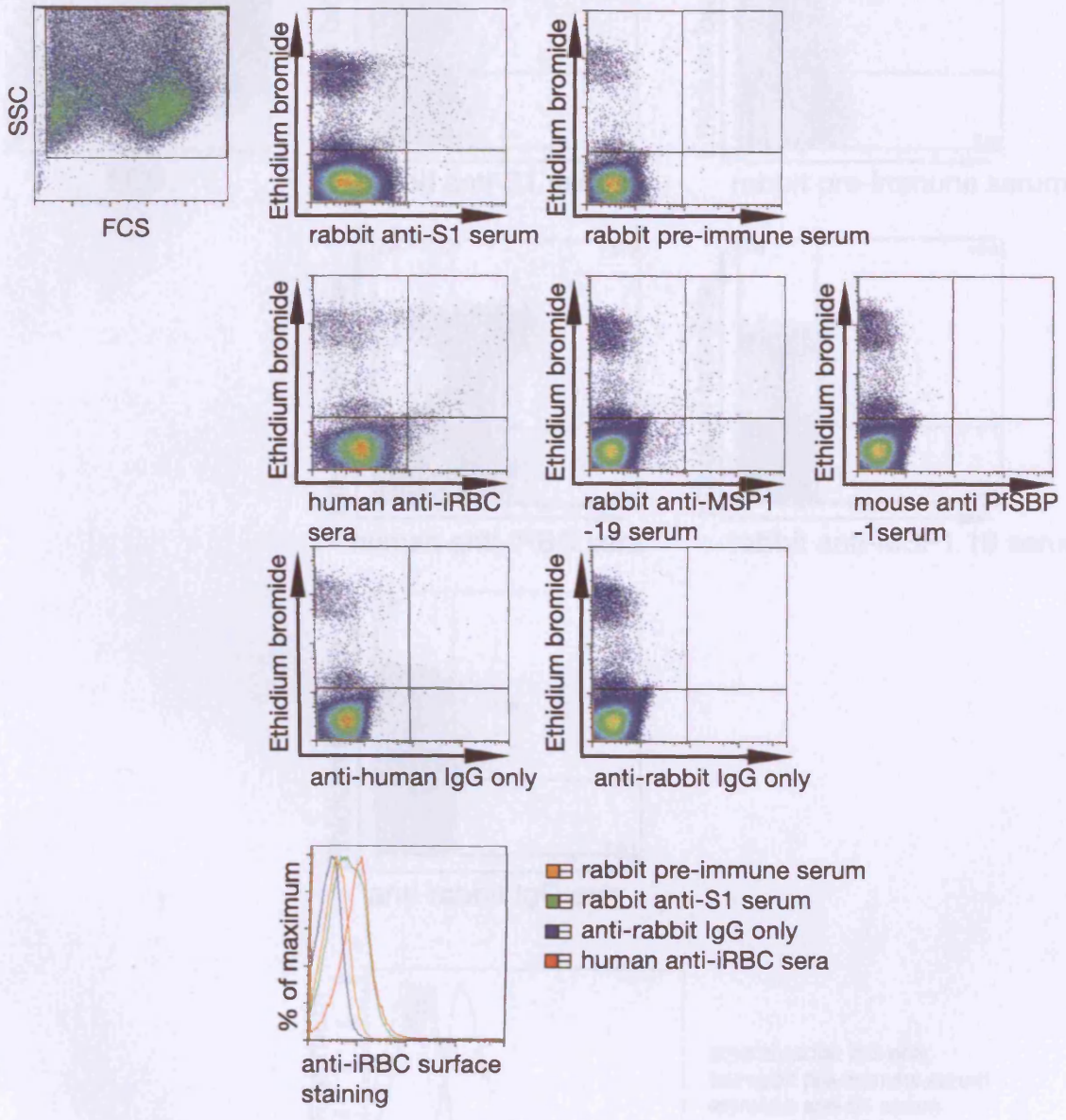
SSC
FCS
Ethidium bromide
rabbit anti-S1 serum
Ethidium bromide
rabbit pre-immune serum
Ethidium bromide
human anti-iRBC sera
Ethidium bromide
rabbit anti-MSP1 -19 serum
Ethidium bromide
mouse anti PfSBP -1serum
Ethidium bromide
anti-human IgG only
Ethidium bromide
anti-rabbit IgG only
% of maximum
anti-iRBC surface staining
rabbit pre-immune serum
rabbit anti-S1 serum
anti-rabbit IgG only
human anti-iRBC sera

B) K1609

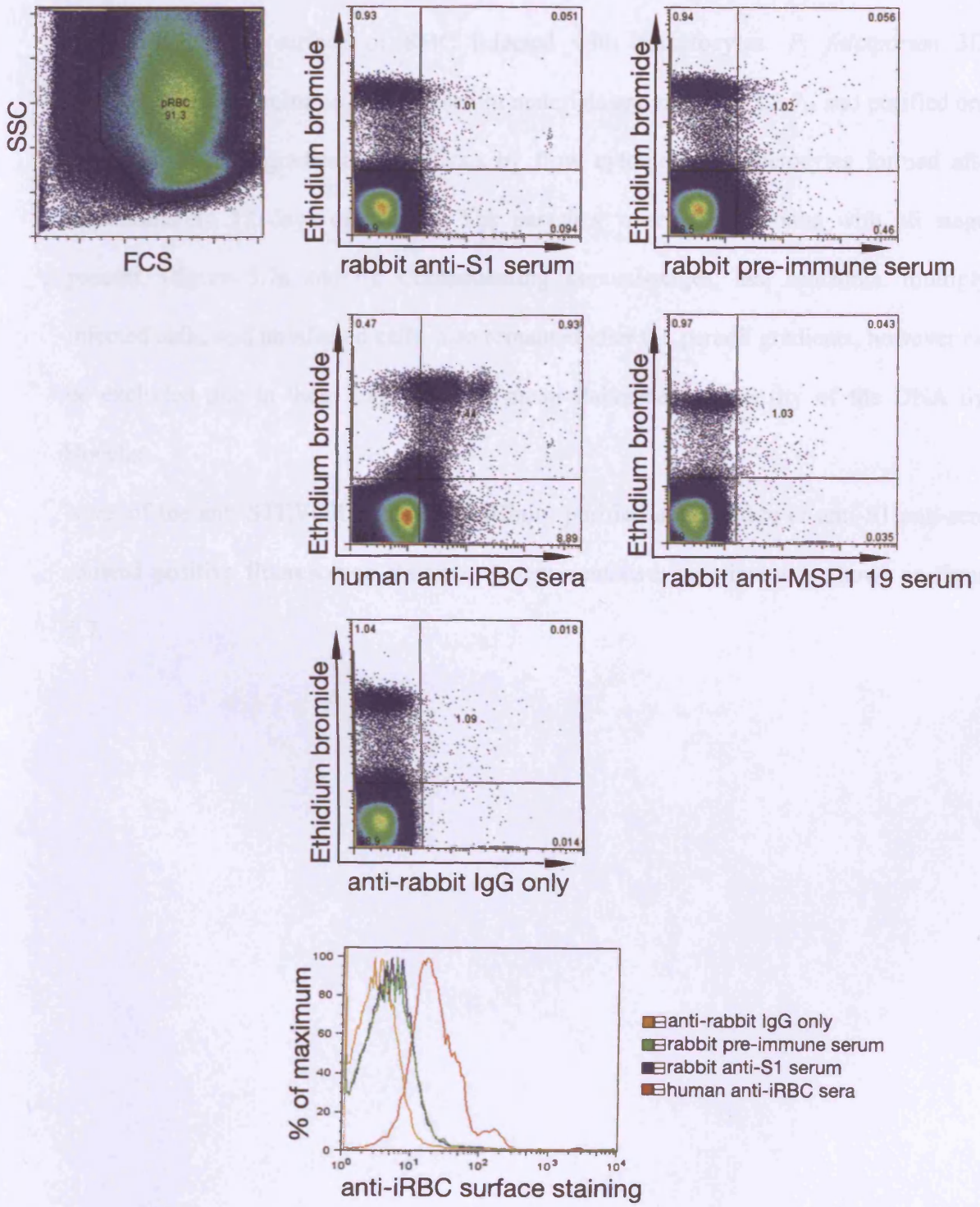
SSC
FCS
pRBC
91.3
Ethidium bromide
rabbit anti-S1 serum
0.93
0.051
1.01
0.094
rabbit pre-immune serum
0.94
0.056
1.02
0.46
human anti-iRBC sera
0.47
0.93
8.89
rabbit anti-MSP1 19 serum
0.97
0.043
1.03
0.035
anti-rabbit IgG only
1.04
0.018
1.09
0.014
% of maximum
anti-iRBC surface staining
anti-rabbit IgG only
rabbit pre-immune serum
rabbit anti-S1 serum
human anti-iRBC sera

5.5. Is STEVOR on the surface of gametocytes

Since expression and localisation of STEVOR in gametocytes is thought to be different from that in asexual-stages (McRobert *et al.*, 2004), it is possible that STEVOR is expressed on the surface of RBC infected with gametocytes. *P. falciparum* 3D7 gametocytes were cultured as described in materials and methods 2.2.7., and purified on a five-layer Percoll gradient for analysis by flow cytometry. Gametocytes formed after approximately 12 days of culture. The parasites were asynchronous with all stages present. (figure 5.7a and b). Contaminating asexual-stages, late schizonts, multiply-infected cells, and uninfected cells, also remained after the percoll gradients, however can be excluded due to their high (or low) mean fluorescence intensity of the DNA dye Hoechst.

None of the anti-STEVOR antibodies (affinity purified anti-peptide or anti-S1 anti-sera) showed positive fluorescence staining. A representative experiment is shown in figure 5.7.

Figure 5.7: FACS cell surface staining of P. falciparum 3D7 day 14 gametocyte cultures using rabbit anti-STEVOR sera.

Giemsa-stained gametocyte culture shown a) before and b) after purification on a Percoll gradient. A representative experiment with rabbit STEVOR anti-peptide sera performed using affinity purified antibodies and P. falciparum *3D7 iRBCs.*

Affinity purified rabbit anti-peptide 1 and anti-peptide 3 sera were used to stain for STEVOR on the iRBC surface. Rabbit post-immunisation sera for STEVOR peptides 1 and 2 are shown. Pre-immunisation serum and affinity-purified serum to a control peptide (A20/B) were used as negative controls. Goat anti-rabbit IgG + IgM FITC-conjugated antibody alone was negative. Parasitised cells were distinguished using Hoechst 33342 dye at 10μg/ml. Cells were initially gated for size and granularity using forward and side scatter. A histogram comparing the surface staining with the various rabbit sera is shown below.

Cells were fixed in 1% paraformaldehyde fixation buffer before acquiring on a BD™ LSR with CellQuest software, and analysed using FlowJo version 6.2.1 software.

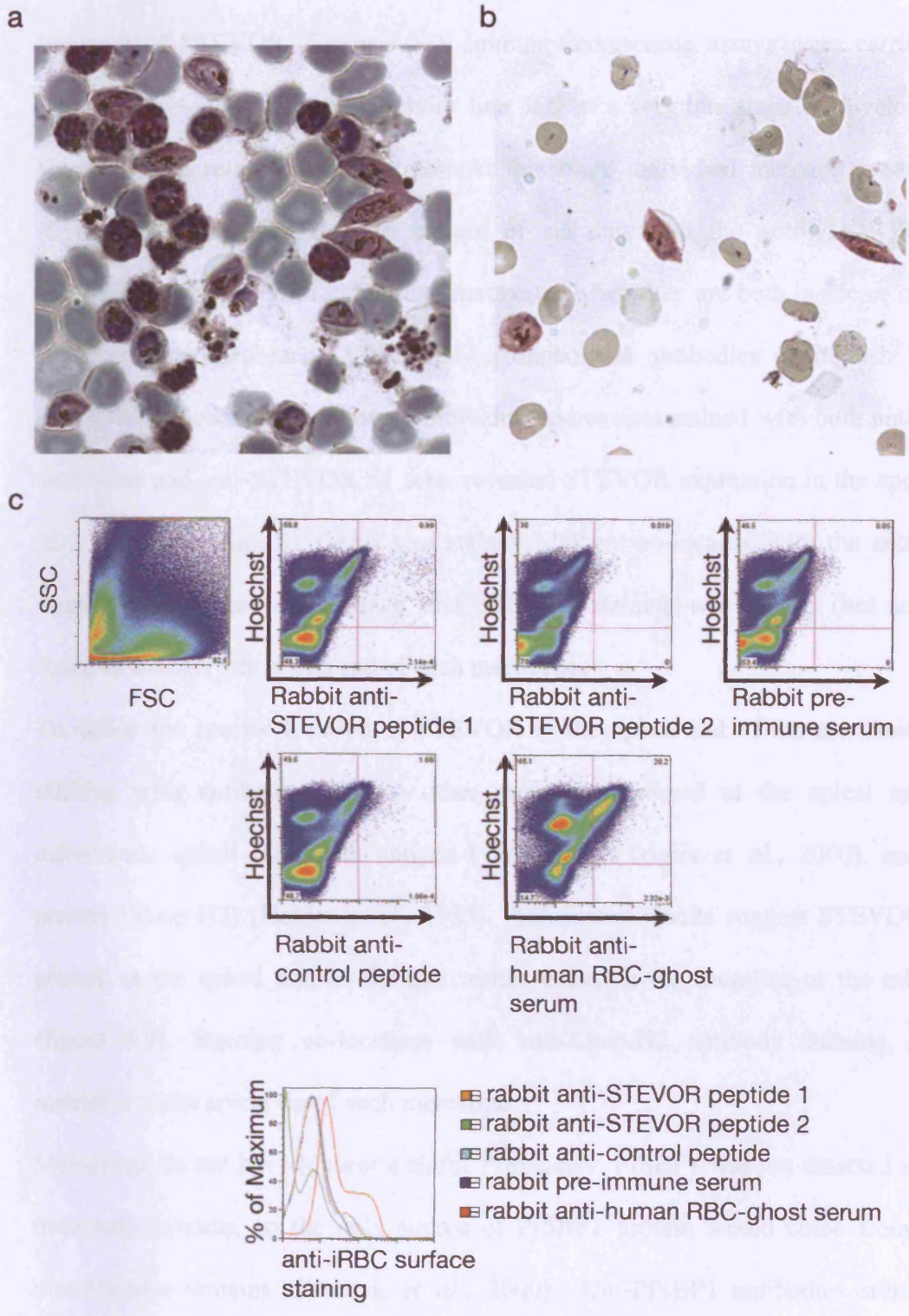
a
b
c
SSC
FSC
Hoechst
Rabbit anti-STEVOR peptide 1
Rabbit anti-STEVOR peptide 2
Rabbit pre-immune serum
Rabbit anti-control peptide
Rabbit anti-human RBC-ghost serum
% of Maximum
anti-iRBC surface staining
rabbit anti-STEVOR peptide 1
rabbit anti-STEVOR peptide 2
rabbit anti-control peptide
rabbit pre-immune serum
rabbit anti-human RBC-ghost serum

5.6. STEVOR expression in the apex of merozoites

Using both anti-S1 mouse and rabbit sera, which recognise the same recombinant fragment of STEVOR (figure 5.2E), Immunofluorescence assays were carried out on schizont-stage iRBC of the laboratory line 3D7 at a very late stage of development i.e. shortly before release of merozoites. At this stage individual merozoites can be seen (figure 5.8). Unexpectedly, the pattern of staining with the anti-STEVOR S1 sera appeared to coincide with individual merozoites when they are both inside or outside the iRBC surface membrane. Anti-MSP1-$_{19}$ monoclonal antibodies distinguish individual merozoites. Closer examination of individual merozoites stained with both anti-MSP1-$_{19}$ antibodies and anti-STEVOR S1 sera, revealed STEVOR expression in the apex of each 3D7 merozoite. Anti-S1 rabbit sera staining did not co-localise with the anti-MSP1-$_{19}$ staining of the merozoite surface, and STEVOR staining was usually (but not always) found in a single site at one end of each merozoite.

To define the precise location of STEVOR in the apical end of the merozoite, double staining with antibodies to two other proteins expressed at the apical end of the merozoites: apical merozoite antigen-1 (AMA-1) (Triglia *et al.*, 2000), and rhoptry protein (Rhop-H2) (Holder *et al.*, 1985). Preliminary results suggest STEVOR may be present at the apical end of the merozoites either in the rhoptries or the micronemes (figure 5.9). Staining co-localises with anti-Rhop-H2 antibody staining, which is restricted to the apical tip of each merozoite.

Merozoites do not have Maurer's clefts. Previously, PfSBP1 was not detected in purified merozoite extracts, so the only source of PfSBP1 protein would come from ruptured membranous remains (Blisnick *et al.*, 2000). Anti-PfSBP1 antibodies were used to determine if Maurer's clefts remained attached to the merozoites here (figure 5.10): As it was a possibility that the distinct foci of STEVOR staining observed were Maurer's clefts containing STEVOR, attached by membrane remnants of the iRBC ghosts. Maurer's

clefts were present in the merozoite slides studied, however they were randomly distributed and not specific to individual merozoite nuclei, by contrast, STEVOR staining within the merozoites was unique to each merozoite apex and restricted to a single point (figure 5.10b and c). The PfSBP1 staining was also quite distinct in size with larger foci than the apical tip STEVOR staining. Therefore despite the fact that Maurer's cleft proteins are present, we conclude that the STEVOR staining in the merozoites is not due to residual Maurer's cleft STEVOR staining.

Figure 5.8: STEVOR immunofluorescence staining of P. falciparum *3D7 merozoites*

STEVOR anti-S1 sera (red) reveal staining in the apical tip of merozoites. MSP1-$_{19}$ anti-sera (green) stain the merozoites' surface. Images of relatively intact, segmented schizonts (a and b), or free merozoites (c-f) are shown.

Goat anti-rabbit IgG FITC conjugated antibody and goat anti-mouse IgG TRITC conjugated antibody were used as secondary antibodies. Parasite nuclei are stained with DAPI (1μg/ml) (blue). Cells were viewed on a Deltavision fluorescence microscope under a 100X oil objective, overall magnification 110X.

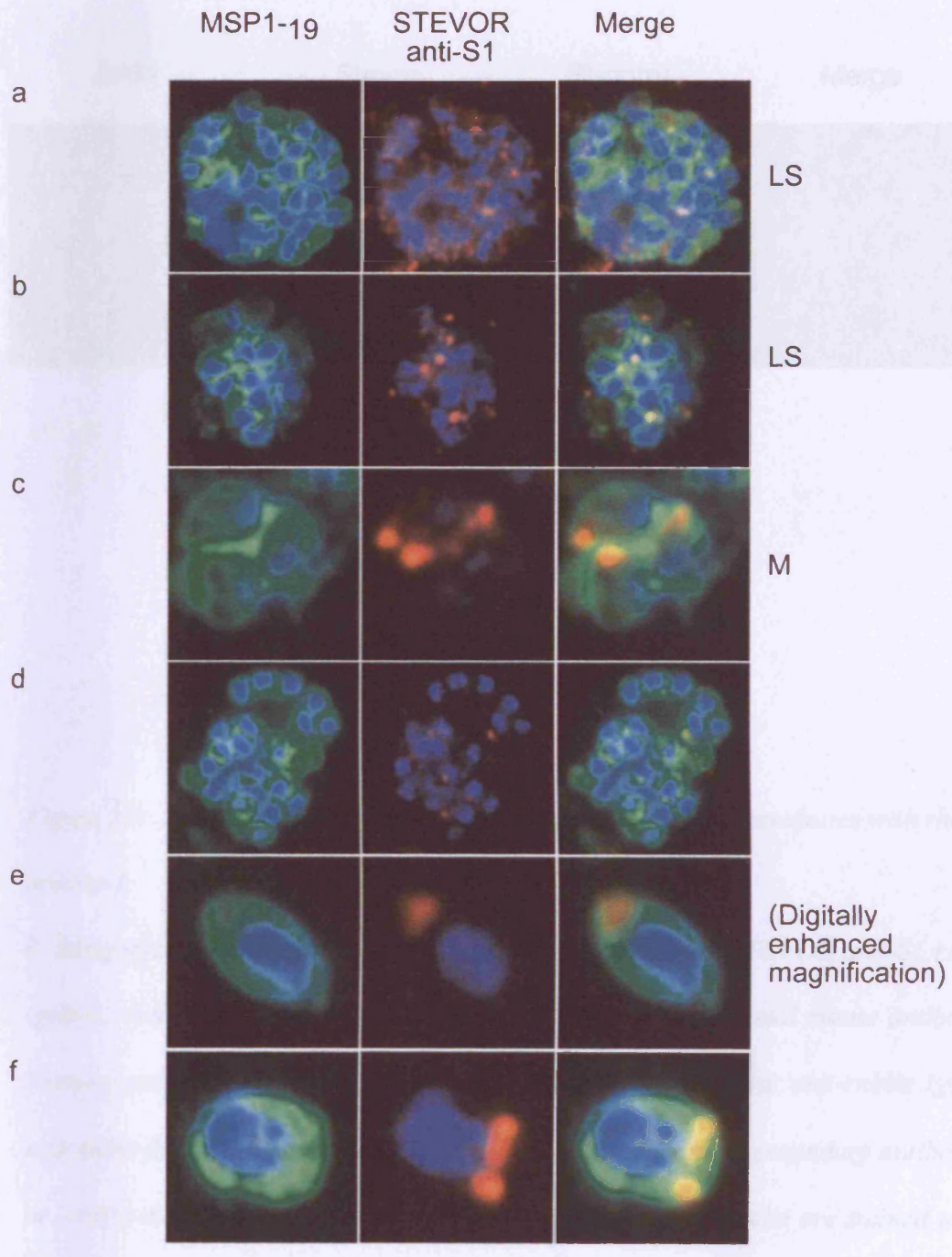
MSP1-19
STEVOR anti-S1
Merge
a
b
c
d
e
f
LS
LS
M
(Digitally enhanced magnification)

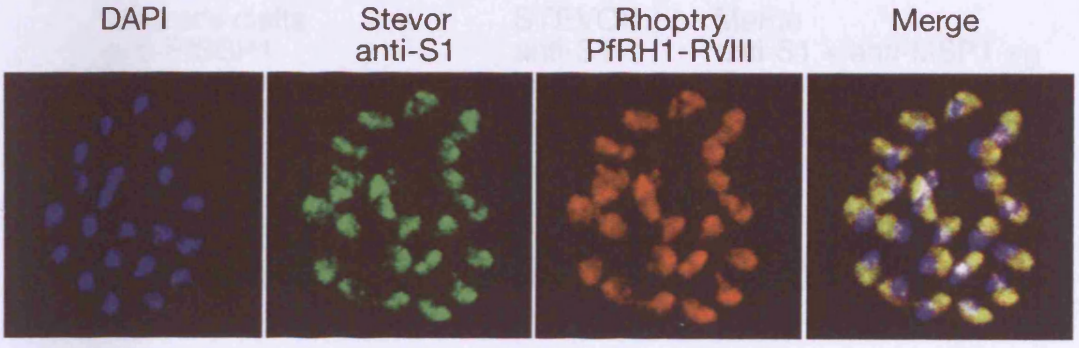

Figure 5.9: STEVOR staining co-localises at the apical tip of merozoites with rhoptry protein-1

P. falciparum *W2mef parasite merozoites were stained with STEVOR anti-S1 rabbit sera (green), and an anti-rhoptry protein 1 (PfRH1-RVIII) monoclonal mouse antibody (red). Primary antibodies were visualised with Alexa fluor® 488 goat anti-rabbit IgG (H+L), and Alexa fluor® 594 goat anti-mouse IgG (H+L) conjugated secondary antibodies used at 1:1000 dilution (Molecular probes, Invitrogen). Parasite nuclei are stained with DAPI (1µg/ml) (blue).*

Cells were viewed on a Zeiss confocal microscope under a 100x oil objective. Images from Peter Preiser, Nanyang Technological University, Singapore.

Figure 5.10: STEVOR foci in the merozoites are not remnants of iRBC membrane bound Maurer's clefts

a) PfSBP1 staining of Maurer's clefts (red) in a ruptured schizont showing these are not within each individual merozoite. b) STEVOR mouse anti-S1 staining in the apex of merozoites (red) c) Merge of anti-S1 and anti-MSP1$_{-19}$ (green) antibody staining showing a single focus of STEVOR per merozoite.

Goat anti-rabbit IgG FITC conjugated antibody and goat anti-mouse IgG TRITC conjugated antibody were used as secondary antibodies. Parasite nuclei are stained with DAPI (1μg/ml) (blue). Cells were viewed on a Deltavision fluorescence microscope under a 100X oil objective, overall magnification 110X.

Discussion

In this chapter, immunofluorescence assays using affinity-purified rabbit anti-peptide 1 antibodies and rabbit anti-recombinant protein S1 sera detected STEVOR in the Maurer's clefts throughout development from early trophozoite to schizont-stages. STEVOR accumulates in the Maurer's clefts from trophozoite to early-mid-schizont-stages. However in the late schizont (once clearly defined merozoite nuclei are visible), the STEVOR staining pattern became more diffuse and was present around the parasite and throughout the iRBC cytosol. This may reflect a proportion of STEVOR that has left the Maurer's clefts and is being exported to the iRBC surface, or that STEVOR functions in the iRBC cytosol at this stage. Although the latter is unlikely given the expected transmembrane orientation of the proteins. This phenomenon appears to be highly specific to this very late developmental stage, which may partially explain why previous studies have not detected STEVOR outside of the Maurer's clefts(Kaviratne *et al.*, 2002; Przyborski *et al.*, 2005).

The redistribution of STEVOR in the late schizont forms was studied by flow cytometry and in IFA studies of unfixed (live) iRBC. Despite IFA data showing STEVOR leaves the Maurer's cleft, reagents against neither the conserved N- nor C-terminals detected STEVOR on the iRBC surface.

These data extend our knowledge of the STEVOR export pathway: STEVOR is expressed during trophozoite development, and is trafficked to the Maurer's clefts in the iRBC cytosol. At the schizont-stage, a proportion of STEVOR leaves the cleft and is exported further towards the iRBC surface membrane, where the hyper-variable loop may be expressed on the iRBC surface.

This export pathway varies dependent on parasite culture adaptation; as *in vitro* cultured parasites did not export significant amounts of STEVOR from the Maurer's clefts compared with field isolates. Additionally, STEVOR was detectable in a larger fraction of

field isolate iRBC than on long-term cultured *P. falciparum* strains. This is consistent with a very recent study of *var* gene transcription in *in vitro* adapted cultures, which showed a significant reduction in transcription within ~10 days of culture (Peters *et al.*, 2007).

Our data also provide the first evidence that parasites express STEVOR in blood-stage merozoites. STEVOR is expressed in the apical tip of the invasive blood-stage merozoites released upon schizont rupture. The export of STEVOR to the apical organelles may be due to a highly conserved YWLY motif identified in the C-terminal of STEVOR (chapter 3.2 and figure 5.9). The orientation of STEVOR within the merozoite-stage is unknown, but orientation and thus function of STEVOR in the merozoite may be different from that in the iRBC.

VSA are exported through the Maurer's clefts *en route* to the surface of the iRBC (Craig & Scherf, 2001). This study agrees with two previous studies where STEVOR was found to be present in the Maurer's clefts. These data are consistent with our findings that STEVOR is co-localised with PfSBP1 in the Maurer's clefts during trophozoite development. In these two studies it was proposed that the Maurer's clefts were the final destination of STEVOR (Kaviratne *et al.*, 2002; Przyborski *et al.*, 2005). However, late schizont-stage parasites were not studied in detail. Thus far, STEVORs are similar to PfEMP1 and RIFINs, in that STEVOR is also present in the Maurer's clefts during the trophozoite-stage in the lifecycle. The IFA studies here show that STEVOR, like PfEMP1 and RIFINs, then pass through the Maurer's clefts *en route* to their final destination perhaps within the (inner) outer surface iRBC membrane.

It is possible that GFP-tagged STEVOR may not reach its final destination within the iRBC despite being exported to the Maurer's clefts (Przyborski *et al.*, 2005). Use of a constitutive promoter, driving expression early in the parasite's development, may influence protein-protein interactions required in the final stages of STEVOR export,

either through absence or low levels of one or more interacting proteins during the trophozoite-stage. In support of this, a recent study where EBA-175 sub-cellular localisation was compared when under a ring/trophozoite-specific promoter or a late schizont-specific promoter. The ring/trophozoite-specific promoter resulted in expression at the wrong time during development; GFP-tagged EBA-175 protein aggregated and was mis-targeted to the parasitophorous vacuole, instead of its correct location in the micronemes. The authors conclude this was due to the absence of the appropriate sorting machinery and predestined organelles (Treeck *et al.*, 2006).

It would be interesting given our data, showing relocation of STEVOR in the schizont-stage iRBC, to observe the distribution of N-terminally GFP-tagged STEVOR later in schizont parasite development. The authors did not look at schizont-stages using these parasites (Jude Przyborski, personal communication). Therefore to ask definitively where STEVOR is located a GFP-construct expressed under the control of the endogenous STEVOR promoter would be required. This has been synthesised, and will be used to answer questions of STEVOR membrane orientation and localisation throughout the erythrocytic cycle (Peter Preiser, personal communication).

A very recent study utilised immunogold localisation of abundantly expressed C-terminal tagged-STEVOR and revealed small amounts at the knobs at the iRBC membrane, in addition to greater amounts in the Maurer's clefts (Lavazec *et al.*, 2006). This same study also placed tags within the HVR but failed to detect this region on the iRBC surface membrane using the same technique. In this thesis IFA data showing STEVOR throughout the cytosol and associated with the iRBC surface membrane is consistent with the location of the STEVOR C-terminal tag in the immunogold localisation.

Only a proportion of total STEVOR protein is relocated, a significant proportion remains in the Maurer's clefts, this may also be a reflection of protein transport deficiencies (particularly in *in vitro* cultured parasites) (Haeggstrom *et al.*, 2004), or that there are sub-

types of STEVOR that function in different parts of the iRBC. Clearly unique-STEVOR specific anti-sera, based upon the hyper-variable loop regions, would be invaluable in determining whether STEVOR sub-types exist. However due to low levels of STEVOR expression, it would be a difficult study without prior knowledge of which STEVORs are being expressed. This would require quantitative (q) RT-PCR data showing exactly which STEVORs are expressed in the parasite population. Recent qRT-PCR data from a *P. falciparum* 3D7 culture, showed PF10_0395; PFI0080w; PFF0850c; and PFD0065w to be the main STEVOR transcripts (highest-lowest) (Sharp *et al.*, 2006). The anti-S1 serum used for our study is therefore specific for the most abundant STEVOR transcript (PF10_0395) in *P. falciparum* 3D7, but despite this STEVOR was still detected at low levels in only a small percentage of parasites (table 5.1). In addition, Kilifi pooled human anti-iRBC sera were not able to recognise antigens on the surface of *P. falciparum* 3D7 iRBC, despite recognising 100% of the Kilifi field isolate parasites tested. These data together with IFA staining data, suggest that this laboratory line is not suitable to detect cell-surface STEVOR.

A comparison of cultured parasites with *in vivo* parasites

An extremely important observation for the application of *in vitro* cultured *P. falciparum* clones is the huge difference in STEVOR expression from that in the field parasite isolates. It is important to note also that not only was the percentage of parasites-positive for STEVOR higher (table 5.1), but the intensity of the staining in the field isolates was brighter and significantly more abundant, suggesting presence of abundant STEVOR. This could imply STEVOR is a non-essential protein for the basic lifecycle of the parasite, but *in vivo*, the maintenance of expression of this multigene family is necessary and perhaps indispensable.

In line with this hypothesis, other large multigene families such as *var* and *rif* are also not vital for the parasite development *in vitro*. RIFIN polypeptides are present on the surface of fresh field isolate trophozoites and *rif* gene expression is detectable by RT-PCR, whereas in tissue culture, RIFIN protein and RNA transcription is low or absent (Fernandez *et al.*, 1999). Fernandez *et al* detected proteins with a molecular weight of 39kDa in the 3D7 and F32 clones but not in R29 or Dd2 clones. This was in contrast to six African clinical isolates where as least two prominent RIFINs were detected in each. However the authors were unable to show the timescale of decline of RIFIN expression over time in culture, as a tracking experiment carried out over 150 generations, did not show a consistent decline in *rif* expression. The lack of RIFIN expression in laboratory clones was corroborated by a second *rif* study in which the rosetting clone R29 did not transcribe or express *rif* (Kyes *et al.*, 1999).

Differences between the 3D7 clone (*in vitro*) and Senegal parasite isolates (*in vivo*) were also detected in a study comparing transcription profiles from these parasites (Daily *et al.*, 2005). Here a single *stevor* (PFD0065w) and two *rifins* were included in a list of just 12 genes found over-expressed in at least four out of five Senegal *in vivo* samples. While the majority of genes transcribed *in vivo* are also found *in vitro*, a closer look at the STEVOR

and RIFIN multigene families revealed they had a greater number of genes transcribed *in vivo* than *in vitro*, with some members of the families transcribed exclusively *in vivo*. In contrast, the number of *var* gene transcripts was greater in the *in vitro* samples.

In addition, *in vitro* maintained clones including the 3D7 parasite clone, may lack fully functional transport machinery and therefore fail to export proteins out into the iRBC cytosol. This is supported by evidence from Haeggstrom *et al*, who observed that on comparison of PfEMP1 and RIFIN export in fresh clinical isolates with that in the 3D7 lineage *in vitro* growth-adapted clones, the 3D7 parasites did not form the large Maurer's cleft structures seen in the fresh isolates. Instead trafficking occurred in smaller less efficient packets (Haeggstrom *et al.*, 2004). This would also suggest that the sole purpose of the iRBC surface proteins exported through the Maurer's clefts, lies in the need to maintain parasite survival under the extreme conditions of the host's immune system.

SURFINs, which have a similar distribution to STEVOR, have been detected in *P. falciparum* clones cultured *in vitro*, but again variable proportions of iRBC express SURFINs (~25% in 3D7S8 - >90 % in FCR3S1.2) but in all cases, they co-localise with PfEMP1 in the Maurer's clefts at the trophozoite-stage (Winter *et al.*, 2005).

The cultured parasite clones proved a difficult model for the study of surface protein expression, as pooled sera known to have high-agglutination properties do not detect surface proteins on *P. falciparum* 3D7 iRBC (Sam Kinyanjui, personal communication). This may suggest either significant loss of 3D7 iRBC surface proteins, potentially due to trafficking defects after long-term *in vitro* culture of these clones, or, an antigenically distinct set of surface proteins. Clearly great care has to be taken when choosing a parasite clone for *in vitro* studies, and where possible fresh clinical isolates should be assessed.

Field isolate iRBC surface proteins were clearly recognised by the human high-agglutination immune anti-iRBC sera (figure 5.5). These same iRBC surface proteins were however not recognised by our STEVOR specific sera in any of the assays.

We cannot conclude that these results rule out the possibility that STEVOR is expressed on the surface of iRBC, as we did not have reagents to the hyper-variable loop region. The reagents used in these assays are specific for either the conserved N-terminus (amino acids 26-180 or peptides within) or the C-terminal (21 amino acids) of the STEVOR proteins. However, if STEVOR is trafficked to the iRBC surface, this data supports the predictions for a surface exposed hyper-variable loop flanked by two transmembrane domains, with conserved N- and C-termini within the iRBC cytosol. Original assessments of STEVOR led to the prediction of a membrane spanning-structure identical to the RIFINs in both gene structure and using probabilistic model analysis (Janssen *et al.*, 2004; Kyes *et al.*, 2001). The topology predicted for both these multigene families is cytoplasmic N- and C-terminal domains, with a hyper-variable loop exposed on the outside of the iRBC. Our data do not contradict this, and add further support for a two transmembrane, theoretical protein-model.

Alternatively, it is possible that due to low levels of STEVOR, combined with a stage-specific surface expression, we may not have been able to detect iRBC surface-exposed STEVOR as the number of late schizont-stage parasites expressing STEVOR on the iRBC surface was too low and below the detection level of the assay. Despite the fact flow cytometry is a sensitive technique.

Figure 5.11: Alternative membrane-spanning topologies for STEVOR and RIFINs

Three alternative interpretations of the proteins' structures based on detailed sequence analysis of multiple alignments (see results chapter 3).

A) 3 potential STEVOR orientations within the Maurer's cleft. Two transmembrane domains as predicted for both STEVOR and RIFIN by Kyes et al 2001, the most likely orientation based on surface localisation results (Kyes et al., 2001). Single C-terminal transmembrane domain, possible topology for both STEVOR and RIFINs, whereby the missing transmembrane domain region forms the internal hydrophobic core of the protein, and therefore both the hyper variable loop and N-termini are on the same side of the membrane. Finally 3 transmembrane spanning domains: possible topology for STEVOR only. STEVOR may have an additional third highly conserved transmembrane domain within the hyper variable loop, whereby the N-terminal only becomes exposed on the outside of the iRBC. B) Same 3 potential membrane-spanning topologies within the iRBC surface membrane.

A. Possible orientation of STEVOR in the Maurer's clefts

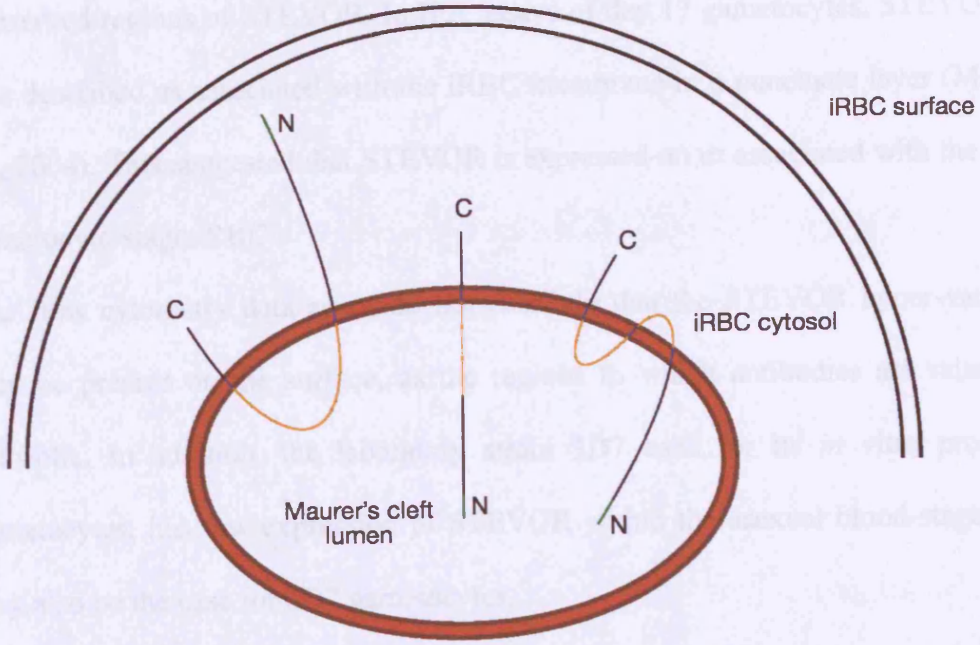

B. Possible orientation of STEVOR at the iRBC surface

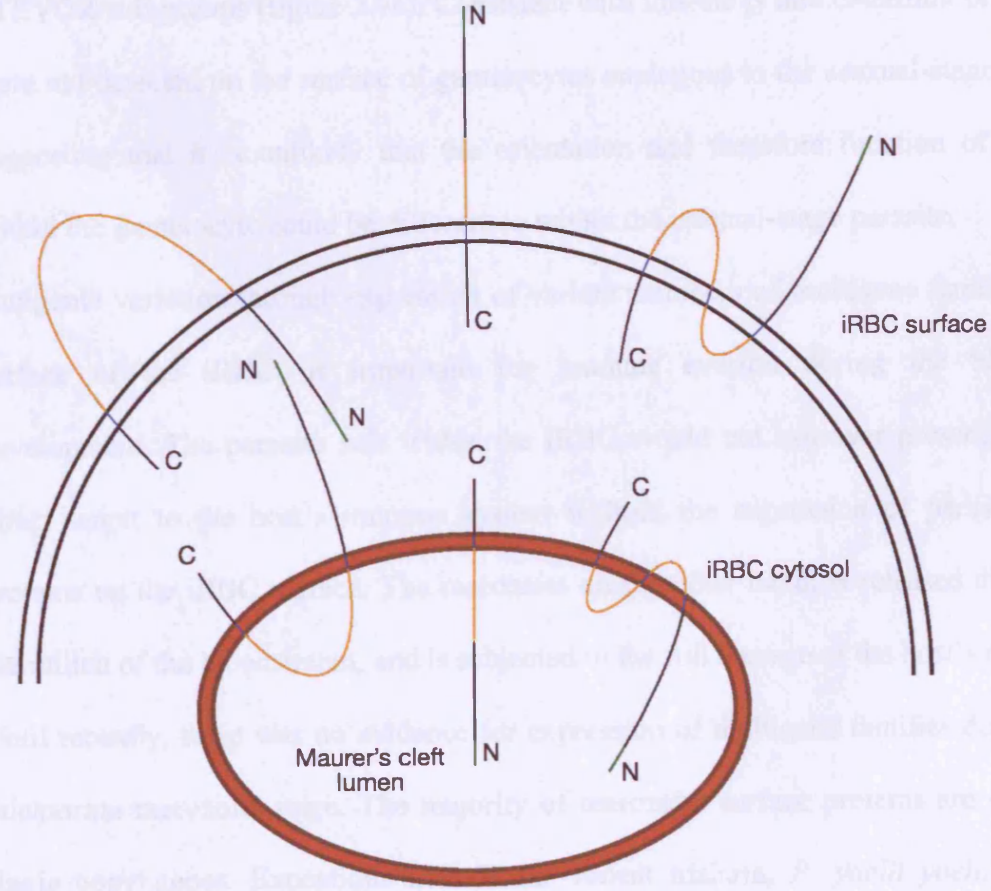

STEVOR was not found on the surface of gametocytes using these same antibodies to conserved regions of STEVOR. In IFA assays of day 17 gametocytes, STEVOR staining was described as associated with the iRBC membrane in a punctuate layer (McRobert *et al.*, 2004). This suggested that STEVOR is expressed on or associated with the surface of gametocyte-stage iRBC.

Our flow cytometry data again do not preclude that the STEVOR hyper-variable loop may be present on the surface, as the regions to which antibodies are raised may be cytosolic. In addition, the laboratory strain 3D7 used for its *in* vitro production of gametocytes, has low expression of STEVOR within the asexual blood-stages, and this may also be the case for 3D7 gametocytes.

Recent work has shown the same main *stevor* variants are transcribed in both gametocytes and asexual parasites (Sharp *et al.*, 2006), consistent with the absence of STEVOR sub-groups (figure 3.7e). Consistent with this the N and C-termini of STEVOR were not detected on the surface of gametocytes analogous to the asexual-stage parasites, suggesting that it is unlikely that the orientation and therefore function of STEVOR within the gametocyte could be different to within the asexual-stage parasite.

Antigenic variation through expression of variant members of multigene families, on the surface of the iRBC, is important for immune evasion during the blood-stage-development. The parasite safe within the iRBC would not however present itself as a direct target to the host's immune system without the expression of parasite-derived proteins on the iRBC surface. The merozoite on the other hand, is released directly into the milieu of the bloodstream, and is subjected to the full barrage of the host's response.

Until recently, there was no evidence for expression of multigene families during the *P. falciparum* merozoite-stage. The majority of merozoite surface proteins are encoded as single copy genes. Exceptions include the rodent malaria, *P. yoelii yoelii* multigene family (Py235), with more than 14 members encoding a 235kDa protein found in the

rhoptries, but not found on the iRBC surface. Homologues are found in both *P. falciparum* and *P. vivax* (Cowman & Crabb, 2006; Galinski *et al.*, 1992; Holder & Freeman, 1981; Kaneko *et al.*, 2002; Rayner *et al.*, 2000; Rayner *et al.*, 2001; Stubbs *et al.*, 2005; Taylor *et al.*, 2001; Triglia *et al.*, 2001a; Triglia *et al.*, 2005; Tsuboi *et al.*, 1994). In *P. falciparum*, 10 surface-associated interspersed genes (*surf* genes) encoding SURFINs found in the merozoites are located, in the words of Winter *et al*, in "an amorphous cap at the parasite apex". In addition, the SURFINs are co-transported with PfEMP1 and RIFINs to the iRBC surface (Winter *et al.*, 2005).

The expression pattern of STEVOR on the merozoite is similar to the much smaller SURFIN protein family. Thus parasites appear to conserve the antigenic composition of iRBC, and merozoite attachment surfaces. Merozoites are totally exposed to immune factors when released from the iRBC, minimising this exposure time whilst providing highly variable targets for the host's immune system may increase the chances of merozoite survival. Since the majority of merozoite surface proteins are single copy genes, these are unsuitable for antigenic variation eg. MSP-1 and AMA1 (Anders *et al.*, 1993; Triglia *et al.*, 2000). The parasite could use polymorphism as an alternative or additional method to avoid immune intervention of merozoite invasion, as the invasion pathways involve polymorphic variants e.g. CLAG 3.1 and 3.2 or the EBA-175 (small) family. However, this is not a viable source of variation for antigenic variation due to the low copy number of these genes (Alfred Cortes, personal communication). Therefore the presence of STEVOR proteins, (and potentially RIFINs also), in the merozoite-stage would provide the merozoite with suitable proteins for antigenic variation.

The N-terminal region of STEVOR proteins can bind RBCs (Peter Preiser, personal communication). Briefly, work from Garcia *et al* also found that synthetic peptides from the conserved N-terminus of STEVOR bound RBCs (Garcia *et al.*, 2005).

The conserved STEVOR N-terminal region could be involved in RBC binding, and combined with the discovery of STEVOR expression in the apical tip of merozoites suggests STEVOR may function in RBC binding and invasion by merozoite-stage parasites, such a function has also been suggested for the *P. falciparum* SURFIN family of proteins although there is no evidence to date (Winter *et al.*, 2005).

Conclusions

A more complicated view of STEVOR has emerged involving almost the complete blood-stage cycle. It has long been the accepted view that STEVOR is a relatively large multigene family of variant Maurer's cleft proteins. The data presented do not contradict the finding that STEVOR co-localises, in trophozoite and schizont-stages, with the Maurer's cleft marker PfSBP1 (Kaviratne *et al.*, 2002). However this more detailed study has revealed stage-specific changes in this localisation, and an additional location within the apex of blood-stage merozoites. A schematic view of the localisation of STEVOR throughout the asexual blood-stages is shown in figure 6.1.

Consistent with the function of STEVOR as an antigenic-variant protein, expression of STEVOR is maximal in fresh clinical isolates, and is significantly reduced in parasite clones that have been cultured long-term in the absence of immune factors. Finally, STEVOR may be a multifunctional protein, contributing to the merozoite's extensive armoury, providing additional antigenically-variable immune targets, and enhanced RBC binding capacity.

Final discussion

The studies presented in this thesis investigated the global repertoire and expression of STEVOR within a range of laboratory lines and field parasites. The *stevor* multigene family is maintained within the genomes of both laboratory and field parasite isolates at a constant number of around 28 copies. The data presented show that *stevor* is consistently transcribed in all *P. falciparum* isolates examined with the exception of one laboratory isolate (A4). Parasite isolates share *stevors* within and between isolates although there is a diverse repertoire worldwide.

Due to its importance as the third largest multigene family in the *P. falciparum* genome, the final cellular localisation of STEVOR proteins is of considerable interest. It has been accepted that STEVORs are a relatively large multigene family of variant Maurer's cleft proteins (Kaviratne *et al.*, 2002). However the detailed study presented in this thesis has revealed that the Maurer's clefts do not appear to be the final or exclusive destination of STEVOR, and therefore the transport mechanism is more complex than initially thought. In addition to the co-localisation of STEVOR with the Maurer's-cleft PfSBP1 protein in late-stage schizonts, STEVOR localisation changes at this stage, and an additional location for STEVOR has been identified within the apex of blood-stage merozoites (figure 6.1).

Both locations may be exposed to the host immune-system, suggesting that *stevor* HVR diversity's may be driven by immune selection, presumably in the form of an effective antibody response. The low level and prevalence of STEVOR expression in *P. falciparum* 3D7 intra-erythrocytic parasites contrasts with that of STEVOR 3D7 merozoites, which includes expression in the majority of merozoites, and suggests expression of STEVOR during the erythrocytic cycle (*in vitro*) is of less importance than its function at the merozoite stage. A more extensive assessment of STEVOR expression in field-isolate merozoites still remains to be addressed.

Consistent with the function of STEVOR as an antigenic-variant protein, the expression of STEVOR is maximal in fresh clinical isolates and in contrast is significantly reduced in parasite-clones that have been cultured long term in the absence of immune selection, suggesting that STEVOR is not essential under these conditions. Location of STEVOR beyond the Maurer's clefts in the late-stage schizont, and in the apical tip of merozoites raises interesting questions about STEVOR's function at these locations. It is tempting to speculate that STEVOR is a multi-functional protein, enhancing the RBC-binding capacity of both iRBCs and merozoites, whilst providing antigenically variable immune targets contributing to the extensive evasive armoury at both these stages. Additionally, it is also possible that variation in the HVR is a parasite mechanism to facilitate adherence to RBC in the face of the huge diversity of human RBC surface proteins. (Baum *et al.*, 2005).

It is also possible that STEVOR, in addition to playing a role in merozoite binding to RBC prior to invasion, could bind RBC from the iRBC surface – a role consistent with rosetting, or even binding to endothelial cells and a shared role in cytoadhesion. The latter was postulated for STEVOR in the binding and sequestering of gametocytes (Rogers *et al.*, 2000). There is also preliminary evidence that STEVOR N-terminal domains can bind RBCs, a view also shared by Garcia *et al,* (Garcia *et al.*, 2005). The SURFIN multigene family, which shares the same localisation, has also been associated with RBC binding of merozoites, although there is no experimental evidence to date (Winter *et al.*, 2005).

The question of how STEVOR may be exported to the iRBC cytosol and surface, as well as to the apical organelles of the developing merozoites, is interesting given that the STEVOR protein structures are the same in both these cases. The various motifs already identified (*e.g.* signal sequence (Burghaus & Lingelbach, 2001; Kyes *et al.*, 2001), PEXEL/VTS (Hiller *et al.*, 2004; Marti *et al.*, 2004), transmembrane domain/hydrophobic region (Kyes *et al.*, 2001; Przyborski *et al.*, 2005), (and perhaps the tyrosine-based motif

identified here) are functional in the export of STEVOR, and possibly RIFIN. Therefore there is no indication that these two proteins should be targeted for export to different locations. No sub-groups have been identified in STEVOR; however, a RIFIN sub-type, which contains two additional cysteines in the distinguishing insert, is more similar to the STEVOR proteins (which also have these two cysteines) than the other larger RIFIN sub-group. STEVOR and the smaller RIFIN sub-group share structural similarities and therefore may also have a similar distribution and function at the merozoite apex.

Unlike PfEMP1, expression of STEVOR in the gametocyte life-cycle stages is not due to transcription and expression of a particular STEVOR sub-group as the major transcripts are not distinct from those in the asexual stages (Sharp *et al.*, 2006). Additionally, in this thesis, no *stevor* sub-groups were identified through analysis of the HVR, however sequencing was not undertaken from merozoite RNA samples. It is still possible that distinct STEVORs are transcribed at the merozoite stage, different from those transcribed during the trophozoite and schizont stages (personal communication Peter Preiser). The presence of two distinct activation stages (one during the trophozoite stage and one during the merozoite stage) could result in expression of distinct sets of *stevor* (and potentially *rifins*). Therefore transcription timing could also play a role, in that earlier or later transcripts may be translated and directed to different locations based on a hierarchy of signals controlling protein export at the time. This could also be due to trafficking requirements and the presence or absence of transporter proteins involved in recognising those signals and in directing STEVOR to a particular location. One way to address this question would be a microarray analysis comparing the transcription of *stevor* and *rifins* between the merozoite and the erythrocytic cycle to identify whether these particular genes are upregulated at specific stages.

Another question raised from this thesis is that of the orientation of STEVOR and the number of transmembrane regions within the membrane. Sequence diversity data

suggests that the HVR is consistent with regions exposed to functional immune pressure. The profound divergence across isolates confined to the HVR would suggest that this region is indeed exposed on the iRBC surface (and potentially the merozoite apical tip surface). Previous protein-domain predictions, locate the HVR between two transmembrane domains, this structure would place both the N and C-terminal domains in the iRBC cytosol. However, in order for STEVOR to function in RBC binding the N-terminal conserved domain would also have to be on the same side of the iRBC membrane as the HVR – an orientation inconsistent with a two-transmembrane prediction.

A very recent study has provided evidence for the presence of STEVOR located at the iRBC surface membrane in the *P. falciparum* NF54 parasite (Lavazec *et al.*, 2006). However, we were unable to detect STEVOR on the surface of iRBC by flow cytometry using antibodies to the N- and C-termini, suggesting no reaction of the parasite surface with these antibodies. This could have been for several reasons. Firstly, it is possible that the N-terminal was exposed, but that the expression levels were too low to detect, or that only a low percentage of iRBC were expressing endogenous STEVOR on the iRBC surface. Secondly, the N- and C-termini may have been concealed and therefore were not recognised by antibodies.

If the HVR is exposed on the surface it is unlikely to be readily detected by flow cytometry (or any other IFA), as antibodies to the HVR probably do not cross-react with other HVRs (as the sequence similarity between STEVOR sequences is low in this region), and it would be necessary to know the repertoire of STEVOR expressed in a given population of iRBC and the likely population of cells expressing a single HVR. In addition to detection problems, studies of this STEVOR have proved extremely challenging due to the low level of protein expression in infected cells and HVR variant-specific antibody reagents are difficult to generate due to the hydrophobic nature of the

STEVOR protein(s). Classic techniques for the study of surface protein localisation, such as trypsinisation of the iRBC surface proteins, are also extremely difficult given the relative proportion of STEVOR relative to the total protein content of the iRBC sample. Various studies (Khattab & Klinkert, 2006; Przyborski *et al.*, 2005) have attempted to increase protein expression levels, for example, using expression of STEVOR conjugated to fluorescent markers such as GFP, and under the control of strong constitutive promoters; however the results of these are inconsistent with other predictions for protein final iRBC surface location, and orientation within the membrane, perhaps due to adverse effects on the timing of protein expression, and therefore export.

The predicted N-terminal (exon 1) hydrophobic signal sequence would result in the entry of STEVOR into the endoplasmic reticulum (ER) (Elmendorf & Haldar, 1993; Elmendorf & Haldar, 1994). The classical secretory pathway (assuming a functional secretory signal) would place the STEVOR HVR on the inside of the ER consistent with the prediction of Pryzborski *et al.*, which places the HVR inside the Maurer's cleft lumen (Przyborski *et al.*, 2005). The HVR would be located within the lumen of secretory vesicles/Maurer's clefts and finally exposed on the iRBC surface. However given the many membranes STEVOR would have to cross to reach the iRBC surface, it is difficult to assess the true final orientation of STEVOR on the iRBC surface using bioinformatics and structural predictions. Our Western blot data support the finding of Przyborski *et al*, that STEVOR is an integral membrane protein (Przyborski *et al.*, 2005).

The question of the topology of STEVOR within the Maurer's clefts is also raised by the incompatible results of the STEVOR and RIFIN orientation at this location. Surprisingly, given the same predicted topology (Kyes *et al.*, 2001), two studies of labelled STEVOR and RIFIN proteins predict alternative orientations for the HVR of these two proteins within the Maurer's cleft (Khattab & Klinkert, 2006; Przyborski *et al.*, 2005). The RIFIN HVR was exposed to the iRBC cytosol (whilst the N and C-terminals were within the

Maurer's cleft lumen), whereas the STEVOR study placed the HVR within the Maurer's cleft lumen (as expected from the classic secretory pathway).

Przyborski *et al*, assumed that the N-terminal of STEVOR is exposed to the iRBC cytosol along with the GFP-labelled C-terminal. However, since only the C-terminal end of STEVOR was labelled, it is not possible to conclude that the N-terminal of STEVOR is not within the Maurer's cleft lumen on the same side as the HVR (as predicted by either the single or three-transmembrane topology). In addition, neither study used multiple examples from the STEVOR and RIFIN families, and therefore may benefit from analysis of further family members. Alternatively, is it possible for STEVOR membrane topology to change from a two-transmembrane protein in the iRBC stage to an alternative structure and membrane orientation form at another stage (*i.e.* the merozoite where the N-terminal may be exposed for assisting the binding to RBCs as well as the HVR) There is currently no experimental evidence to suggest this is likely.

Permeabilisation with streptolysin-o (Ansorge *et al.*, 1997), which permeabilises specific membranes leaving Maurer's cleft membranes intact, in combination with affinity purified antibodies against the N and C-terminals may be useful approaches to elucidate the orientation of STEVOR. This would enable the orientation of STEVOR within the Maurer's clefts to be determined under the natural *stevor* promoter. However, again due to low level of expression, laboratory strain parasites may not be ideal for this type of experiment, and field-isolate samples are not always readily available.

Given our finding that STEVOR may be on the surface of merozoites, the effect of anti-STEVOR antibodies on merozoite invasion of RBC would be interesting to study, as it is possible they may prevent attachment of the merozoites. However, the correct structure conformation of recombinant STEVOR fragments would be key to the generation of antibodies able to recognise the native protein, and it is known from MSP1 studies that not all antibodies may be functional in this kind of study (Uthaipibull *et al.*, 2001).

Preliminary studies have tentatively shown that STEVOR binds RBC (Peter Preiser, personal communication). In future studies, as well as documenting the binding ability of the protein, it will be necessary to determine if corresponding recombinant proteins or antibodies can competitively inhibit this RBC binding to eliminate the possibility of general protein 'stickiness'.

The results presented in this thesis contribute significantly to the discussion on multigene families and have significant implications for the investigation of associations between the transcription and expression of multigene families and clinical manifestations of parasites that have undergone *in vitro* culture. In the future, comparative studies between field isolates and laboratory strains may reveal clues as to which proteins are driven by host factors.

In conclusion, the potential function of STEVOR needs to be re-evaluated. The identification of a new location of the STEVOR (and potentially RIFIN) proteins in the merozoite necessitates this revision in function, from immuno-variant proteins protecting the Maurer's clefts to a multifunctional protein that may enable RBC binding, whilst providing an additional source for antigenic variation (seemingly independent of PfEMP1), for both schizont iRBC and merozoite stages.

Figure 6.1: Schematic view of STEVOR localisation throughout the asexual blood-stage cycle of P. falciparum

STEVOR is first expressed in the trophozoite stage, where it traffics from within the parasite across the parasitophorous vacuole membrane and accumulates in Maurer's clefts within the iRBC cytosol. Once the parasite develops into a mature schizont (where individual merozoites become visible, and Maurer's clefts are pushed to the periphery of the iRBC), the STEVOR proteins are observed throughout the cytosol of the iRBC. They are closely associated with the iRBC surface, either within the clefts, or at the iRBC membrane. Here the hyper-variable loop may be on the iRBC surface. On schizont rupture, STEVOR may remain within the Maurer's clefts and attached to the broken iRBC membrane (ghosts); however, merozoites are observed to have a single focus of STEVOR at their apex. At this stage, this multigene family could protect against antibodies, targeting important proteins necessary for the invasion of new RBC, and may additionally assist in the binding of merozoites to fresh RBC.

Localisation of STEVOR during the erythrocytic cycle

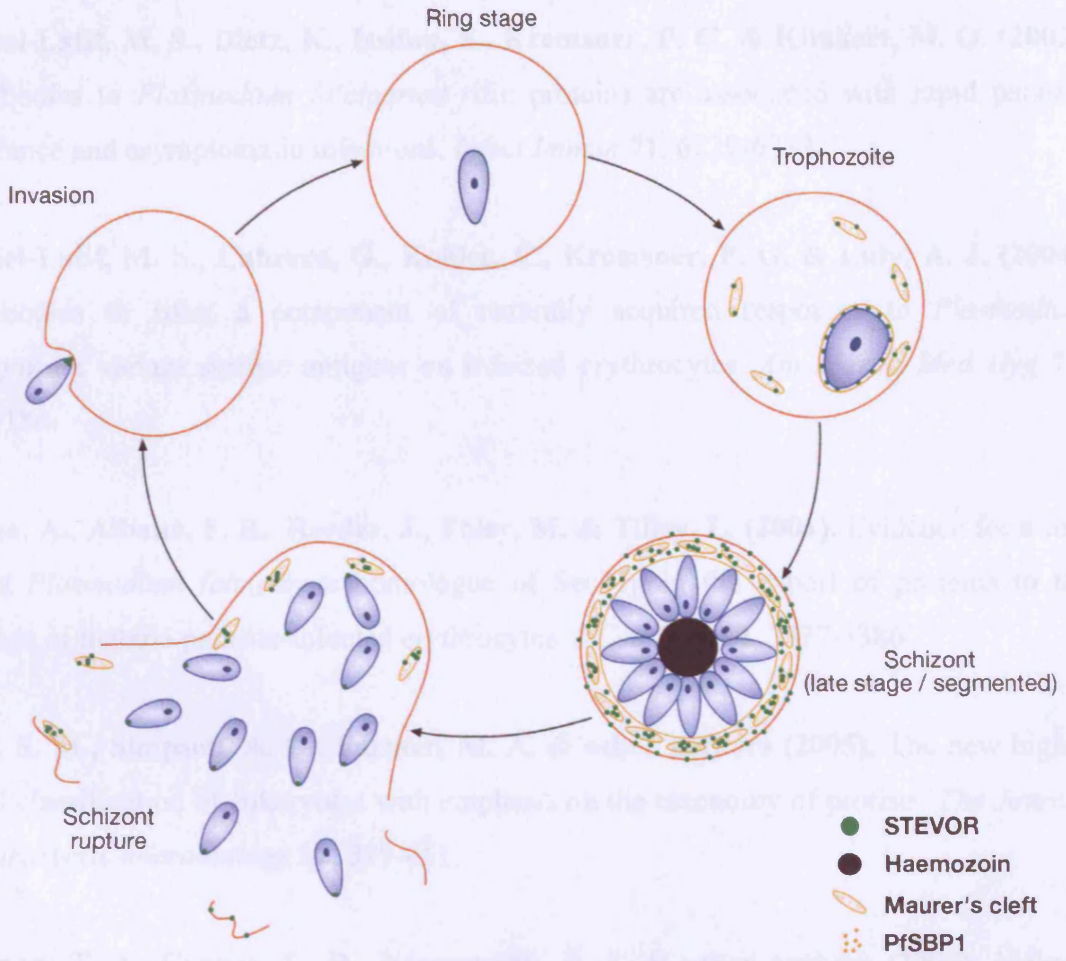

References

Abdel-Latif, M. S., Khattab, A., Lindenthal, C., Kremsner, P. G. & Klinkert, M. Q. (2002). Recognition of variant Rifin antigens by human antibodies induced during natural *Plasmodium* falciparum infections. *Infect Immun* **70**, 7013-7021.

Abdel-Latif, M. S., Dietz, K., Issifou, S., Kremsner, P. G. & Klinkert, M. Q. (2003). Antibodies to *Plasmodium falciparum* rifin proteins are associated with rapid parasite clearance and asymptomatic infections. *Infect Immun* **71**, 6229-6233.

Abdel-Latif, M. S., Cabrera, G., Kohler, C., Kremsner, P. G. & Luty, A. J. (2004). Antibodies to rifin: a component of naturally acquired responses to *Plasmodium falciparum* variant surface antigens on infected erythrocytes. *Am J Trop Med Hyg* **71**, 179-186.

Adisa, A., Albano, F. R., Reeder, J., Foley, M. & Tilley, L. (2001). Evidence for a role for a *Plasmodium falciparum* homologue of Sec31p in the export of proteins to the surface of malaria parasite-infected erythrocytes. *J Cell Sci* **114**, 3377-3386.

Adl, S. M., Simpson, A. G., Farmer, M. A. & other authors (2005). The new higher level classification of eukaryotes with emphasis on the taxonomy of protists. *The Journal of eukaryotic microbiology* **52**, 399-451.

Aitman, T. J., Cooper, L. D., Norsworthy, P. J. & other authors (2000). Malaria susceptibility and CD36 mutation. *Nature* **405**, 1015-1016.

Albano, F. R., Berman, A., La Greca, N., Hibbs, A. R., Wickham, M., Foley, M. & Tilley, L. (1999). A homologue of Sar1p localises to a novel trafficking pathway in malaria-infected erythrocytes. *Eur J Cell Biol* **78**, 453-462.

Albrecht, L., Merino, E. F., Hoffmann, E. H. & other authors (2006). Extensive variant gene family repertoire overlap in Western Amazon *Plasmodium falciparum* isolates. *Mol Biochem Parasitol* **150**, 157-165.

Alexander, E. L., Titus, J. A. & Segal, D. M. (1979). Human leukocyte Fc (IgG) receptors: quantitation and affinity with radiolabeled affinity cross-linked rabbit IgG. *J Immunol* **123**, 295-302.

Allen, S. J., O'Donnell, A., Alexander, N. D., Mgone, C. S., Peto, T. E., Clegg, J. B., Alpers, M. P. & Weatherall, D. J. (1999). Prevention of cerebral malaria in children in Papua New Guinea by southeast Asian ovalocytosis band 3. *Am J Trop Med Hyg* **60**, 1056-1060.

Anders, R. F., McColl, D. J. & Coppel, R. L. (1993). Molecular variation in *Plasmodium falciparum*: polymorphic antigens of asexual erythrocytic stages. *Acta Trop* **53**, 239-253.

Ang, H. H., Chan, K. L. & Mak, J. W. (1996). Clonal diversity in single isolates of Malaysian *Plasmodium falciparum*. *Med Trop (Mars)* **56**, 349-351.

Ansorge, I., Paprotka, K., Bhakdi, S. & Lingelbach, K. (1997). Permeabilization of the erythrocyte membrane with streptolysin O allows access to the vacuolar membrane of *Plasmodium falciparum* and a molecular analysis of membrane topology. *Mol Biochem Parasitol* **84**, 259-261.

Arevalo-Herrera, M., Castellanos, A., Yazdani, S. S., Shakri, A. R., Chitnis, C. E., Dominik, R. & Herrera, S. (2005). Immunogenicity and protective efficacy of recombinant vaccine based on the receptor-binding domain of the *Plasmodium vivax* Duffy binding protein in *Aotus* monkeys. *Am J Trop Med Hyg* **73**, 25-31.

Artavanis-Tsakonas, K., Eleme, K., McQueen, K. L., Cheng, N. W., Parham, P., Davis, D. M. & Riley, E. M. (2003). Activation of a subset of human NK cells upon contact with *Plasmodium falciparum*-infected erythrocytes. *J Immunol* **171**, 5396-5405.

Ashburner, M., Ball, C. A., Blake, J. A. & other authors (2000). Gene ontology: tool for the unification of biology. The Gene Ontology Consortium. *Nature genetics* **25**, 25-29.

Aucan, C., Walley, A. J., Hennig, B. J., Fitness, J., Frodsham, A., Zhang, L., Kwiatkowski, D. & Hill, A. V. (2003). Interferon-alpha receptor-1 (IFNAR1) variants are associated with protection against cerebral malaria in the Gambia. *Genes and immunity* **4**, 275-282.

Ayi, K., Turrini, F., Piga, A. & Arese, P. (2004). Enhanced phagocytosis of ring-parasitized mutant erythrocytes: a common mechanism that may explain protection against *falciparum* malaria in sickle trait and beta-thalassemia trait. *Blood* **104**, 3364-3371.

Bahl, A., Brunk, B., Crabtree, J. & other authors (2003). PlasmoDB: the *Plasmodium* genome resource. A database integrating experimental and computational data. *Nucleic Acids Res* **31**, 212-215.

Bannister, L. & Mitchell, G. (2003). The ins, outs and roundabouts of malaria. *Trends Parasitol* **19**, 209-213.

Bannister, L. H., Hopkins, J. M., Dluzewski, A. R., Margos, G., Williams, I. T., Blackman, M. J., Kocken, C. H., Thomas, A. W. & Mitchell, G. H. (2003). *Plasmodium falciparum* apical membrane antigen 1 (PfAMA-1) is translocated within micronemes along subpellicular microtubules during merozoite development. *J Cell Sci* **116**, 3825-3834.

Barnwell, J. W., Howard, R. J. & Miller, L. H. (1982). Altered expression of *Plasmodium knowlesi* variant antigen on the erythrocyte membrane in splenectomized *rhesus* monkeys. *J Immunol* **128**, 224-226.

Baruch, D. I., Pasloske, B. L., Singh, H. B., Bi, X., Ma, X. C., Feldman, M., Taraschi, T. F. & Howard, R. J. (1995). Cloning the *P. falciparum* gene encoding PfEMP1, a malarial variant antigen and adherence receptor on the surface of parasitized human erythrocytes. *Cell* **82**, 77-87.

Baum, J., Maier, A. G., Good, R. T., Simpson, K. M. & Cowman, A. F. (2005). Invasion by *P. falciparum* merozoites suggests a hierarchy of molecular interactions. *PLoS pathogens* **1**, e37.

Beck, H. P. (2002). Extraction and purification of *Plasmodium* parasite DNA. *Methods Mol Med* **72**, 159-163.

Billker, O., Lindo, V., Panico, M., Etienne, A. E., Paxton, T., Dell, A., Rogers, M., Sinden, R. E. & Morris, H. R. (1998). Identification of xanthurenic acid as the putative inducer of malaria development in the mosquito. *Nature* **392**, 289-292.

Blackman, M. J., Scott-Finnigan, T. J., Shai, S. & Holder, A. A. (1994). Antibodies inhibit the protease-mediated processing of a malaria merozoite surface protein. *J Exp Med* **180**, 389-393.

Blisnick, T., Morales Betoulle, M. E., Barale, J. C., Uzureau, P., Berry, L., Desroses, S., Fujioka, H., Mattei, D. & Braun Breton, C. (2000). Pfsbp1, a Maurer's cleft *Plasmodium falciparum* protein, is associated with the erythrocyte skeleton. *Mol Biochem Parasitol* **111**, 107-121.

Bock, J. B., Matern, H. T., Peden, A. A. & Scheller, R. H. (2001). A genomic perspective on membrane compartment organization. *Nature* **409**, 839-841.

Bowman, S., Lawson, D., Basham, D. & other authors (1999). The complete nucleotide sequence of chromosome 3 of *Plasmodium falciparum*. *Nature* **400**, 532-538.

Brabin, B. J. (1983). An analysis of malaria in pregnancy in Africa. *Bull World Health Organ* **61**, 1005-1016.

Brewster, D. R., Kwiatkowski, D. & White, N. J. (1990). Neurological sequelae of cerebral malaria in children. *Lancet* **336**, 1039-1043.

Brown, K. N. & Brown, I. N. (1965). Immunity to malaria: antigenic variation in chronic infections of *Plasmodium knowlesi*. *Nature* **208**, 1286-1288.

Bull, P. C., Lowe, B. S., Kortok, M., Molyneux, C. S., Newbold, C. I. & Marsh, K. (1998). Parasite antigens on the infected red cell surface are targets for naturally acquired immunity to malaria. *Nat Med* **4**, 358-360.

Bull, P. C., Berriman, M., Kyes, S., Quail, M. A., Hall, N., Kortok, M. M., Marsh, K. & Newbold, C. I. (2005). *Plasmodium falciparum* variant surface antigen expression patterns during malaria. *PLoS pathogens* **1**, e26.

Burghaus, P. A. & Lingelbach, K. (2001). Luciferase, when fused to an N-terminal signal peptide, is secreted from transfected *Plasmodium falciparum* and transported to the cytosol of infected erythrocytes. *J Biol Chem* **276**, 26838-26845.

Burgner, D., Usen, S., Rockett, K., Jallow, M., Ackerman, H., Cervino, A., Pinder, M. & Kwiatkowski, D. P. (2003). Nucleotide and haplotypic diversity of the NOS2A promoter region and its relationship to cerebral malaria. *Human genetics* **112**, 379-386.

Cabrera, G., Cot, M., Migot-Nabias, F., Kremsner, P. G., Deloron, P. & Luty, A. J. (2005). The sickle cell trait is associated with enhanced immunoglobulin G antibody responses to *Plasmodium falciparum* variant surface antigens. *J Infect Dis* **191**, 1631-1638.

Calle, J. M., Nardin, E. H., Clavijo, P., Boudin, C., Stuber, D., Takacs, B., Nussenzweig, R. S. & Cochrane, A. H. (1992). Recognition of different domains of the *Plasmodium falciparum* CS protein by the sera of naturally infected individuals compared with those of sporozoite-immunized volunteers. *J Immunol* **149**, 2695-2701.

Camus, D. & Hadley, T. J. (1985). A *Plasmodium falciparum* antigen that binds to host erythrocytes and merozoites. *Science* **230**, 553-556.

Cappadoro, M., Giribaldi, G., O'Brien, E., Turrini, F., Mannu, F., Ulliers, D., Simula, G., Luzzatto, L. & Arese, P. (1998). Early phagocytosis of glucose-6-phosphate dehydrogenase (G6PD)-deficient erythrocytes parasitized by *Plasmodium falciparum* may explain malaria protection in G6PD deficiency. *Blood* **92**, 2527-2534.

Carcy, B., Bonnefoy, S., Guillotte, M., Le Scanf, C., Grellier, P., Schrevel, J., Fandeur, T. & Mercereau-Puijalon, O. (1994). A large multigene family expressed during the erythrocytic schizogony of *Plasmodium falciparum*. *Mol Biochem Parasitol* **68**, 221-233.

Carlton, J., Silva, J. & Hall, N. (2005). The genome of model malaria parasites, and comparative genomics. *Current issues in molecular biology* **7**, 23-37.

Carlton, J. M., Angiuoli, S. V., Suh, B. B. & other authors (2002). Genome sequence and comparative analysis of the model rodent malaria parasite *Plasmodium yoelii yoelii*. *Nature* **419**, 512-519.

Carlton, J. M. & Carucci, D. J. (2002). Rodent models of malaria in the genomics era. *Trends Parasitol* **18**, 100-102.

Chen, P., Lamont, G., Elliott, T., Kidson, C., Brown, G., Mitchell, G., Stace, J. & Alpers, M. (1980). *Plasmodium falciparum* strains from Papua New Guinea: culture characteristics and drug sensitivity. *Southeast Asian J Trop Med Public Health* **11**, 435-440.

Chen, Q., Barragan, A., Fernandez, V., Sundstrom, A., Schlichtherle, M., Sahlen, A., Carlson, J., Datta, S. & Wahlgren, M. (1998). Identification of *Plasmodium falciparum* erythrocyte membrane protein 1 (PfEMP1) as the rosetting ligand of the malaria parasite *P. falciparum*. *J Exp Med* **187**, 15-23.

Cheng, Q., Cloonan, N., Fischer, K., Thompson, J., Waine, G., Lanzer, M. & Saul, A. (1998). *stevor* and *rif* are *Plasmodium falciparum* multicopy gene families which potentially encode variant antigens. *Mol Biochem Parasitol* **97**, 161-176.

Cockburn, I. A., Mackinnon, M. J., O'Donnell, A., Allen, S. J., Moulds, J. M., Baisor, M., Bockarie, M., Reeder, J. C. & Rowe, J. A. (2004). A human complement receptor 1 polymorphism that reduces *Plasmodium falciparum* rosetting confers protection against severe malaria. *Proc Natl Acad Sci U S A* **101**, 272-277.

Cohen, S., Mc, G. I. & Carrington, S. (1961). Gamma-globulin and acquired immunity to human malaria. *Nature* **192**, 733-737.

Collins, W. E. & Jeffery, G. M. (1999a). A retrospective examination of secondary sporozoite- and trophozoite-induced infections with *Plasmodium falciparum*:

development of parasitologic and clinical immunity following secondary infection. *Am J Trop Med Hyg* **61**, 20-35.

Collins, W. E. & Jeffery, G. M. (1999b). A retrospective examination of sporozoite- and trophozoite-induced infections with *Plasmodium falciparum* in patients previously infected with heterologous species of *Plasmodium*: effect on development of parasitologic and clinical immunity. *Am J Trop Med Hyg* **61**, 36-43.

Conway, D. J., Cavanagh, D. R., Tanabe, K. & other authors (2000). A principal target of human immunity to malaria identified by molecular population genetic and immunological analyses. *Nat Med* **6**, 689-692.

Cooke, B. M., Buckingham, D. W., Glenister, F. K., Fernandez, K. M., Bannister, L. H., Marti, M., Mohandas, N. & Coppel, R. L. (2006). A Maurer's cleft-associated protein is essential for expression of the major malaria virulence antigen on the surface of infected red blood cells. *The Journal of cell biology* **172**, 899-908.

Cortes, A., Mellombo, M., Mgone, C. S., Beck, H. P., Reeder, J. C. & Cooke, B. M. (2005). Adhesion of *Plasmodium falciparum*-infected red blood cells to CD36 under flow is enhanced by the cerebral malaria-protective trait South-East Asian ovalocytosis. *Mol Biochem Parasitol* **142**, 252-257.

Cowman, A. F. & Crabb, B. S. (2006). Invasion of red blood cells by malaria parasites. *Cell* **124**, 755-766.

Cox, H. W. (1958). The roles of time and atabrine in inducing chronic *Plasmodium berghei* infections of white mice. *J Immunol* **81**, 72-75.

Craig, A. & Scherf, A. (2001). Molecules on the surface of the *Plasmodium falciparum* infected erythrocyte and their role in malaria pathogenesis and immune evasion. *Mol Biochem Parasitol* **115**, 129-143.

Crandall, I., Collins, W. E., Gysin, J. & Sherman, I. W. (1993). Synthetic peptides based on motifs present in human band 3 protein inhibit cytoadherence/sequestration of the malaria parasite *Plasmodium falciparum*. *Proc Natl Acad Sci U S A* **90**, 4703-4707.

Crandall, I., Land, K. M. & Sherman, I. W. (1994). *Plasmodium falciparum*: pfalhesin and CD36 form an adhesin/receptor pair that is responsible for the pH-dependent portion of cytoadherence/sequestration. *Exp Parasitol* **78**, 203-209.

Crandall, I. & Sherman, I. W. (1994a). Antibodies to synthetic peptides based on band 3 motifs react specifically with *Plasmodium falciparum* (human malaria)-infected erythrocytes and block cytoadherence. *Parasitology* **108 (Pt 4)**, 389-396.

Crandall, I. & Sherman, I. W. (1994b). Cytoadherence-related neoantigens on *Plasmodium falciparum* (human malaria)-infected human erythrocytes result from the exposure of normally cryptic regions of the band 3 protein. *Parasitology* **108 (Pt 3)**, 257-267.

Daily, J. P., Le Roch, K. G., Sarr, O. & other authors (2005). In vivo transcriptome of *Plasmodium falciparum* reveals overexpression of transcripts that encode surface proteins. *J Infect Dis* **191**, 1196-1203.

Day, K. P., Karamalis, F., Thompson, J., Barnes, D. A., Peterson, C., Brown, H., Brown, G. V. & Kemp, D. J. (1993). Genes necessary for expression of a virulence determinant and for transmission of *Plasmodium falciparum* are located on a 0.3-megabase region of chromosome 9. *Proc Natl Acad Sci U S A* **90**, 8292-8296.

Day, K. P., Hayward, R. E., Smith, D. & Culvenor, J. G. (1998). CD36-dependent adhesion and knob expression of the transmission stages of *Plasmodium falciparum* is stage specific. *Mol Biochem Parasitol* **93**, 167-177.

de Bruin, D., Lanzer, M. & Ravetch, J. V. (1994). The polymorphic subtelomeric regions of *Plasmodium falciparum* chromosomes contain arrays of repetitive sequence elements. *Proc Natl Acad Sci U S A* **91**, 619-623.

De Souza, J. B., Williamson, K. H., Otani, T. & Playfair, J. H. (1997). Early gamma interferon responses in lethal and nonlethal murine blood-stage malaria. *Infect Immun* **65**, 1593-1598.

Del Giudice, G., Tougne, C., Renia, L. & other authors (1991). Characterization of murine monoclonal antibodies against a repetitive synthetic peptide from the circumsporozoite protein of the human malaria parasite, *Plasmodium falciparum*. *Molecular immunology* **28**, 1003-1009.

Delves, C. J., Goman, M., Ridley, R. G., Matile, H., Lensen, T. H., Ponnudurai, T. & Scaife, J. G. (1989). Identification of *Plasmodium falciparum*-infected mosquitoes using a probe containing repetitive DNA. *Mol Biochem Parasitol* **32**, 105-112.

Duraisingh, M. T., Voss, T. S., Marty, A. J. & other authors (2005). Heterochromatin silencing and locus repositioning linked to regulation of virulence genes in *Plasmodium falciparum*. *Cell* **121**, 13-24.

Eaton, M. (1938). The agglutination of *Plasmodium knowlesi* by immune serum. *J Expt Med* **67**.

Eda, S., Lawler, J. & Sherman, I. W. (1999). *Plasmodium falciparum*-infected erythrocyte adhesion to the type 3 repeat domain of thrombospondin-1 is mediated by a modified band 3 protein. *Mol Biochem Parasitol* **100**, 195-205.

Elmendorf, H. G. & Haldar, K. (1993). Identification and localization of ERD2 in the malaria parasite *Plasmodium falciparum*: separation from sites of sphingomyelin synthesis and implications for organization of the Golgi. *Embo J* **12**, 4763-4773.

Elmendorf, H. G. & Haldar, K. (1994). *Plasmodium falciparum* exports the Golgi marker sphingomyelin synthase into a tubovesicular network in the cytoplasm of mature erythrocytes. *The Journal of cell biology* **124**, 449-462.

English, M., Murphy, S., Mwangi, I., Crawley, J., Peshu, N. & Marsh, K. (1995). Interobserver variation in respiratory signs of severe malaria. *Archives of disease in childhood* **72**, 334-336.

Escalante, A. A., Freeland, D. E., Collins, W. E. & Lal, A. A. (1998). The evolution of primate malaria parasites based on the gene encoding cytochrome b from the linear mitochondrial genome. *Proc Natl Acad Sci U S A* **95**, 8124-8129.

Esposito, F., Lombardi, S., Modiano, D., Zavala, F., Reeme, J., Lamizana, L., Coluzzi, M. & Nussenzweig, R. S. (1988). Prevalence and levels of antibodies to the circumsporozoite protein of *Plasmodium falciparum* in an endemic area and their relationship to resistance against malaria infection. *Trans R Soc Trop Med Hyg* **82**, 827-832.

Fairhurst, R. M., Fujioka, H., Hayton, K., Collins, K. F. & Wellems, T. E. (2003). Aberrant development of *Plasmodium falciparum* in hemoglobin CC red cells: implications for the malaria protective effect of the homozygous state. *Blood* **101**, 3309-3315.

Felsenstein, J. (1988). Phylogenies from molecular sequences: inference and reliability. *Annual review of genetics* **22**, 521-565.

Fernandez, V., Hommel, M., Chen, Q., Hagblom, P. & Wahlgren, M. (1999). Small, clonally variant antigens expressed on the surface of the *Plasmodium falciparum*-infected erythrocyte are encoded by the *rif* gene family and are the target of human immune responses. *J Exp Med* **190**, 1393-1404.

Filisetti, D., Bombard, S., N'Guiri, C., Dahan, R., Molet, B., Abou-Bacar, A., Hansmann, Y., Christmann, D. & Candolfi, E. (2002). Prospective assessment of a new polymerase chain reaction target (STEVOR) for imported *Plasmodium falciparum* malaria. *Eur J Clin Microbiol Infect Dis* **21**, 679-681.

Florens, L., Washburn, M. P., Raine, J. D. & other authors (2002). A proteomic view of the *Plasmodium falciparum* life cycle. *Nature* **419**, 520-526.

Freitas-Junior, L. H., Hernandez-Rivas, R., Ralph, S. A. & other authors (2005). Telomeric heterochromatin propagation and histone acetylation control mutually exclusive expression of antigenic variation genes in malaria parasites. *Cell* **121**, 25-36.

Friedman, M. J., Roth, E. F., Nagel, R. L. & Trager, W. (1979). The role of hemoglobins C, S, and Nbalt in the inhibition of malaria parasite development in vitro. *Am J Trop Med Hyg* **28**, 777-780.

Gabriel, J. & Berzins, K. (1983). Specific lysis of *Plasmodium yoelii* infected mouse erythrocytes with antibody and complement. *Clin Exp Immunol* **52**, 129-134.

Galinski, M. R., Medina, C. C., Ingravallo, P. & Barnwell, J. W. (1992). A reticulocyte-binding protein complex of *Plasmodium vivax* merozoites. *Cell* **69**, 1213-1226.

Garcia, J. E., Puentes, A., Curtidor, H. & other authors (2005). Peptides from the *Plasmodium falciparum* STEVOR putative protein bind with high affinity to normal human red blood cells. *Peptides* **26**, 1133-1143.

Gardner, M. J. (1999). The genome of the malaria parasite. *Curr Opin Genet Dev* **9**, 704-708.

Gardner, M. J., Hall, N., Fung, E. & other authors (2002). Genome sequence of the human malaria parasite *Plasmodium falciparum. Nature* **419**, 498-511.

Genton, B., al-Yaman, F., Mgone, C. S., Alexander, N., Paniu, M. M., Alpers, M. P. & Mokela, D. (1995). Ovalocytosis and cerebral malaria. *Nature* **378**, 564-565.

Goel, V. K., Li, X., Chen, H., Liu, S. C., Chishti, A. H. & Oh, S. S. (2003). Band 3 is a host receptor binding merozoite surface protein 1 during the *Plasmodium falciparum* invasion of erythrocytes. *Proc Natl Acad Sci U S A* **100**, 5164-5169.

Greenwood, B. & Mutabingwa, T. (2002). Malaria in 2002. *Nature* **415**, 670-672.

Guevara Patino, J. A., Holder, A. A., McBride, J. S. & Blackman, M. J. (1997). Antibodies that inhibit malaria merozoite surface protein-1 processing and erythrocyte invasion are blocked by naturally acquired human antibodies. *J Exp Med* **186**, 1689-1699.

Haeggstrom, M., Kironde, F., Berzins, K., Chen, Q., Wahlgren, M. & Fernandez, V. (2004). Common trafficking pathway for variant antigens destined for the surface of the *Plasmodium falciparum*-infected erythrocyte. *Mol Biochem Parasitol* **133**, 1-14.

Hall (1998). BioEdit. Biological sequence alignment editor for Windows.

Hawthorne, P. L., Trenholme, K. R., Skinner-Adams, T. S. & other authors (2004). A novel *Plasmodium falciparum* ring stage protein, REX, is located in Maurer's clefts. *Mol Biochem Parasitol* **136**, 181-189.

Hayward, R. E., Tiwari, B., Piper, K. P., Baruch, D. I. & Day, K. P. (1999). Virulence and transmission success of the malarial parasite *Plasmodium falciparum*. *Proc Natl Acad Sci U S A* **96**, 4563-4568.

Helmby, H., Cavelier, L., Pettersson, U. & Wahlgren, M. (1993). Rosetting *Plasmodium falciparum*-infected erythrocytes express unique strain-specific antigens on their surface. *Infect Immun* **61**, 284-288.

Hermsen, C. C., Konijnenberg, Y., Mulder, L. & other authors (2003). Circulating concentrations of soluble granzyme A and B increase during natural and experimental *Plasmodium falciparum* infections. *Clin Exp Immunol* **132**, 467-472.

Higgins, D. G. & Sharp, P. M. (1988). CLUSTAL: a package for performing multiple sequence alignment on a microcomputer. *Gene* **73**, 237-244.

Hill, A. V., Allsopp, C. E., Kwiatkowski, D. & other authors (1991). Common west African HLA antigens are associated with protection from severe malaria. *Nature* **352**, 595-600.

Hiller, N. L., Bhattacharjee, S., van Ooij, C., Liolios, K., Harrison, T., Lopez-Estrano, C. & Haldar, K. (2004). A host-targeting signal in virulence proteins reveals a secretome in malarial infection. *Science* **306**, 1934-1937.

Hobbs, M. R., Udhayakumar, V., Levesque, M. C. & other authors (2002). A new NOS2 promoter polymorphism associated with increased nitric oxide production and protection from severe malaria in Tanzanian and Kenyan children. *Lancet* **360**, 1468-1475.

Hogh, B., Marbiah, N. T., Burghaus, P. A. & Andersen, P. K. (1995). Relationship between maternally derived anti-*Plasmodium falciparum* antibodies and risk of infection and disease in infants living in an area of Liberia, West Africa, in which malaria is highly endemic. *Infect Immun* **63**, 4034-4038.

Holder, A. A. & Freeman, R. R. (1981). Immunization against blood-stage rodent malaria using purified parasite antigens. *Nature* **294**, 361-364.

Holder, A. A., Freeman, R. R., Uni, S. & Aikawa, M. (1985). Isolation of a *Plasmodium falciparum* rhoptry protein. *Mol Biochem Parasitol* **14**, 293-303.

Holt, D. C., Gardiner, D. L., Thomas, E. A. & other authors (1999). The cytoadherence linked asexual gene family of *Plasmodium falciparum*: are there roles other than cytoadherence? *Int J Parasitol* **29**, 939-944.

Hommel, M., David, P. H. & Oligino, L. D. (1983). Surface alterations of erythrocytes in *Plasmodium falciparum* malaria. Antigenic variation, antigenic diversity, and the role of the spleen. *J Exp Med* **157**, 1137-1148.

Hoppe, H. C., Verschoor, J. A. & Louw, A. I. (1991). *Plasmodium falciparum*: a comparison of synchronisation methods for in vitro cultures. *Exp Parasitol* **72**, 464-467.

Hoppe, H. C., Ngo, H. M., Yang, M. & Joiner, K. A. (2000). Targeting to rhoptry organelles of *Toxoplasma gondii* involves evolutionarily conserved mechanisms. *Nature cell biology* **2**, 449-456.

Horai, S., Hayasaka, K., Kondo, R., Tsugane, K. & Takahata, N. (1995). Recent African origin of modern humans revealed by complete sequences of hominoid mitochondrial DNAs. *Proc Natl Acad Sci U S A* **92**, 532-536.

Howard, R. J., Barnwell, J. W., Rock, E. P., Neequaye, J., Ofori-Adjei, D., Maloy, W. L., Lyon, J. A. & Saul, A. (1988). Two approximately 300 kilodalton *Plasmodium falciparum* proteins at the surface membrane of infected erythrocytes. *Mol Biochem Parasitol* **27**, 207-223.

Hutagalung, R., Wilairatana, P., Looareesuwan, S., Brittenham, G. M., Aikawa, M. & Gordeuk, V. R. (1999). Influence of hemoglobin E trait on the severity of *falciparum* malaria. *J Infect Dis* **179**, 283-286.

Jagers, P. (1983). Stochastic models for cell kinetics. *Bulletin of mathematical biology* **45**, 507-519.

Janssen, C. S., Phillips, R. S., Turner, C. M. & Barrett, M. P. (2004). *Plasmodium* interspersed repeats: the major multigene super-family of malaria parasites. *Nucleic Acids Res* **32**, 5712-5720.

Jeffares, D. C., Pain, A., Berry, A. & other authors (2007). Genome variation and evolution of the malaria parasite *Plasmodium falciparum*. *Nature genetics* **39**, 120-125.

Jennings, R. M., JB, D. E. S., Todd, J. E., Armstrong, M., Flanagan, K. L., Riley, E. M. & Doherty, J. F. (2006). Imported *Plasmodium falciparum* malaria: are patients originating from disease-endemic areas less likely to develop severe disease? A prospective, observational study. *Am J Trop Med Hyg* **75**, 1195-1199.

John, C. C., Zickafoose, J. S., Sumba, P. O., King, C. L. & Kazura, J. W. (2003). Antibodies to the *Plasmodium falciparum* antigens circumsporozoite protein, thrombospondin-related adhesive protein, and liver-stage antigen 1 vary by ages of subjects and by season in a highland area of Kenya. *Infect Immun* **71**, 4320-4325.

Kaneko, O., Tsuboi, T., Ling, I. T., Howell, S., Shirano, M., Tachibana, M., Cao, Y. M., Holder, A. A. & Torii, M. (2001). The high molecular mass rhoptry protein, RhopH1, is encoded by members of the clag multigene family in *Plasmodium falciparum* and *Plasmodium yoelii*. *Mol Biochem Parasitol* **118**, 223-231.

Kaneko, O., Mu, J., Tsuboi, T., Su, X. & Torii, M. (2002). Gene structure and expression of a *Plasmodium falciparum* 220-kDa protein homologous to the *Plasmodium vivax* reticulocyte binding proteins. *Mol Biochem Parasitol* **121**, 275-278.

Kaneko, O., Yim Lim, B. Y., Iriko, H. & other authors (2005). Apical expression of three RhopH1/Clag proteins as components of the *Plasmodium falciparum* RhopH complex. *Mol Biochem Parasitol* **143**, 20-28.

Kassim, O. O., Ako-Anai, K. A., Torimiro, S. E., Hollowell, G. P., Okoye, V. C. & Martin, S. K. (2000). Inhibitory factors in breastmilk, maternal and infant sera against in vitro growth of *Plasmodium falciparum* malaria parasite. *Journal of tropical pediatrics* **46**, 92-96.

Kats, L. M., Black, C. G., Proellocks, N. I. & Coppel, R. L. (2006). *Plasmodium* rhoptries: how things went pear-shaped. *Trends Parasitol* **22**, 269-276.

Kaviratne, M., Khan, S. M., Jarra, W. & Preiser, P. R. (2002). Small variant STEVOR antigen is uniquely located within Maurer's clefts in *Plasmodium falciparum*-infected red blood cells. *Eukaryot Cell* **1**, 926-935.

Kay, M. M., Marchalonis, J. J., Hughes, J., Watanabe, K. & Schluter, S. F. (1990). Definition of a physiologic aging autoantigen by using synthetic peptides of membrane protein band 3: localization of the active antigenic sites. *Proc Natl Acad Sci U S A* **87**, 5734-5738.

Khattab, A. & Klinkert, M. Q. (2006). Maurer's clefts-restricted localization, orientation and export of a *Plasmodium falciparum* RIFIN. *Traffic (Copenhagen, Denmark)* **7**, 1654-1665.

Kikuchi, M., Looareesuwan, S., Ubalee, R. & other authors (2001). Association of adhesion molecule PECAM-1/CD31 polymorphism with susceptibility to cerebral malaria in Thais. *Parasitology international* **50**, 235-239.

Knight, J. C., Udalova, I., Hill, A. V., Greenwood, B. M., Peshu, N., Marsh, K. & Kwiatkowski, D. (1999). A polymorphism that affects OCT-1 binding to the TNF promoter region is associated with severe malaria. *Nature genetics* **22**, 145-150.

Knuepfer, E., Rug, M., Klonis, N., Tilley, L. & Cowman, A. F. (2005a). Trafficking determinants for PfEMP3 export and assembly under the *Plasmodium falciparum*-infected red blood cell membrane. *Mol Microbiol* **58**, 1039-1053.

Knuepfer, E., Rug, M., Klonis, N., Tilley, L. & Cowman, A. F. (2005b). Trafficking of the major virulence factor to the surface of transfected P. *falciparum*-infected erythrocytes. *Blood* **105**, 4078-4087.

Koch, O., Awomoyi, A., Usen, S., Jallow, M., Richardson, A., Hull, J., Pinder, M., Newport, M. & Kwiatkowski, D. (2002). IFNGR1 gene promoter polymorphisms and susceptibility to cerebral malaria. *J Infect Dis* **185**, 1684-1687.

Kooij, T. W., Carlton, J. M., Bidwell, S. L., Hall, N., Ramesar, J., Janse, C. J. & Waters, A. P. (2005). A *Plasmodium* whole-genome synteny map: indels and synteny breakpoints as foci for species-specific genes. *PLoS pathogens* **1**, e44.

Krettli, A. U., Nussenzweig, V. & Nussenzweig, R. S. (1976). Complement alterations in rodent malaria. *Am J Trop Med Hyg* **25**, 34-41.

Kriek, N., Tilley, L., Horrocks, P., Pinches, R., Elford, B. C., Ferguson, D. J., Lingelbach, K. & Newbold, C. I. (2003). Characterization of the pathway for transport of the cytoadherence-mediating protein, PfEMP1, to the host cell surface in malaria parasite-infected erythrocytes. *Mol Microbiol* **50**, 1215-1227.

Kumar, K. A., Sano, G., Boscardin, S., Nussenzweig, R. S., Nussenzweig, M. C., Zavala, F. & Nussenzweig, V. (2006). The circumsporozoite protein is an immunodominant protective antigen in irradiated sporozoites. *Nature* **444**, 937-940.

Kumar, S., Tamura, K. & Nei, M. (2004). MEGA3: Integrated software for Molecular Evolutionary Genetics Analysis and sequence alignment. *Brief Bioinform* **5**, 150-163.

Kun, J. F., Mordmuller, B., Perkins, D. J., May, J., Mercereau-Puijalon, O., Alpers, M., Weinberg, J. B. & Kremsner, P. G. (2001). Nitric oxide synthase 2(Lambarene) (G-954C), increased nitric oxide production, and protection against malaria. *J Infect Dis* **184**, 330-336.

Kwiatkowski, D., Molyneux, M. E., Stephens, S. & other authors (1993). Anti-TNF therapy inhibits fever in cerebral malaria. *The Quarterly journal of medicine* **86**, 91-98.

Kyes, S., Pinches, R. & Newbold, C. (2000). A simple RNA analysis method shows *var* and *rif* multigene family expression patterns in *Plasmodium falciparum*. *Mol Biochem Parasitol* **105**, 311-315.

Kyes, S., Horrocks, P. & Newbold, C. (2001). Antigenic variation at the infected red cell surface in malaria. *Annu Rev Microbiol* **55**, 673-707.

Kyes, S. A., Rowe, J. A., Kriek, N. & Newbold, C. I. (1999). Rifins: a second family of clonally variant proteins expressed on the surface of red cells infected with *Plasmodium falciparum*. *Proc Natl Acad Sci U S A* **96**, 9333-9338.

Langhorne, J., Simon-Haarhaus, B. & Meding, S. J. (1990). The role of CD4+ T cells in the protective immune response to *Plasmodium chabaudi in vivo*. *Immunology letters* **25**, 101-107.

Langhorne, J., Quin, S. J. & Sanni, L. A. (2002). Mouse models of blood-stage malaria infections: immune responses and cytokines involved in protection and pathology. *Chem Immunol* **80**, 204-228.

Lauer, S., VanWye, J., Harrison, T., McManus, H., Samuel, B. U., Hiller, N. L., Mohandas, N. & Haldar, K. (2000). Vacuolar uptake of host components, and a role for cholesterol and sphingomyelin in malarial infection. *Embo J* **19**, 3556-3564.

Lavazec, C., Sanyal, S. & Templeton, T. J. (2006). Hypervariability within the Rifin, Stevor and Pfmc-2TM superfamilies in *Plasmodium falciparum*. *Nucleic Acids Res* **34**, 6696-6707.

Le Roch, K. G., Zhou, Y., Blair, P. L. & other authors (2003). Discovery of gene function by expression profiling of the malaria parasite life cycle. *Science* **301**, 1503-1508.

Leech, J. H., Barnwell, J. W., Miller, L. H. & Howard, R. J. (1984). Identification of a strain-specific malarial antigen exposed on the surface of *Plasmodium falciparum*-infected erythrocytes. *J Exp Med* **159**, 1567-1575.

Lensen, A., Bril, A., van de Vegte, M., van Gemert, G. J., Eling, W. & Sauerwein, R. (1999). *Plasmodium falciparum*: infectivity of cultured, synchronized gametocytes to mosquitoes. *Exp Parasitol* **91**, 101-103.

Levine, N. D. (1988). Progress in taxonomy of the Apicomplexan protozoa. *The Journal of protozoology* **35**, 518-520.

Limpaiboon, T., Taylor, D. W., Jones, G., Geysen, H. M. & Saul, A. (1990). Characterization of a *Plasmodium falciparum* epitope recognized by a monoclonal antibody with broad isolate and species specificity. *Southeast Asian J Trop Med Public Health* **21**, 388-396.

Ling, I. T., Florens, L., Dluzewski, A. R. & other authors (2004). The *Plasmodium falciparum clag9* gene encodes a rhoptry protein that is transferred to the host erythrocyte upon invasion. *Mol Microbiol* **52**, 107-118.

Llinas, M., Bozdech, Z., Wong, E. D., Adai, A. T. & DeRisi, J. L. (2006). Comparative whole genome transcriptome analysis of three *Plasmodium falciparum* strains. *Nucleic Acids Res* **34**, 1166-1173.

Lobo, C. A., Rodriguez, M., Reid, M. & Lustigman, S. (2003). Glycophorin C is the receptor for the *Plasmodium falciparum* erythrocyte binding ligand PfEBP-2 (baebl). *Blood* **101**, 4628-4631.

Lopez-Estrano, C., Bhattacharjee, S., Harrison, T. & Haldar, K. (2003). Cooperative domains define a unique host cell-targeting signal in *Plasmodium falciparum*-infected erythrocytes. *Proc Natl Acad Sci U S A* **100**, 12402-12407.

Low, P. S., Waugh, S. M., Zinke, K. & Drenckhahn, D. (1985). The role of hemoglobin denaturation and band 3 clustering in red blood cell aging. *Science* **227**, 531-533.

Luoni, G., Verra, F., Arca, B., Sirima, B. S., Troye-Blomberg, M., Coluzzi, M., Kwiatkowski, D. & Modiano, D. (2001). Antimalarial antibody levels and IL4 polymorphism in the Fulani of West Africa. *Genes and immunity* **2**, 411-414.

Luse, S. A. & Miller, L. H. (1971). *Plasmodium falciparum* malaria. Ultrastructure of parasitized erythrocytes in cardiac vessels. *Am J Trop Med Hyg* **20**, 655-660.

Luty, A. J., Kun, J. F. & Kremsner, P. G. (1998). Mannose-binding lectin plasma levels and gene polymorphisms in *Plasmodium falciparum* malaria. *J Infect Dis* **178**, 1221-1224.

Macintosh, C. (2006). Naturally occurring antibody responses to recombinant protein domains of *Plasmodium falciparum* erythrocyte membrane protein 1.

Mackintosh, C. L., Beeson, J. G. & Marsh, K. (2004). Clinical features and pathogenesis of severe malaria. *Trends Parasitol* **20**, 597-603.

Maier, A. G., Duraisingh, M. T., Reeder, J. C., Patel, S. S., Kazura, J. W., Zimmerman, P. A. & Cowman, A. F. (2003). *Plasmodium falciparum* erythrocyte invasion through glycophorin C and selection for Gerbich negativity in human populations. *Nat Med* **9**, 87-92.

Manski-Nankervis, J. A., Gardiner, D. L., Hawthorne, P., Holt, D. C., Edwards, M., Kemp, D. J. & Trenholme, K. R. (2000). The sequence of *clag 9*, a subtelomeric gene of *Plasmodium falciparum* is highly conserved. *Mol Biochem Parasitol* **111**, 437-440.

Marks, M. S., Woodruff, L., Ohno, H. & Bonifacino, J. S. (1996). Protein targeting by tyrosine- and di-leucine-based signals: evidence for distinct saturable components. *The Journal of cell biology* **135**, 341-354.

Marsh, K. & Howard, R. J. (1986). Antigens induced on erythrocytes by *P. falciparum*: expression of diverse and conserved determinants. *Science* **231**, 150-153.

Marsh, K., Forster, D., Waruiru, C. & other authors (1995). Indicators of life-threatening malaria in African children. *The New England journal of medicine* **332**, 1399-1404.

Marsh, K. & Snow, R. W. (1997). Host-parasite interaction and morbidity in malaria endemic areas. *Philosophical transactions of the Royal Society of London* **352**, 1385-1394.

Marsh, K. & Kinyanjui, S. (2006). Immune effector mechanisms in malaria. *Parasite Immunol* **28**, 51-60.

Marti, M., Good, R. T., Rug, M., Knuepfer, E. & Cowman, A. F. (2004). Targeting malaria virulence and remodeling proteins to the host erythrocyte. *Science* **306**, 1930-1933.

Mbogo, C. N., Snow, R. W., Kabiru, E. W., Ouma, J. H., Githure, J. I., Marsh, K. & Beier, J. C. (1993). Low-level *Plasmodium falciparum* transmission and the incidence of severe malaria infections on the Kenyan coast. *Am J Trop Med Hyg* **49**, 245-253.

McBride, J. S., Walliker, D. & Morgan, G. (1982). Antigenic diversity in the human malaria parasite *Plasmodium falciparum*. *Science* **217**, 254-257.

McGregor, I. A., Hall, P. J., Williams, K. & Hardy, C. L. (1966). Demonstration of circulating antibodies to *Plasmodium falciparum* by gel-diffusion techniques. *Nature* **210**, 1384-1386.

McGuire, W., Hill, A. V., Allsopp, C. E., Greenwood, B. M. & Kwiatkowski, D. (1994). Variation in the TNF-alpha promoter region associated with susceptibility to cerebral malaria. *Nature* **371**, 508-510.

McRobert, L., Preiser, P., Sharp, S., Jarra, W., Kaviratne, M., Taylor, M. C., Renia, L. & Sutherland, C. J. (2004). Distinct trafficking and localization of STEVOR proteins in three stages of the *Plasmodium falciparum* life cycle. *Infect Immun* **72**, 6597-6602.

Mehlin, C., Boni, E., Buckner, F. S. & other authors (2006). Heterologous expression of proteins from *Plasmodium falciparum*: results from 1000 genes. *Mol Biochem Parasitol* **148**, 144-160.

Menendez, C., Ordi, J., Ismail, M. R., Ventura, P. J., Aponte, J. J., Kahigwa, E., Font, F. & Alonso, P. L. (2000). The impact of placental malaria on gestational age and birth weight. *J Infect Dis* **181**, 1740-1745.

Miller, L. H., Baruch, D. I., Marsh, K. & Doumbo, O. K. (2002). The pathogenic basis of malaria. *Nature* **415**, 673-679.

Min-Oo, G., Fortin, A., Tam, M. F., Nantel, A., Stevenson, M. M. & Gros, P. (2003). Pyruvate kinase deficiency in mice protects against malaria. *Nature genetics* **35**, 357-362.

Mockenhaupt, F. P., Ehrhardt, S., Cramer, J. P. & other authors (2004). Hemoglobin C and resistance to severe malaria in Ghanaian children. *J Infect Dis* **190**, 1006-1009.

Modiano, D., Luoni, G., Sirima, B. S. & other authors (2001). Haemoglobin C protects against clinical *Plasmodium falciparum* malaria. *Nature* **414**, 305-308.

Mohan, K., Moulin, P. & Stevenson, M. M. (1997). Natural killer cell cytokine production, not cytotoxicity, contributes to resistance against blood-stage *Plasmodium chabaudi* AS infection. *J Immunol* **159**, 4990-4998.

Molineaux, L., Trauble, M., Collins, W. E., Jeffery, G. M. & Dietz, K. (2002). Malaria therapy reinoculation data suggest individual variation of an innate immune response and independent acquisition of antiparasitic and antitoxic immunities. *Trans R Soc Trop Med Hyg* **96**, 205-209.

Molyneux, M. E. (1989). Malaria--clinical features in children. *Journal of the Royal Society of Medicine* **82 Suppl 17**, 35-38.

Morahan, G., Boutlis, C. S., Huang, D. & other authors (2002). A promoter polymorphism in the gene encoding interleukin-12 p40 (IL12B) is associated with

mortality from cerebral malaria and with reduced nitric oxide production. *Genes and immunity* **3**, 414-418.

Mota, M. M., Pradel, G., Vanderberg, J. P., Hafalla, J. C., Frevert, U., Nussenzweig, R. S., Nussenzweig, V. & Rodriguez, A. (2001). Migration of *Plasmodium* sporozoites through cells before infection. *Science* **291**, 141-144.

Mu, J., Awadalla, P., Duan, J., McGee, K. M., Joy, D. A., McVean, G. A. & Su, X. Z. (2005). Recombination hotspots and population structure in *Plasmodium falciparum*. *PLoS Biol* **3**, e335.

Nardin, E., Zavala, F., Nussenzweig, V. & Nussenzweig, R. S. (1999). Pre-erythrocytic malaria vaccine: mechanisms of protective immunity and human vaccine trials. *Parassitologia* **41**, 397-402.

Newbold, C., Warn, P., Black, G., Berendt, A., Craig, A., Snow, B., Msobo, M., Peshu, N. & Marsh, K. (1997). Receptor-specific adhesion and clinical disease in *Plasmodium falciparum*. *Am J Trop Med Hyg* **57**, 389-398.

Oduola, A. M., Milhous, W. K., Weatherly, N. F., Bowdre, J. H. & Desjardins, R. E. (1988). *Plasmodium falciparum*: induction of resistance to mefloquine in cloned strains by continuous drug exposure in vitro. *Exp Parasitol* **67**, 354-360.

Okamura, H., Kashiwamura, S., Tsutsui, H., Yoshimoto, T. & Nakanishi, K. (1998). Regulation of interferon-gamma production by IL-12 and IL-18. *Curr Opin Immunol* **10**, 259-264.

Omi, K., Ohashi, J., Patarapotikul, J., Hananantachai, H., Naka, I., Looareesuwan, S. & Tokunaga, K. (2003). CD36 polymorphism is associated with protection from cerebral malaria. *American journal of human genetics* **72**, 364-374.

Oquendo, P., Goman, M., Mackay, M., Langsley, G., Walliker, D. & Scaife, J. (1986). Characterisation of a repetitive DNA sequence from the malaria parasite, *Plasmodium falciparum*. *Mol Biochem Parasitol* **18**, 89-101.

Page, R. D. (1996). TreeView: an application to display phylogenetic trees on personal computers. *Comput Appl Biosci* **12**, 357-358.

Pain, A., Urban, B. C., Kai, O., Casals-Pascual, C., Shafi, J., Marsh, K. & Roberts, D. J. (2001). A non-sense mutation in Cd36 gene is associated with protection from severe malaria. *Lancet* **357**, 1502-1503.

Papakrivos, J., Newbold, C. I. & Lingelbach, K. (2005). A potential novel mechanism for the insertion of a membrane protein revealed by a biochemical analysis of the *Plasmodium falciparum* cytoadherence molecule PfEMP-1. *Mol Microbiol* **55**, 1272-1284.

Pasvol, G., Wainscoat, J. S. & Weatherall, D. J. (1982). Erythrocytes deficiency in glycophorin resist invasion by the malarial parasite *Plasmodium falciparum*. *Nature* **297**, 64-66.

Peters, J. M., Fowler, E. V., Krause, D. R., Cheng, Q. & Gatton, M. L. (2007). Differential Changes in *Plasmodium falciparum var* Transcription during Adaptation to Culture. *J Infect Dis* **195**, 748-755.

Peterson, D. S. & Wellems, T. E. (2000). EBL-1, a putative erythrocyte binding protein of *Plasmodium falciparum*, maps within a favored linkage group in two genetic crosses. *Mol Biochem Parasitol* **105**, 105-113.

Phillips, R. S. (2001). Current status of malaria and potential for control. *Clinical microbiology reviews* **14**, 208-226.

Piper, K. P., Hayward, R. E., Cox, M. J. & Day, K. P. (1999a). Malaria transmission and naturally acquired immunity to PfEMP-1. *Infect Immun* **67**, 6369-6374.

Piper, K. P., Roberts, D. J. & Day, K. P. (1999b). *Plasmodium falciparum*: analysis of the antibody specificity to the surface of the trophozoite-infected erythrocyte. *Exp Parasitol* **91**, 161-169.

Pleass, R. J. & Holder, A. A. (2005). Opinion: antibody-based therapies for malaria. *Nat Rev Microbiol* **3**, 893-899.

Prescott, N., Stowers, A. W., Cheng, Q., Bobogare, A., Rzepczyk, C. M. & Saul, A. (1994). *Plasmodium falciparum* genetic diversity can be characterised using the polymorphic merozoite surface antigen 2 (MSA-2) gene as a single locus marker. *Mol Biochem Parasitol* **63**, 203-212.

Przyborski, J. M. & Lanzer, M. (2005). Protein transport and trafficking in *Plasmodium falciparum*-infected erythrocytes. *Parasitology* **130**, 373-388.

Przyborski, J. M., Miller, S. K., Pfahler, J. M., Henrich, P. P., Rohrbach, P., Crabb, B. S. & Lanzer, M. (2005). Trafficking of STEVOR to the Maurer's clefts in *Plasmodium falciparum*-infected erythrocytes. *Embo J.*

Purkerson, J. & Isakson, P. (1992). A two-signal model for regulation of immunoglobulin isotype switching. *Faseb J* **6**, 3245-3252.

Ralph, S. A., Scheidig-Benatar, C. & Scherf, A. (2005). Antigenic variation in *Plasmodium falciparum* is associated with movement of *var* loci between subnuclear locations. *Proc Natl Acad Sci U S A* **102**, 5414-5419.

Rasti, N., Wahlgren, M. & Chen, Q. (2004). Molecular aspects of malaria pathogenesis. *FEMS Immunol Med Microbiol* **41**, 9-26.

Rayner, J. C., Galinski, M. R., Ingravallo, P. & Barnwell, J. W. (2000). Two *Plasmodium falciparum* genes express merozoite proteins that are related to *Plasmodium vivax* and *Plasmodium yoelii* adhesive proteins involved in host cell selection and invasion. *Proc Natl Acad Sci U S A* **97**, 9648-9653.

Rayner, J. C., Vargas-Serrato, E., Huber, C. S., Galinski, M. R. & Barnwell, J. W. (2001). A *Plasmodium falciparum* homologue of *Plasmodium vivax* reticulocyte binding protein (PvRBP1) defines a trypsin-resistant erythrocyte invasion pathway. *J Exp Med* **194**, 1571-1581.

Recker, M., Nee, S., Bull, P. C., Kinyanjui, S., Marsh, K., Newbold, C. & Gupta, S. (2004). Transient cross-reactive immune responses can orchestrate antigenic variation in malaria. *Nature* **429**, 555-558.

Reyburn, H., Mbatia, R., Drakeley, C. & other authors (2005). Association of transmission intensity and age with clinical manifestations and case fatality of severe *Plasmodium falciparum* malaria. *Jama* **293**, 1461-1470.

Rihet, P., Flori, L., Tall, F., Traore, A. S. & Fumoux, F. (2004). Hemoglobin C is associated with reduced *Plasmodium falciparum* parasitemia and low risk of mild malaria attack. *Human molecular genetics* **13**, 1-6.

Roberts, D. J., Craig, A. G., Berendt, A. R., Pinches, R., Nash, G., Marsh, K. & Newbold, C. I. (1992). Rapid switching to multiple antigenic and adhesive phenotypes in malaria. *Nature* **357**, 689-692.

Rogers, N. J., Hall, B. S., Obiero, J., Targett, G. A. & Sutherland, C. J. (2000). A model for sequestration of the transmission stages of *Plasmodium falciparum*: adhesion of gametocyte-infected erythrocytes to human bone marrow cells. *Infect Immun* **68**, 3455-3462.

Rost, B. & Sander, C. (1993). Secondary structure prediction of all-helical proteins in two states. *Protein Eng* **6**, 831-836.

Rost, B., Casadio, R., Fariselli, P. & Sander, C. (1995). Transmembrane helices predicted at 95% accuracy. *Protein Sci* **4**, 521-533.

Rost, B. & Liu, J. (2003). The PredictProtein server. *Nucleic Acids Res* **31**, 3300-3304.

Rotman, H. L., Daly, T. M., Clynes, R. & Long, C. A. (1998). Fc receptors are not required for antibody-mediated protection against lethal malaria challenge in a mouse model. *J Immunol* **161**, 1908-1912.

Rowe, J. A., Moulds, J. M., Newbold, C. I. & Miller, L. H. (1997). *P. falciparum* rosetting mediated by a parasite-variant erythrocyte membrane protein and complement-receptor 1. *Nature* **388**, 292-295.

Sabchareon, A., Burnouf, T., Ouattara, D., Attanath, P., Bouharoun-Tayoun, H., Chantavanich, P., Foucault, C., Chongsuphajaisiddhi, T. & Druilhe, P. (1991). Parasitologic and clinical human response to immunoglobulin administration in *falciparum* malaria. *Am J Trop Med Hyg* **45**, 297-308.

Sabeti, P., Usen, S., Farhadian, S., Jallow, M., Doherty, T., Newport, M., Pinder, M., Ward, R. & Kwiatkowski, D. (2002). CD40L association with protection from severe malaria. *Genes and immunity* **3**, 286-291.

Sacks, D. & Sher, A. (2002). Evasion of innate immunity by parasitic protozoa. *Nature immunology* **3**, 1041-1047.

Sam-Yellowe, T. Y., Florens, L., Johnson, J. R. & other authors (2004). A *Plasmodium* gene family encoding Maurer's cleft membrane proteins: structural properties and expression profiling. *Genome Res* **14**, 1052-1059.

Schmidt, J. A., Udeinya, I. J., Leech, J. H., Hay, R. J., Aikawa, M., Barnwell, J., Green, I. & Miller, L. H. (1982). *Plasmodium falciparum* malaria. An amelanotic melanoma cell line bears receptors for the knob ligand on infected erythrocytes. *J Clin Invest* **70**, 379-386.

Schrevel, J., Sinou, V., Grellier, P., Frappier, F., Guenard, D. & Potier, P. (1994). Interactions between docetaxel (Taxotere) and *Plasmodium falciparum*-infected erythrocytes. *Proc Natl Acad Sci U S A* **91**, 8472-8476.

Sehgal, V. M., Siddjiqui, W. A. & Alpers, M. P. (1989). A seroepidemiological study to evaluate the role of passive maternal immunity to malaria in infants. *Trans R Soc Trop Med Hyg* **83 Suppl**, 105-106.

Seixas, E., Fonseca, L. & Langhorne, J. (2002). The influence of gammadelta T cells on the CD4+ T cell and antibody response during a primary *Plasmodium chabaudi chabaudi* infection in mice. *Parasite Immunol* **24**, 131-140.

Sharp, S., Lavstsen, T., Fivelman, Q. L. & other authors (2006). Programmed transcription of the *var* gene family, but not of *stevor*, in *Plasmodium falciparum* gametocytes. *Eukaryot Cell* **5**, 1206-1214.

Shear, H. L., Nussenzweig, R. S. & Bianco, C. (1979). Immune phagocytosis in murine malaria. *J Exp Med* **149**, 1288-1298.

Shulman, C. E. & Dorman, E. K. (2003). Importance and prevention of malaria in pregnancy. *Trans R Soc Trop Med Hyg* **97**, 30-35.

Sinden, R. E. & Smalley, M. E. (1979). Gametocytogenesis of *Plasmodium falciparum in vitro*: the cell-cycle. *Parasitology* **79**, 277-296.

Smith, J. D., Chitnis, C. E., Craig, A. G., Roberts, D. J., Hudson-Taylor, D. E., Peterson, D. S., Pinches, R., Newbold, C. I. & Miller, L. H. (1995). Switches in expression of *Plasmodium falciparumvar*genes correlate with changes in antigenic and cytoadherent phenotypes of infected erythrocytes. *Cell* **82**, 101-110.

Snow, R. W., Omumbo, J. A., Lowe, B. & other authors (1997). Relation between severe malaria morbidity in children and level of *Plasmodium falciparum* transmission in Africa. *Lancet* **349**, 1650-1654.

Snow, R. W., Nahlen, B., Palmer, A., Donnelly, C. A., Gupta, S. & Marsh, K. (1998). Risk of severe malaria among African infants: direct evidence of clinical protection during early infancy. *J Infect Dis* **177**, 819-822.

Snow, R. W. & Marsh, K. (2002). The consequences of reducing transmission of *Plasmodium falciparum* in Africa. *Adv Parasitol* **52**, 235-264.

Snow, R. W., Guerra, C. A., Noor, A. M., Myint, H. Y. & Hay, S. I. (2005). The global distribution of clinical episodes of *Plasmodium falciparum* malaria. *Nature* **434**, 214-217.

Spycher, C., Klonis, N., Spielmann, T., Kump, E., Steiger, S., Tilley, L. & Beck, H. P. (2003). MAHRP-1, a novel *Plasmodium falciparum* histidine-rich protein, binds ferriprotoporphyrin IX and localizes to the Maurer's clefts. *J Biol Chem* **278**, 35373-35383.

Stanley, H. A. & Reese, R. T. (1986). *Plasmodium falciparum* polypeptides associated with the infected erythrocyte plasma membrane. *Proc Natl Acad Sci U S A* **83**, 6093-6097.

Steketee, R. W., Nahlen, B. L., Parise, M. E. & Menendez, C. (2001). The burden of malaria in pregnancy in malaria-endemic areas. *Am J Trop Med Hyg* **64**, 28-35.

Stevenson, M. M. & Urban, B. C. (2006). Antigen presentation and dendritic cell biology in malaria. *Parasite Immunol* **28**, 5-14.

Stubbs, J., Simpson, K. M., Triglia, T., Plouffe, D., Tonkin, C. J., Duraisingh, M. T., Maier, A. G., Winzeler, E. A. & Cowman, A. F. (2005). Molecular mechanism for switching of P. *falciparum* invasion pathways into human erythrocytes. *Science* **309**, 1384-1387.

Su, X. Z., Heatwole, V. M., Wertheimer, S. P., Guinet, F., Herrfeldt, J. A., Peterson, D. S., Ravetch, J. A. & Wellems, T. E. (1995). The large diverse gene family *var* encodes proteins involved in cytoadherence and antigenic variation of *Plasmodium falciparum*-infected erythrocytes. *Cell* **82**, 89-100.

Su, Z. & Stevenson, M. M. (2002). IL-12 is required for antibody-mediated protective immunity against blood-stage *Plasmodium chabaudi* AS malaria infection in mice. *J Immunol* **168**, 1348-1355.

Suss, G., Eichmann, K., Kury, E., Linke, A. & Langhorne, J. (1988). Roles of CD4- and CD8-bearing T lymphocytes in the immune response to the erythrocytic stages of *Plasmodium chabaudi. Infect Immun* **56**, 3081-3088.

Sutherland, C. J. (2001). Stevor transcripts from *Plasmodium falciparum* gametocytes encode truncated polypeptides. *Mol Biochem Parasitol* **113**, 331-335.

Swofford (2003).PAUP. Phylogenetic Analysis Using Parsimony and other methods. Sunderland: Sinauer Associates.

Taylor, H. M., Triglia, T., Thompson, J., Sajid, M., Fowler, R., Wickham, M. E., Cowman, A. F. & Holder, A. A. (2001). *Plasmodium falciparum* homologue of the genes for *Plasmodium vivax* and *Plasmodium yoelii* adhesive proteins, which is transcribed but not translated. *Infect Immun* **69**, 3635-3645.

Taylor, H. M., Grainger, M. & Holder, A. A. (2002). Variation in the expression of a *Plasmodium falciparum* protein family implicated in erythrocyte invasion. *Infect Immun* **70**, 5779-5789.

Taylor, T. E., Molyneux, M. E., Wirima, J. J., Fletcher, K. A. & Morris, K. (1988). Blood glucose levels in Malawian children before and during the administration of intravenous quinine for severe *falciparum* malaria. *The New England journal of medicine* **319**, 1040-1047.

Taylor, T. E., Borgstein, A. & Molyneux, M. E. (1993). Acid-base status in paediatric *Plasmodium falciparum* malaria. *The Quarterly journal of medicine* **86**, 99-109.

Thaithong, S., Beale, G. H., Fenton, B., McBride, J., Rosario, V., Walker, A. & Walliker, D. (1984). Clonal diversity in a single isolate of the malaria parasite *Plasmodium falciparum. Trans R Soc Trop Med Hyg* **78**, 242-245.

Thompson, J. K., Triglia, T., Reed, M. B. & Cowman, A. F. (2001). A novel ligand from *Plasmodium falciparum* that binds to a sialic acid-containing receptor on the surface of human erythrocytes. *Mol Microbiol* **41**, 47-58.

Trager, W. & Jensen, J. B. (1976). Human malaria parasites in continuous culture. *Science* **193**, 673-675.

Trape, J. F. & Rogier, C. (1996). Combating malaria morbidity and mortality by reducing transmission. *Parasitology today (Personal ed* **12**, 236-240.

Treeck, M., Struck, N. S., Haase, S., Langer, C., Herrmann, S., Healer, J., Cowman, A. F. & Gilberger, T. W. (2006). A conserved region in the EBL proteins is implicated in microneme targeting of the malaria parasite *Plasmodium falciparum*. *J Biol Chem* **281**, 31995-32003.

Trenholme, K. R., Gardiner, D. L., Holt, D. C., Thomas, E. A., Cowman, A. F. & Kemp, D. J. (2000). *clag9*: A cytoadherence gene in *Plasmodium falciparum* essential for binding of parasitized erythrocytes to CD36. *Proc Natl Acad Sci U S A* **97**, 4029-4033.

Triglia, T., Healer, J., Caruana, S. R., Hodder, A. N., Anders, R. F., Crabb, B. S. & Cowman, A. F. (2000). Apical membrane antigen 1 plays a central role in erythrocyte invasion by *Plasmodium* species. *Mol Microbiol* **38**, 706-718.

Triglia, T., Thompson, J., Caruana, S. R., Delorenzi, M., Speed, T. & Cowman, A. F. (2001a). Identification of proteins from *Plasmodium falciparum* that are homologous to reticulocyte binding proteins in *Plasmodium vivax*. *Infect Immun* **69**, 1084-1092.

Triglia, T., Thompson, J. K. & Cowman, A. F. (2001b). An EBA175 homologue which is transcribed but not translated in erythrocytic stages of *Plasmodium falciparum*. *Mol Biochem Parasitol* **116**, 55-63.

Triglia, T., Duraisingh, M. T., Good, R. T. & Cowman, A. F. (2005). Reticulocyte-binding protein homologue 1 is required for sialic acid-dependent invasion into human erythrocytes by *Plasmodium falciparum*. *Mol Microbiol* **55**, 162-174.

Trimnell, A. R., Kraemer, S. M., Mukherjee, S., Phippard, D. J., Janes, J. H., Flamoe, E., Su, X. Z., Awadalla, P. & Smith, J. D. (2006). Global genetic diversity and evolution of *var* genes associated with placental and severe childhood malaria. *Mol Biochem Parasitol* **148**, 169-180.

Tsuboi, T., Kappe, S. H., al-Yaman, F., Prickett, M. D., Alpers, M. & Adams, J. H. (1994). Natural variation within the principal adhesion domain of the *Plasmodium vivax* duffy binding protein. *Infect Immun* **62**, 5581-5586.

Turner, G. D., Morrison, H., Jones, M. & other authors (1994). An immunohistochemical study of the pathology of fatal malaria. Evidence for widespread endothelial activation and a potential role for intercellular adhesion molecule-1 in cerebral sequestration. *The American journal of pathology* **145**, 1057-1069.

Udeinya, I. J., Schmidt, J. A., Aikawa, M., Miller, L. H. & Green, I. (1981). *Falciparum* malaria-infected erythrocytes specifically bind to cultured human endothelial cells. *Science* **213**, 555-557.

Uthaipibull, C., Aufiero, B., Syed, S. E. & other authors (2001). Inhibitory and blocking monoclonal antibody epitopes on merozoite surface protein 1 of the malaria parasite *Plasmodium falciparum*. *J Mol Biol* **307**, 1381-1394.

Vincensini, L., Richert, S., Blisnick, T., Van Dorsselaer, A., Leize-Wagner, E., Rabilloud, T. & Braun Breton, C. (2005). Proteomic analysis identifies novel proteins of the Maurer's clefts, a secretory compartment delivering *Plasmodium falciparum* proteins to the surface of its host cell. *Mol Cell Proteomics* **4**, 582-593.

Vindelol, L. L. (1978). A new method for Rapid Isolation and Staining of Nuclei for FTF-Analysis of Nuclear DNA in cells from Solid Tissues and Cell Suspensions. In *Pulse-Cytophotometry*, pp. 483-488. Edited by D. Lutz. Ghent: European Press.

Volkman, S. K., Hartl, D. L., Wirth, D. F. & other authors (2002). Excess polymorphisms in genes for membrane proteins in *Plasmodium falciparum*. *Science* **298**, 216-218.

Volkman, S. K., Lozovsky, E., Barry, A. E. & other authors (2007a). Genomic heterogeneity in the density of noncoding single-nucleotide and microsatellite polymorphisms in *Plasmodium falciparum*. *Gene* **387**, 1-6.

Volkman, S. K., Sabeti, P. C., DeCaprio, D. & other authors (2007b). A genome-wide map of diversity in *Plasmodium falciparum*. *Nature genetics* **39**, 113-119.

Waller, R. F., Reed, M. B., Cowman, A. F. & McFadden, G. I. (2000). Protein trafficking to the plastid of *Plasmodium falciparum* is via the secretory pathway. *Embo J* **19**, 1794-1802.

Walliker, D., Quakyi, I. A., Wellems, T. E., McCutchan, T. F., Szarfman, A., London, W. T., Corcoran, L. M., Burkot, T. R. & Carter, R. (1987). Genetic analysis of the human malaria parasite *Plasmodium falciparum*. *Science* **236**, 1661-1666.

Wambua, S., Mwangi, T. W., Kortok, M. & other authors (2006). The effect of alpha+-thalassaemia on the incidence of malaria and other diseases in children living on the coast of Kenya. *PLoS medicine* **3**, e158.

Waterkeyn, J. G., Wickham, M. E., Davern, K. M., Cooke, B. M., Coppel, R. L., Reeder, J. C., Culvenor, J. G., Waller, R. F. & Cowman, A. F. (2000). Targeted mutagenesis of *Plasmodium falciparum* erythrocyte membrane protein 3 (PfEMP3) disrupts cytoadherence of malaria-infected red blood cells. *Embo J* **19**, 2813-2823.

Watson, J. V. (1981). Dual laser beam focussing for flow cytometry through a single crossed cylindrical lens pair. *Cytometry* **2**, 14-19.

White, N. J., Warrell, D. A., Looareesuwan, S., Chanthavanich, P., Phillips, R. E. & Pongpaew, P. (1985). Pathophysiological and prognostic significance of cerebrospinal-fluid lactate in cerebral malaria. *Lancet* **1**, 776-778.

Wickham, M. E., Rug, M., Ralph, S. A., Klonis, N., McFadden, G. I., Tilley, L. & Cowman, A. F. (2001). Trafficking and assembly of the cytoadherence complex in *Plasmodium falciparum*-infected human erythrocytes. *Embo J* **20**, 5636-5649.

Williams, T. N., Mwangi, T. W., Wambua, S., Alexander, N. D., Kortok, M., Snow, R. W. & Marsh, K. (2005). Sickle cell trait and the risk of *Plasmodium falciparum* malaria and other childhood diseases. *J Infect Dis* **192**, 178-186.

Williams, T. N. (2006). Human red blood cell polymorphisms and malaria. *Curr Opin Microbiol* **9**, 388-394.

Winter, G., Kawai, S., Haeggstrom, M., Kaneko, O., von Euler, A., Kawazu, S., Palm, D., Fernandez, V. & Wahlgren, M. (2005). SURFIN is a polymorphic antigen expressed on *Plasmodium falciparum* merozoites and infected erythrocytes. *J Exp Med* **201**, 1853-1863.

Wootton, J. C., Feng, X., Ferdig, M. T., Cooper, R. A., Mu, J., Baruch, D. I., Magill, A. J. & Su, X. Z. (2002). Genetic diversity and chloroquine selective sweeps in *Plasmodium falciparum*. *Nature* **418**, 320-323.